



Universidad de Valladolid

ESCUELA DE INGENIERÍAS INDUSTRIALES

DEPARTAMENTO DE INGENIERÍA QUÍMICA Y TECNOLOGÍA DEL

MEDIO AMBIENTE

**Studies in the development of SCWO
vessel reactors with hydrothermal flame
as an internal heat source**

Pablo Cabeza Pérez



Universidad de Valladolid

ESCUELA DE INGENIERÍAS INDUSTRIALES

DEPARTAMENTO DE INGENIERÍA QUÍMICA Y TECNOLOGÍA DEL

MEDIO AMBIENTE

**Desarrollo de reactores de tanque
para oxidación en agua supercrítica con llama
hidrotermal como fuente de energía interna**

Pablo Cabeza Pérez

Memoria para optar al grado de Doctor,
con Mención de doctorado Europeo,
presentada por el Ingeniero Químico:

Pablo Cabeza Pérez

Valladolid, Julio de 2012

UNIVERSIDAD DE VALLADOLID
ESCUELA DE INGENIERÍAS INDUSTRIALES

Secretaría

La presente tesis doctoral queda registrada en el folio N^o _____
del correspondiente Libro de Registro con el N^o _____

Valladolid, a _____ de _____ de 2012

Fdo. El encargado del Registro

María Dolores Bermejo Roda

Profesora Ayudante Doctor del Departamento de Ingeniería Química
y Tecnología del Medio Ambiente
Universidad de Valladolid

y

María José Cocero Alonso

Profesora titular del Departamento de Ingeniería Química
y Tecnología del Medio Ambiente
Universidad de Valladolid

CERTIFICAN QUE:

PABLO CABEZA PEREZ ha realizado bajo su dirección el trabajo *“Studies in the development of SCWO vessel reactors with hydrothermal flame as an internal heat source”*, en el Departamento de Ingeniería Química y Tecnología del Medio Ambiente de la Escuela de Ingenierías Industriales de la Universidad de Valladolid. Considerando que dicho trabajo reúne los requisitos para ser presentado como Tesis Doctoral expresan su conformidad con dicha presentación.

Valladolid a ____ de _____ de 2012.

Fdo. María José Cocero Alonso

Fdo. María Dolores Bermejo Roda

Reunido el tribunal que ha juzgado la tesis doctoral "*Studies in the development of SCWO vessel reactors with hydrothermal flame as an internal heat source*" presentada por Pablo Cabeza Pérez y en cumplimiento con lo establecido por el Real Decreto 861/2010 (BOE 03.07.2010) ha acordado conceder por _____
_____ la calificación de _____.

Valladolid, a de de 2012

PRESIDENTE

SECRETARIO

1^{er} Vocal

2^{do} Vocal

3^{er} Vocal

TABLE OF CONTENTS

RESUMEN	1
1. ANTECEDENTES	1
2. OBJETIVOS	4
3. RESULTADOS	5
4. CONCLUSIONES	26
SUMMARY	33
CHAPTER 1: INTRODUCTION	37
1.1. SUPERCRITICAL FLUIDS	39
1.2. SUPERCRITICAL WATER OXIDATION	40
1.3. HYDROTHERMAL FLAMES	59
1.4. REFERENCES	63
CHAPTER 2: OBJETIVES	73
CHAPTER 3: EXPERIMENTAL SETUP	77
3.1. REACTORS	79
3.2. PLANT OPERATION	88
3.3. COMMON EQUIPMENT	103
CHAPTER 4: TUBULAR REACTORS	117
4.1 EXPERIMENTAL STUDY OF HYDROTHERMAL FLAMES INITIATION USING DIFFERENT STATIC MIXER CONFIGURATIONS	119
4.1.1. INTRODUCTION	120
4.1.2. EXPERIMENTAL	122
4.1.3. RESULTS AND DISCUSSION	127
4.1.4. CONCLUSIONS	138
4.1.5. REFERENCES	139
4.2. EXPERIMENTAL STUDY OF THE SUPERCRITICAL WATER OXIDATION OF RECALCITRANT COMPOUNDS UNDER HYDROTHERMAL FLAMES USING TUBULAR REACTORS	143
4.2.1. INTRODUCTION	145
4.2.2. EXPERIMENTAL	147
4.2.3. RESULTS AND DISCUSSION	151
4.2.4. CONCLUSIONS	162
4.2.5. REFERENCES	165

CHAPTER 5: TRANSPIRING WALL REACTOR.....	169
5.1 ANALYSIS OF THE SCALE UP OF A TRANSPIRING WALL REACTOR WITH A HYDROTHERMAL FLAME AS A HEAT SOURCE FOR THE SUPERCRITICAL WATER OXIDATION.....	173
5.1. INTRODUCTION.....	175
5.2. EXPERIMENTAL.....	177
5.3. RESULTS AND DISCUSSION.....	182
5.4. CONCLUSIONS.....	200
5.5. REFERENCES.....	203
CHAPTER 6: NEW COOLED WALL REACTOR DESIGN.....	207
6.1 EXPERIMENTAL STUDY OF HYDROTHERMAL FLAMES FORMATION USING A TUBULAR INJECTOR IN A REFRIGERATED REACTION CHAMBER. INFLUENCE OF THE OPERATIONAL AND GEOMETRICAL PARAMETERS.....	211
6.1.1. INTRODUCTION.....	213
6.1.2. EXPERIMENTAL.....	216
6.1.3. RESULTS AND DISCUSSION.....	224
6.1.4. CONCLUSIONS.....	232
6.1.5. REFERENCES.....	234
6.2. SLUDGE DESTRUCTION BY MEANS OF A HYDROTHERMAL FLAME. OPTIMIZATION OF AMMONIA DESTRUCTION CONDITIONS.....	237
6.2.1. INTRODUCTION.....	239
6.2.2. EXPERIMENTAL.....	242
6.2.3. RESULTS AND DISCUSSION.....	245
6.2.4. CONCLUSIONS.....	261
6.2.5. REFERENCES.....	263
6.3. ANALYSIS OF THE BEHAVIOR OF A SCWO COOLED WALL REACTOR WORKING WITH TWO OUTLETS. EXPERIMENTAL RESULTS AND ENERGETIC STUDY.....	267
6.3.1. INTRODUCTION.....	269
6.3.2. EXPERIMENTAL.....	272
6.3.3. RESULTS AND DISCUSSION.....	277
6.3.4. CONCLUSIONS.....	285
6.3.5. REFERENCES.....	287
CHAPTER 7: CONCLUSIONS AND FUTURE WORK.....	291
APPENDIX I: SUPPORTING INFORMATION CHAPTER 6.....	297
APPENDIX II: PROCESS DATA SHEETS.....	301
LIST OF PUBLICATIONS.....	319

RESUMEN

Desarrollo de reactores de tanque para oxidación en agua supercrítica con llama hidrotermal como fuente de energía interna

PABLO CABEZA PÉREZ

RESUMEN

1. ANTECEDENTES

El agua en condiciones supercríticas (ASC) posee propiedades físicas características que hacen que sea un excelente medio de oxidación de residuos industriales. Por ejemplo, el agua supercrítica actúa como un gas denso no polar, y sus propiedades de solvatación son equivalentes a las de un disolvente orgánico de baja polaridad, lo que justifica la alta solubilidad de los hidrocarburos en agua supercrítica. Además gases como nitrógeno, oxígeno, y dióxido de carbono son totalmente miscibles, por lo tanto las reacciones de oxidación son reacciones homogéneas, sin limitaciones a la transferencia de materia. Los productos de la oxidación en ASC de hidrocarburos son dióxido de carbono y agua. Los compuestos nitrogenados se oxidan para dar nitrógeno molecular (N_2), y los heteroátomos pasan a óxidos, sales o ácidos con un elevado grado de oxidación. Estas características hacen que actualmente la principal aplicación del agua supercrítica sea la “oxidación en agua supercrítica” (OASC) ó (Supercritical water oxidation (SCWO)), que se basa en la oxidación homogénea de compuestos químicos presentes en corrientes acuosas, realizada a presión y temperatura superiores a la del punto crítico del agua, $P_C = 22.1$ MPa y $T_C = 374^\circ C$.

La principal aplicación de la OASC es la destrucción de contaminantes recalcitrantes, xenobióticos ó no biodegradables, representando una alternativa a procesos convencionales como la oxidación química ó la incineración.

A pesar de las evidentes ventajas de este proceso su comercialización se ha visto dificultada por una serie de inconvenientes asociados al proceso [1]:

- Corrosión: Las duras condiciones de operación en presión y temperatura hacen que el proceso requiera equipos no convencionales. Las elevadas temperaturas y la atmósfera oxidante llevan a problemas de corrosión que hay que tener en cuenta en el diseño de los reactores y de los intercambiadores de calor [2]. Como materiales de construcción se utilizan aleaciones con alto contenido en níquel (625, C-276), titanio y materiales cerámicos. [3, 4]

- Precipitación de sales: Debido a los valores reducidos de la constante dieléctrica en ASC, la solubilidad de las sales inorgánicas es prácticamente nula, lo que lleva asociado problemas de deposición de sales y de taponamiento.
- Elevado consumo energético y costes de operación: Las elevadas presiones ($P > 23$ MPa) y temperaturas de operación ($T > 400^\circ\text{C}$), hacen que el acondicionamiento de los reactivos requiera un elevado consumo energético. Por esto es importante maximizar la recuperación del calor del proceso para el precalentamiento de reactivos, ó incluso para la producción de energía eléctrica [5].

El adecuado diseño del reactor es un factor importante para evitar el taponamiento y la corrosión, así como para maximizar la recuperación energética.

Con este propósito se han empleado en este trabajo diferentes tipos de reactores, desde el reactor tubular, que es la configuración más sencilla hasta otros diseños más complejos como el reactor de pared transpirable o el reactor de pared enfriada.

Reactor tubular

El reactor tubular es el diseño más simple de los existentes por lo que es uno de los más utilizados. Se emplea para investigación en pequeñas plantas de laboratorio [6] ó también para obtener parámetros cinéticos o calores de reacción [7, 8]. También es el más utilizado a nivel industrial [1, 9, 10] Los reactores tubulares también presentan desventajas, como son la facilidad de taponamiento debida a la precipitación de sales y la posibilidad de formación de puntos.

Reactor de pared transpirable

El reactor de pared transpirable (TWR) consiste en una cámara de reacción rodeada por una pared a través de la cual circula agua limpia de enfriamiento y protección, de manera que se evitan los problemas de corrosión, la deposición de sales y altas temperaturas.

Existen diferentes tipos de reactores de pared transpirable. El elemento principal y común en todos ellos es la pared porosa; un tubo poroso que constituye la cámara de reacción y es fabricado de metal sinterizado o cerámica.

Reactor de pared enfriada

El reactor de pared enfriada posee un diseño que hace capaz de considerar independientemente los efectos de la temperatura y la presión en la OASC. Consta de un recipiente a presión y de una cámara interna de reacción contenida en éste. La pared del recipiente a presión se mantiene a temperaturas inferiores a 400°C mediante la acción del agua de enfriamiento que fluye entre las cámaras externa e interna. Como no tiene que soportar temperaturas mayores de 400°C, ni atmósferas corrosivas, puede construirse de un material de menor precio como el acero inoxidable. La cámara de reacción, en la que los reactivos son mezclados y tiene lugar la reacción de oxidación, está construida de materiales capaces de soportar la atmósfera oxidante hasta temperaturas de hasta 700°C, y el coste de construcción se abarata ya que no tiene que soportar presión y tiene un espesor pequeño.

Llamas hidrotermales, aplicación al proceso OASC

Con concentraciones lo suficientemente elevadas de materia orgánica y oxígeno es posible operar a temperaturas por encima de la de autoignición y formar llamas, denominadas llamas hidrotermales cuando dicha ignición se produce en medio acuoso. Las llamas hidrotermales fueron descubiertas por Franck en 1988 [11] y presentan ventajas en el proceso OASC tales como:

- Reducir el tiempo de reacción a milisegundos, lo que permite reducir el tamaño de los equipos.
- Es posible inyectar los reactivos a temperaturas más bajas evitando precalentamiento externo, lo que reduce los problemas de corrosión y deposición de sales en el sistema de precalentamiento.
- Mejorar el aprovechamiento energético del efluente a temperaturas altas.

A la hora de seleccionar el tipo de reactor adecuado para trabajar con llamas hidrotermales se ha observado que los reactores del tanque en comparación con los reactores tubulares presentan ciertas ventajas como la posibilidad de inyectar los reactivos a temperatura por debajo del punto crítico ó la producción de una llama más estable. [12, 13]

2. OBJETIVOS

El objetivo de esta tesis es desarrollar un nuevo diseño de reactor para el proceso de oxidación en agua supercrítica, que trabaje con una llama hidrotermal como fuente de calor interno y que sea capaz de permitir la inyección de alimentaciones a temperatura ambiente, de manejar residuos con cierto contenido en sales inorgánicas y de optimizar el aprovechamiento energético.

Para ello se han propuesto varios objetivos parciales:

1) Estudio de la influencia de parámetros de operación en la formación de las llamas hidrotermales.

En primer lugar usando dispositivos tubulares, se estudiará en primer lugar la iniciación de de llamas hidrotermales de compuestos inflamables con el fin de determinar la influencia de parámetros como la mezcla, la velocidad de inyección, la concentración y la temperaturas de inyección.

También se estudiará la ignición de compuestos recalcitrantes, como el amoniaco o el ácido acético, para los que se valorará la necesidad del uso de un co-fuel.

Usando reactores de tanque se determinara la influencia de los parámetros geométricos en la formación y comportamiento de las lamas hidrotermales.

Con esta información se determinarán los parámetros que influyen en la inyección de reactivos a temperatura ambiente sobre una llama hidrotermal y se identificarán los parámetros más importantes a la hora de diseñar un reactor con llama hidrotermal como fuente de calor interna.

2) Diseño, construcción y puesta a punto de un reactor tipo tanque que trabaje con una llama hidrotermal como fuente de calor interna.

3) Estudio del comportamiento del reactor con diferentes alimentaciones:

Compuestos inflamables

Alimentaciones con alto contenido en sales

Alimentaciones conteniendo compuestos recalcitrantes

4) Modificaciones en la configuración del reactor para mejorar la recuperación de energía

3. RESULTADOS

Capítulo 4: Reactores tubulares.

4.1 Estudio experimental de iniciación de llamas hidrotermales utilizando diferentes configuraciones de reactor tubular

En el trabajo desarrollado para este capítulo se realizaron experimentos para el estudio de la iniciación de llamas hidrotermales en varios reactores tubulares con distintos tamaños y formas trabajando con diferentes flujos de alimentación, temperaturas de inyección y concentraciones isopropanol. (La descripción completa de cada tipo de reactor se encuentra desarrollada en el capítulo 4.1 de esta tesis, figura 4.1.2).

Dependiendo de las condiciones de operación, se han obtenido hasta tres tipos de perfiles de temperatura a lo largo de los reactores tubulares.

Los ejemplos se muestran en la Figura 1. En el perfil a, la temperatura aumentó de forma pronunciada desde el punto de mezcla. En el tipo de perfil b, la temperatura de la mezcla de reacción creció lentamente hasta alcanzar una temperatura en la que se observa un aumento mucho más rápido de temperatura. Por último, en el perfil de temperatura c, los reactivos aumentan de temperatura muy lentamente a lo largo del reactor. Perfiles de temperatura similares se obtuvieron trabajando con los otros reactores empleados para el estudio.

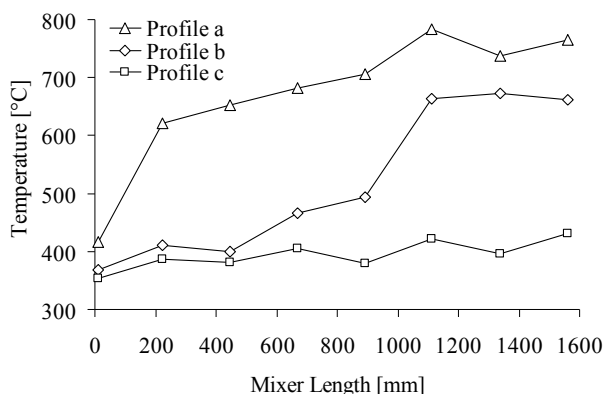


Figura 1: Ejemplos de perfiles de temperatura encontrados en el mezclador 1. Perfil a) Flujo: 12,9 kg / h, temperatura de inyección: 417°C, perfil de b) flujo de alimentación: 7,51 kg / h, temperatura de inyección: 368°C, perfil c) Flujo: 7,51 kg / h; temperatura de inyección: 353°C

Los perfiles de temperatura se han comparado con los resultados de un modelo que considera un reactor de flujo pistón en estado estacionario. Dos modelos cinéticos fueron probados y comparados con los perfiles de temperatura experimentales: el modelo presentado por Li et al. [14] y el modelo de Hunter [15]. Únicamente se ha logrado reproducir el caso del perfil tipo c el cual se puede reproducir mediante el modelo de cinética desarrollada por Li et al [14]. La comparación de algunos de los resultados experimentales con los obtenidos mediante los modelos cinéticos se muestran en la Figura 2.

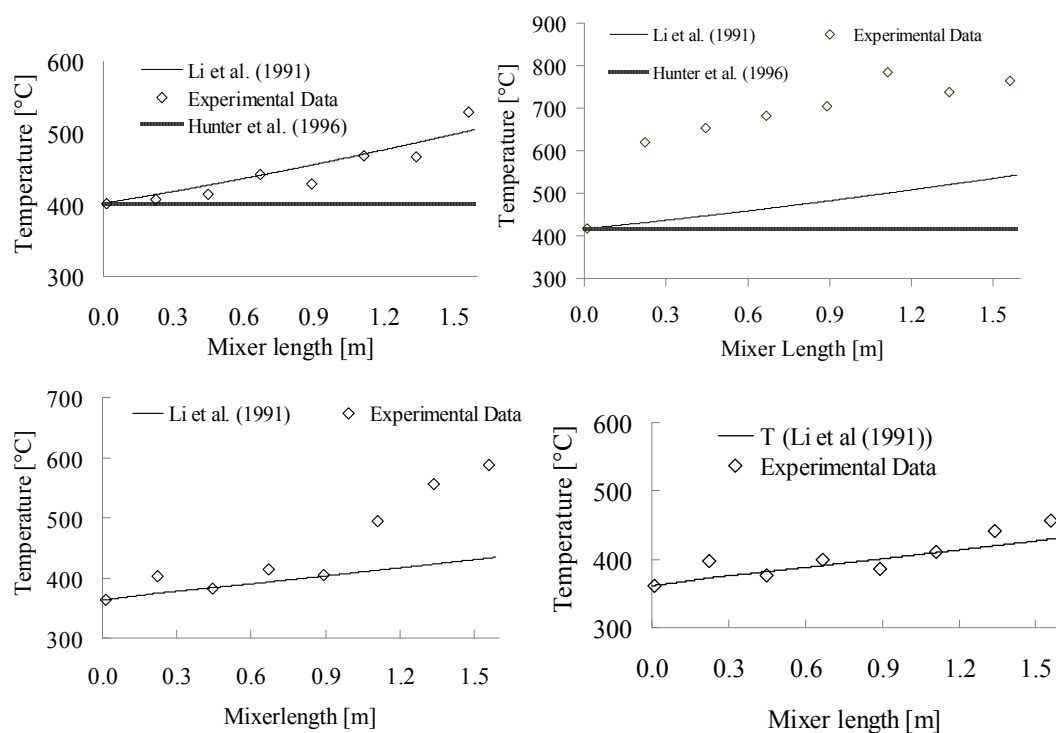


Figura 2: Comparación del perfil de temperaturas experimentales con las predicciones de los modelos cinéticos

Debido a que todos los mezcladores (reactores tubulares) utilizados trabajan de forma autotérmica, y todos los modelos cinéticos estudiados resultaron ser más lentos que los datos experimentales, el rápido incremento de temperatura se puede asociar con un cambio en el mecanismo de reacción favorecido por las altas temperaturas. El fenómeno observado es muy similar a la formación de llamas hidrotermales descrito en literatura [11, 16-20][13 - 18].

A partir de este punto se ha llevado a cabo un estudio de la influencia de las distintas variables de operación en el proceso de ignición para los distintos tipos de reactores tubulares probados.

La Figura 3 muestra el tiempo de residencia de arranque (tiempo hasta que se produce la ignición) frente a la temperatura de entrada para las diferentes configuraciones de mezcladores con un flujo de alimentación constante de 7,5 kg/h y una concentración del 4% de IPA.

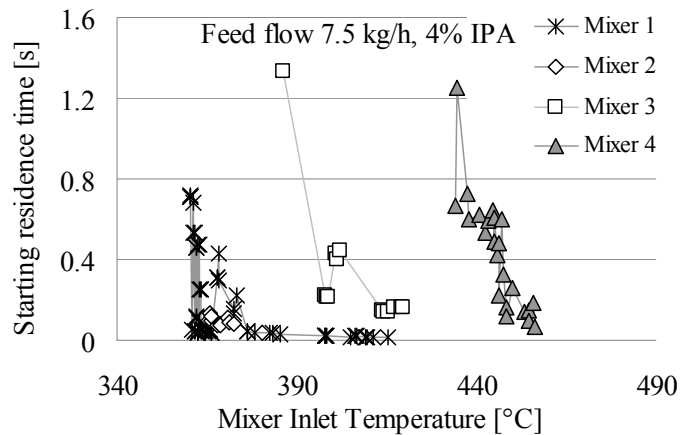


Figura 3: Tiempo de residencia de arranque frente a la temperatura de entrada con las diferentes configuraciones de mezcladores con un flujo de alimentación constante de 7,5 kg / h y 4% de IPA.

Para el mezclador 1, se observa que la temperatura de inyección con la que se produce la oxidación con llama es de aproximadamente 360 °C. Para esta temperatura el tiempo de residencia de arranque es de 0,7 s. Cuando la temperatura de inyección se incrementa por encima de 375 °C la ignición se produce casi en la entrada del reactor.

El mezclador 2 presenta resultados similares al mezclador 1.

En el caso del mezclador 3, para lograr la ignición han sido necesarias temperaturas de inyecciones superior a 390° C y un tiempo de residencia para el arranque de 1,4 s, pero con mayores temperaturas el tiempo de residencia de arranque puede reducirse a 0,2 s.

Para el mezclador 4, la temperatura de entrada mínima es de 430°C y los tiempos de residencia de 1,2 s. A temperaturas superiores a 450°C la ignición se produce casi de inmediato a la entrada del mezclador.

Los resultados respecto a la eliminación del TOC se muestran en la Tabla 1. Se observa que la eliminación máxima del TOC fue del 93% mientras que la mínima eliminación fue del 55%, siendo los tiempos de residencia máximos de 1,7 s.

Los datos con mayor eliminación de TOC se pueden asociar con el proceso de ignición. Es destacable que incluso cuando la configuración de los reactores tubulares no era la óptima para producir ó mantener una llama, los valores de eliminación del TOC obtenidos con tiempos de residencia inferiores a 2 s fueron altos.

Tabla 1: Eliminaciones de TOC y tiempos de residencia

Mixer	% IPA	Feed Mass Flow [kg/h]	TOC Removal [%]		Total residence time [s]	
			min	max	min	max
1	4	7.5	55.43	99.97	0.35	0.63
		6	94.27	99.92	0.43	0.54
	5	12.6	89.84	95.99	0.19	0.24
2	4	7.5	57.38	94.27	0.14	0.19
3	4	6	98.88	99.91	1.07	1.52
		7.5	97.39	99.91	0.72	1.15
		9	76.02	99.95	0.60	1.22
		10	89.89	99.18	0.60	0.80
4	4	6	92.58	99.48	1.13	1.68
		8	90.87	100.00	0.93	1.58
		9	92.77	98.46	0.78	1.08
		10	56.18	93.63	0.81	1.09

4.2 Estudio experimental de la oxidación en agua supercrítica de compuestos recalcitrantes en llamas hidrotermales mediante reactores tubulares

El objetivo de este trabajo es el análisis del aprovechamiento de la formación de llamas hidrotermales en un reactor tubular para la eliminación de compuestos de difícil eliminación denominados recalcitrantes. Los compuestos estudiados fueron el ácido acético y el amoníaco:

Oxidación de mezclas acuosas de ácido acético-isopropanol

Para este caso se realizaron experimentos con concentraciones del 1% al 4% (en masa) de ácido acético (procedente de un residuo industrial cuyo componente principal es ácido acético, composición completa en la tabla 4.2.1) mezclado con la concentración de isopropanol (IPA) necesaria con el fin de mantener el valor de la temperatura en el reactor alrededor de 650-750 °C.

Todos los experimentos se realizaron con un flujo de alimentación de 9 kg/h, a una temperatura de inyección constante entre 390 a 410 °C, una presión de 23 MPa y empleando oxígeno como agente oxidante en concentraciones superiores a la estequiométrica para asegurar una conversión completa.

Tras varios experimentos realizados con diferentes composiciones de ácido acético e isopropanol, tal como se esperaba, se puede observar que aumentando la cantidad de material orgánico en la alimentación, la temperatura máxima alcanzada en el reactor es mayor y, en consecuencia, la conversión de TOC también. Los resultados se presentan en la Figura 4a, donde se muestra la eliminación de TOC frente a la temperatura máxima registrada en el reactor para las distintas alimentaciones tratadas.

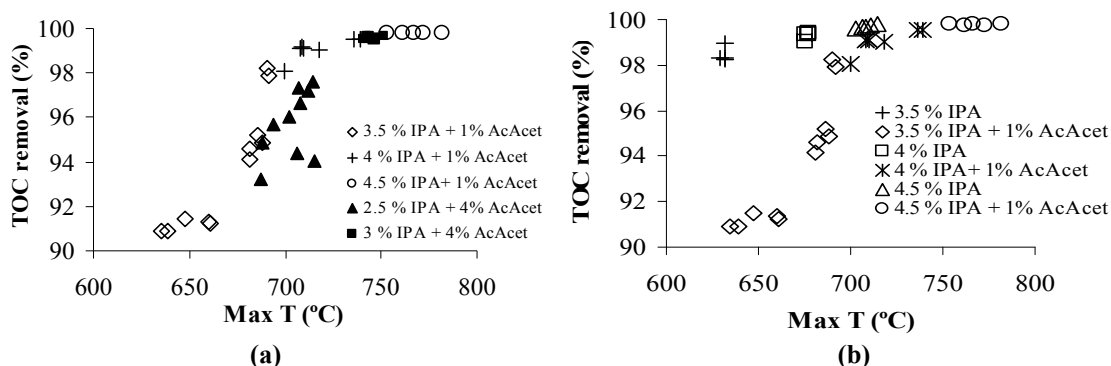


Figura 4a: Eliminación de TOC frente a la temperatura de reacción para diferentes concentraciones de isopropanol y ácido acético al 1% y al 4%

Figura 4b: Eliminación de TOC frente a la temperatura de reacción para diferentes concentraciones de isopropanol solo y de mezclas de isopropanol y ácido acético al 1%.

Condiciones experimentales: Flujo de alimentación 9.50 kg/h Flujo de Oxígeno en exceso respecto al estequiométrico, $P=23\text{MPa}$.

En la Figura 4b, se muestran por un lado la eliminación del TOC para alimentaciones con diferentes concentraciones únicamente de IPA a distintas temperaturas, y a la vez, de la misma manera, alimentaciones preparadas con la misma concentración de IPA más un 1% de ácido acético.

Se puede apreciar que se dan mayores eliminaciones de TOC para las mezclas que no contienen ácido acético así como que las mezclas requieren mayores temperaturas de reacción para lograr una eliminación completa cuando la concentración de IPA es la misma.

A pesar de los buenos resultados de eliminación de TOC de las mezclas de ácido acético-isopropanol, no se pudieron probar concentraciones más altas de ácido acético debido a problemas de corrosión detectados en la zona de precalentamiento.

Oxidación de mezclas acuosas de amoníaco-isopropanol

Para este segundo estudio, se realizaron experimentos con concentraciones de amoníaco del 2% al 6% (en masa), mezclados con la concentración de isopropanol necesaria para mantener el valor de la temperatura en el reactor alrededor de 650-750 °C.

Al igual que en el estudio de mezclas de ácido acético-isopropanol, todos los experimentos se realizaron con un flujo de alimentación de 9 kg/h, a una temperatura de inyección constante entre 390 a 410 °C, una presión de 23 MPa y empleando oxígeno como agente oxidante.

En este caso fue posible obtener eliminaciones de TOC más del 99%, pero en el caso de la eliminación de amoníaco, la eliminación máxima fue del 94% incluso a temperaturas superiores a 750 °C. En las Figuras 5a y 5b se muestra la eliminación del TOC (Figura 5a) y la eliminación de nitrógeno (Figura 5b) frente a la temperatura máxima registrada en el reactor para diferentes concentraciones de IPA y amoníaco.

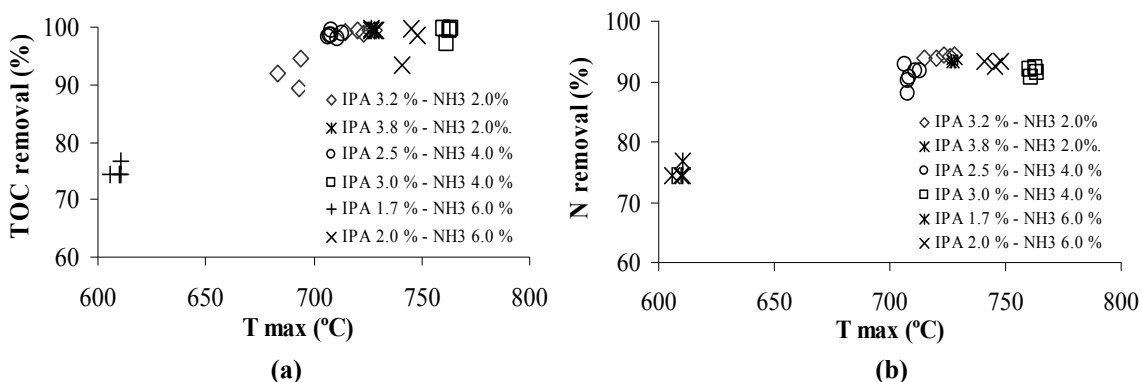


Figura 5a: Eliminación de TOC frente a la temperatura de reacción para diferentes concentraciones de amoníaco e isopropanol

Figura 5b: Eliminación de amoníaco (nitrógeno total) frente a la temperatura de reacción para diferentes concentraciones de amoníaco e isopropanol

Se puede observar que cuando la eliminación de TOC mejora lo hace también la eliminación de nitrógeno total (TN), debido principalmente al aumento de la temperatura dentro del reactor, pero también se observa que no es posible eliminar más del 94% de amoníaco a pesar de incrementar la temperatura de reacción.

En un trabajo anterior del grupo [18], fue posible obtener más de 99% de eliminación de amoníaco con temperaturas cercanas a 800 °C en un reactor de cámara con pared enfriada con un tiempo de residencia total de 1 minuto. De esta manera, se puede pensar que para la destrucción total de amoníaco se requieren tiempos de residencia más largos (el tiempo de residencia en el reactor tubular empleado es menor de 1 segundo).

En la Figura 6 se muestran perfiles de temperatura a lo largo del reactor para experimentos realizados con diferentes concentraciones de IPA y de NH₃. Se puede observar que a medida que la concentración de IPA disminuye, la posición de la llama se desplaza alejándose del punto de inyección del reactor, lo que significa que para la formación de la llama hidrotermal con amoníaco la temperatura de autoignición tiene que ser superior a la de autoignición de IPA.

Con concentraciones de IPA del 1%. La ignición de IPA no se produce al igual que no fue posible lograr la ignición de llama empleando sólo NH₃ como combustible, incluso a concentraciones del 10% en peso de NH₃.

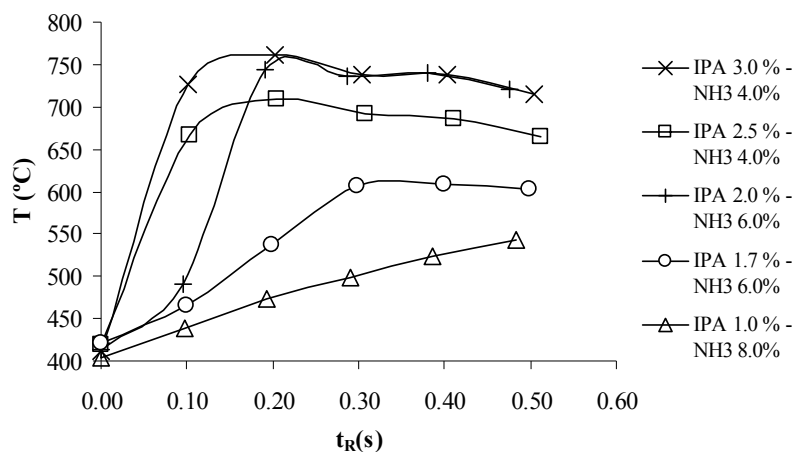


Figura 6: Influencia de la concentración de amoníaco en la formación de la llama hidrotermal

Capítulo 5: Reactor de pared transpirable

5.1. Análisis del escalado de un reactor de pared transpirable con llama hidrotérmica como fuente de calor para la oxidación en agua supercrítica

En este capítulo se expone el funcionamiento de un reactor de pared transpirable una vez que ha sido instalado en una planta piloto de mayor capacidad que en previa en la cual el reactor fue empleado en trabajos previos [21-25] (cambio de escala de planta de 23 kg/h a 200 kg/h). Los primeros estudios se basaron en el estudio de la formación de llamas en este tipo de reactores tras la experiencia previa obtenida en el estudio de las llamas en reactores tubulares.

En la Figura 7 se observa que la temperatura en el interior del inyector permanece a temperaturas menores de 350°C, elevándose hasta 650-750°C solo fuera del mezclador en la cámara de reacción.

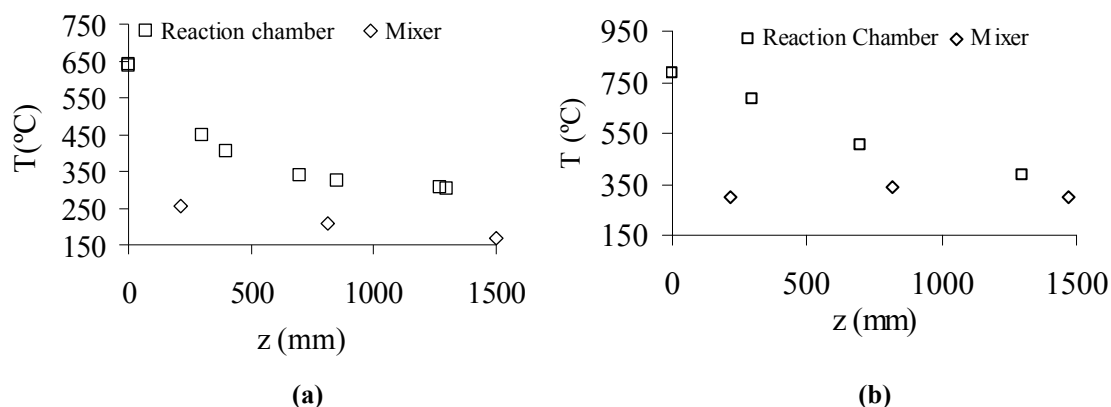


Figura 7: Perfiles de temperatura en el reactor escalado: (a) Alimentación= 35 kg/h; Oxidante: aire; $C_{IPA}=10\%wt$; $T_{Inyección}= 169^{\circ}C$; $T_{air}=320^{\circ}C$; (b) Alimentación= 61.6 kg/h; Oxidante: O_2 ; $C_{IPA}=8\%wt$; $T_{Inyección}=303^{\circ}C$

De esta manera se ha observado que en los reactores de cámara, la llama no se forma en el inyector sino una vez que los reactivos pasan por la cámara de reacción, el hecho de que la llama se produzca fuera del inyector también afecta a lograr una llama mucho más estable que en los reactores tubulares donde la llama permite temperaturas de inyecciones más bajas.

Estudio de la influencia de las variables de operación del reactor

Con el fin de estudiar el escalado del reactor se ha trabajado aumentando progresivamente el flujo de reactivos a tratar y el flujo transpirable para buscar el flujo óptimo de trabajo del nuevo reactor.

Influencia del flujo de alimentación

En la Figura 8 se observa que al aumentar el flujo de la alimentación, la temperatura media del reactor sube. Esto se puede deber a que más volumen de reactor es útil para la oxidación.

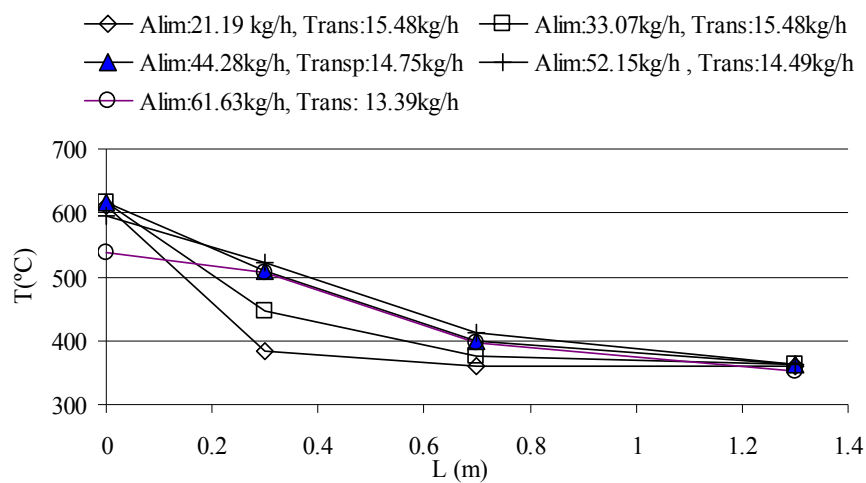


Figura 8: Perfiles de temperatura en el reactor a diferentes flujos de alimentación

Influencia del flujo transpirable

En la Figura 9 se observa que a elevados flujos de alimentación la influencia reguladora de la temperatura del flujo transpirable es menor y la influencia en el tiempo de residencia útil (tiempo de residencia en la zona del reactor en el que $T > 400^{\circ}\text{C}$) es pequeña como se muestra a continuación.

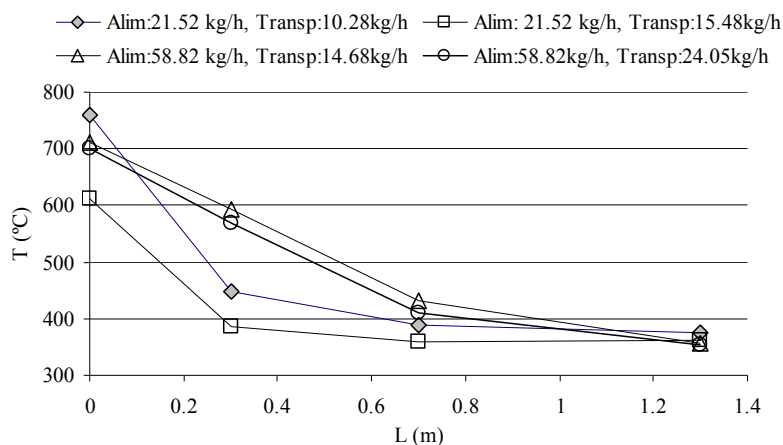


Figura 9: Perfiles de temperatura en el reactor a diferentes flujos transpirables

Tiempo útil de residencia

Si se define la relación de flujo transpirable R , como la relación entre el flujo transpirable y la suma de los flujos de alimentación más aire:

$$R = \frac{\text{Flujo_Transpirable}}{\text{Flujo_Alimentación} + \text{Flujo_O}_2}$$

En la Figura 10 se observa que el tiempo de residencia útil en el reactor es del orden de 20s con una alimentación de 58 kg/h. El aumento del flujo transpirable apenas influye en el tiempo de residencia útil en el reactor.

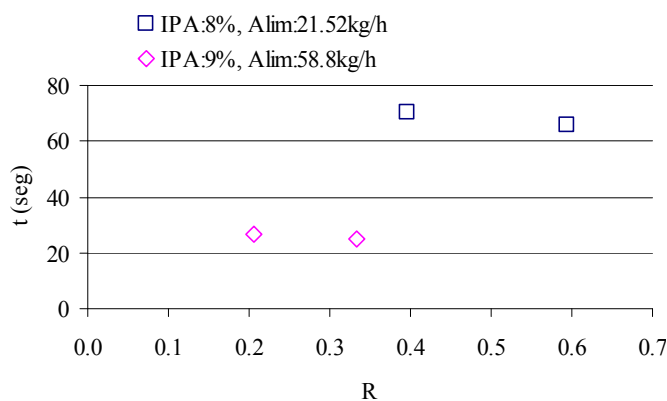


Figura 10: Tiempo de residencia útil en el reactor $T > 400^\circ\text{C}$ para diferentes flujos de alimentación y diferentes relaciones de flujo transpirable

Influencia de la concentración de isopropanol

En la Figura 11 se observa que un cambio de solo un 1% en la concentración de nuestro combustible modelo, isopropanol, puede conducir a cambios dramáticos en la temperatura de reacción. Es importante encontrar el calor de reacción óptimo de la alimentación para cada flujo a tratar.

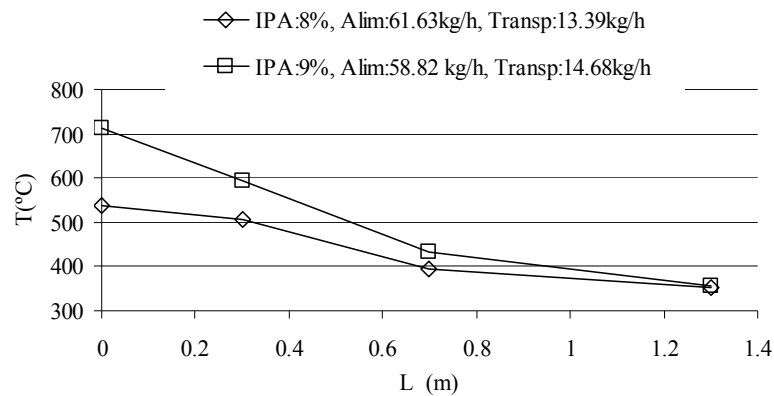


Figura 11: Perfiles de temperatura en el reactor para diferentes tiempos de residencia

Velocidad del frente de llama

En condiciones de 23 MPa y 700 °C los valores de la velocidad del frente de llama son entre 0,1 y 0,01 m/s, mucho menores que las velocidades típicas del frente de llama en la combustión convencional. Estas velocidades son menores que la velocidad en el interior del inyector (3-24 m/s) y de los reactores tubulares, y del mismo orden de magnitud que los de la cámara de reacción (0,04 m/s). Por lo tanto, se espera que la llama se estabilice en la cámara de reacción y no en el inyector, como se ha observado experimentalmente. Con estos valores se puede establecer una regla indicativa para el diseño de reactores de cámara con llamas hidrotermales como fuente de energía, en la que se puede establecer que la velocidad del fluido en el interior de la cámara de reacción debe ser entre 0.1-0.01 m / s, mientras que la velocidad en el inyector debe ser mayor que 1 m/s.

Capítulo 6: Nuevo diseño de reactor de pared enfriada

En los siguientes capítulos se muestran los resultados obtenidos de diversos estudios con un nuevo diseño de reactor de pared enfriada

El reactor diseñado es una modificación del reactor de pared enfriada. Consiste en un inyector tubular por donde se introduce la alimentación y el aire dentro de una cámara de reacción refrigerada vacía, de 2 L. La llama se forma a la salida del inyector. La cámara de reacción está contenida en un recipiente a presión refrigerado con agua limpia que circula entre la cámara de reacción y el recipiente a presión

En la figura 12 se muestra un esquema del nuevo diseño del reactor con una salida y con dos:

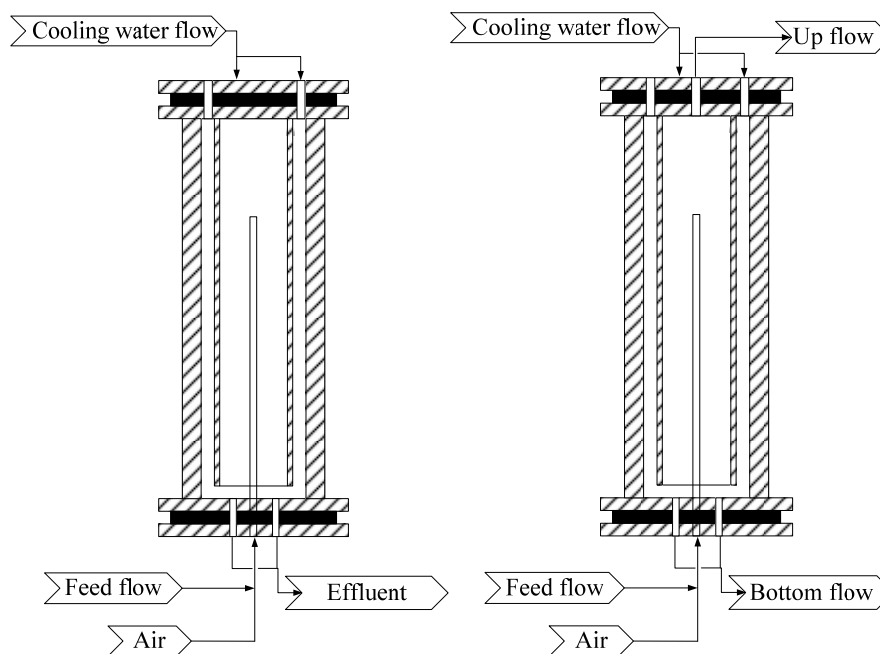


Figura 12: Esquema del nuevo reactor de pared enfriada con una salida y con dos

6.1 Experimentos realizados con inyectores tubulares en una cámara de reacción refrigerada para el estudio de la influencia de la geometría del mezclador en la formación de llamas hidrotermales

Tras el diseño y la instalación del nuevo reactor, se llevaron a cabo los primeros estudios acerca del comportamiento del mismo y la influencia de la posición y geometría de uno de sus componentes principales: el inyector.

Se estudiaron tres tipos de inyectores: 2 de tubo de 1/4" de diferentes longitudes (inyector 1 y 3) y otro de 1/8" (inyector 2) en la misma posición que el inyector 1.

Estudio de la estabilidad de la llama y la eliminación de TOC

La reacción se logró iniciar con facilidad en la gran mayoría de los casos estando el reactor trabajando a régimen estable en tiempos inferiores a 20 minutos desde el momento de iniciar la operación, resultando ser más ágil que otros reactores desarrollados previamente. En cuanto a la eliminación de TOC se han conseguido eliminaciones superiores al 99.95% con efluentes con concentraciones inferiores a 20 ppm en la inmensa mayoría de los casos. En la Figura 13 se muestra la eliminación de TOC y el TOC del efluente en uno de los inyectores evaluados.

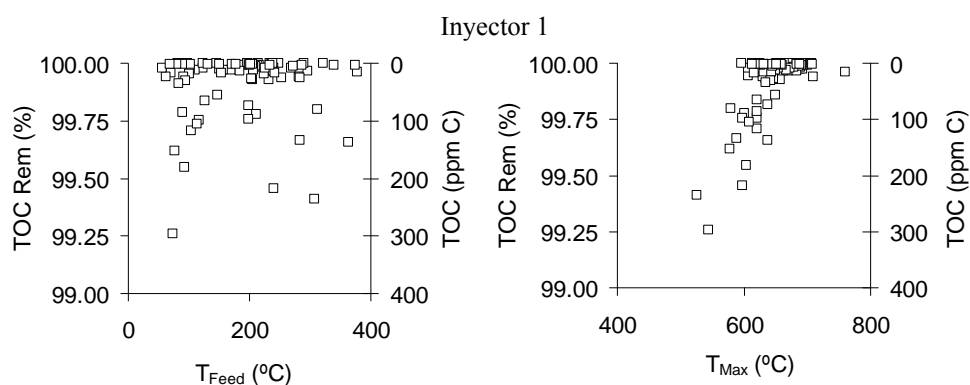


Figura 13: Eliminación de TOC (TOC rem.) y TOC del efluente en función de la temperatura máxima (T_{Max}) y de la temperatura de alimentación (T_{Feed}) para uno de inyectores estudiados

En la Figura 14 se pueden observar las temperaturas máximas de reacción alcanzadas para diferentes concentraciones de IPA a diferentes flujos, para temperaturas de inyección de la alimentación decrecientes, para inyectores de 1/4" y para el inyector de 1/8". Se ha conseguido operar de forma estable con el reactor a temperaturas de inyección bastante por debajo de 100°C consiguiendo similares eliminaciones de TOC a las conseguidas a temperaturas de inyección más altas. Se observa que al disminuir la temperatura de inyección, es necesario aumentar la concentración de isopropanol para aportar a la mezcla de reacción el calor necesario para alcanzar una temperatura de reacción de aproximadamente 650°C

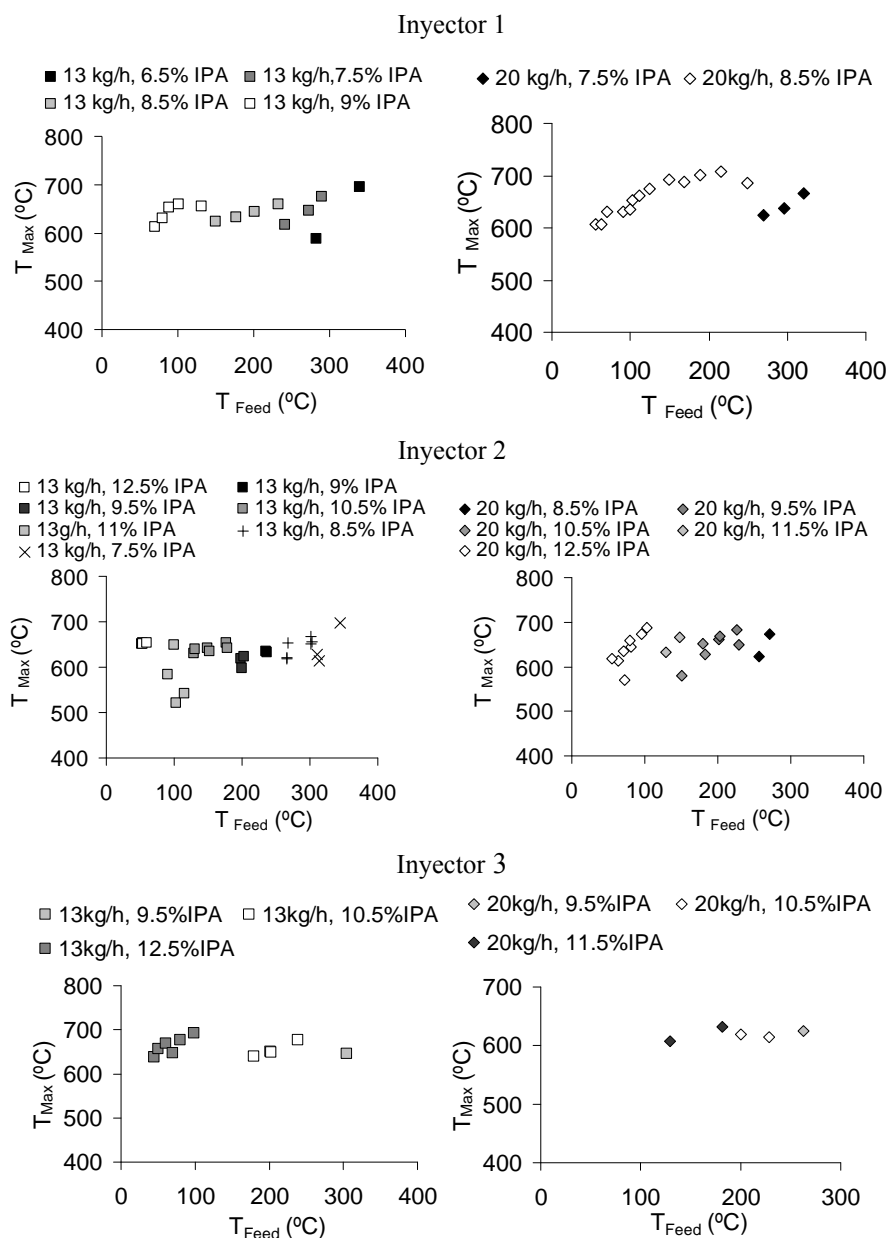


Figura 14: Temperaturas máximas alcanzadas en la cámara de reacción para diferentes concentraciones de isopropanol (IPA) y diferentes flujos de alimentación, para los inyectores estudiados

También se ha podido observar un retroceso de la posición de la llama desde la salida del inyector a medida que disminuye la temperatura de inyección ó la concentración de isopropanol (IPA) ó aumenta la velocidad de salida del mezclador, siendo más acusado en los experimentos realizados con el mezclador de 1/8”.

Influencia de la longitud del mezclador

Para estudiar la influencia de la longitud del mezclador se han representado los perfiles de temperatura obtenidos con los inyectores 1 y 3 de la Figura 15. Se observa que la temperatura máxima se produce cerca de la salida del inyector independientemente de la longitud de éste.

Usar el inyector 3, más corto, tiene la ventaja de que la temperatura máxima de reacción se produce más alejada del techo del reactor, aumentando la vida útil de los materiales.

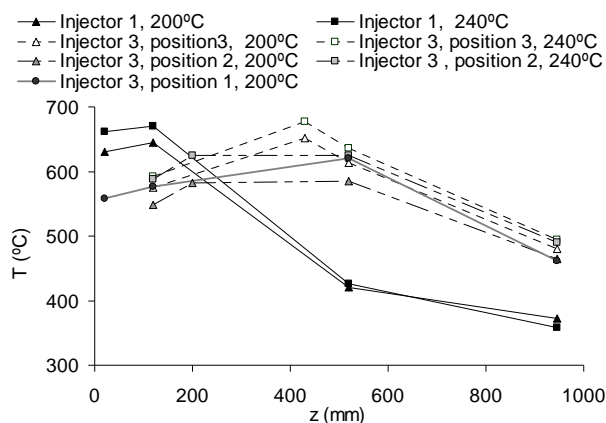


Figura 15: Perfiles de temperatura obtenidos con el inyector 1 de 95 cm (línea sólida), y con el inyector 3 de 55 cm (línea discontinua)

Operación del reactor con sales inorgánicas

Por último se trató el funcionamiento del reactor trabajando con alimentaciones con alto contenido en sales inorgánicas. En general fue posible la operación en régimen estacionario con concentraciones de sales (Na_2SO_4) en la alimentación de hasta el 2.5%. Pudieron introducirse con éxito en el reactor sin que se produjeran taponamientos y la presencia de sales no redujo la eliminación de materia orgánica en las diferentes muestras respecto a lo observado en los experimentos anteriores.

6.2 Destrucción de lodos por medio de una llama hidrotermal. Optimización de las condiciones de destrucción de amoníaco

Operación del reactor con alimentaciones del alto contenido en amonios

Para evaluar la eliminación de amonios en el reactor desarrollado han probado alimentaciones con concentraciones de amoníaco entre el 1% y el 8% usando isopropanol como co-fuel. Un resumen de los resultados se muestra en la Tabla 2. Se observa que la temperatura mínima para mantener la reacción disminuye con la concentración de amoníaco. Pasa de ser 710°C para 8% de NH₃, a 629°C para 3% de NH₃ y 563°C para 1% de NH₃. Incluso a las temperaturas más bajas es posible conseguir eliminaciones de amonios superiores al 99,7% con efluentes con concentraciones menores de 50 ppm, siendo estos resultados sustancialmente mejores a otros resultados anteriores encontrados en bibliografía.

Tabla 2: Resumen resultados de oxidación de alimentaciones con alta concentración de NH₄⁺

C _{0NH3} (%)	T _{Max} (°C)	Exc aire (%)	X _{NH4+} (%)	C _{N nitrico} efluente (ppm)	C _{NH4+} efluente (ppm)
8	787	10	99,91	552	38
8	710	10	99,93	448	32
3	788	5	99,73	702	46
3	752	4	99,77	525	40
3	721	6	99,75	712	44
3	632	3	99,98	97	3
3	629	11	99,74	588	45
1	737	7	99,71	326	23
1	722	5	99,80	257	16
1	672	4	99,90	203	8
1	563	4	99,84	83	13
0,5	626	1	99,60	12	11

No se ha detectado NH₃ o NO_x (límite mínimo de detección 5 ppm y 0,5 ppm respectivamente) en el efluente gaseoso incluso a temperaturas de alimentación de casi 800°C. Por otro lado se puede observar que la formación de nitratos se ve favorecida por las altas concentraciones iniciales de amonios, las altas temperaturas y el exceso de oxidante. Se hicieron estudios con concentraciones menores de amonio de 0.5%, un valor típico de amonios para fangos de depuradora. Los resultados de la influencia de exceso de oxidante para una temperatura de reacción de 670°C se muestran en la Figura 16. Se observa que la proporción de nitrógeno convertido a nitratos disminuye del 2.5%

al 1% al disminuir el exceso de aire del 6% al 2%. La eliminación de amonios no se ve afectada por la reducción del exceso de oxidante.

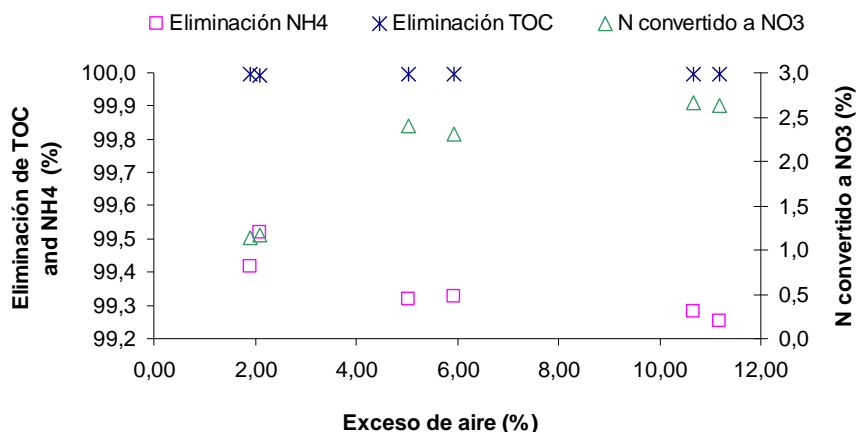


Figura 16: Influencia del exceso de oxidante en la eliminación de TOC y NH_4^+ y en la formación de amonios.

Operación con fango sintético

En la Tabla 3 se muestra un resumen de los resultados de la oxidación de un fango sintético que se preparó mezclando celulosa, amoníaco e isopropanol y café soluble para simular el color del fango. La inyección de la suspensión en el reactor se produjo de forma estable sin que se produjeran taponamientos. Las eliminaciones de materia orgánica obtenidas han sido superiores al 99% y las eliminaciones de amoníaco superiores al 99.3% incluso trabajando a temperaturas de 605°C.

Tabla 3: Resumen de resultados de de la oxidación del fango sintético

Flujo (kg/h)	Exc aire (%)	T_{Max} (°C)	X_{TOC} (%)	$X_{\text{NH}_4^+}$ (%)	$C_{\text{N nitrico efluente}}$ (ppm)	$C_{\text{NH}_4^+ \text{ efluente}}$ (ppm)
13,6	134	6379	99,92	99,57	75	35
13,6	134	641	99,94	99,63	54	31
14,5	13	606	99,90	99,33	15	50
14,5	-2	626	99,93	99,79	32	17

El color del fango sintético también fue eliminado en su totalidad como se muestra en la imagen de la Figura 17.

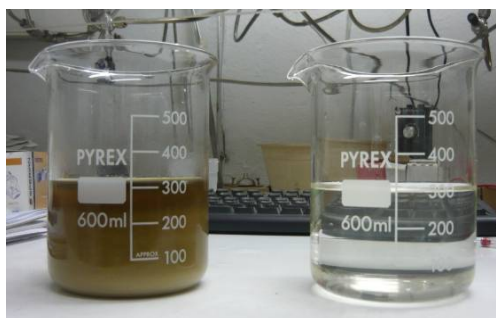


Figura 17: Fango sintético (izquierda) y efluente (derecha)

Operación del reactor con alimentaciones con fango real

Finalmente tras las pruebas con fango sintético se procedió a probar la oxidación en el nuevo reactor de un fango real. En la Tabla 4 se muestran los resultados obtenidos al introducir en el reactor una alimentación cuya composición era de 11% de isopropanol y 22% de un fango real (contenido del 6% en sólidos volátiles).

Tabla 4: Resumen de resultados de de la oxidación del fango sintético

Flujo (kg/h)	Exc aire (%)	T _{Max} (°C)	X _{TOC} (%)	X _{NH4+} (%)	C _N nítrico efluente (ppm)	C _{NH4+} efluente (ppm)
13,6	4	512	99,90	94,46	13	24
13,6	9	518	99,87	94,17	17	25
13,6	6	531	99,82	94,03	21	26
13,6	7	522	99,85	95,37	18	20
13,6	8	531	99,89	95,22	11	20
13,6	11	553	99,85	94,83	14	22
13,6	4	512	99,90	94,46	13	24

Se logró obtener un efluente con concentraciones de carbono orgánico, amoníaco y nitratos por debajo de los límites de vertido. La Figura 18 muestra el perfil de temperaturas durante la operación con el fango real, se puede observar como la temperatura de reacción disminuyó pero se mantuvo la llama encendida de manera que tanto el fango como el isopropanol fueron eliminados sin taponamientos y sin necesidad de precalentar la alimentación ya que ésta se inyectó a temperatura ambiente

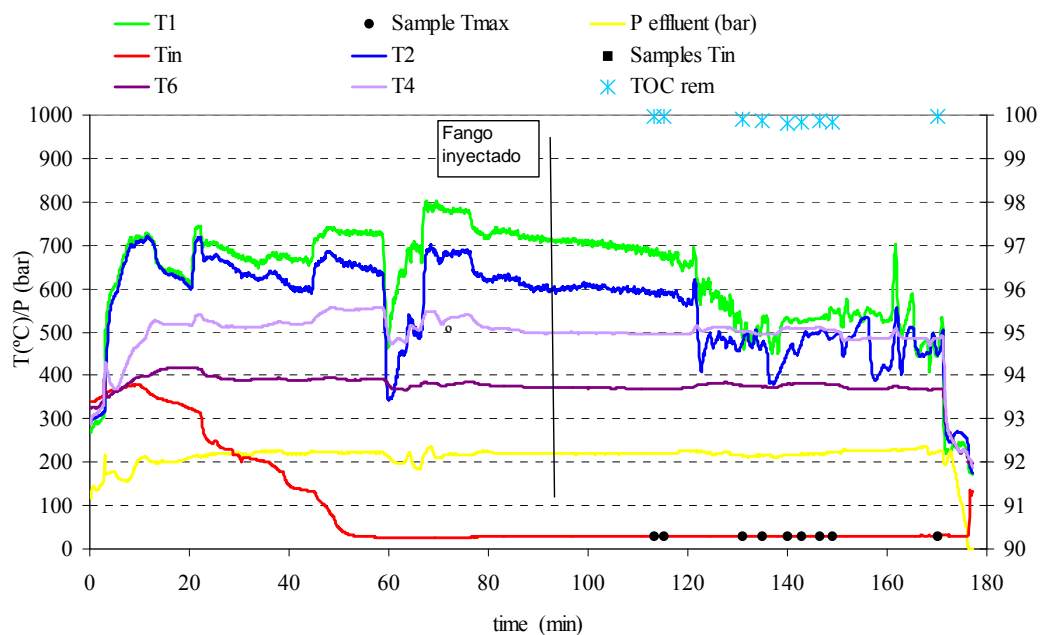


Figura 18: Perfil de temperaturas, presión, eliminaciones de TOC

*Análisis del comportamiento de un reactor de pared enfriada OASC con dos salidas.
Resultados experimentales y estudio energético*

El último trabajo realizado con el nuevo reactor trató de la prueba de una nueva configuración del reactor consistente en la instalación de una nueva salida por la zona superior del reactor manteniendo también la salida inferior, permitiendo obtener dos flujos de productos procedentes del mismo reactor. El flujo superior a temperaturas superior a 600°C y libre de sales minerales y el flujo inferior a temperatura subcrítica y donde se espera que salgan disueltas las sales minerales. Con esta nueva configuración se llevaron a cabo diversas pruebas analizando la influencia de esta nueva salida:

Influencia de la relación de flujo de salida superior e inferior (Flujo salida superior/Flujo salida inferior)

En este estudio se realizaron experimentos variando el flujo de las dos salidas. Como se puede observar en la Figura 21, a medida que el flujo de salida por la salida superior es mayor, la temperatura en el interior del reactor es menor debido a que al estar el inyector más cerca de la salida superior que de la inferior, menor cantidad de los productos calientes bajan a través del reactor.

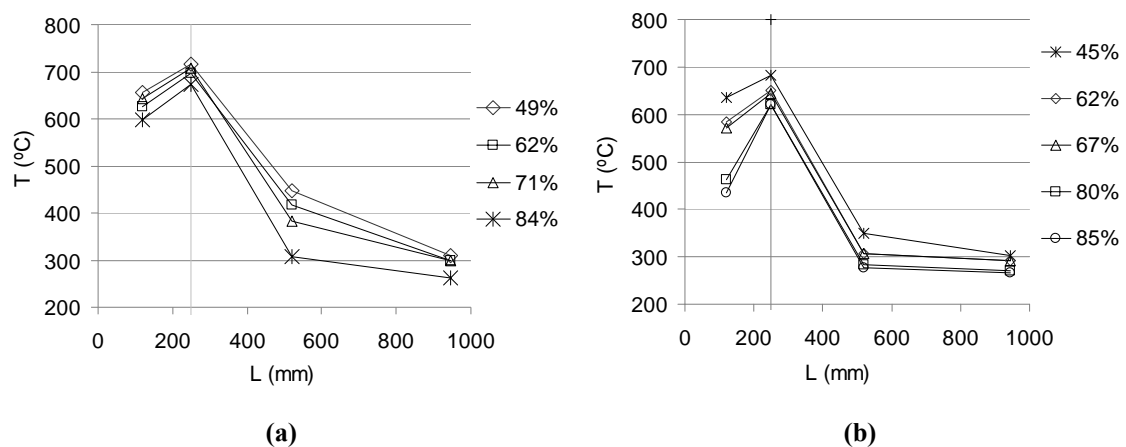


Figura 21a: Perfiles de temperatura para distintas distribuciones de flujo para alimentaciones inyectadas a 20°C,

Figura 21b: Perfiles de temperatura para distintas distribuciones de flujo para alimentaciones inyectadas a 200°C, la línea vertical indica la posición de la salida del inyector

Influencia del flujo de refrigeración

Se observa que con el flujo de refrigeración se cumple una de las sus funciones que es disminuir la temperatura en la cámara de reacción. Al aumentar el flujo de refrigeración, las temperaturas en el interior del reactor disminuyen. El cambio de temperaturas es más notorio en el inferior donde se produce una pequeña acumulación de agua líquida. La Figura 22 muestra los resultados comentados.

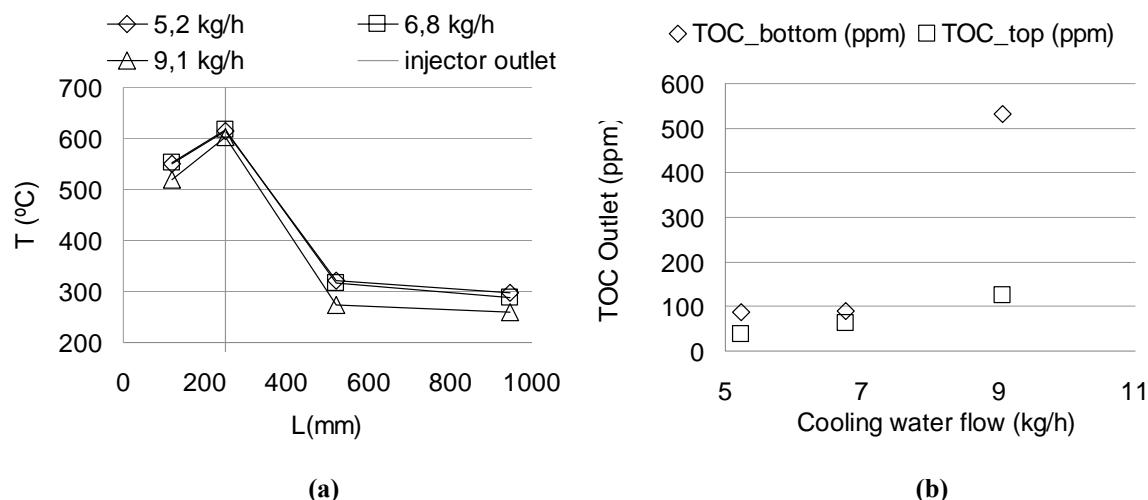


Figura 22 a: Perfiles de temperatura para distintos flujos de agua de enfriamiento. **b:** Valores de TOC de muestras tomadas con los diferentes flujos de agua de enfriamiento de la pared.

Eliminación de amoníaco

Se realizaron una serie de experimentos con diferentes cantidades de isopropanol y de amoníaco en la alimentación para poder de esta manera comparar la eliminación de estas mezclas cuando se trabaja con el reactor con esta nueva configuración o con una sola salida cuyos resultados se encuentran en el apartado anterior (6.2) de este mismo capítulo.

Las eliminaciones obtenidas de TOC y de nitrógeno total con respecto a la temperatura de reacción se muestran en la Gráfica 23 donde se puede observar que se requieren temperaturas cercanas a 700° C para obtener una eliminación superior al 99% de amoníaco. Los resultados reflejan que se produce mayor eliminación en la salida inferior que en la superior, debido a que la cinética de la oxidación de amoníaco es una de las más lentas y ya que según el diseño del reactor, la proximidad del inyector a la salida superior no permite que el tiempo de residencia de los reactivos que salen por dicha salida no sea el suficiente para conseguir la oxidación completa de amoníaco.

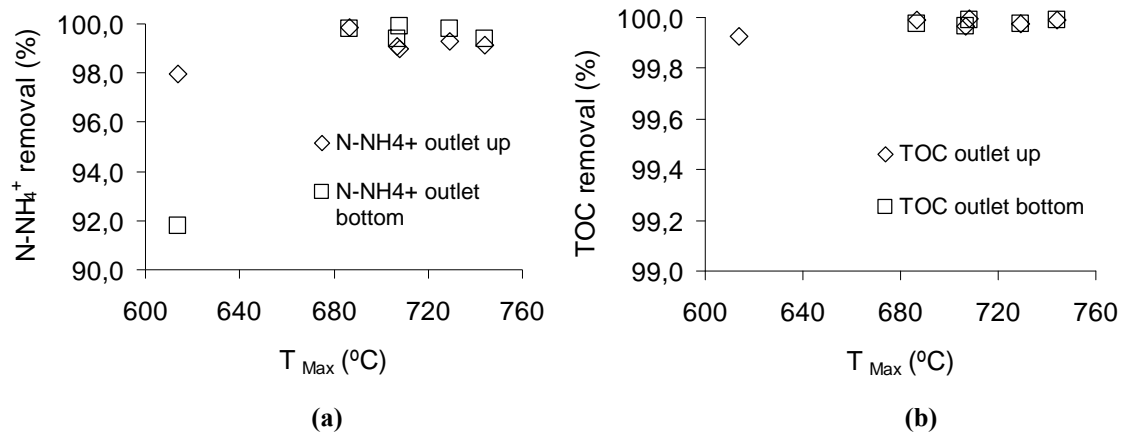


Figura 23a: Eliminación de amoníaco frente a la temperatura máxima registrada en el reactor para alimentaciones con concentraciones de amoníaco entre el 0,5 y 3% y de IPA entre el 9 - 11,5%

Figura 23b: Eliminación de TOC frente a la temperatura máxima registrada en el reactor para alimentaciones con concentraciones de amoníaco entre el 0,5 y 3% y de IPA entre el 9 - 11,5%

Eliminación de alimentaciones con altas concentraciones de sales inorgánicas

Para este estudio inyectaron alimentaciones con Na₂SO₄ concentraciones de hasta 2,5% utilizando con IPA como combustible para obtener temperaturas de reacción de 700°C mientras que los flujos de alimentación se fijaron entre 13-14 kg/h.

Es posible conseguir un flujo libre de sales (concentración de Na₂SO₄ inferior a 0,02% en peso) y a temperaturas superiores a 500°C, disponible para ser expandido en una turbina o para la producción de vapor a alta temperatura que puede ser también expandido en una turbina. La recuperación en la zona inferior del reactor resultó no ser completamente estable debido a la posible formación de agregados de sales.

4. CONCLUSIONES

En esta tesis se han estudiado el desarrollo y escalado de reactores de tanque para la oxidación en agua supercrítica trabajando con una llama hidrotermal como fuente de calor interno, desarrollando un nuevo diseño de reactor de pared enfriada para la oxidación en agua supercrítica capaz de permitir la inyección de alimentaciones a temperatura ambiente, de manejar residuos con cierto contenido en sales inorgánicas y de optimizar el aprovechamiento energético.

En el desarrollo de este equipo se han obtenido las siguientes conclusiones:

- 1) Se ha estudiado la iniciación de llamas hidrotermales en diferentes reactores tubulares, obteniendo que la temperatura de inyección es el parámetro decisivo en la ignición de llamas hidrotermales, siendo necesario temperaturas cercanas a la de ignición de la mezcla.
- 2) Se ha estudiado la iniciación de llamas de compuestos recalcitrantes como ácido acético o amoniaco en reactores tubulares. En el caso de ácido acético, los importantes problemas de corrosión no permitieron trabajar con concentraciones superiores al 4% en masa. En el caso de amoniaco no fue posible la formación de llamas hidrotermales exclusivamente de amoniaco, y siempre fue necesario la presencia de isopropanol como cofuel.
- 3) Aunque se consiguieron eliminaciones de compuestos inflamables del 99% en tiempos de residencia menores de 1 s en presencia de la llama hidrotermal, con compuestos recalcitrantes, como el amoniaco, no fue posible conseguir eliminaciones totales, ni siquiera a temperaturas de 750°C en tiempos de residencia menos de 1 s.
- 4) Se ha probado el comportamiento de un reactor de pared transpirable con llama hidrotermal como fuente de calor interna, con flujos de alimentación de hasta 60 kg/h. Elementos constructivos como la pared transpirable de aleación de níquel sinterizada y los inyectores rellenos de partículas han probado ser poco robustos y se han desechado para el diseño final.

5) Se ha propuesto un método de diseño de reactores basado en la velocidad de frente de llama. La velocidad de frente de llama en condiciones supercríticas se ha estimado entre 0,01 y 0,1 m/s, un orden de magnitud menor que las típicas de las llamas atmosféricas. El método propuesto consiste en diseñar inyectores con velocidades de flujo superiores a las velocidades de frente de llama para evitar la ignición en el inyector y fijar velocidades del orden de las de frente de llama en la cámara de reacción para permitir que la llama permanezca inmóvil en la cámara de reacción permitiendo así la inyección de reactivos a temperatura ambiente en la llama.

6) Se ha estudiado la influencia de los parámetros geométricos en la formación de llamas hidrotermales. La longitud del inyector juega un papel importante ya que la llama se forma justo a la salida del mismo y puede determinar la mayor distancia a las paredes de la cámara de reacción, favoreciendo la conservación de los materiales.

7) Se ha construido y puesto a punto un nuevo diseño de reactor de pared enfriada que consta de los siguientes elementos:

- Inyector tubular
- Cámara de reacción refrigerada, que permite la entrada del agua de enfriamiento por su parte inferior
- Carcasa de presión con una brida inferior y otra superior que permite el fácil ensamblaje y desensamblaje del aparato para su mantenimiento.

El reactor se ha probado en la planta piloto de la Universidad de Valladolid con flujos de alimentación de hasta 23 kg/h, concluyendo que se trata de un equipo de fácil manejo, versátil y robusto.

El nuevo reactor permite la eliminación de carbono orgánico total y de amonio hasta el 99,99% , incluso inyectando la alimentación a temperatura ambiente. Usando el nuevo reactor es posible la inyección de alimentaciones con sales hasta el 2,5% de Na_2SO_4 , obteniendo unas recuperaciones de hasta 20%.

Se ha mejorado la recuperación energética del nuevo reactor, añadiendo al diseño una salida superior para los productos calientes. Trabajando con esta configuración se ha determinado que el óptimo de trabajo se encuentra al recuperar hasta el 70% de la alimentación por la salida superior.

Para mayores fracciones de flujo por la salida superior las eliminaciones de carbono orgánico total son menores. Se ha obtenido una corriente superior a temperaturas mayores de 600°C, con un contenido en sales menor de 20 ppm, apta para su utilización en la producción de energía. La recuperación de sales por la salida inferior ha sido superior al 40%.

Trabajando con compuesto recalcitrantes como el amonio la eliminación de compuestos como el amonio es inferior debido al bajo tiempo de residencia de esta corriente en el reactor

Se ha propuesto y solicitado la patente (PCT/ES2011/070727) de este nuevo diseño de reactor de pared enfriada.

5. REFERENCIAS

- [1] M.D. Bermejo, M.J. Cocero, Supercritical water oxidation: A technical review, *AICHE Journal*, 52 (2006) 3933-3951.
- [2] P. Kritzer, Corrosion in high-temperature and supercritical water and aqueous solutions: A review, *Journal of Supercritical Fluids*, 29 (2004) 1-29.
- [3] E. Asselin, A. Alfantazi, S. Rogak, Thermodynamics of the corrosion of alloy 625 Supercritical water oxidation reactor tubing in ammoniacal sulfate solution, *Corrosion*, 64 (2008) 301-314.
- [4] P. Kritzer, Corrosion in high-temperature and supercritical water and aqueous solutions: a review, *Journal of Supercritical Fluids*, 29 (2004) 1-29.
- [5] M.D. Bermejo, M.J. Cocero, F. Fernandez-Polanco, A process for generating power from the oxidation of coal in supercritical water, *Fuel*, 83 (2004) 195-204.
- [6] B. Veriansyah, T.-J. Park, J.-S. Lim, Y.-W. Lee, Supercritical water oxidation of wastewater from LCD manufacturing process: kinetic and formation of chromium oxide nanoparticles, *Journal of Supercritical Fluids*, 34 (2005) 51-61.
- [7] J.R. Portela, Nebot E., M.d.l.O. E., Kinetic comparison between subcritical and supercritical water oxidation of phenol, *Chemical Engineering Journal*, 81 (2001) 287-299.
- [8] Steven F. Rice, R.R. Steeper, Oxidation rates of common organic compounds in supercritical water, *Journal of Hazardous Materials*, 59 (1998) 261-278.
- [9] J.W. Griffith, D.H. Raymond, The first commercial supercritical water oxidation sludge processing plant, *Waste Management*, 22 (2002) 453-459.
- [10] L. Stenmark, Aqua Critox®: The Chematur engineering AB concept for SCWO, *Proceedings of the Workshop on Supercritical Water Oxidation - Achievements and Challenges in Commercial Applications*, (2001).
- [11] W. Schilling, E.U. Franck, Combustion and diffusion flames at high-pressures to 2000 bar, *Berichte Der Bunsen-Gesellschaft-Physical Chemistry Chemical Physics*, 92 (1988) 631-636.
- [12] M.D. Bermejo, P. Cabeza, J.P.S. Queiroz, C. Jiménez, M.J. Cocero, Analysis of the scale up of a transpiring wall reactor with a hydrothermal flame as a heat source for the supercritical water oxidation, *Journal of Supercritical Fluids*, 56 (2011) 21-32.

- [13] P. Cabeza, M.D. Bermejo, C. Jimenez, M.J. Cocero, Experimental study of the supercritical water oxidation of recalcitrant compounds under hydrothermal flames using tubular reactors, *Water Research*, 45 (2011) 2485-2495.
- [14] L.X.C. Li, P. S. Gloyna, E. F., Generalized kinetic-model for wet oxidation of organic-compounds, *AIChE Journal*, 37 (1991) 1687-1697.
- [15] S.F. Rice, T.B. Hunter, A° .C. Ryde'n, R.G. Hanush, Raman spectroscopic measurement of oxidation in supercritical water. 1. Conversion of methanol to formaldehyde, *Industrial & Engineering Chemistry Research* , 35 (7) (1996) 2161-2171.
- [16] T. Hirth, E.U. Franck, Oxidation and hydrothermolysis of hydrocarbons in supercritical water at high-pressures, *Berichte Der Bunsen-Gesellschaft-Physical Chemistry Chemical Physics*, 97 (1993) 1091-1098.
- [17] G.M. Pohsner, E.U. Franck, Spectra and temperatures of diffusion flames at high-pressures to 1000 bar, *Berichte Der Bunsen-Gesellschaft-Physical Chemistry Chemical Physics*, 98 (1994) 1082-1090.
- [18] A. Sobhy, I.S. Butler, J.A. Kozinski, Selected profiles of high-pressure methanol-air flames in supercritical water, *Proceedings of the Combustion Institute*, 31 (2007) 3369-3376.
- [19] R.R. Steeper, S.F. Rice, M.S. Brown, S.C. Johnston, Methane and methanol diffusion flames in supercritical water, *Journal of Supercritical Fluids*, 5 (1992) 262-268.
- [20] R.M. Serikawa, T. Usui, T. Nishimura, H. Sato, S. Hamada, H. Sekino, Hydrothermal flames in supercritical water oxidation: investigation in a pilot scale continuous reactor, *Fuel*, 81 (2002) 1147-1159.
- [21] M.D. Bermejo, F. Fdez-Polanco, M.J. Cocero, Experimental study of the operational parameters of a transpiring wall reactor for supercritical water oxidation, *Journal of Supercritical Fluids*, 39 (2006) 70-79.
- [22] M.D. Bermejo, F. Fdez-Polanco, M.J. Cocero, Effect of the transpiring wall on the behavior of a supercritical water oxidation reactor: Modeling and experimental results, *Industrial & Engineering Chemistry Research*, 45 (2006) 3438-3446.
- [23] M.D. Bermejo, I. Bielsa, M.J. Cocero, Experimental and theoretical study of the influence of pressure on SCWO, *AIChE Journal*, 52 (2006) 3958-3966.
- [24] M.D. Bermejo, M.J. Cocero, Destruction of an industrial wastewater by supercritical water oxidation in a transpiring wall reactor, *Journal of Hazardous Materials*, 137 (2006) 965-971.

[25] M.D. Bermejo, F. Fernandez-Polanco, M.J. Cocero, Modeling of a transpiring wall reactor for the supercritical water oxidation using simple flow patterns: Comparison to experimental results, *Industrial & Engineering Chemistry Research*, 44 (2005) 3835-3845.

SUMMARY

The supercritical water oxidation (SCWO) is a promising technology for the destruction of wastes, but its commercialization has been delayed by the problems of corrosion and salt deposition associated to this technology and as well for its high energetic consumes. The uses of reactors working with a hydrothermal flame as a heat source contribute to overcome many of the challenges presented by this technology.

Injection of the reagents over an hydrothermal flame can avoid the reagents preheating as the feed can be injected into the reactor at low temperatures, avoiding plugging and corrosion problems in a preheating system. Also the kinetics are much faster allowing complete destructions of the pollutants in residence times lower than 1 s. Next to this the high temperatures associated to the hydrothermal flames contribute to a better energy recovery of the heat released in the reaction for electricity production

Through this thesis, different studies about the process of supercritical water oxidation working with hydrothermal flames were carried out in order to develop a new reactor design for supercritical water oxidation able to inject feeds at room temperature, to work with wastes containing some inorganic salt and to optimize the energetic use

The first step was to study the initiation of the SCWO reaction with concentrated isopropyl alcohol (IPA) solutions, using different tubular reactors at different operational conditions (temperature, fuel concentration and velocity)

It was found that at temperatures lower than 450-500°C, depending on the tubular reactor design, the reaction proceeded slowly, and when reaching higher temperatures a sharp increase in temperature was produced indicating a much faster reaction mechanism. The description of the phenomenon is similar to the ignition of hydrothermal flames described in literature. In these cases TOC removals higher than 99% were reached in residence times as low as 0.4 s. Ignition was not possible injecting feeds at room temperature using tubular reactors.

Using a similar experimental device, the destruction of high concentrations of recalcitrant compounds such as ammonia and an industrial waste containing acetic acid in the presence of a hydrothermal flame were studied using IPA as a co-fuel. For mixtures with acid acetic total elimination of TOC was achieved at temperatures higher than 750°C and in the case of mixtures with ammonia TOC removal were over 99.9% while maximum removals of N-NH_4^+ was never higher than 94%, even for reaction temperatures higher than 710°C

The scaling up of vessel reactors was analyzed using a transpiring wall reactor (TWR) operating with a hydrothermal flame as a heat source. Results of the TWR show that steady operation with a hydrothermal flame inside is possible even when reagents are injected at subcritical conditions. Temperature measurements show that reaction is not initiated in the injector but in the reaction chamber, where fluid velocity is similar to the flame front velocity of a hydrothermal flame that is of the order of 0.1 m/s. In this way a design and scale up method for vessel reactors with a hydrothermal flame inside was developed.

Basing on the results obtained using the TWR, a new reactor design was developed. The new design of cooled wall reactor was designed, constructed, installed and tested successfully in different operating conditions.

This new reactor design makes possible to work with lower injection temperatures than previously tested reactors. Stationary and stable operations were feasible even at room injection temperatures with TOC removal over 99.99% (TOC < 10 ppm) in all operating conditions when working with IPA as model compound. It was possible to work with feeds containing up to 2.5% wt of Na₂SO₄ without plugging, nevertheless low recovery of salt was obtained. The reactor was tested with recalcitrant compounds such as ammonia being able to destroy high concentrations of NH₄⁺ with efficiencies up to 99.99% at temperatures as low as 600°C in residence times of 20 seconds, and finally it was possible the destruction of synthetic and real sludge with TOC removals of 99.95% (TOC < 80 ppm) was possible.

Finally the new reactor design was tested working with a second effluent from the top of the reactor obtaining an effluent at temperatures between 500 and 600°C TOC removal over 99,99% were obtained when the fraction of products leaving the reactor in the upper effluent is lower than 70% of the feed flow. Removals higher than 99% of N-NH₄⁺ are achieved in both effluent. Effluents with 2.5% Na₂SO₄ were injected in the reactor without plugging problems. Average salt recoveries in the lower effluent were of 40% while salt concentration on the upper effluent was as low as 20 ppm. Thus, this top effluent is appropriate for the energy production both by steam generation and expansion in a Rankine cycle or by direct expansion of the effluent.

This new reactor has been presented as an European patent. The reactor is prepared to be tested with real industrial waste in long continuous operational periods.

CHAPTER 1

INTRODUCTION

CHAPTER 1

INTRODUCTION

TABLE OF CONTENTS

1.1. SUPERCRITICAL FLUIDS	39
1.2. SUPERCRITICAL WATER OXIDATION.....	40
1.2.1 Properties of supercritical of water.....	40
1.2.2 Process of Supercritical Water Oxidation	42
1.2.3 Types of reactor for SCWO.....	47
1.2.3.1 Tubular Reactor	47
1.2.3.2 Vessel reactor	48
1.2.3.3 Cooled wall reactor.....	48
1.2.3.4 Transpiring wall Reactor	49
1.2.3.5 Other reactor designs	51
1.2.4 Industrial Applications of SCWO: Current SCWO companies	53
1.2.4.1 SuperWater Solutions	53
1.2.4.2 General atomic	53
1.2.4.3 SuperCritical Fluids International (SCFI)	54
1.2.4.4 Innoveox	55
1.2.4.5 Hanwha Chemical Corporation.....	55
1.2.4.6 SRI International	56
1.2.5 Current status of commercial SCWO plants.....	56
1.2.6 Current status of SCWO research: pilot plants.....	57
1.3. HYDROTHERMAL FLAMES.....	59
1.4. REFERENCES	63

1.1. SUPERCRITICAL FLUIDS

A pure supercritical fluid (SCF) is any compound at a temperature and pressure above its critical values. Above the critical temperature of a compound the pure, gaseous component cannot be liquefied regardless of the pressure applied. The critical pressure is the vapor pressure of the gas at the critical temperature. In the supercritical environment only one phase exists. The fluid, as it is termed, is neither a gas nor a liquid and is best described as intermediate to the two extremes.

The critical point represents the limit of the gas-liquid equilibrium conditions and stability. Mathematically, it is defined as the point at which the first, second and third derivatives of the energy function of a system are aborted: When the temperature remains constant, the derivative of the pressure respect the volume is equal to zero for a pure compound [1].

SFCs share physical properties of gases and liquids. At the critical point two or more fluid phases can coexist, resulting indistinguishable. A supercritical fluid does not have phase changes, so that its physical properties vary continuously with changes of temperature and pressure, showing typical values intermediate between liquids and gases. Depending on the supercritical fluid, its density, solvent power, transport properties (such as viscosity and diffusivity), among others, are closer to the properties of liquids or gases. Significant changes in the values of these properties can be achieved with small variations in pressure, especially when it is near the critical point. The combination of solvent power of a liquid and transport properties of a gas, and the ability to adjust these properties with pressure, makes possible that SCFs would be a good choice for many engineering applications, such as extraction or as substitutes of organic solvents. In the region of gas-liquid transition, it present a combination of properties that make them well suited for development of new process impossible to do with conventional solvents.

Table 1.1: Comparison of physical and transport properties of gases, liquids, and SCFs

Property	Density (kg/m³)	Viscosity (cP)	Diffusivity (mm²/s)
Gas	1	0.01	1-10
SCF	100-800	0.05-0.1	0.01-0.1
Liquid	1000	0.5-1.0	0.001

1.2. SUPERCRITICAL WATER OXIDATION

1.2.1. Properties of supercritical of water

Water offers many favorable properties at elevated temperatures and pressures that make it therefore an excellent solvent and reaction medium for numerous applications. Figure 1.1 shows a P-T-diagram of water at elevated temperatures and pressures, including the critical point at $T_c = 647\text{K}$ and $p_c = 22.1\text{MPa}$.

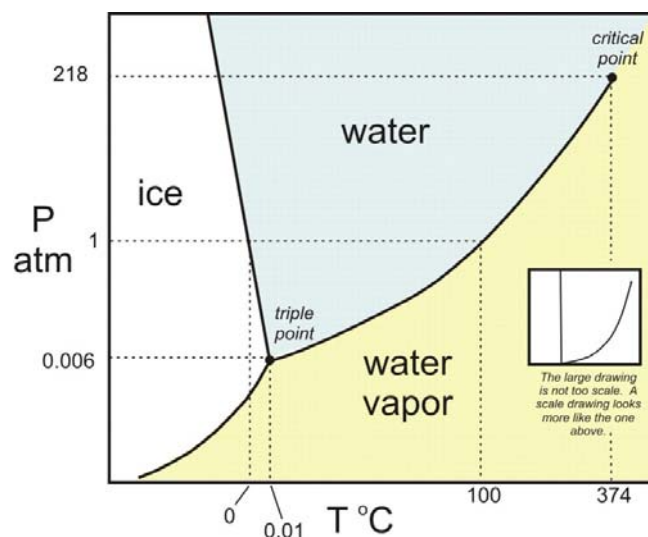


Figure 1.1: P-T diagram of water

In the vicinity of the critical point the thermodynamic properties of water change drastically compared to those of liquid water. The density for example, with a value of 378 kg/m^3 , at the supercritical point, lies in between those of water vapor (1 kg/m^3) and liquid water (1000 kg/m^3). If increasing simultaneously pressure and temperature of a mixture consisting of gas and liquid at equilibrium conditions, the liquid becomes less dense, while the density of the gas increases due to compression. At the critical point both densities are identical and the distinction between gas and liquid disappears. The degree of dissolution at supercritical conditions also differs compared to ambient conditions. An estimation of the solvation power can be obtained by having a look at the dielectric constant and the dissociation constant of water. The dielectric constant is a function of temperature and pressure. Figure 1.2 illustrates a constant drop of the dielectric constant from a value about 78.5 As/Vm at ambient conditions to 6 As/Vm at the critical point [2].

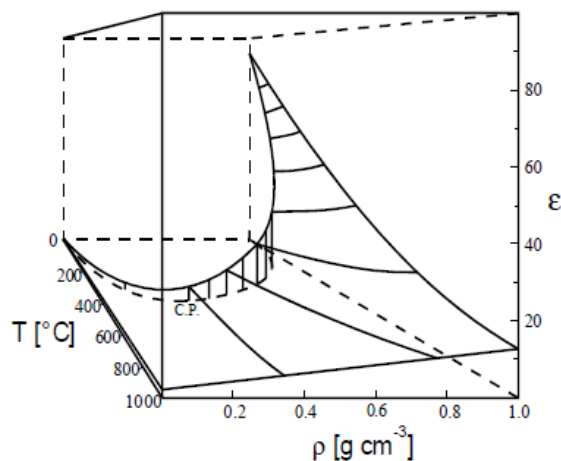


Figure 1.2: Dielectric constant of water[2]

The significant drop in the dielectric strength leads to a considerable increase in the solubility of hydrocarbons in supercritical water. In correlation, the solubility of inorganic salts reduces drastically. Supercritical water acts like a non-polar dense gas with solvation properties equivalent to those of low polar organic solvents.

The dissociation of water leads to the formation of hydronium and hydroxyl ions and determines the pH of pure water. The ionic product changes drastically from ambient to supercritical conditions. Figure 1.3 shows the ionic product of water as a function of pressure and temperature.

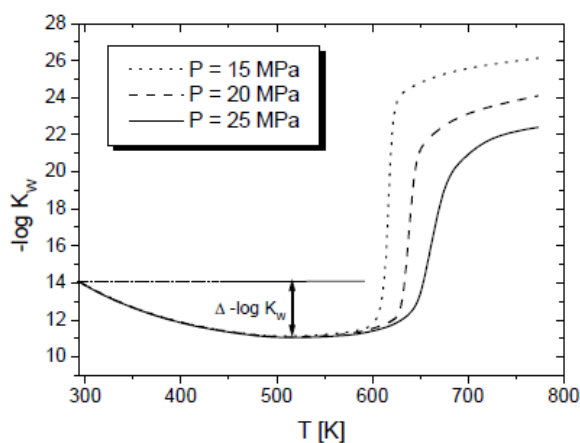


Figure 1.3: Ionic product of water[3]

The ionic product increases from a value of 10^{-14} at ambient conditions to values of about 10^{-11} at 300°C to drop to values of 10^{-18} at the critical point and up to 10^{-23} at supercritical conditions [3]. These physical properties are the reason to consider supercritical water as an ideal media for the oxidation of organic compounds. The reaction takes place in a single phase, avoiding interfacial mass transfer resistances.

1.2.2. Process of Supercritical Water Oxidation

The process known as supercritical water oxidation (SCWO) or hydrothermal oxidation (HTO) consists of the homogeneous oxidation of chemical compounds in an aqueous medium using air, oxygen or hydrogen peroxide as oxidizing agent, at temperatures and pressures above the critical point of water (374°C and 22.4 MPa).

At SCWO conditions, pollutants are totally mineralized, Organic compounds are oxidized to CO₂ and water, nitrogen passes N₂ and the other heteroatoms are oxidized to oxides or salts in high oxidation states.

The most common application of SCWO is the destruction of organic wastes (sewage and sludge, especially those containing recalcitrant xenobiotics and non-biodegradable pollutants). Consequently, the SCWO competes with other processes such as wet air oxidation (WAO) and incineration.

From an environmental perspective, this process achieves complete removal of oxidizable matter. With suitable temperatures, pressures and residence times, almost any contaminant reaction can be completely destroyed, with residence times less than one minute.

Until now, SCWO has been used in order to oxidize various pollutants such as pesticides, organic compounds such as ammonia or inorganic cyanides, being converted to CO₂, water and N₂, and observing no partial oxidation products such as dioxin, NO_x or CO. Thus, the resultant effluents comply with environmental regulations and may be available without secondary process [4].

From the perspective of sustainability, studies show that SCWO is favorable compared to other processes such as WAO and incineration [5]. Companies involved in developing the SCWO process present favorable economic balances with the use of this process [6] [7].

Technically, the SCWO has the advantage of simple, fast and homogeneous reactions without mass transfer limitations. It also has some limitations related to extreme operating conditions and their effect on the materials equipment. These must be overcome before the widespread industrial use of the process. Therefore, the main challenges of SCWO are corrosion and deposition of salts, which are being resolved by the use of special construction materials and the development of new reactor designs able to soften the conditions that the materials must resist [8].

Some industrial applications of SCWO that have been developed have been the oxidation of sludge [6] or the destruction of chemical weapons [9]. To develop new industrial applications of supercritical water, research should focus on developing equipment that resists the operating conditions, also trying to reduce costs. This way, it could allow the joint of advantages in respect to the environmental benefits with the economic viability of the process [10].

There are many specific variations of the flow chart of the main process, depending on the application, but all have the same basic steps. The SCWO takes place in four steps:

- 1 Feed preparation and pressurization
- 2 Reaction
- 3 Salt separation
- 4 Depressurization and heat recovery.

Due to the fact of there is high energy consume at the pressurizing and preheating of reactants, The energy integration of the process with true use of the product streams to preheat or produce energy [11]. Figure 1.4 shows a general diagram of the SCWO process.

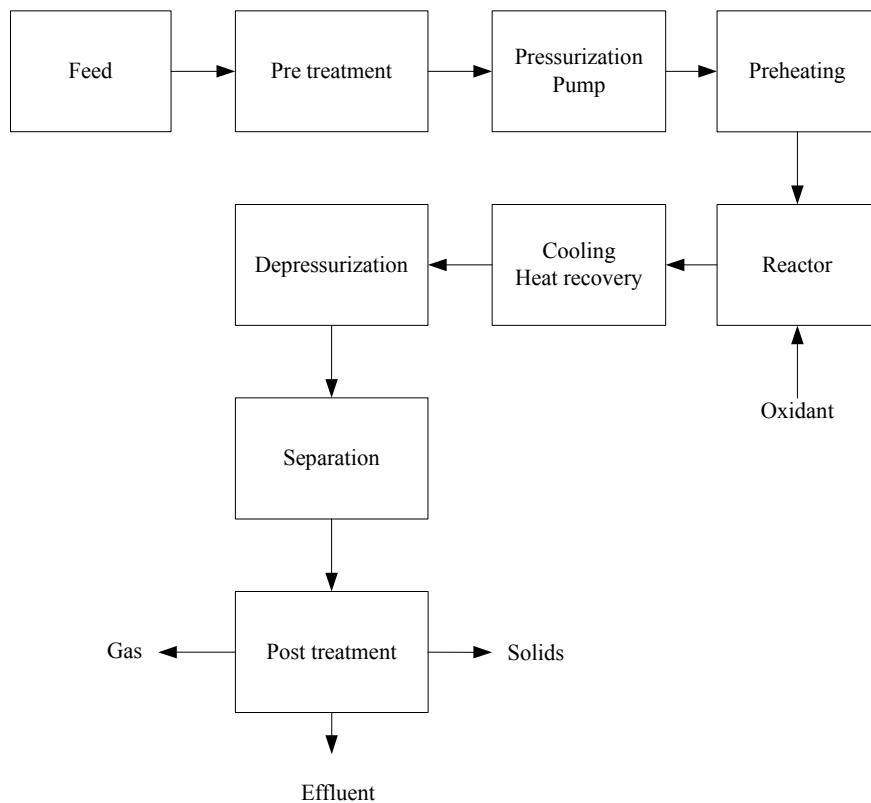


Figure 1.4: General diagram of the SCWO process

Feed preparation and pressurization

The feed flow of the supercritical water oxidation process consists of the wastewater and the oxidant stream. The efficiency of the process is independent of the chosen oxidant [12], as there can be used: liquid oxygen, air or hydrogen peroxide and therefore the election depends on economic factors. Using liquid oxygen increases the raw material costs, but results in lower costs for compression, compared to those for air on equivalent oxygen basis. The use of hydrogen peroxide may be considered in bench-scale applications, but would result in very high costs in industrial scale.

The wastewater or sludge stream is pressurized up to working pressure ($P > 22.1$ MPa) and fed into the reactor. Feed streams with high organic load can be diluted with water or mixed with streams of lower organic load to stay inside the limits of the process (upper oxidation temperature limited to 700 - 750°C). The feed flow can be preheated by means of a heat exchanger using the heat of the effluent leaving the reactor.

Reaction

As oxidant can be used oxygen or air, although it is also common hydrogen peroxide, (especially at laboratory scale due its price is higher for a bigger plants purpose), and nitrate salts, when there are special conditions [1] [12].

The choice depends mainly on economic factors. Pure oxygen is the simplest, but requires added expensive cost of transporting and storing cryogenic liquid. On the other hand, the use of air requires air compressors and also requires bigger reactors due to the significant amount of nitrogen (contained in the air) that has to pass through the system.

Once compressed, the oxidant may be added to feed before reaching the reactor or directly into the reactor. These substances are added so that the control of the reactor conditions is improved. For example, kerosene is used as auxiliary fuel, which keeps the temperature in the reactor with a low calorific waste or a stream of water that lends the maintenance of the reactor temperature or the addition of bases which neutralizes the acids formed during the oxidation.

Salt separation

Because of the low salt solubility of water at supercritical state, Solid particles (both precipitated sticky salts and nonstick solids completely insoluble in SCW) are present in SCWO processes.

These particles can cause equipment fouling, plugging, and erosion. Nevertheless, the low solubility of salts in supercritical water allows them, in theory, to be removed by a solid–fluid separation, for instance, by means of hydrocyclons or filtration systems, making possible the recovery of valuable products. Micro filtration systems are appropriated when a high purity on the filtrate is necessary, although it presents disadvantages such as mechanical placement, corrosion, erosion, fouling, and process control.[13] All these methods of recovering solids at the outlet of the reactor are effective only when the solids do not tend to stick to the wall of the reactor. This can happen if the solids are not sticky or if a system for removing the solids from the walls is implemented in the reactor (such as transpiring wall reactor).

Depressurization and heat recovery

The product stream, after leaving the reactor, is cooled, and finally depressurized, these steps can be done also in reverse way. The product flows through a heat exchanger, decreasing its temperature. For dilute aqueous wastes, with low heat of reaction, it is possible to use the heat content of the products to preheat the waste up to the operation conditions, using a heat exchanger. The minimum organic matter content necessary depends on the heat exchanged.

The effluent produced can preheat the feed from room temperature to the required injection temperature, or can be expanded in a turbine producing electricity that can be used to supply the energy requirements of the plant. [11].

To decompress the product stream a pressure control valve or capillary tubes can be used, in one or more stages, with the total flow of effluent or with gas and liquid phases separated, in the case that the separation is carried out before the complete decompression. If the effluent has high concentration of solids, pressure reducing components can be damaged. To avoid this, It can be used a decompression system especially designed for this type of fluids.

On a larger scale system, heat recovery may be carried out by direct expansion of the reaction products with a supercritical steam turbine. A system of this type could produce large amounts of energy. Such a system would be capable of generating a significant power in excess of that required for air compression, or oxygen and feed pumping [14].

Separation

The phase separation is performed after the depressurization, but can also occur at high pressure. When conditions change from supercritical to subcritical, gaseous products (mainly CO₂, N₂ and O₂) contained in the gas flow can be separated from the liquid flow by a single separator or a flash device. Depending on the number of existing depressurization steps there can be more than one gas-liquid separation.

The vapor phase is emitted directly to atmosphere or to a ventilation system or sent to a system to recovery the CO₂.

When the feed has little amount of solids, liquid effluent generally has an aspect similar to mineral water, also may occur as a brine (ie, high concentration of dissolved salt) or sludge (ie, high concentration of suspended solids).

Operational Problems: corrosion in SCWO systems

The two main difficulties of the process are corrosion and solids handling. They take place when the organic compounds treated contain heteroatoms. Acids formed from the degradation of these substances are aggressive to the system, especially in the temperature range from 250 to 350°C, normally in the heating and cooling area, where there are still subcritical conditions, and particularly, the dissociation constant of water is at its maximum. When the temperature is supercritical no dissociation of acids occurs in their corresponding ions, which can cause corrosion. Also, this phenomenon can occur when are injected dense or molten salt solutions.

At room temperature the corrosion process is controlled by the kinetics of the oxidation of materials. In contrast, the corrosion at high temperatures is controlled by the process of dissolution of the protective oxide layer which contains metal.

When temperatures are higher than 600-700 °C it has to be taken in account other corrosion mechanism: corrosion at high temperature, also called creeping. Under these conditions, metals such as iron, nickel and chromium create volatile corrosion products, being removed from the metal surface or melted fast on the wall, which generates a fast corrosion.

Respect to the construction materials of these reactors, most employ alloys with high content of nickel, Inconel or Hastelloy for their components and also for the pipes under supercritical conditions.[15] These alloys are more resistant to corrosion and temperature compared with carbon steel or stainless steel [16]. Also, when temperatures are below 400 °C, titanium should be used when the feed contains high concentrations of chlorides.[17, 18]

1.2.3. Types of reactors for SCWO

SCWO can be carried out in different reactor types. It is important to note that depending on the design of the reactor main problems of this process, corrosion and deposition of salts, can be avoided in greater or less way.

The main classification of reactors was developed by Shmieder and Abeln [19], which classified them by tubular reactors, vessel reactors, transpiring wall and cooled wall.

1.2.3.1 Tubular Reactor

The tubular reactor is the simplest design of existing ones, and therefore, the most used. It is mainly used for testing in small laboratory plants new applications of SCWO [20, 21], to obtain kinetic parameters and reaction heats. [22-25]. In addition most big and industrial plants constructed so far uses this kind of reactor [7] [26]

The main disadvantages of these reactors are easy plugging due to precipitation of salts and the possible formation of hot spots when uncontrollable exothermic reactions are produced at high speeds.

In this type of reactor the effects of pressure and temperature can not be isolated, this way tubular reactors are generally expensive and heavy due to the needs of a

considerable thickness reactor wall and expensive material (such a niquel alloys) to make it possible to resist the high temperatures and pressures present inside the reactor. The diameters of the tubular reactors have to be small enough for obtaining a high speed of the circulating fluid in order to prevent the deposition of salts. Even that, the precipitated salts can stick to the reactor walls.

In cases where the concentration of organic matter in the feed is considerably high, there is even greater possibility of existence of hot spots within the reactor. To avoid this, multi-injection systems, incorporating air, cooling water or cold feed at different points along the reactor are used, as shown in figure 1.5.

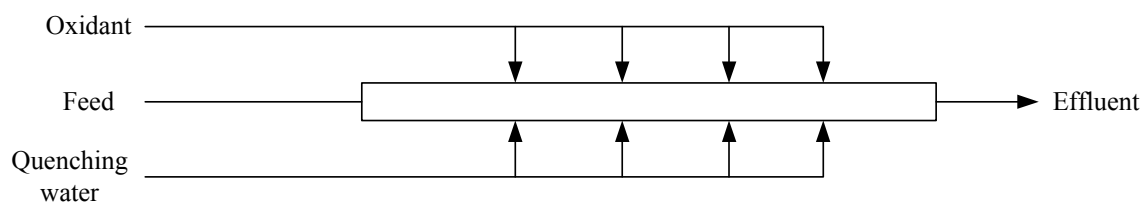


Figure 1.5: Tubular reactor with multiple injections

In industrial applications AquaCritox ® and AQUACAT ® they solve the problems of plugging by using reactors in parallel: when one is in operation, the other is in the cleanup phase.

1.2.3.2 MODAR vessel reactor

The vessel reactor consists of a container in which two zones can be distinguished: the upper zone, at high temperature reaction, and the lower zone, at low temperature (in subcritical conditions) where the salts are dissolved. A film of water falling down the wall prevents the deposition of salts on the computer [10]. Can see the outline of this reactor in figure 1.6 [27]

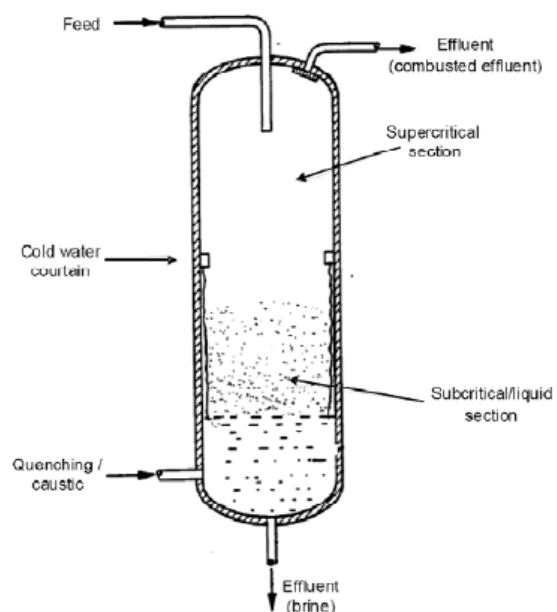


Figure 1.6: MODAR vessel reactor

1.2.3.3 Cooled wall reactor

The cooled wall reactor has a design that makes it available the independence of the effects of temperature and pressure in the SCWO. The external wall which keeps the pressure, is maintained at about 400 °C by the action of a cooling water flow pumped downward between the external and internal walls, it can be constructed of stainless steel because it does not suffer oxidizing atmosphere and high temperatures. The internal wall, also called reaction chamber, is where the reactants are mixed and takes place the oxidation reaction. It is built with a special material capable of resist the oxidizing atmosphere at temperatures up to 800 °C.

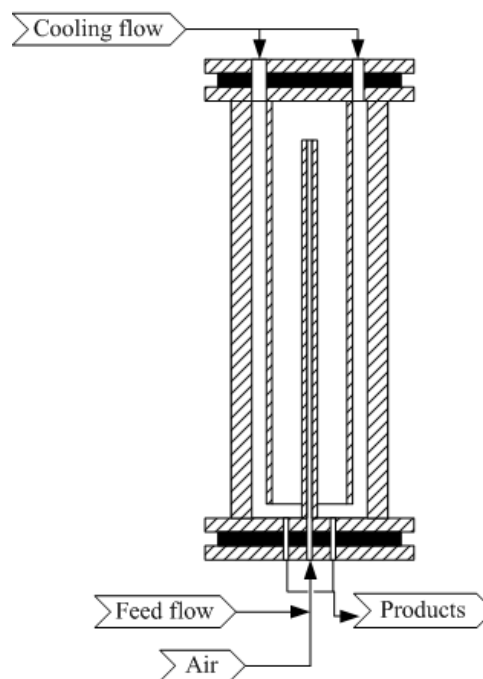


Figure 1.7: Example of cooled wall reactor

1.2.3.4 Transpiring wall Reactor

The transpiring wall reactor (TWR) consists of a reaction chamber surrounded by a wall through which clean water circulates for cooling and protection, avoiding the action of corrosive agents, salt deposition and high temperatures.

There are different types of transpiring wall reactors, the main and common element in all of them is a porous wall, a porous tube which constitutes the reaction chamber, made of sintered metal or ceramic.

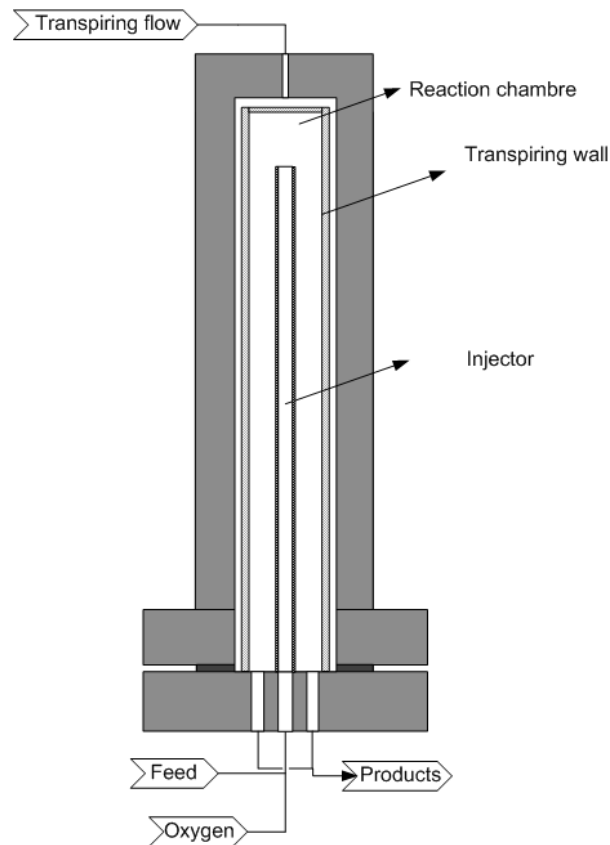


Figure 1.8: Example of cooled wall reactor

The main disadvantage to be considered for the TWR is the heat recovery. Hot products introduced are cooled and diluted by mixing with the cold water that transpires through the wall. Heat recovery is not as good as it could be suppose because the water used to dissolve the salts as much as possible has to be at temperatures below the critical point. So the outlet temperature of the products is not high enough for a good heat recovery [28].

With regard to the operational results, the data obtained with this kind of reactors have been successful in contaminants removal. The biggest problem is the recovery of existing salts introduced with the feed, although the problem of plugging is improved. [29]

Alternative designs have been developed, as proposed by Ahluwalia [30, 31] consisting of a concentric plate reactor being the reaction zone an intermediate annular section between them, Bermejo et al. [32] have carried out and extensive research for the development of TWR (Figure 1.8).

1.2.3.5 Other reactor designs

Reactor tank reverse flow with a brine pool

This type of reactor consists of an elongated cylinder, closed at its ends, which constitutes the inner reaction chamber. Inside there are two different zones: an upper zone at supercritical temperature, and a lower zone temperature subcritical. The oxidation reaction takes place in the zone in which supercritical conditions are achieved.

Cause inorganic salts or other dense material introduced with the feed or formed by chemical reactions are insoluble in supercritical fluids they precipitate to the subcritical zone where they are dissolved in the brine pool. Furthermore, to avoid the deposition of these substances inside the wall reactor, it has a water film which covers the wall.

MODAR Inc. (Natick, MA) developed and patented [33] the first reactor of this type. An application of that is the commercial plant Nittetsu (Japan), for the destruction of waste from the manufacture of semiconductors (63 kg/h of capacity) [34]. Stone and Webster designed a compact automated plant to keep on board [35], using also this design of reactor

Fluidized bed reactor

Developed by SRI International, this reactor consists of a variation of the SCWO process that uses a bed of fluidized solids functioning as both reactant and adsorptive surface for salt control. The process is referred to as "assisted hydrothermal oxidation" (AHO), and works at lower temperatures and pressures than the conventional SCWO process (T 380–420°C and $P < 22.1$ MPa).[34]

Reverse-flow tubular reactor

Patented by Abitibi-Price, the inverse tubular flow reactor consists on a tube which only differ in two thermal zones, so that the process fluid can be fed in both directions. Thus, when the reagents flow through the interior of the reactor, it can redissolve salts layer formed when the reactor was operating in the reverse direction (when the inlet was the outlet and vice versa) [34].

Double-walled tank reactor:

This design of a stirred reactor has a double titanium wall, through which prevents corrosion and a mechanical stirrer which provides a turbulent flow, preventing the precipitation of salts and favoring heat transmission, It was developed by the CEA (Commissariat à l'Énergie Atomique, Commission for Atomic Energy, France). [36].

Process SUWOX:

The reactor employed for the process SUWOX consists on a cooled wall reactor , with its two corresponding chambers: the external chamber where a pressurized water flows, and the internal chamber where the reaction takes place at 420 - 490 °C and pressures above 70.0 MPa. This way it is achieved a high enough density to maintain the salts dissolved (Figure 1.9).

It was developed after the creation of a process in the IKET (Institut für Kern-und Energietechnik, Institute of Nuclear and Energetic Technology, Karlsruhe) and FZK (Focusing Zentrum Karlsruhe, Germany) [37, 38].

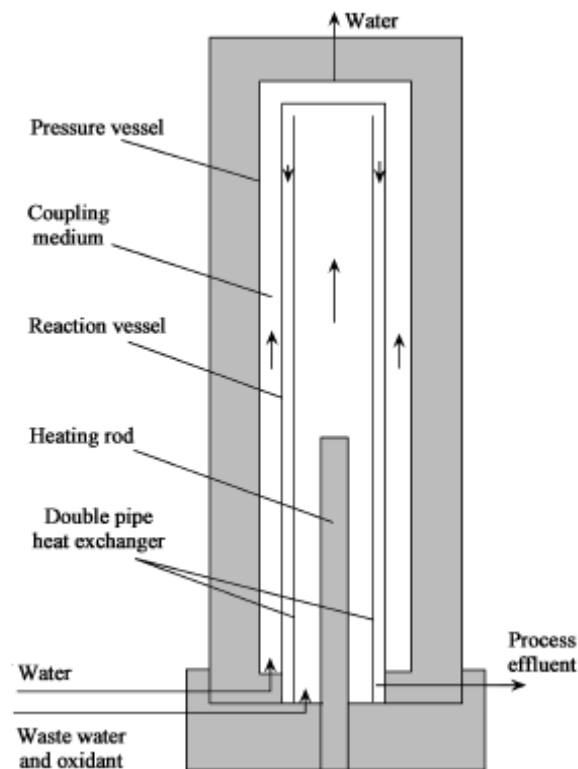


Figure 1.9: SUWOX reactor [38]

1.2.4. Industrial Applications of SCWO: Current SCWO companies

Here is presented a summary of some actual companies which work with SCWO technology.

1.2.4.1 SuperWater Solutions [39]

Co-founded by Dr Michael Modell,, SuperWater started in 2006 in Wellington (Florida). Its main work has been focused on the treatment of non-corrosive sludge. Working with systems based on similar designs of Modell's previous company, MODEC, SuperWater Solutions features a tubular reactor system with a mechanical brushes for control/removal of salts/solids accumulation [40]. Currently a full scale SCWO plant for sludge oxidation with a capacity of 5 t/day in dry basis, is in trials since 2009 in Iron Bridge Regional Water Treatment Facility (Florida, USA), since February 2011 is operating with sludge [41].

1.2.4.2 General atomic [42]

Created in San Diego, General Atomic (GA) has the longest tenure in SCWO of all active SCWO companies (The subdivision of SCWO was created in 1991).

GA has typically utilized a vessel type reactor design and has had extensive experience with several different methods for controlling corrosion and salt precipitation / accumulation, such as the use of liners, coatings, feed additives, and mechanical scrapers [9, 10].



Figure 1.10: SCWO reactor of Bluegrass Chemical Agent Pilot Plant System (GA) [42]

A number of SCWO systems have been or are being built and delivered. Most of GA's work has been for government / military entities but they have also worked with industrial clients as well:

A system to treat pink and red water from TNT operations was provided to DAC for a facility in Korea (Korea System, 4,5 L/min). A system to treat hazardous wastes and sewage sludge was provided to partner commercial companies in Japan for evaluation in the Japanese hazardous waste destruction market. (Japan System). The Bluegrass chemical munitions demilitarization plant will use SCWO systems to destroy hydrolysate from chemical agent and energetic neutralization operations (BGCAPP System).

A simplified SCWO system utilizing over 20 years of development experience is being supplied to Tooele Army Depot (TEAD System) for destruction of energetic hydrolysate from the CAD demilitarization plant (11,4 L/min). The Bluegrass Army Depot will use SCWO to destroy hydrolysate from the hydrolysis of excess explosives and propellants (BGAD System with a capacity of 38 L/min).

1.2.4.3 SuperCritical Fluids International (SCFI) [43]

The origin of SCFI is based on the company Chematur:

In 1995 the Swedish company Chematur AB bought a license for the EWT (Eco Waste Technologies) SCWO process in Europe and then in 1999 it bought the worldwide rights to EWT SCWO, finally, Chematur developed their version of SCWO process under the name Aquacritox®. In 2007, Chematur sold their supercritical fluids division and equipment to SCFI after developed and named different customized versions of the Aquacritox® process in collaboration with various clients, this way, SCFI was founded in 2007 to commercialize AquaCritox® in the industrial and municipal market.

SCFI utilizes a tubular reactor design and has chosen to focus primarily on sewage sludge and digestate feed applications [44]

SCFI has installed one of their models: the Aqua Critox® A10, in the European Validation Centre (EVC) in Ringaskiddy, Cork, Ireland. The Aquacritox A10 has been used to process waste streams that include precious metal catalysts, municipal sewage and drinking water sludge and high strength pharmaceutical waste streams.



Figure 1.11: AquaCritox's sewage-to-energy demonstration plant in Cork, Ireland [43]

1.2.4.4 Innoveox [45]

Paris-based Innoveox has exclusive global rights to the version of SCWO developed and patented by Cansell's group at CNRS in France.

The special point of Innoveox's SCWO design is the use of multiple injection points for oxidant along the length of its tubular reactor. This is done in order to control the temperature for greatest reaction efficiencies and to avoid thermal losses.

Innoveox's focus and business model is based on providing waste treatment as a service at a customer's site rather than just designing and selling SCWO equipment [46]. In addition to the SCWO system already in operation at Arthez-de-Béarn,

1.2.4.5 Hanwha Chemical Corporation.

Created in Seoul, South Korea, they have been working with supercritical water-based technologies since 1994. Hanwha Chemical Corporation is one of the most versatile companies involved with hydrothermal technologies.

They have utilized both vessel and tubular reactor types in their systems and have several pilot scale systems on which they have performed testing of various feeds by hydrothermal treatment.

About their work in SCWO process, they have built two full-scale SCWO plants; a 2000 kg/h system for dinitrotoluene (DNT) wastewater and a 5500 kg/h system for terephthalic acid (TPA) wastewater [47]. Both of these plants are no longer operating [48].

1.2.4.6 SRI International

Located in Menlo Park The scientific research institute SRI International developed the AHO version of SCWO. This is the technology that is being utilized in the full-scale facility built for JESCO and currently in operation in Tokyo Japan for destruction of PCBs, (described later in current commercial SCWO plants).

1.2.5. Current status of commercial SCWO plants

Despite of all these companies involved in the SCWO business, nowadays only two commercial SCWO plants are in operation and one else is being building nowadays.

The first plant currently in operation was built in Tokyo by Mitsubishi Heavy Industries utilizing the Advanced Hydrothermal Oxidation (AHO) variation of SCWO that was developed by SRI International [49]. It was built for the Japan Environmental Safety Corporation (JESCO), an agency of the Japanese government.

The plant has a capacity of 2000 kg/day of PCBs and 100,000 kg/day of water. The reactor used is a fluidized bed vessel. Operating conditions are typically in the range of 370-400°C (just hot enough to keep the fluidizing salt in the solid phase) and 265 bar. The Tokyo plant has a second tubular reactor to ensure adequate destruction [50]. This plant has been in operation since November 2005.

The second commercial SCWO plant currently in operation was built by Innoveox and is located in Arthez-de-Béarn in southwestern France [51].

The system was built for a private customer to process hazardous industrial waste at a relatively low capacity of 100 kg/hr. The system utilizes a tubular reactor with oxygen injected at multiple points

Operating conditions range from 250-550°C (increasing down the length of the reactor due to the multiple oxygen injections) and 265 bar. Feed composition is limited to < 1 g/L chloride and < 10 g/L salt. This system has been in operation since June 2011. [48]

Finally, SCFI is currently building their first commercial system (2500 kg/h) for the waste treatment and recycling firm Eras Eco in Youghal, Ireland [48] This system will include the option of power generation from the process effluent heat via a waste heat boiler and turbine.

1.2.6. Current status of SCWO research: pilot plants

Outside the commercial point of view, there are several actual non-commercial pilot or demonstration-scale plants of SCWO in use owned mostly by university research groups them primarily for research and development work:

Donghai Xu et al [52] have developed the first SCWO pilot scale plant in China for the treatment of sludge with a maximum capacity of 125 kg/h.

A reverse flow tank reactor configuration and a porous transpiring wall are combined to design a novel TWM reactor (Transpiring Wall reactor and MODAR reactor), which aims to overcome reactor corrosion and plugging problems.

V.I. Anikeev et al[53], developed a pilot stationary installation for supercritical water oxidation of organic compounds, first created in Russia. The design output capacity of this installation is 40–60 kg/h and the reactor of the installation was fabricated from a VT-9 titanium alloy in the form of a tube (tubular reactor)

Kim et al designed and manufactured a pilot plant with the capacity of 30 kg/h at Hanwha Chemical R&D centre in the Republic of Korea. The plant can work with a tubular reactor [54, 55] or with a vessel reactor [56]



Figure 1.12: Picture of pilot plant at Hanwha Chemical R&D centre [56]

Also in China, Fengming Zhang et al [57] designed and manufactured a SCWO pilot plant with a transpiring wall reactor with a capacity of 25 kg/h successfully operated in Shandong University of China

In the university of Cadiz (Spain), the group of Food Technology and Environmental Technologies designed a pilot plant to treat up to 25 kg/h working with a tubular reactor [58, 59], they have also collaborated in the develop of a pilot plant of 100 kg/h owned by EMASESA and BEFESA for the treatment of sludge with a tubular reactor [60].



Figure 1.13: Image of the pilot plant of University of Cadiz [61]

In the Supercritical Fluids and Membranes Laboratory (CEA Marcoule, France) it has been developed a SCWO process with a stirred double shell reactor with a flow rate ranging between 500 and 3000 L/h. with the purpose of treating contaminated organic wastes from nuclear industry [62, 63]

Finally, the work presented in this thesis has been done in the pilot plants owned by the group of High Pressure Process of the University of Valladolid. one a pilot plant with a capacity of 23 kg/h [64] and other with a capacity of 200 kg/h (demonstration plant, Figure 1.14) [65] both plants designed to work with different kind of reactors (tubular, transpiring wall and cooled wall reactors)



Figure 1.14: Demonstration plant of University of Valladolid [10]

1.3. HYDROTHERMAL FLAMES

Hydrothermal flames are combustion flames produced in aqueous environments at conditions above the critical point of water ($P > 221$ bar and $T > 374^\circ\text{C}$).

The flame is defined as the surface where combustion is produced. This surface separates the oxidant from the fuel in the case of diffusion or non-premixed flames, in which fuel is injected into the oxidant. In the case of premixed flames, that is that the fuel and oxidant are injected already mixed, the flame is the surface separating the reagents from the reaction product. In premixed flames, the surface is moving towards the reagents with a flame front velocity. If this velocity is the same as the fluid velocity the flame will remain still in a fixed position. If flow velocity is higher than flame front velocity the flame is blown away from the tube. An scheme of each kind of flame is show in Figure 1.15

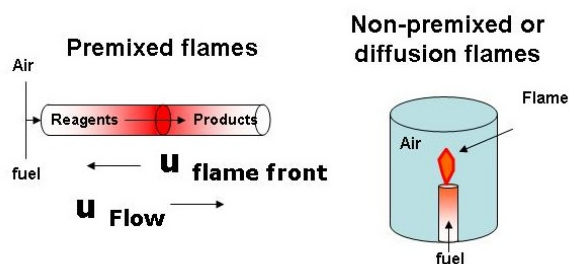


Figure 1.15: Scheme of premixed flames and diffusion flames

When the temperature of the mixture is higher than the autoignition temperature, supercritical water oxidation proceeds in the form of flames called hydrothermal flames. The term “hydrothermal combustion” was first used by Franck to describe oxidation processes taking place in dense aqueous environments [66]

The presence of a flame in a SCWO system would be expected to enhance the destructive abilities of the SCW medium [67, 68]. However, only a few works about hydrothermal flames have been published, among them the works of Steeper et al [69]; Serikawa et al [70] and Sobhy et al [68]

First experiments mostly carried out by Franck and coworkers consisted in studying the ignition of fuel + water mixtures. In general, the device used consisted of reaction chambers in which an oxidant stream (air, or pure oxygen) was introduced into a chamber containing a mixture of a fuel (generally methane, methanol or isopropyl alcohol) with supercritical water. [66, 67, 71]

In general, flames ignited spontaneously beyond a certain temperature, normally between 400 and 500°C [72]. This auto ignition temperature was decreased for higher pressures and fuel concentrations. There was a minimum temperature and a concentration under which flames were not produced. As the fuel concentration decreased the flame lost temperature and luminosity, but even when the luminosity was gone, the flame structure was maintained. In general, the conditions of the flame ignition depended on the fuel, the oxidant, the ratio of fuel/oxidant and the geometry of the injection system (an example is shown in figure 1.17.) Serikawa and coworkers [70] developed a continuous refrigerated facility for observing hydrothermal flames oxidizing isopropanol. In figure 1.16 can be observed how a flame is ignited and extinct inside a visual cell [70]



Figure 1.16: Ignition and extinction of hydrothermal flame (taken from[70])

Sobhy et al [68] also designed a semi-batch bench-scale visual flame cell system where they studied flames formed with air and methanol. Figure 1.17 shows some frames where the flow of air is changed and it can be observed how the size of the flame changes depending on the air injected.

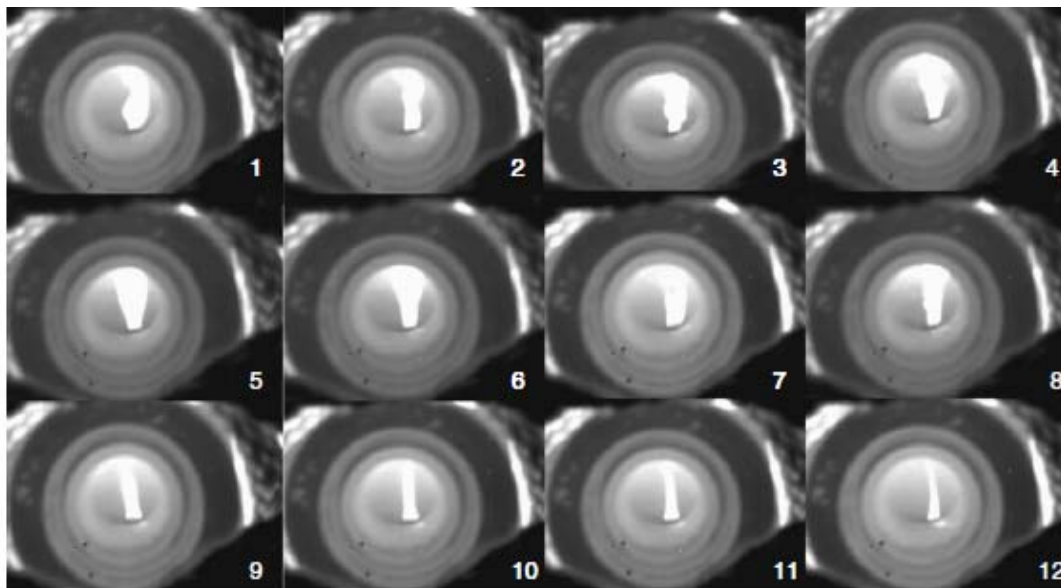


Figure 1.17: Snapshots 1–12 showing an SCW air–methanol flame being stabilized by reducing air-flow from 1.5 to 0.5 ml/min. Picture sequence captured using a FLIR thermal imaging NIR camera. Reaction conditions: 23% methanol, SCW– methanol at 380°C / 23 MPa air at 350°C / 30 MPa. [73]

The first reactor probably working with a hydrothermal flame inside was the MODAR reactor, working in conditions of concentration, temperature and pressure above the ignition conditions of methanol being able to work with injection temperatures of 25°C and injecting the air at 220°C [7]. In the reactor used in the university of Valladolid, operational conditions were above the ignition conditions of IPA according to Serikawa, thus they can be described as working at hydrothermal flame regime.[65, 74]

The ETH Zurich has been since 1992 developing different continuous hydrothermal burners [75, 76]. They used the hydrothermal flame as an internal heat source in a transpiring wall reactor. The direct injection of the waste into a hydrothermal flame generated inside the reactor was developed as a solution to avoid the external preheating of the wastes up to supercritical conditions [77-79]. Recently some authors have proposed using them in the breaking of rocks by thermal drilling spallation to make wells of more than 3 km deep, where water or sludge is used to maintain the structure of the well [79-81].

The subject has been thoroughly revised by Augustine & Tester [82].

SCWO with a hydrothermal flame has a number of advantages over the flameless process. Some of these advantages permit overcoming the traditional challenges that make the successful and profitable commercialization of SCWO technology difficult.

The advantages include the following [82]:

- It allows the destruction of the pollutants in residence times of a few milliseconds, which permits the construction of smaller reactors.
- It is possible to initiate the reaction with feed injection temperatures near to room temperature when using vessel reactors [32, 83, 84]. This avoids problems such as plugging and corrosion in a preheating system, having an advantage from the operational and energy integration perspective.
- Higher operation temperatures improve the energy recovery

Even though the most immediate application of hydrothermal flames is in the Supercritical Water Oxidation (SCWO) process for waste destruction [70, 72, 79, 85-87], which is the most industrially developed hydrothermal process, it is possible to move from the idea of hydrothermal flame as a technology for the destruction of wastes to considering the hydrothermal flame as a technology for the generation of clean

energy, which could eventually substitute the actual technologies based on atmospheric combustion

For this purpose a new point in the SCWO studies of new reactor design which could be able to use all the heat from the flame not only in the possibility of inject reactants at room temperature but also use other purposes as the energetic integration of the process [58, 88] or for production of electricity by turbines. In the case of waste with high concentration of inorganic substances, new reactor designs able to separate these salts from the effluent must be developed in order to make it possible to directly expand the effluent in an electricity production turbine.

For a sustainable society with a decentralized production based on renewable resources, Arai [89] proposed the supercritical oxidation of biomass wastes and other sustainable any kind of waste with high energetic content. fuels with a hydrothermal flame as a clean energy source. Augustine and Tester [82] also propose its utilization with low grade fuels. In general, this technology can be applied to the valorisation of wastes such as wastewater treatment plant sludge, biomass or plastic wastes and in general

1.4. REFERENCES

- [1] P.A. Marrone, G.T. Hong, Supercritical Water oxidation, in: M. Kutz (Ed.) Environmentally Conscious Materials and Chemicals Processing, John Wiley & Sons Inc, Hoboken (NJ), (2007), 385-443
- [2] R. Deul, E.U. Franck, The static dielectric-constant of the water-benzene mixture system to 400-degrees-c and 2800-bar, *Berichte Der Bunsen-Gesellschaft-Physical Chemistry Chemical Physics*, 95 (1991) 847-853.
- [3] W.M. Marshall, E.U. Franck, Ion Product of Water Substance, 0-1000°C, 1-10,000 Bars: New International Formulation and Its Background, American Chemical Society and the American Institute of Physics for the National Bureau of Standards, (1981).
- [4] J.W. Tester, H.R. Holgate, F.J. Armellini, P.A. Webley, W.R. Killilea, G.T. Hong, H.E. Barner, Supercritical Water Oxidation Technology - Process-Development and Fundamental Research, *Acs Symposium Series*, 518 (1993) 35-76.
- [5] M. Svanstrom, M. Froling, M. Modell, W.A. Peters, J. Tester, Environmental assessment of supercritical water oxidation of sewage sludge, *Resources, Conservation and Recycling*, 41 (2004) 321-338.
- [6] J.W. Griffith, D.H. Raymond, The first commercial supercritical water oxidation sludge processing plant, *Waste Management*, 22 (2002) 453-459.
- [7] L. Stenmark, Aqua Critox®: The Chematur engineering AB concept for SCWO, *Proceedings of the Workshop on Supercritical Water Oxidation - Achievements and Challenges in Commercial Applications*, (2001).
- [8] P. Kritzer, E. Dinjus, An assessment of supercritical water oxidation (SCWO): Existing problems, possible solutions and new reactor concepts, *Chemical Engineering Journal*, 83 (2001) 207-214.
- [9] P.A. Marrone, S.D. Cantwell, D.W. Dalton, SCWO system designs for waste treatment: Application to chemical weapons destruction, *Industrial & Engineering Chemistry Research*, 44 (2005) 9030-9039.
- [10] M.D. Bermejo, M.J. Cocero, Supercritical water oxidation: A technical review, *AIChE Journal*, 52 (2006) 3933-3951.
- [11] M.J. Cocero, E. Alonso, M.T. Sanz, F. Fdz-Polanco, Supercritical water oxidation process under energetically self-sufficient operation, *Journal of Supercritical Fluids*, 24 (2002) 37-46.

- [12] B.D. Phenix, J.L. DiNaro, J.W. Tester, J.B. Howard, K.A. Smith, The Effects of Mixing and Oxidant Choice on Laboratory-Scale Measurements of Supercritical Water Oxidation Kinetics, *Industrial & Engineering Chemistry Research*, 41 (2002) 624-631.
- [13] M.G.E. Goemans, F.M. Tiller, L. Li, E.F. Gloyna, Separation of metal oxides from supercritical water by crossflow microfiltration, *Journal of Membrane Science*, 124 (1997) 129-145.
- [14] M.D. Bermejo, D. Rincón, V. Vazquez, M.J. Cocero., Supercritical Water Oxidation: Fundamentals and Reactor Modeling, *CI & CEQ*, 13 (2007) 79-87.
- [15] H. Kim, D.B. Mitton, R.M. Latanision, Stress Corrosion Cracking of Alloy 625 in pH 2 Aqueous Solution at High Temperature and Pressure, *Corrosion*, 67 (2011).
- [16] E. Asselin, A. Alfantazi, S. Rogak, Thermodynamics of the corrosion of alloy 625 Supercritical water oxidation reactor tubing in ammoniacal sulfate solution, *Corrosion*, 64 (2008) 301-314.
- [17] P. Kritzer, Corrosion in high-temperature and supercritical water and aqueous solutions: a review, *Journal of Supercritical Fluids*, 29 (2004) 1-29.
- [18] B. Veriansyah, J.D. Kim, J.C. Lee, A double wall reactor for supercritical water oxidation: Experimental results on corrosive sulfur mustard simulant oxidation, *Journal of Industrial and Engineering Chemistry*, 15 (2009) 153-156.
- [19] H. Schmieder, J. Abeln, Supercritical water oxidation: State of the art, *Chemical Engineering & Technology*, 22 (1999) 903-908.
- [20] B. Veriansyah, T.-J. Park, J.-S. Lim, Y.-W. Lee, Supercritical water oxidation of wastewater from LCD manufacturing process: kinetic and formation of chromium oxide nanoparticles, *Journal of Supercritical Fluids*, 34 (2005) 51-61.
- [21] H.C. Lee, J.H. Kim, J.H. In, C.H. Lee, NaFeEDTA decomposition and hematite nanoparticle formation in supercritical water oxidation, *Industrial & Engineering Chemistry Research*, 44 (2005) 6615-6621.
- [22] J.R. Portela, Nebot E., M.d.l.O. E., Kinetic comparison between subcritical and supercritical water oxidation of phenol, *Chemical Engineering Journal*, 81 (2001) 287-299.
- [23] S.F. Rice, R.R. Steeper, Oxidation rates of common organic compounds in supercritical water, *Journal of Hazardous Materials*, 59 (1998) 261-278.
- [24] C. Aymonier, A. Gratiás, J. Mercadier, F. Cansell, Global reaction heat of acetic acid oxidation in supercritical water, *Journal of Supercritical Fluids*, 21 (2001) 219-226.

- [25] K.M. Benjamin, P.E. Savage, Supercritical Water Oxidation of Methylamine, *Industrial & Engineering Chemistry Research*, 44 (2005) 5318-5324.
- [26] <http://www.chematur.se/>, (last accessed 27th June 2012)
- [27] Huang CY, Barner HE, Albano JV, Killilea WR, Hong GT, Method for supercritical water oxidation, WO9221621, (1992)
- [28] M.D. Bermejo, I. Bielsa, M.J. Cocero, Experimental and theoretical study of the influence of pressure on SCWO, *AIChE Journal*, 52 (2006) 3958-3966.
- [29] M.D. Bermejo, F. Fdez-Polanco, M.J. Cocero, Effect of the transpiring wall on the behavior of a supercritical water oxidation reactor: Modeling and experimental results, *Industrial & Engineering Chemistry Research*, 45 (2006) 3438-3446.
- [30] K. Ahluwalia, Internal Platelet Heat Source and Method for Use in a Supercritical Water Oxidation Reactor, US 5571424, (1996)
- [31] K. Ahluwalia, Internal Platelet Heat Source and Method for Use on a Supercritical Water Oxidation Reactor, US 5670040 (1997)
- [32] M.D. Bermejo, E. Fdez-Polanco, M.J. Cocero, Experimental study of the operational parameters of a transpiring wall reactor for supercritical water oxidation, *Journal of Supercritical Fluids*, 39 (2006) 70-79.
- [33] G. Hong, WR Killilea, T. Thomason, Method for Solids Separation in a Wet Oxidation Type Process, US 4822497, (1989)
- [34] P.A. Marrone, M. Hodes, K.A. Smith, J.W. Tester, Salt precipitation and scale control in supercritical water oxidation - part B: commercial/full-scale applications, *Journal of Supercritical Fluids*, 29 (2004) 289-312.
- [35] L.S. Cohen, D. Jensen, G. Lee, D.W. Ordway, Hydrothermal oxidation of Navy excess hazardous materials, *Waste Management*, 18 (1998) 539-546.
- [36] Y. Calzavara, C. Jousset-Dubien, H.A. Turc, E. Fauvel, S. Sarrade, A new reactor concept for hydrothermal oxidation, *Journal of Supercritical Fluids*, 31 (2004) 195-206.
- [37] V. Casal, H. Schmidt, SUWOX - a facility for the destruction of chlorinated hydrocarbons, *Journal of Supercritical Fluids*, 13 (1998) 269-276.
- [38] S. Baur, H. Schmidt, A. Kramer, J. Gerber, The destruction of industrial aqueous waste containing biocides in supercritical water - development of the SUWOX process for the technical application, *Journal of Supercritical Fluids*, 33 (2005) 149-157.
- [39] <http://www.superwatersolutions.com/>, (last accessed 22th June 2012)
- [40] D.S. Sloan, M. Modell, R.A. Pelletie, Sludge Management in the City of Orlando- It's Supercritical!, *Florida water resources journal*, 60 (2008) 46-54.

- [41] http://www.cityoforlando.net/cityclerk/citycouncil/workshop_files/presentations/2011-04-25_oxidation.pdf, (last accessed 22th March 2012)
- [42] <http://www.ga.com/index.php>, (last accessed 28th June 2010)
- [43] <http://www.scfi.eu/>, (last accessed 24th June 2012)
- [44] Waste and wastewater newsletter, 13 (2011)
http://www.waterandwastewater.com/www_services/newsletter/april_4_2011.htm (last accessed 4th July 2012)
- [45] <http://www.innoveox.com>, (last accessed 4th July 2012)
- [46] G. Ondrey, Supercritical water oxidation for organic waste treatment, Chemical Engineering, (2011) 11.
- [47] www.hanwhachemical.co.kr/english/pro/psu_panc_idx.jsp, (last accessed 30th June 2012)
- [48] P.A. Marrone, Supercritical Water Oxidation – Current Status of Full-scale Commercial Activity for Waste Destruction, in: ISSF (Ed.) 10th International Symposium on Supercritical Fluids San Francisco. CA, 2012.
- [49] I.S. Jayaweera, D.S. Ross, D. Bomberger, An emerging hydrothermal technology for treatment of industrial waste, Abstracts of Papers of the American Chemical Society, 216 (1998) U946-U946.
- [50] I.S. Jayaweera, Chemical Degradation Methods for Wastes and Pollutants: Environmental and Industrial Applications, Tarr, M.A., (2003).
- [51] <http://www.usinenouvelle.com/article/innoveox-inaugure-sa-1ere-unite-de-traitement-de-dechets-par-oxydation-hydrothermale-supercritique-a-arthez-de-bearn.N153617>, (last accessed 31th June 2012)
- [52] D. Xu, S. Wang, X. Tang, Y. Gong, Y. Guo, Y. Wang, J. Zhang, Design of the first pilot scale plant of China for supercritical water oxidation of sewage sludge, Chemical Engineering Research and Design, 90 (2012) 288–297.
- [53] V.I. Anikeev, A. Yermakova, Technique for Complete Oxidation of Organic Compounds in Supercritical Water, Russian Journal of Applied Chemistry, 84 (2011) 88-94.
- [54] K. Kim, S.H. Son, K. Kim, K. Kim, Y.-C. Kim, Environmental effects of supercritical water oxidation (SCWO) process for treating transformer oil contaminated with polychlorinated biphenyls (PCBs), Chemical Engineering Journal, 165 (2010) 170-174.

- [55] K. Kim, K. Kim, S.H. Son, J. Cho, Y.-C. Kim, Supercritical water oxidation of transformer oil contaminated with PCBs—A road to commercial plant from bench-scale facility, *Journal of Supercritical Fluids*, 58 (2011) 121-130.
- [56] K. Kim, K. Kim, M. Choi, S.H. Son, J.H. Han, Treatment of ion exchange resins used in nuclear power plants by super- and sub-critical water oxidation – A road to commercial plant from bench-scale facility, *Chemical Engineering Journal*, 189–190 (2012) 213-221.
- [57] F. Zhang, S. Chen, C. Xu, G. Chen, J. Zhang, C. Ma, Experimental study on the effects of operating parameters on the performance of a transpiring-wall supercritical water oxidation reactor, *Desalination*, 294 (2012) 60-66.
- [58] F. Jimenez-Espadafor, J.R. Portela, V. Vadillo, J. Sanchez-Oneto, J.A.B. Villanueva, M.T. Garcia, E.J.M. de la Ossa, Supercritical Water Oxidation of Oily Wastes at Pilot Plant: Simulation for Energy Recovery, *Industrial & Engineering Chemistry Research*, 50 (2011) 775-784.
- [59] V. Vadillo, M.B. García-Jarana, J. Sánchez-Oneto, J.R. Portela, E.J.M. de la Ossa, Supercritical water oxidation of flammable industrial wastewaters: Economic perspectives of an industrial plant, *Journal of Chemical Technology and Biotechnology*, 86 (2011) 1049-1057.
- [60] V. Vadillo, Estudio del proceso de oxidación en agua supercritica para su escalamiento industrial: Implantación de nuevas solucioens tecnologias. simulacion y optimizacion, in: Dpto Ingenieria Quimica y TA, UCA, 2012.
- [61] www.uca.es, (last accessed 7th July 2010)
- [62] Y. Calzavara, C. Jousot-Dubien, H.A. Turc, E. Fauvel, S. Sarrade, A new reactor concept for hydrothermal oxidation, *Journal of Supercritical Fluids*, 31 (2004) 195-206.
- [63] A. Leybros, A. Roubaud, P. Guichardon, O. Boutin, Ion exchange resins destruction in a stirred supercritical water oxidation reactor, *Journal of Supercritical Fluids* 51 (2010) 369-375.
- [64] M.J. Cocero, D. Vallelado, R. Torio, E. Alonso, F. Fdez-Polanco, Optimisation of the operation variables of a supercritical water oxidation process, *Water Science and Technology*, 42 (2000) 107-113.
- [65] M.D. Bermejo, D. Rincon, A. Martin, M.J. Cocero, Experimental Performance and Modeling of a New Cooled-Wall Reactor for the Supercritical Water Oxidation, *Industrial & Engineering Chemistry Research*, 48 (2009) 6262-6272.

- [66] W. Schilling, E.U. Franck, Combustion and diffusion flames at high-pressures to 2000 bar, *Berichte Der Bunsen-Gesellschaft-Physical Chemistry Chemical Physics*, 92 (1988) 631-636.
- [67] G.M. Pohnsner, E.U. Franck, Spectra and temperatures of diffusion flames at high-pressures to 1000 bar, *Berichte Der Bunsen-Gesellschaft-Physical Chemistry Chemical Physics*, 98 (1994) 1082-1090.
- [68] A. Sobhy, I.S. Butler, J.A. Kozinski, Selected profiles of high-pressure methanol-air flames in supercritical water, *Proceedings of the Combustion Institute*, 31 (2007) 3369-3376.
- [69] R.R. Steeper, S.F. Rice, M.S. Brown, S.C. Johnston, Methane and methanol diffusion flames in supercritical water, *Journal of Supercritical Fluids*, 5 (1992) 262-268.
- [70] R.M. Serikawa, T. Usui, T. Nishimura, H. Sato, S. Hamada, H. Sekino, Hydrothermal flames in supercritical water oxidation: investigation in a pilot scale continuous reactor, *Fuel*, 81 (2002) 1147-1159.
- [71] T. Hirth, E.U. Franck, Oxidation and hydrothermolysis of hydrocarbons in supercritical water at high-pressures, *Berichte Der Bunsen-Gesellschaft-Physical Chemistry Chemical Physics*, 97 (1993) 1091-1098.
- [72] A. Sobhy, R.I.L. Guthrie, I.S. Butler, J.A. Kozinski, Naphthalene combustion in supercritical water flames, *Proceedings of the Combustion Institute*, 32 (2009) 3231-3238.
- [73] A. Sobhy, R.I.L. Guthrie, L.S. Butler, J.A. Kozinski, Naphthalene combustion in supercritical water flames, in, *Montreal, QC, 2009*, pp. 3231-3238.
- [74] M. Dolores Bermejo, F. Fdez-Polanco, M.J. Cocero, Effect of the transpiring wall on the behavior of a supercritical water oxidation reactor: Modeling and experimental results, *Industrial and Engineering Chemistry Research*, 45 (2006) 3438-3446.
- [75] H.L. La Roche, M. Weber, C. Trepp, Rationale for the filmcooled coaxial hydrothermal burner (FCHB) for supercritical water oxidation (SCWO), in: *Briefing Book of the First International Workshop on Supercritical Water Oxidation*, Jacksonville, FL, USA, 1995.
- [76] H.L. LaRoche, M. Weber, C. Trepp, Design rules for the Wallcooled Hydrothermal Burner (WHB), *Chemical Engineering & Technology*, 20 (1997) 208-211.

- [77] B. Wellig, K. Lieball, P. Rudolf Von Rohr, Operating characteristics of a transpiring-wall scwo reactor with a hydrothermal flame as internal heat source, *Journal of Supercritical Fluids*, 34 (2005) 35 - 50.
- [78] K. Prikopský, B. Wellig, P.R. von Rohr, SCWO of salt containing artificial wastewater using a transpiring-wall reactor: Experimental results, *Journal of Supercritical Fluids*, 40 (2007) 246-257.
- [79] B. Wellig, M. Weber, K. Lieball, K. Prikopský, P. Rudolf von Rohr, Hydrothermal methanol diffusion flame as internal heat source in a SCWO reactor, *Journal of Supercritical Fluids*, 49 (2009) 59-70.
- [80] T. Wideman, J. Potter, R. Potter, D. Dreesen, Methods and apparatus for thermal drilling, WO2010042723, (2010)
- [81] r.P. Rudolf von Roh, T. Rothenfluh, M. Schuler, Rock drilling in great depths by thermal fragmentation using highly exothermic reactions evolving in the environment of a water-based drilling fluid, WO2010072407, (2010)
- [82] C. Augustine, J.W. Tester, Hydrothermal flames: From phenomenological experimental demonstrations to quantitative understanding, *Journal of Supercritical Fluids*, 47 (2009) 415-430.
- [83] C.H. Oh, R.J. Kochan, T.R. Charlton, A.L. Bourhis, Thermal-hydraulic modeling of supercritical water oxidation of ethanol, *Energy & Fuels*, 10 (1996) 326-332.
- [84] M.D. Bermejo, P. Cabeza, J.P.S. Queiroz, C. Jiménez, M.J. Cocero, Analysis of the scale up of a transpiring wall reactor with a hydrothermal flame as a heat source for the supercritical water oxidation, *Journal of Supercritical Fluids*, 56 (2011) 21-32.
- [85] C. Narayanan, C. Frouzakis, K. Boulouchos, K. Prikopsky, B. Wellig, P.R. von Rohr, Numerical modelling of a supercritical water oxidation reactor containing a hydrothermal flame, *Journal of Supercritical Fluids*, 46 (2008) 149-155.
- [86] P.R. Von Rohr, K. Prikopsky, Hydrothermal flames in a novel supercritical water oxidation (Scwo) reactor, in, San Francisco, CA, (2006).
- [87] B. Wellig, K. Lieball, P. Rudolf von Rohr, Operating characteristics of a transpiring-wall SCWO reactor with a hydrothermal flame as internal heat source, *Journal of Supercritical Fluids*, 34 (2005) 35-50.
- [88] E.D. Lavric, H. Weyten, J. De Ruyck, V. Pleşu, V. Lavric, Supercritical water oxidation improvements through chemical reactors energy integration, *Applied Thermal Engineering*, 26 (2006) 1385-1392.

[89] K. Arai, R.L. Smith Jr, T.M. Aida, Decentralized chemical processes with supercritical fluid technology for sustainable society, *Journal of Supercritical Fluids*, 47 (2009) 628-636.

CHAPTER 2

OBJECTIVES

CHAPTER 2

OBJETIVES

The aim of this research is to develop a new reactor design for the process of supercritical water oxidation, working with a hydrothermal flame as internal heat source and able to inject feeds at room temperature, to work with waste containing some inorganic salt and to optimize the energetic use.

To do so several partial objectives must be fulfilled:

1) Study of the influence of the operational parameters in the hydrothermal flame initiation.

In first place tubular devices will be used to study the influence of operational parameters such as mixing, injection flowrate and temperature as well as fuel concentration in the ignition of hydrothermal flames from flammable compounds. The ignition of recalcitrant compounds such as ammonia or acetic acid will be studied as well, evaluating the necessity of using a co-fuel.

Using vessel reactors, the influence of the geometrical parameters in the formation and behavior of will be determined.

Using this information, the parameters controlling the injection of reagents at room temperature on a hydrothermal flame will be determined and the key parameters to consider when designing a reactor with a hydrothermal flame as a heat source will be identified.

2) Design, construction, set up and start up of a new reactor working with hydrothermal flame as internal heat source in the supercritical water oxidation process.

3) Study the behavior of the reactor with different kind of feeds.

Flammable compounds

Feeds with high salt content

Feeds containing recalcitrant compounds

4) Modifications in the reactor configuration in order to improve energy recovery.

CHAPTER 3

EXPERIMENTAL SETUP

CHAPTER 3

EXPERIMENTAL SETUP

TABLE OF CONTENTS

3.1.REACTORS.....	79
3.1.1 Reactors studied in the facility of CETRANSA, (Santovenia de Pisuerga, UVa)	79
3.1.1.1 Tubular reactor	79
3.1.1.2. Transpiring Wall reactor.....	80
3.1.2 Reactors studied in the facility of Science Faculty (Department of Chemical Engineering, UVa).....	82
3.1.2.1 Tubular reactors.....	82
3.1.2.2 Cooled wall reactor.....	85
3.2.PLANT OPERATION: WORKING EQUIPMENT AND FLOW CHARTS.....	88
3.2.1 Facility of CETRANSA, Santovenia de Pisuerga, UVa.....	88
3.2.1.1 Introduction	88
3.2.1.2 Process description	90
3.2.1.3 Main equipment of the pilot plant	91
3.2.2 Facility of Sciences Faculty, UVa	96
3.2.2.1 Introduction	96
3.2.2.2 Process description	98
3.2.2.3 Main equipment of the pilot plant	99
3.3. COMMON EQUIPMENT OF BOTH FACILITIES.....	103
3.3.1 Valves and pipes.....	103
3.3.2 Instrumentation.....	106
3.3.3 Data acquisition system.....	108

3.1. REACTORS

Different types of reactor has been used along this work. In the following section a description of each one is presented together with an indication in which of the facilities used in this work they were used.

3.1.1. Reactors studied in the facility of CETRANSA, (Santovenia de Pisuerga, University of Valladolid)

3.1.1.1. Tubular reactor

This reactor consisted of a straight and empty tube made of Ni alloy C-276 with a total length of 5400 mm and a diameter of $\frac{1}{4}$ " (i.d. 3.86 mm) giving an internal volume of 63.2 mL. It was thermally isolated. Temperatures were measured with 6 thermocouples type K (temperature range from 0 to 1000 °C) with an accuracy of 1%, placed every 390 mm along the reactor. The thermocouples where connected using conventional "tee" tubing fittings

The diameter of the tubular reactor was chosen to be similar to that of the mixer used in the transpiring wall reactor. In its end, a quenching water stream is introduced in the reactor in order to stop the oxidation reaction. A scheme of this reactor is shown in figure 3.1.

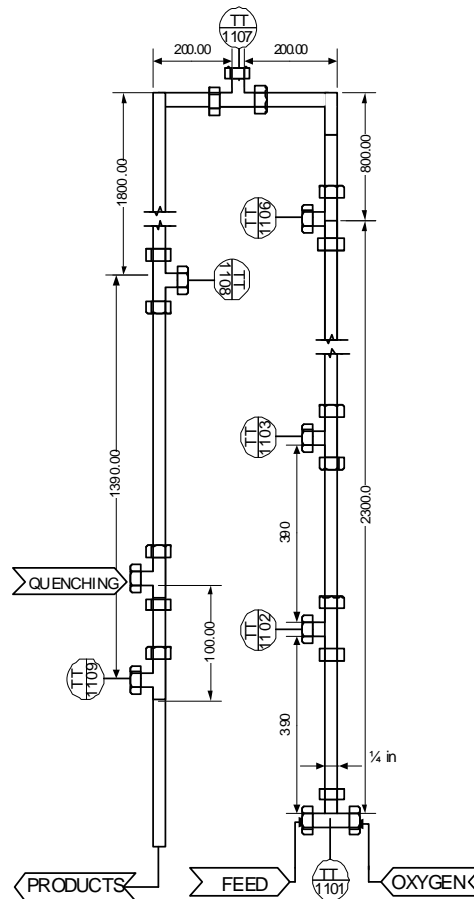


Figure 3.1: Tubuar reactor

3.1.1.2. Transpiring wall reactor

The transpiring wall reactor of the University of Valladolid (UVa) consists of a stainless steel pressure shell with a volume of 6.3 L. It contains a reaction chamber surrounded by a porous wall through which clean water circulates. The feed and the oxidant are introduced into the reactor through its lower part, and they are feed through a tubular injector up to the upper part of the reaction chamber where the hydrothermal flame is ignited. After passing through the flame, the products of the reaction flow down mixing with the clean water that enters the reactor through the transpiring wall, and decontaminated water leaves the reactor through its lower part. an scheme of the reactor is shown in figure 3.2

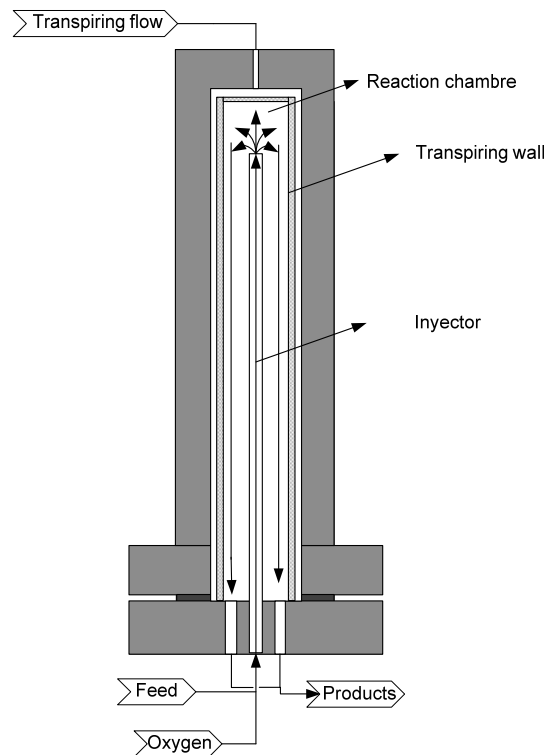


Figure 3.2: Transpiring wall reactor of the University of Valladolid (UVa)

The transpiring wall consists on three sections. Upper and lower sections are made of non-transpiring Ni alloy 625. It is porous only the central section of the reactor, that is made of porous sintered Ni alloy 600. The mixer is designed in such a way that the ignition was produced in the reaction chamber and not in the mixer. Thus, the injector was constructed as a tube with an internal diameter of 9mm filled with alloy 625 particles of different sizes, placing the smallest in the higher part of the mixer. A double

thermocouple contained in a 1/8" tube, with two measurements position is placed inside of the injector., in figure 3.3 a scheme of the reactor with the position of the thermocouples is shown.

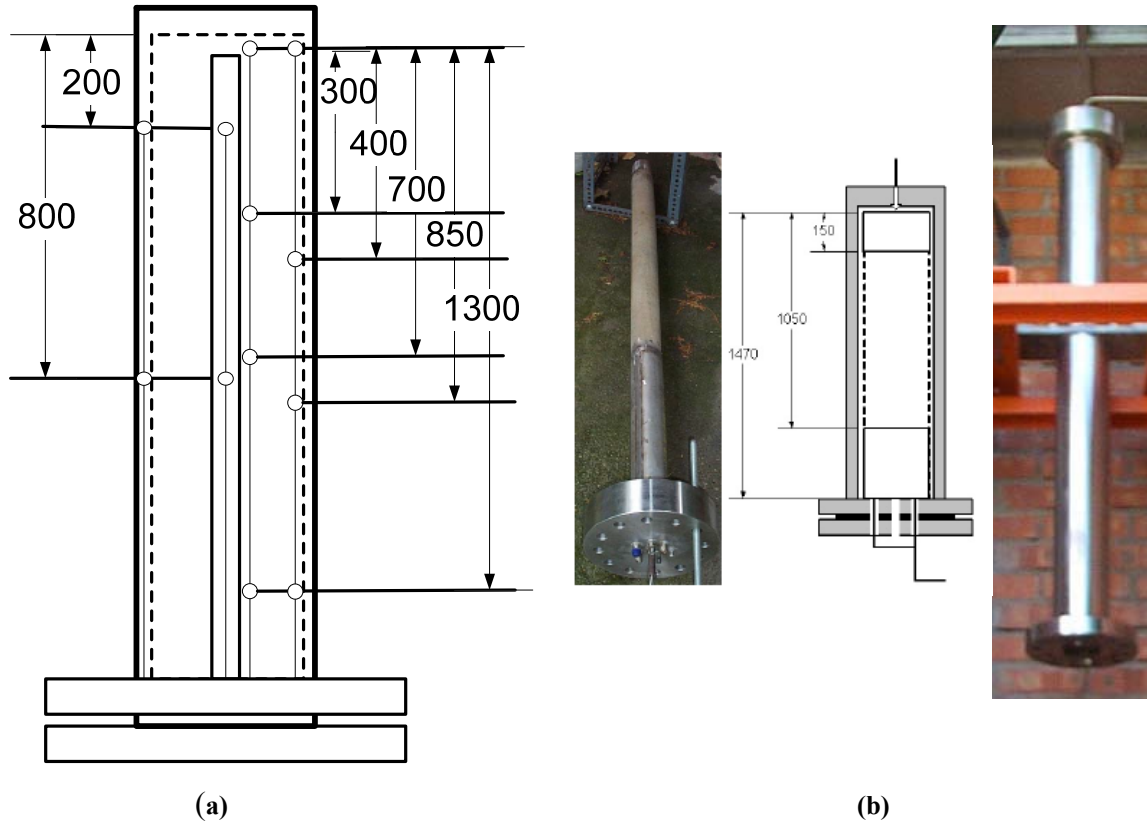


Figure 3.3 a: Position fo the thermocouples inside the reactor, **(b):** Pictures of traspiring wall (right), and external (left) wall of the transpirign wall reactor.

Electrical preheating of the reactor:

Electric preheating reactor is performed with three electric heaters resistances (Figure 3.4), which are placed outside the reactor wall. Next to each of these resistances is installed a thermocouple to control the heating.

Properties of each resistance

- Dimensions: 145 x 345 mm
- Power: 1,5 kW



Figure 3.4: Electrical resistances

3.1.2. Reactors studied in the facility of Science Faculty (Department of chemical Engineering, University of Valladolid)

3.1.2.1. Tubular reactors

Several tubular reactors were tested in the pilot plant. All the tubular reactor were constructed with commercial Ni alloy C-276 tubing of $\frac{1}{4}$ " (i.d. 3.86 mm) and $\frac{1}{8}$ " (i.d. 1.75 mm). The dimensions of the reactors were selected in order to be used as injectors or mixers in the vessel reactors, because in the first moment the mixture was thought to play an important role in ignition phenomenon. Thus, in some parts of the work , these reactors are referred as mixer.

All of them were thermally isolated. Temperatures were measured with thermocouples type K (temperature range from 0 to 1000°C) with an accuracy of 1%.

Mixer 1

Consisted of an $\frac{1}{4}$ " straight and empty tube with a length of 1584 mm and an internal volume of 18.5 mL. As it is shown in figure 3.5, the flow inside the tube was upwards. Temperature was monitored using 8 thermocouples. Feed was injected in the lower end of the tube while air is injected perpendicularly. (Figure 3.5)

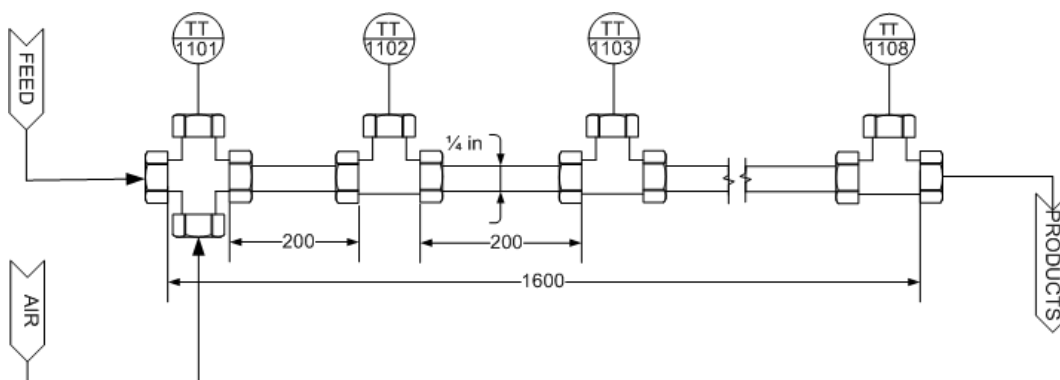


Figure 3.5: Scheme of mixer 1

Mixer 2

The second reactor consisted of an $\frac{1}{8}$ " straight and empty tube with a length of 2344 mm and an internal volume of 5.63 mL. The flow inside the tube was upwards. Temperature was monitored using 8 thermocouples. Feed was injected to the bottom while air is injected perpendicularly. (figure 3.6)

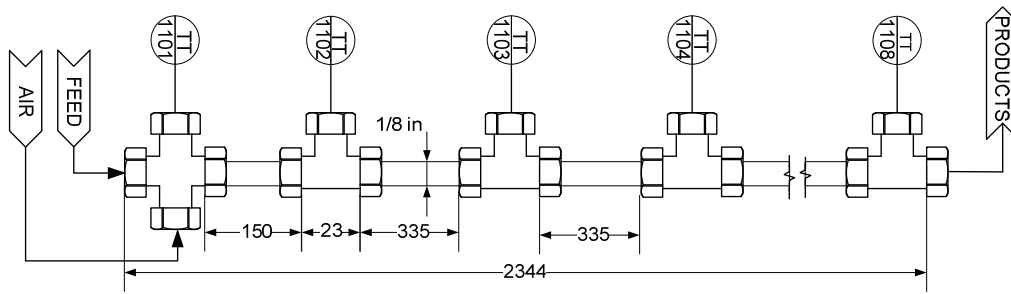


Figure 3.6: Scheme of mixer 2

Mixer 3

Consisted of 1/4" straight and empty tube portions connected by portions where the flow is bifurcated and reversed, before being mixed again, producing a general upward flow. In this way the fluid elements containing air and feed are cut and mixed as shown in figure 3.7 The mixer had an internal volume of 31.75 mL. Temperature was monitored with 6 thermocouples. In this design feed and air inlets are opposite each other.

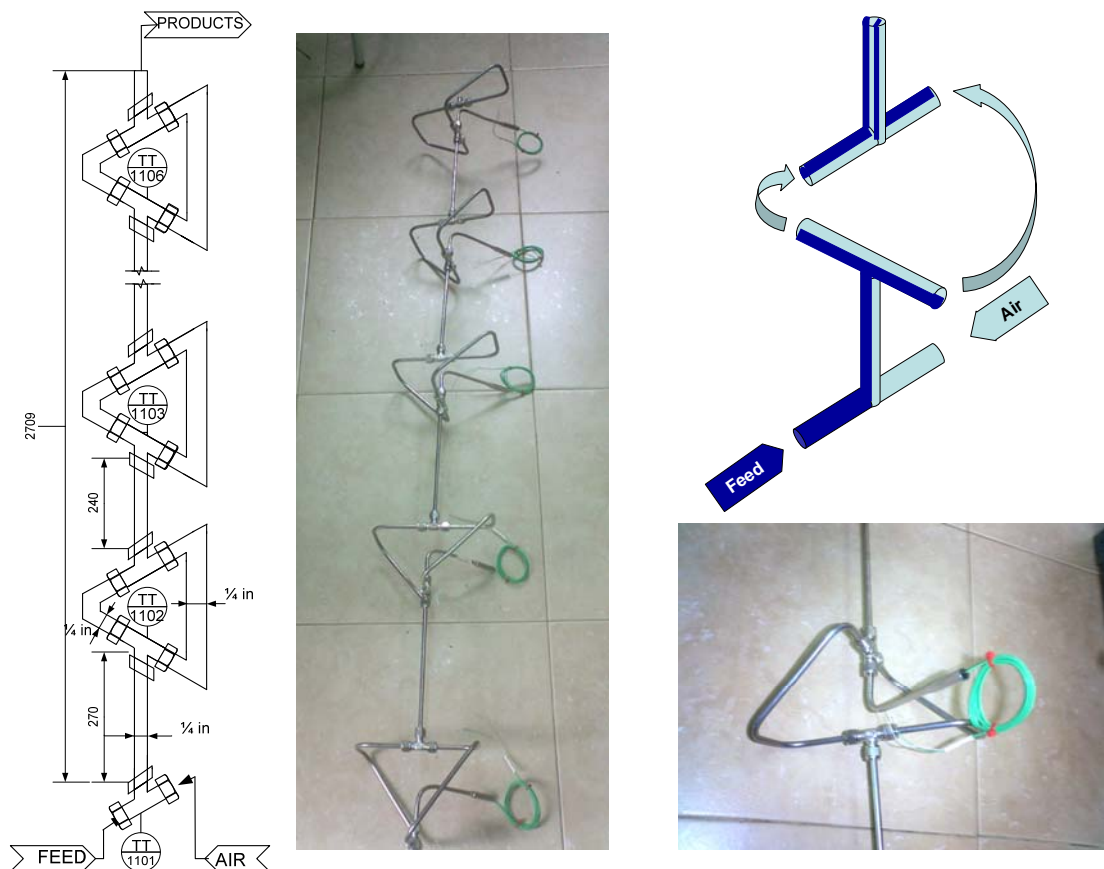


Figure 3.7: Scheme and pictures of different parts of mixer 3

Mixer 4

Consisted of four sections constructed using $\frac{1}{4}$ " straight tube. The first one has an upward flow and was filled with 2-3 mm AISI 316 rings (example in figure 3.8) giving a porosity of 50% and an internal volume of 12.2 mL. In this tram temperature was monitored by 6 thermocouples. After this tram there was an upflow empty tube of the same dimensions followed by a horizontal tram, where temperature was also monitored and a downflow tram where temperature was monitored as well. In this way it was possible to monitor if the reaction ignited after the filled tube. The total internal volume was 47.3 mL. An scheme of the reactor is shown in figure 3.9



Figure 3.8: Samples of the fill used in the reactor

(2-3 mm AISI 316 rings)

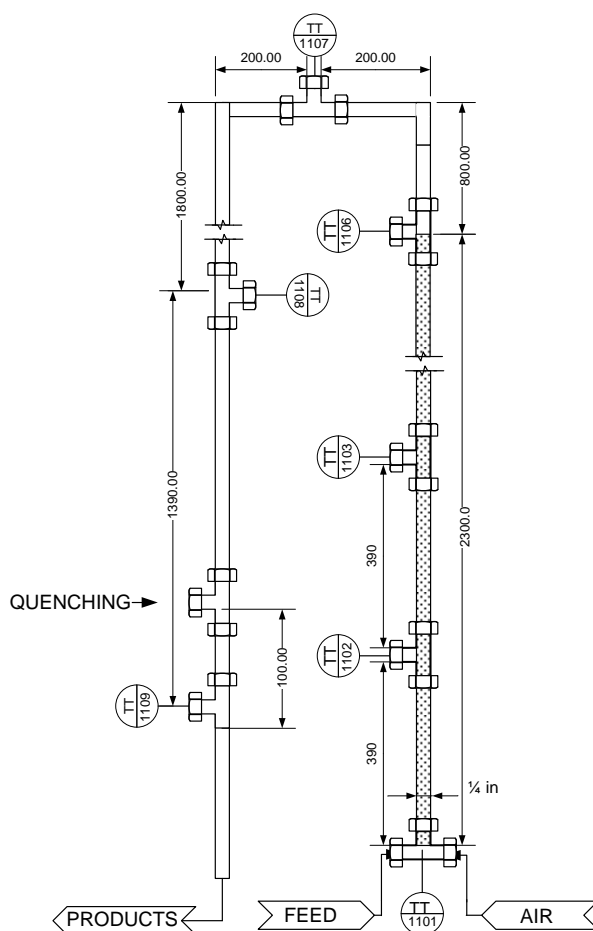


Figure 3.9: Scheme of mixer 4

3.1.2.2. Cooled wall reactor

The reactor consists of a vertical Ni-alloy reaction chamber of 53.4 mm of internal diameter and 1 m high. It is inside of a pressure vessel made of AISI 316 able to stand a maximum pressure of 30 MPa and 400°C. Between the walls of the two vessels a stream of cold water refrigerates the reaction vessel. The reagents (feed and air) are introduced in the reactor through a tubular injector up to the top of the reaction chamber. The flame is produced outside of the injector, normally at the top of the reaction chamber, where the maximum temperature is registered. Reaction chamber is refrigerated with room temperature pressurized water that flowed between the reaction chamber wall and the inner wall which supported the pressure, keeping the pressurized wall at temperatures lower than 400°C, and entering in the reaction chamber by its lower part mixing with the reaction products. The products flowed down the reactor leaving it by its lower part together with the cooling water. A scheme of the reactor is shown in figure 3.9

One of the advantages of this reactor is that the injector is not welded to the flange so its position can be changed or a different injector can be installed easily, this way three injectors constructed with empty tubes were used according with the results of the chapter 4.1 where different injectors are studied.

Characteristics of those injectors are summarized in Table 3.1.

Table 3.1: Characteristics of the three injectors studied in this work

Injector	Injector 1	Injector 2	Injector 3
Material	Ni-alloy 625	Ni-alloy 625	Ni-alloy 625
External Diameter (in)	1/4	1/8	1/4
Internal Diameter (mm)	3.86	2.16	3.86
Length (mm)	950	950	550

Other configuration of this reactor is working with an outlet at the top of the reactor having this way two outlets one at high temperature and other at subcritical temperatures with the salt dissolved with the cooling water.

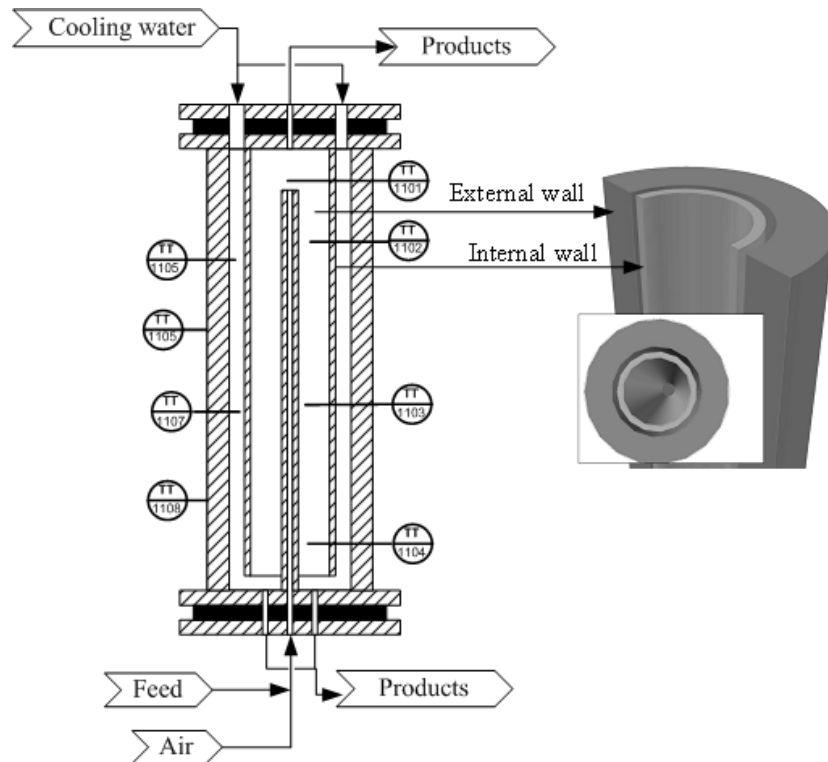


Figure 3.10: Scheme of the new cooled wall reactor of the University of Valladolid (UVa)

The cooling water is injected through the top of the reactor, descending between the internal and external walls. In the bottom of the reactor this cooling water take contact with the reaction products, forming a "pool" where it is possible to dissolve the precipitated salts.

To keep the pressure inside the reactor this one is closed by flanges located on the upper and lower sides closed with bolt.

Electrical preheating of the reactor:

Electric preheating reactor is performed with two electric heaters resistances with different sizes, which are placed outside the reactor wall. Next to each of these resistances is installed a thermocouple to control the heating.

Properties

Resistance placed at the top

- Dimensions: 358 x 300 mm
- Power: 1,5 kW

Resistance placed at the bottom

- Dimensions: 358 x 400 mm
- Power: 2,5 kW

A thermocouple contained in a 1/8" tube, with 3 measurements position is placed inside the reaction chamber., in figure 3.11.a scheme of the reactor with the position of the thermocouples is shown

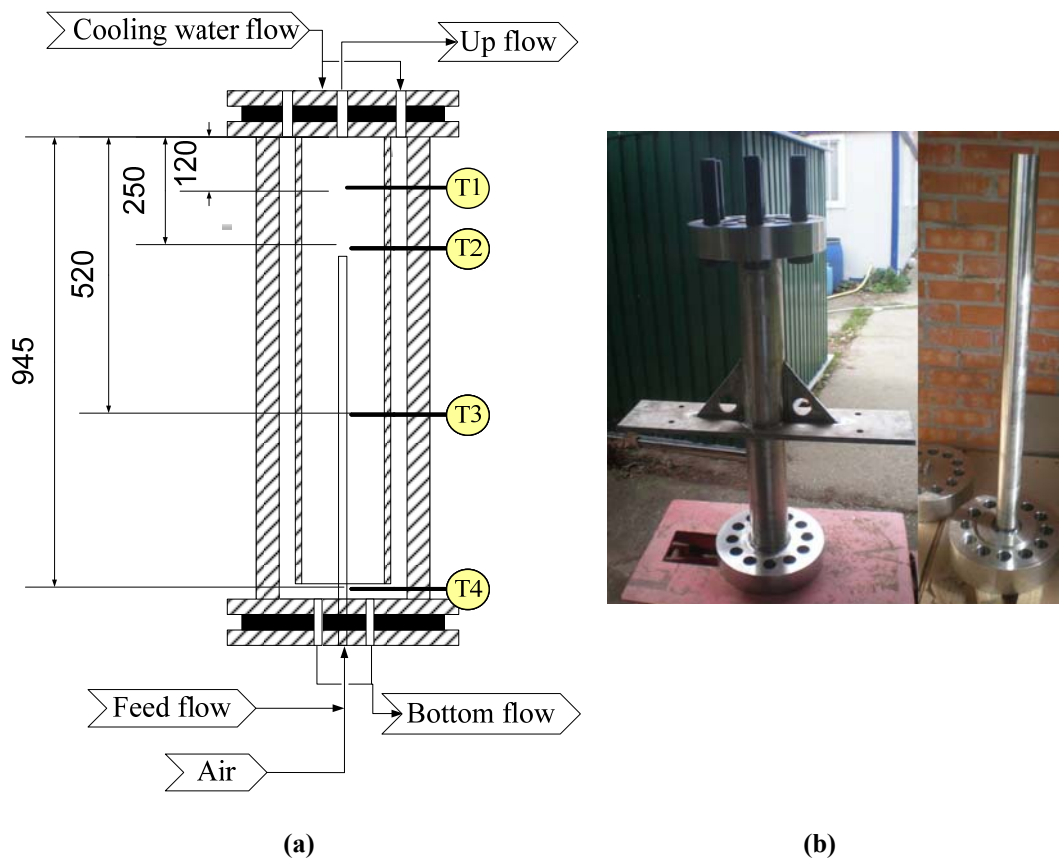


Figure 3.11.a : Position fo the thermocouples inside the reactor. **(b):** Pictures of the external (right) and internal (left) wall of the new cooled wall reactor

3.2. PLANT OPERATION: WORKING EQUIPMENT AND FLOW CHARTS

3.2.1. Demonstration plant sited in CETRANSA, (Santovenia de Pisuerga)

3.2.1.1. Introduction

The demonstration Plant of SCWO is located on the premises of CETRANSA (Santovenia de Pisuerga), it was designed to test the destruction of various compounds by oxidation in supercritical water, using oxygen as oxidizing agent.

The plant operates in continuous and has a treatment capacity of 200 kg / h. It has been designed to operate at pressures up to 300 MPa and temperatures up to 400 °C and 700 °C inside of the reaction chamber.

Figure 3.12 and 3.13 show the diagram flow of the plant with the transpiring wall reactor and the tubular reactor:

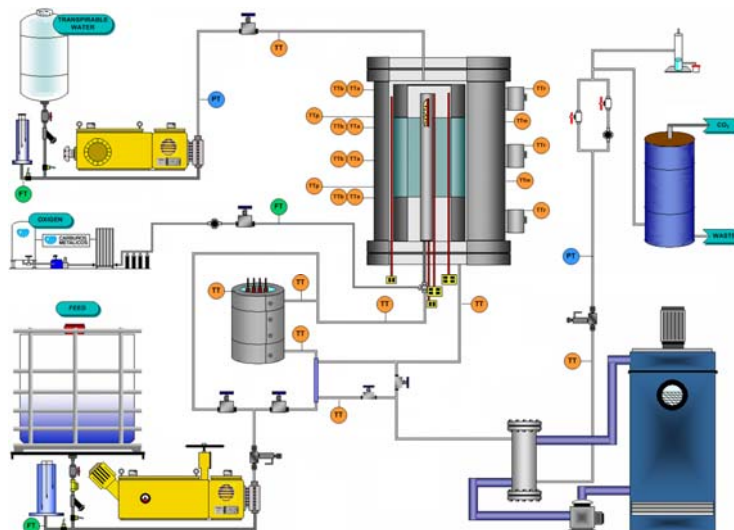


Figure 3.12: Flow diagram of the facility with a transpiring wall reactor

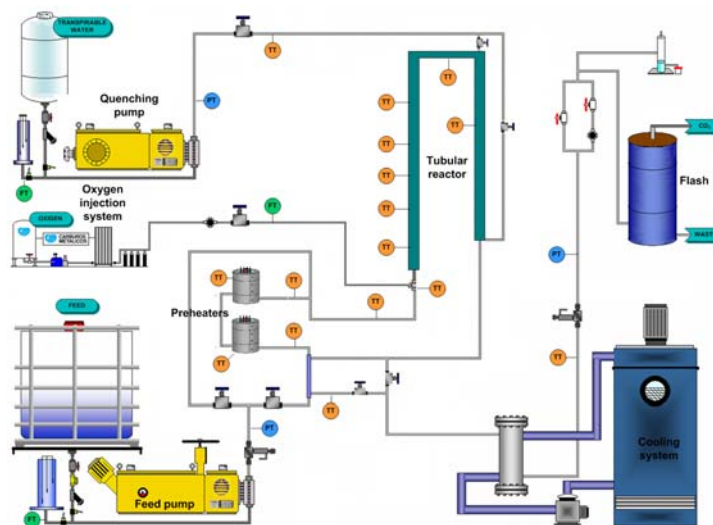


Figure 3.13: Flow diagram of the facility with a tubular reactor

This plant has four main lines of work.

- Feed Supply

They handle aqueous solutions of flammable and sometimes toxic, are pressurized and heated electrically.

The main equipment of this line is:

- Membrane pump, P-350. $P_{max} = 300$ bar. Flow = 200 kg /h
- Electric preheaters, E-370 ($W = 6000W$, $T_{max} = 600^{\circ}C$) E-380 ($W = 8000W$, $T_{max} = 600^{\circ}C$)

- O₂ line

The oxidizer is introduced into the reactor after being compressed and evaporated into the O₂ bottles.

The main equipment of this line is:

- Cryogenic pump, P-220
- Air cooler, E-230
- O₂ Tank, T-210
- Bottles of O₂ storage, T-240

- Quenching line

The main equipment of this line is:

- Piston Pump P-120. $P_{max} = 300$ bar, flow max = 72 L / h

- Line outlet reactor.

The Products from the reactor are subsequently cooled and decompressed.

The main equipment of this line is:

- Cooler: E-420, It consists of a stainless steel coil $\frac{1}{4}$ "and 0.049" thick, inserted in a container of galvanized steel.
- Double needle valve VREL SENTRY ® 11. $P_{max} = 345$ bar, flows of P: 9-240 L / h.

3.2.1.2. Process description

The waste to be treated is stored in the tank T-310, with a capacity of 700 liters and is pumped through a centrifugal pump, P-330, to a second smaller tank of 200 liters, where the mixture is homogenized. This tank has a stirring system consists of a motor connected to a propeller mixer. From the second tank, through the piston pump, P-350, the waste is conducted to the reactor.

The feed is conditioned by preheater E-370, which heats the feed till around 350 – 400°C. This exchanger is system formed by a set of four electrical resistances of 2500 W each one, inserted into a bronze cylinder and with a tube of 6 meters of inconel 600 placed around the cylinder. The device is isolated and has a thermocouple inside the central solid block to characterize and control its temperature. At the outlet there is a thermocouple connected to the circuit, which allows to determine the inlet temperature of the waste to the reactor.

Oxygen is stored as a liquid in a pallet-tank with a capacity of approximately 750 kg of O₂. This pallet-tank is an isolated cryogenic tank (Dewar) that keeps the oxygen in liquid state at a pressure of 2.5 - 3 bar.

The liquid O₂ is pumped from the bottom by a cryogenic pump, P-220, to an evaporator E-230, where oxygen is gasified to be stored at a pressure between 250 and 270 bar in four cylindrical bottles acting as a gas storage tank. The pump is automatically controlled by a stop-start cycle. The pump is switched on when the pressure in the bottles falls below the minimum set point (230 bar) and switched off when it reaches the maximum set point (270 bar). The safety valve for the bottles is rated at 280 bar. Once the cycle of the cryogenic pump starts, a first valve opens throwing out oxygen to the pump inlet in order to decrease the temperature till -140 °C to avoid the evaporation of O₂ before the outlet of the pump. Once this temperature is reached in the pump, the liquid oxygen can pass trough to the piston, being vaporizing at the vaporizer. All the cryogenic system is lubricated by dry N₂, this flow of N₂ is maintained during operation of the pump as well as 30 minutes before and after the switch off of the pump.

Oxygen is introduced into the reactor by pressure difference between the bottles and inside the reactor. At the end of the cylinders the pressure regulator PI-203 lets select and set the outlet pressure

The oxygen and the residue are mixed and enter through the bottom of the reactor and the reaction of oxidation is produced.

At the outlet of the reactor, the products are cooled (up to room temperature) through the cooler E-420, which uses a closed cooling system, where the water of the cooling is cooled in a cooling tower D-430. Then the products are depressurize with the valve HV-422, which is electrically heated to prevent freezing caused by decompression.

The products at atmospheric pressure are introduced into a flash chamber V-460 where it is separated the liquid and gas phase There is also a V-450 sampler, which takes the liquid sample to analyze their OCD.

3.2.1.3. Main equipment of the pilot plant

Pumping equipment.

In the plant of SCWO there are three different types of pumps.

- A cryogenic pump for liquid oxygen.
- Centrifugal pumps for the transfer of waste, fuel and water dilutions.
- Piston pump for pumping the waste-mixture at high pressure and the quenching water.

P-320. Centrifugal pump

This equipment is mounted on a support with wheels for manual transport and dispose of a versatile system of transport.

Mainly used for filling the tank F-110 with the residue. It allows pumping till a maximum height of 15 m. and a maximum flow of 100 L / min. (Picture in figure 3.14)



Figure 3.14: Centrifugal pump P-320

P-330. Centrifugal pump.

This pump is installed on the floor of the plant, by screwing. It has two external filters in the PVC pipe, placed at the outlet and inlet to protect the drive of sediments from the dilution water.

Working in the line of waste, its main function is pumping the diluted residue from the main tank to the secondary tank. The connection system is manual, and the pump can load the residue till a maximum height of 28 meters.

(Picture in figure 3.15)



Figure 3.15:
Centrifugal pump P-330

P-440. Centrifugal pump cooling system.

This pump is connected to the tower cooling.

Its function is to pump the refrigeration water through the whole refrigeration system. The water is conducted to the top of the cooling tower where it falls as rain through the tower fill to the pool at the bottom.

The pump operates in the regime 2800 rev / min.

(Picture in figure 3.16)



Figure 3.16:
Centrifugal pump P-440

P-350. Piston pump

Positive displacement pump Dossapro-MiltonRoyal Maxroyal C 4kW for pumping and pressurising the feed. The aspiration is connected to PVC pipe, meanwhile the output is connected to pipe of 1/4 of AISI 316. Both connections have commercial check valves.

The pump has a three phases drive that turning an articulated device that moves a piston compresses against a body closed. The device needs oil to lubricate the shaft and has a security system formed by a relief valve rated at 300 bar. The maximum pumping capacity is 200 kg/h at a pressure of 25 MPa. The control of the race is performed by a percentage wheel located at the top. (Picture in figure 3.17)



Figure 3.17: Piston pump P-350

P-120. Piston pump

The quenching is pumped by the piston pump P-120 Dosapro Milton Roy, model M6-140 L – 14 M 300/JVV1. The maximum flow that supplies the pump is 23 kg/h. Maximum pressure supply is 300 bars. Picture in Figure 3.18



Figure 3.18: Piston pump P-120

P-220. Cryogenic pump

The operation of this device is similar to a piston pump, but with certain peculiarities. The pump is connected to a control system which regulates the pressure in the oxygen tanks; T-240 The pump has two chambers, one for the inlet and other for the outlet. Picture in figure 3.19



Figure 3.19: Cryogenic pump P-220

T-310. Waste tank

This fiberglass tank with a capacity up to 700 liters is mounted on a metal fixed platform with a external level measurement system.

This system consists on a methacrylate tube graduated with a valve plug to the bottom. The dilution water inlet takes place by a pipe of 50 mm diameter PVC. The tank has a stirrer mounted on a metal arm welded to the platform.

The discharge of waste is performed through the bottom to the pump, P-330.

T-340. Tank mixtures

Fiberglass tank with a top cover and load by the top of the container, there is also a mixer system and the outlet is at the bottom. The drain of the tank is performed through a tube of 20 mm.

V-460. Separation tank

Separator used in the for the effluent to divide the effluent in two streams, one of vapor and a other as liquid. The flash is done by depressurizing to the atmosphere the cooled fluid from for the cooler.

T-210. Oxygen Tank.

Oxygen is stored as a liquid in a pallet-tank capacity of approximately 750 kg of O₂. This pallet-tank is an isolated cryogenic tank (Dewar) that holds the liquid oxygen in equilibrium with vapor at pressures between 1 and 4 bar

T-240. Deposit bottles.

This set of four pressurized cylinders acts such a regulating system pressure in the oxygen line. The gas is stored at a pressure of between 250 and 280 bar. The outlet is performed under control through a valve which controls the flow of O₂. A pressure regulator connected at the outlet of the system ensures

that the pressure in line input is not higher than 280 bar at any time. Below the pressure set point, the cryogenic pump is switch on to increase ensure the pressure in the bottles.

Above the maximum pump stops to reload. Picture in figure 3.20



Figure 3.20:
Deposit bottles T-240

D-430. Cooling tower.

Cooling tower with forced flow with a fan fixed at the top. The fill consists in plastic material uniformly distributed in the central part of the tower. The bottom is a pool from where is carry out the load of the refrigeration water for the cooler. Picture in figure 3.21



Figure 3.21: Cooling tower
D-430

E-370. Electrical Preheater

This equipment is used during the heating plant startup to preheat the feed to a temperature of about 400 °C.

It consists on a central cylinder of brass with 4 holes where it is housed 4 electrical resistances of 2500 W of power. Around this cylinder passes a spiral stainless tube with a externally of a conductive paste to facilitate heat transfer. The whole assembly is insulated with rock wool and aluminum structure. Picture in figure 3.22



Figure 3.22: Electrical preheater E-370

In the central part of the brass cylinder there is a thermocouple which controls the power of resistance by temperature. At the inlet and the outlet there are two thermocouples respectively, to measure the behavior equipment and the heating feed.

E-420. Cooler

This device is located at the outlet of the reactor and allows decrease the temperature of the effluent before the decompression. The cooler is integrated into the cooling system which includes the tower, D-430 and P-440 pump for cooling water. The system consists on a stainless steel casing by flowing cooling water and a central cylinder on which a coil is wound titanium alloy. Picture in figure 3.23



Figure 3.23: Cooler E-420

E-230. Evaporator

This machine is a heat exchanger where increased surface produces the phase change to gas of oxygen for storage in the deposits at high pressure.. The equipment consists on a circuit of finned tubes through which oxygen circulates evaporating the liquid by direct contact with environment. Picture in figure 3.24



Figure 3.24:
Evaporator E-230

3.2.2. Pilot plant of Sciences Faculty, University of Valladolid

3.2.2.1. Introduction

The pilot Plant of SCWO is located on the Faculty of Science at the University of Valladolid. It was designed to test the destruction of various compounds by oxidation in supercritical water, using air as oxidizing agent.

The plant operates in continuous and has a treatment capacity of 25 kg / h, it has been designed to operate at pressures up to 300 MPa and temperatures between 400 °C and 700 °C inside of the reaction chamber. , diagram flow of the pilot plant with the different reactors used are shown in figure 3.25 (tubular reactor), figure 3.26 (cooled wall reactor with one outlet) and 3.27 (cooled wall reactor with two outlets)

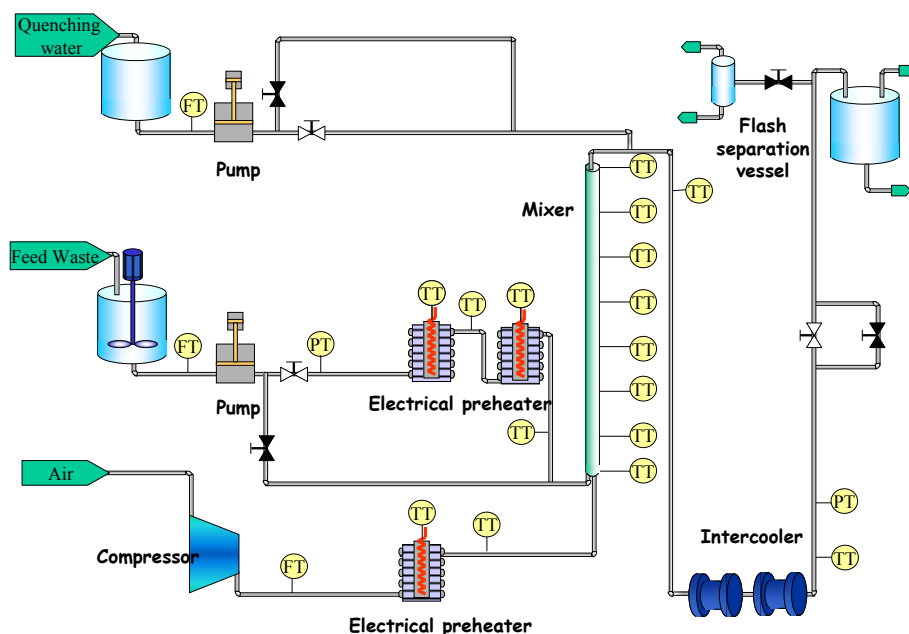


Figure 3.25: Diagram of SCWO facility of sciences faculty with the tubular reactor

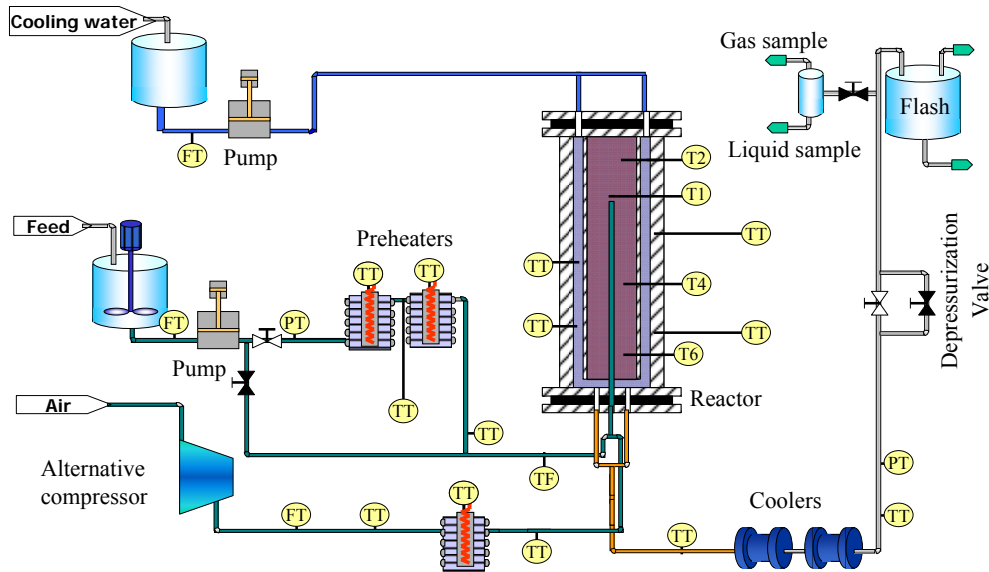


Figure 3.26: of SCWO facility of sciences faculty with the cooled wall reactor with one outlet

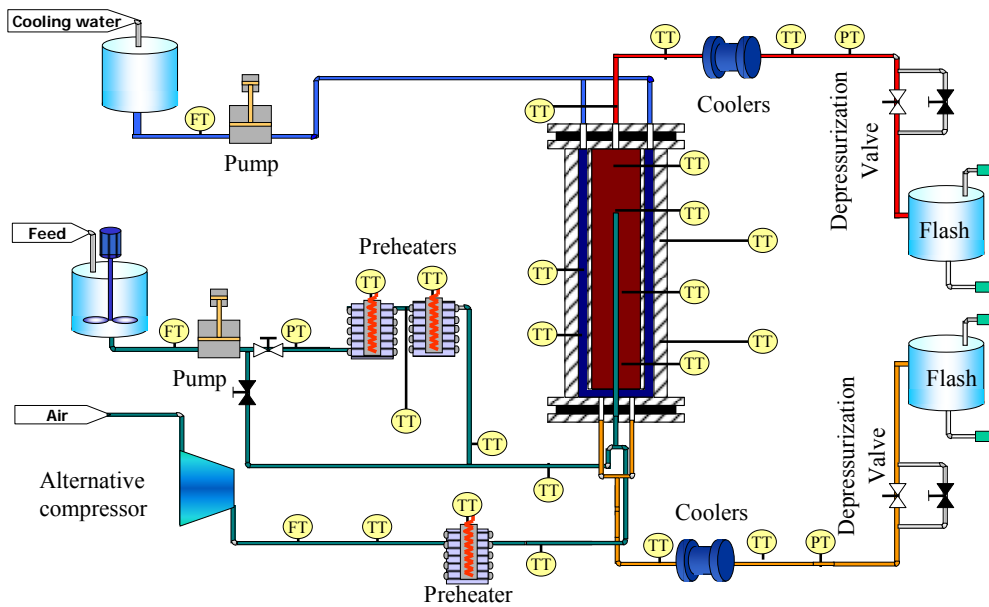


Figure 3.27: Diagram of SCWO facility of sciences faculty with the cooled wall reactor with two outlets

This plant has four main lines.

- Feed line

Aqueous solutions of flammable and sometimes toxic, are pressurized and preheated electrically.

The main equipment of this line is:

- Membrane pump, P-240. $P_{max} = 300$ bar. Flow = 22.3 L / h
- Electric preheaters, E-250 ($W = 6000$ W, $T_{max} = 600^{\circ}$ C) E-260 ($W = 8000$ W, $T_{max} = 600^{\circ}$ C)

- Air Line.

Air is introduced into the reactor after compression and heating.

The main equipment of this line is:

- 4-stage reciprocating compressor G-220. P max = 300 bar
- Electric preheater E-230 (W = 6000 W, T max = 600°C)

- Cooling water line

Introduce an auxiliary flow of water in the reactor.

The main equipment of this line is:

- Membrane Pump P-210. P max = 300 bar, flow max = 72 L / h

- Line reactor outlet.

The products from the reactor are subsequently cooled and decompressed.

The main equipment of this line is:

- Coolers: E-120, E-130 and E-170. Each cooler consists of a stainless steel coil $\frac{1}{4}$ ", L=6 m and 0.049" thick, inserted in a vessel of galvanized steel.
- Double needle valve VREL SENTRY ® 11. P max = 345 bar, flows of P: 9-240 L / h.

3.2.2.2. Process description

Feed is pumped through the P-212 pump to the tank T-241 where it is stirred to obtain a homogeneous feed. The feed (at room temperature) is pumped and pressurized by the membrane pump P-240 with a maximum flow of 22.5L/h. Then the Feed is preheated before entering the reactor through the exchangers E-250 and E-260 heating the residue to about 400 to 350 °C, in order to get the ignition temperature to create the hydrothermal flame, after that the injection temperature can be lowered to try to operate at lower inlet temperatures till room temperature

As oxidant, it is used ambient air is supplied through the compressor G-220. The air is preheated through heat exchanger E-230

The feed stream and air are mixed before entering the reactor R-110. In the reactor the oxidation process takes place which oxidize the feed reaching temperatures over

600°C–700°C. To preserve the external wall of the reactor, water is pumped into the reactor through the membrane pump P-210.

The reactor effluent is cooled by the cooler E-120 and E-130 to room temperature using cooling water system. Then the effluent is decompressed using a double needle valve V-160 Sentry VREL electrically heated to prevent freezing.

Products already cold and at atmospheric pressure are introduced in the Flash T-140 where liquid and gas are separated. There is also a T-150 sampler that is designed as a camera flash and allowing take liquid and gas samples to analyze them TOC and be able to know the percentage of removal.

For the case of the reactor with two outlets, part of the products leave the reactor by the top outlet are cooled down in the intercoolers and depressurized in a new line of the system identical at the outlet line existent.

3.2.2.3. Main equipment of the pilot plant

G-220 Air Compressor

It is a four-stage reciprocating compressor with intercooling between stages from AIR INGERSOLL_RAND, model H15T4 with a consume of 15 kW, that supports a maximum pressure of 30MPa and give a maximum and constant flow of air up to 28 kg/h. It is equipped with safety valves at the outlet of each stage and a switch able to stop if the pressure exceeds the pressure limit set by the user. Picture in figure 3.28



Figure 3.28: Air Cmpressor G-220

P-212. Centrifugal pump

The feed line has a charge pump model L-242 PRISMA 15 3M, whose function is to introduce the solutions into the tank T-241. This pump can work with maximum flows of 66L/h and a maximum height of 34m.

P-240 Membrane n pump

The feed is introduced to the reactor by the membrane pump P-240 Dosapro Milton Roy, model MB. 112.S (L) 12.M 300/VV2. The maximum flow that supplies the pump is 23 kg/h. Maximum pressure supply is 300 bar. Picture in figure 3.29



Figure 3.29: Membrane pump P-240

P-210 Piston pump

For quenching line uses a piston pump MILTON ROY Dosapro brand, model MILROYAL C - MC 61 S (Q) 20 N. This pump operates at a maximum pressure of 300 bar and offers a maximum flow of 72kg /h. Picture in figure 3.30



Figure 3.30: Piston pump P-210

T-241 Tank feed

Plastic tank as the T-241 with top cover and load by the top of the container. There is also a system agitation and the bottom outlet. The drain of the tank performed through tube 20 mm and passes through a filter. Picture in figure 3.31



Figure 3.31: Tank feed T-241

T -140, T-150. Flash tanks

Separator used in the plant effluent to separate into two streams, one of vapor and other of liquid. The flash is done by depressurizing to the atmosphere the old fluid cold from the cooler. Picture in figure 3.32



Figure 3.32: Flash tank T-140 & T-150

E -230, E-250 E-260. Electric preheaters

Electric preheaters are used during startup and operation of the plant to heat the reactants. Consist of a central cylinder of brass, with four holes which are located the electrical resistances of different powers, and Ni-alloy tube 600 ¼ externally coated by a conductive paste to facilitate heat transfer. This is isolated with rock wool and glass and coated with an aluminum casing.

There are three electric preheaters, two to the feed and one for air. All are based in the same design, but the power of the resistors are different.

Feed line E-250 and E-260 has two heaters, one of 8000W of 10 meters and a length of 6 meters 6000W pipe length, arranged in series.

Air Line E-240 has a 6000W preheater and 6 meter long tube.

Picture of the three preheaters in figure 3.33



Figure 3.33: Electrical preheaters E-230, E-250 & E-260

E-120, E-130, E-180 Coolers

For cooling the effluent there are two heat exchangers which consist on a steel coil of 6 meters length of $\frac{1}{4}$ and 0.049 thickness inserted into a container of galvanized steel.

The reactor effluent flows downstream favoring the fall of the condensates. On the exterior of the coil circulates cooling water upstream. To facilitate



Figure 3.34: Cooler E-120

contact with cooling water, the coil section has been reduced with a free flowing water welding galvanized steel pipe to the top flange. As independent units can be increased or decreased based on cooling needs. To control their right operation it is measured the inlet temperature and outlet of the reactor effluent with respective thermocouples. Picture in figure 3.34

In appendix II are collected all equipment process data sheets.

3.3. COMMON EQUIPMENT OF BOTH FACILITIES

3.3.1. Valves and pipes

Relief valves

Model HR6000 (Hoke. Figure 3.35)

Technical data

- Body construction: 316 stainless steel
- Spring material: 17-7PH CRES
- Seal material: Silicone
- Connection sizes: 1/4"
- Orifice size: 0.094"
- Cracking Pressure: 150–5000 psig (10–345 bar)
- Maximum Operating Pressure: 150–7000 psig (10–482 bar)
- Proof : 9000 psig (620 bar)
- Burst: Over 24,000 psig (1652 bar)
- Reseat Pressure: 85% min. of CP
- Temperature range -20°C to +400°C
- Cv Factors: 0.16-0.07

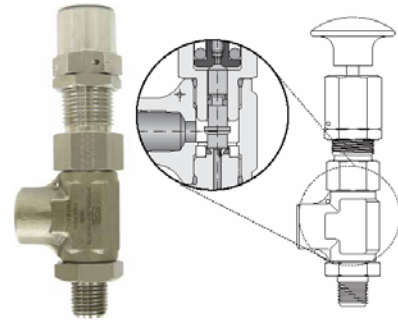


Figure 3.35: Scheme of a relief valve

Check valves

Model: 6100 series (Hoke. Figure 3.36)

Technical data

- Body Material: 316 stainless steel
- Maximum Operating Pressure: 6000 psig @ 70° F (414 bar @ 21° C)
- Standard cracking pressure: 2 psig
- Operating Temperature Range: -29° C to +177 °C
- Orifice Sizes: 0.187" (4.75mm), 0.422" (10.7mm)
- Cv Factors: 0.3 - 2.4



Figure 3.36: Check valve

Regulation valves

The control of the pressure in the reactor is carry out by a system of two valves in parallel at the outlet of the cooler as shown in figure 3,37. This dual system of pressure control is done by a needle valve and a twin screw valve for fine tuning, VREL-SENTRY. The second one is the most employed during the experiments for controlling the pressure in the range of 200-240 bar, while the first valve allows bigger pressure changes. The pipes connected to both valves wear a coiled electrical resistance to heating the pipes and compensate the effect of cooling during decompression avoiding the ice formation.



Figure 3.37: Dual system

A micrometer filter protects the sentry valve from obstructions of particles coming from the reactor outlet

VREL® - High Pressure Sample Flow Control Valve (Figure 3.38)

The VREL® is an adjustable sample pressure reducer for sample pressures above 500 psig (35 bar). A precisely machined tapered rod assembly moves inside precision holes within the barrel of the VREL®. Pressure drop is a function of the length of the rods inserted into the barrel.

- Wetted Materials: 316 stainless steel
- Weight: 4 lbs. (2 kg)
- Ratings: 5000 psig at 300°F (345 bar at 149°C)
- Standard end connection: 1/4" (6.4 mm) O.D. bare tube ends

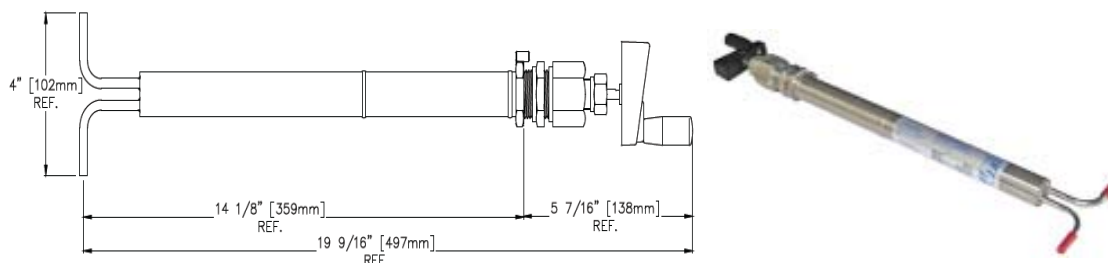


Figure 3.38: Scheme an picture of the SENTRY valve

Needle valves

Model: 1711G4Y (Hoke. Figure 3.39)

Technical data

- Inlet A 1/4" Gyrolok: 1/4" male NPT
- Outlet B 1/4" Gyrolok: 1/4" male NPT
- Body Material: 316 Stainless Steel
- Maximum Operating Pressure: 6000 psig at 70° F (414 Bar at 21° C)
- Operating Temperature Range: -65° to +450° F (-54° to +232° C)
- Cv Factor: 0.31



Figure 3.39: needle valve
Hoke

Model: 20SM4071 (Autoclave Engineers. Figure 3.40)

Technical data

- Inlet A 1/4" Gyrolok: 1/4" male NPT
- Outlet B 1/4" Gyrolok: 1/4" male NPT
- Body Material: 316 Stainless Steel
- Maximum Operating Pressure: 15000 psig at 70° F (1034 Bar at 21° C)
- Operating Temperature Range: -100° to +450° F (-72° to +232° C)
- Cv Factor: 0.20



Figure 3.40: needle valve
Autoclave Engineers

Metering Valves

Model: 1345M4Y (Hoke. Figure 3.41)

Technical data

- Connections - Inlet: 1/4" NPT Male 1/8" Gyrolok
- Connections - Outlet: 1/4" NPT Male 1/8" Gyrolok
- Flow Pattern: Globe
- Body Material: 316 Stainless Steel
- Operating Pressure Range: 5000 psig at 70° F (345 bar at 21° C)
- Operating Temperature Range: -65 to +450 °F -54 to +232°C
- Cv Factor: 0.010



Figure 3.41:
Metering valve

Burst disc

The system consists of a metal disc rating to break at 280 bar placed on a tee in the pipe service. In the SCWO plant there are available a burst discs before the entrance of the reactors and at the outlet of heaters



Figure 3.42: Device where burst disc is installed

Model: Device : SS4600 ¼-A (Autoclave Eng. Figure 3.42)

Burst Disc P-7317 ¼”

Technical data

- Max Pressure : 4056 psig a 72°F (280 bar at 23°C)

Pipes

High pressure accessories used for build a pilot plant are critical when it is build a high pressure plant as it operates. These elements are chosen in stainless steel or other materials exceptionally as Inconel or titanium in some pipes subjected to high temperatures.

The piping of the lines in the plant are made of the following materials:

- SS316 stainless steel ¼ "tubing, to service temperature and pressure.
- Inconel 600 ¼ "tubing for high temperature service
- PVC tubing 25 to 50 mm for pipes of water service.

3.3.2. Instrumentation

The control of the process is performed by measuring the temperature along the system and especially in the reactor, feed streams and air/oxygen pressure along the circuit.

The following item describes the measuring instruments used for the monitoring temperature, pressure and flow in the plant

Temperature measuring instruments

All temperature sensors used in the set up are thermocouples Type K. The installed thermocouples measure temperatures of up to either 800°C or 1200°C with an accuracy of 1% depending on the integrated transmitter producing an output signal of 4-20 mA. All temperature measurements are registered in a data base.

Pressure measurement systems

There are two types of pressure measurers, the analogical and digital, through pressure transducer that sends the electrical signal to the computer.

The analogue measurement is performed by a bourdon pressure gauge, connected to a coiled tube, as a protection system, to the line. There are available type Bourdon gauge after each pump system (precision of ± 5 bar),.

Pressure sensors, with the capacity of measuring pressures between 0 and 40MPa are located in the feed line behind the pump and at the exit of the reactors, behind the coolers. They allow the visualisation of the pressure on the computer and the registration of the pressure in the data base by transmitting a 4 to 20 mA signal.

Flow measurement

· Feed and quenching flow

To measure the liquid volume flows, which are produced by the pumps in the feed and cooling water line, a system consisting of a recipient with a determined volume and two electro valves is used. The recipient is filled by gravity while both electro valves are open. Once recipient is filled, the electro valve connected between the feed tank and the pump is closed and the pump aspirates the liquid out of the volume flow measuring device instead of the feed tank. The volume flow is now evaluated by measuring the time necessary to empty the reservoir. The calculated volume flow appears on the computer screen and is also included in the data base. (Precision ± 100 ml)

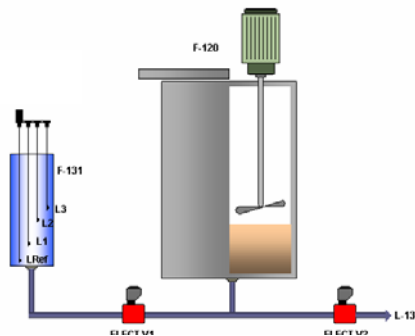


Figure 3.43: Scheme of the system for measuring the feed flow

· Air / Oxygen flow

The air / oxygen flow is measured using a Coriolis Micro Motion model brand RFT9739 R2BS, which provides a direct reading on the panel with a "display" and also sends a signal to the computer to store the value of continuous mass flow with a precision of ± 100 g.

3.3.3. Data acquisition system.

The variables measured in the plant are collected through an acquisition system data which transform the signal to the computer and record information.

The data acquisition system is based on the program LabSCADA, which has been realized by the staff of the High Pressure Processes Group of the Chemical Engineering and Environmental Technology Department at the University of Valladolid. With this program, it is possible to communicate between the data transmitters and the user interface, it covers all functions of a SCADA (Supervisory Control And Data Acquisition):

- Indication and registration of measurements
- Management of different types and levels of alarms in the measured variables
- Execution of security actions and switch off in respond to the alarms
- Permits recording of events: notes, sampling time etc.
- Permits representation of the measured variables graphically (across the whole experiment or a tendency)
- Equipped with embedded calculators to facilitate the preparation of the feed solution, the calculation of the oxidant flow and the necessary quenching flow
- Automatic calculations that facilitate the preparation of solutions of feed, and calculation of the oxidant flow ratio.

The program was adapted to the specific needs of each plant at each configuration for the different reactors used.

Location of plant control instrumentation.

The variables of the process are incorporated into a file in the operating Labscada program, where the control is carry on. However, during the operation, the plant operators must have quick and direct access to the pressure information in the pressure discharge points and outlet of the reactor, as well as temperatures within the system. The pressure is a critical variable in terms of security of the container and have analog gauges mounted two large clear panel for being viewing by the operators.

The temperature is recorded in the screening program and the flow of oxygen may be continue on the display of Coriolis. All information is just a glance at the work panel as figure 3.44 (pilot plant of Faculty of sciences) and figure 3.45 (pilot plant of CETRANSA) show.

Valves for selection of hot and cold circuits of the waste input oxygen, pressure control and security are all in the same panel.

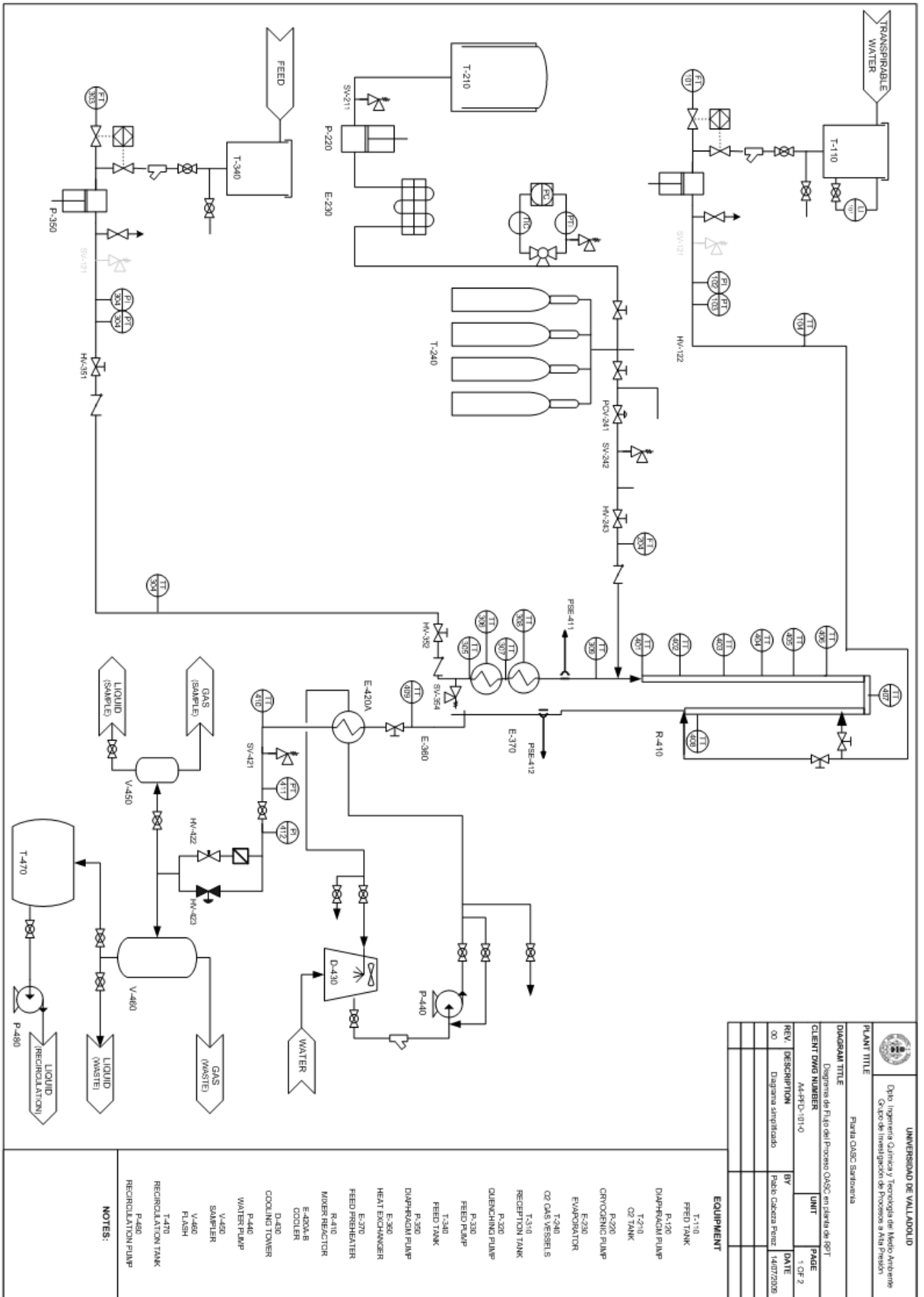


Figure 3.44: Control panel of the pilot plant of Faculty of Sciences

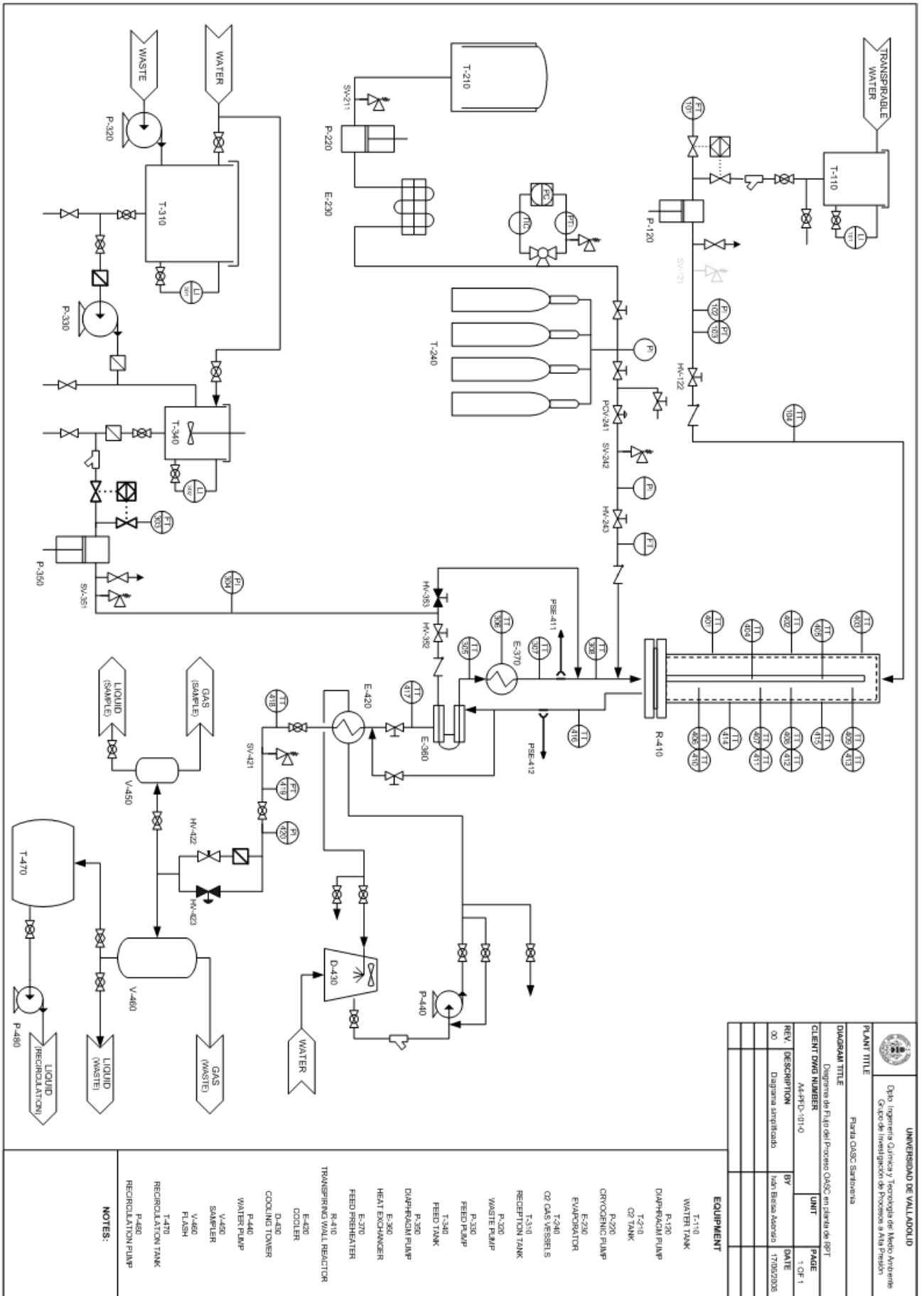


Figure 3.45: Control panel of the pilot plant of CETRANSA

In the next pages is shown the different diagram flows for the different setup used in each pilot plant:



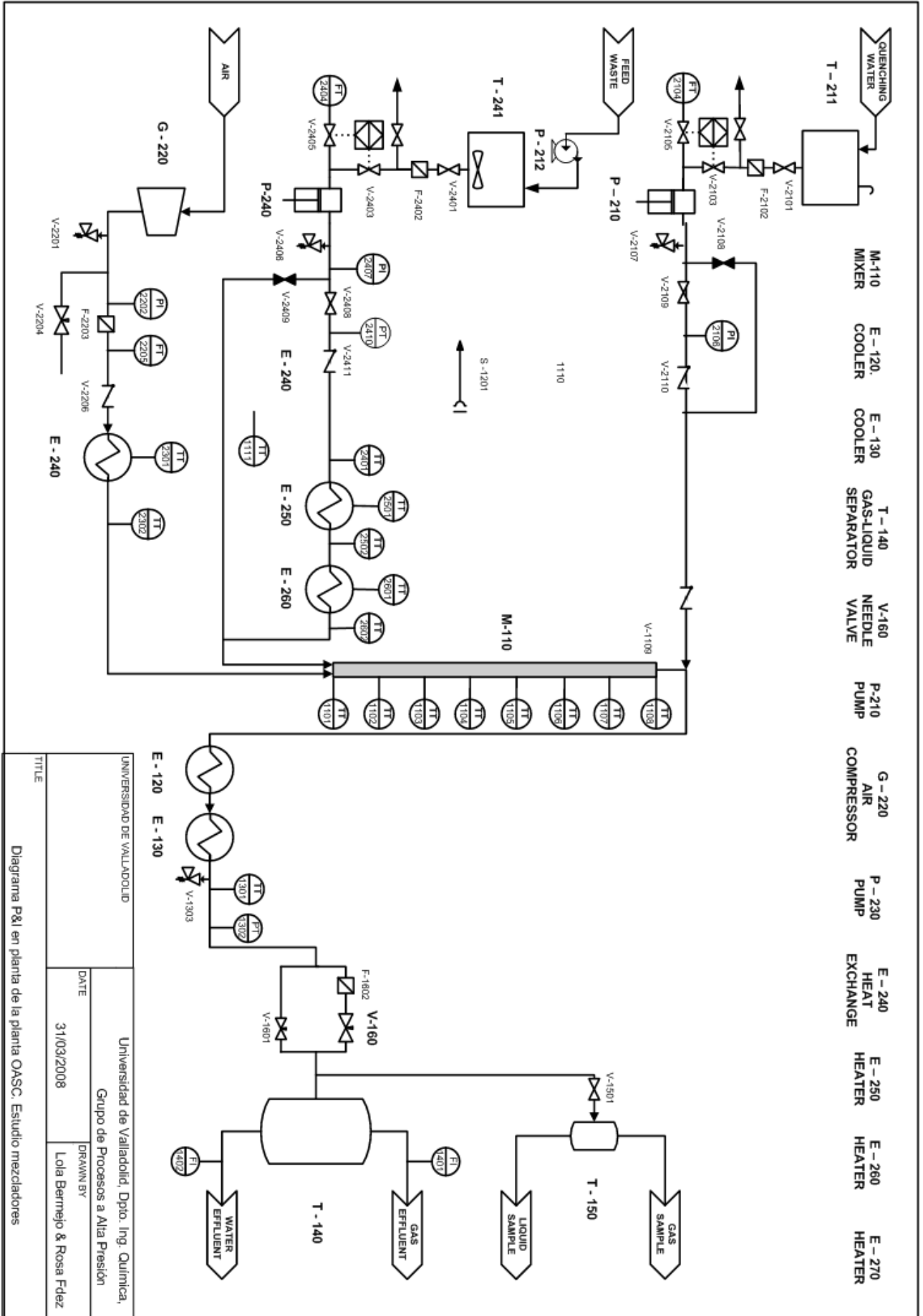
UNIVERSIDAD DE VALPARAÍSO Centro Ingeniería Química y Tecnología de Medio Ambiente Grupo de Investigación de Procesos y Alta Presión	
PLAN TITLE Planta OASB Sabinera	
DIAGRAM TITLE Diagrama de Flujo del Proceso OASB en planta de 80T	
CLIENT DWG NUMBER	UNIT
REV. DESCRIPTION	DATE
00	14/07/2008



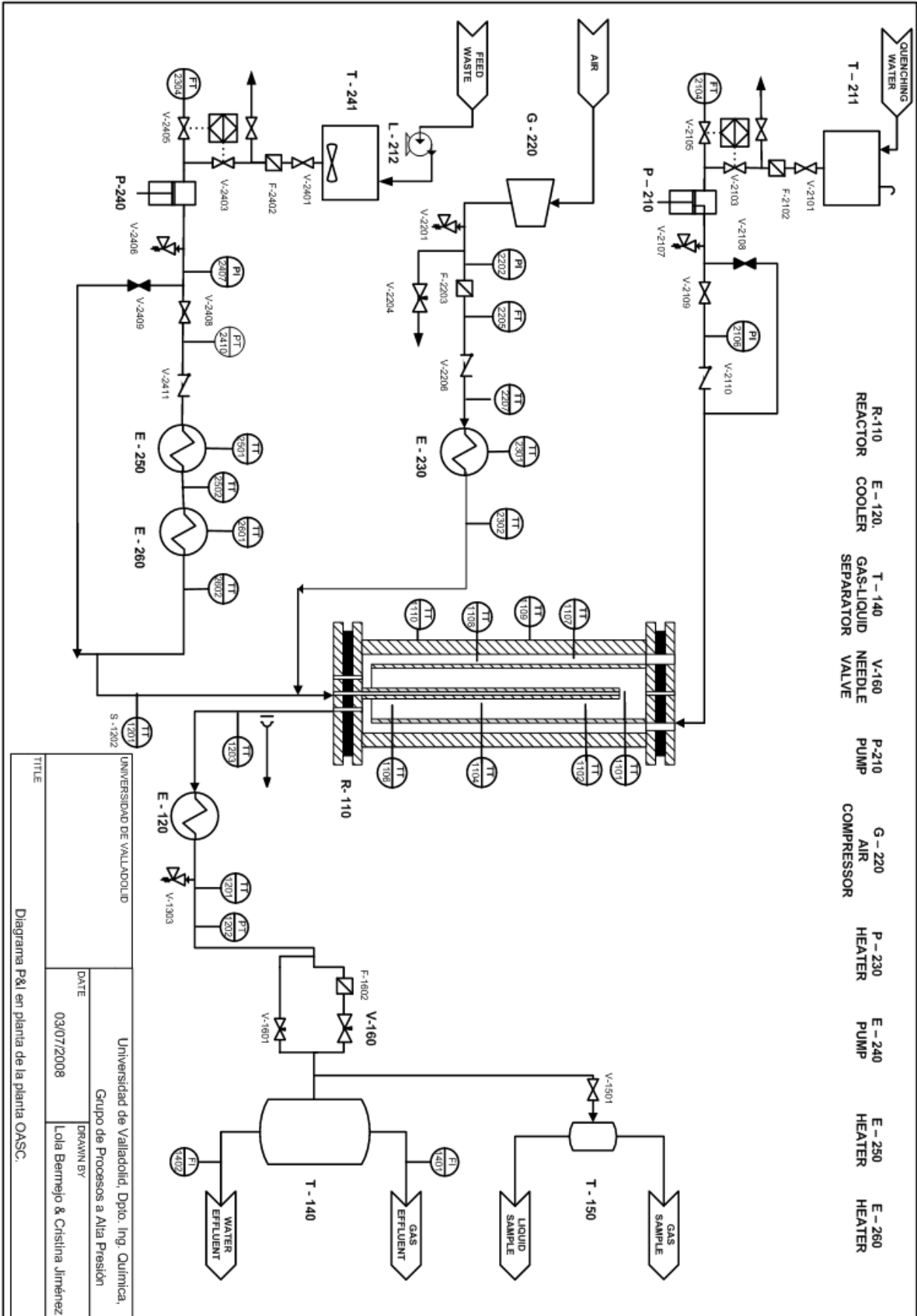
		UNIVERSIDAD DE VALPARAÍSO	
		Depto. Ingeniería Química y Tecnología de Medio Ambiente Grupo de Investigación de Procesos y Fluidos	
PLANT TITLE		Flujo QASC Saturated	
DIAGRAM TITLE		Diagrama de Flujo del proceso QASC en flujo de 80T	
CLIENT	DWG NUMBER	UNIT	PAGE
MA-FPD-011-0			1 of 1
REV / DESCRIPTION	BY	DATE	
00 Diagrama simplificado	Yván Belsa Azevedo	17/02/2008	

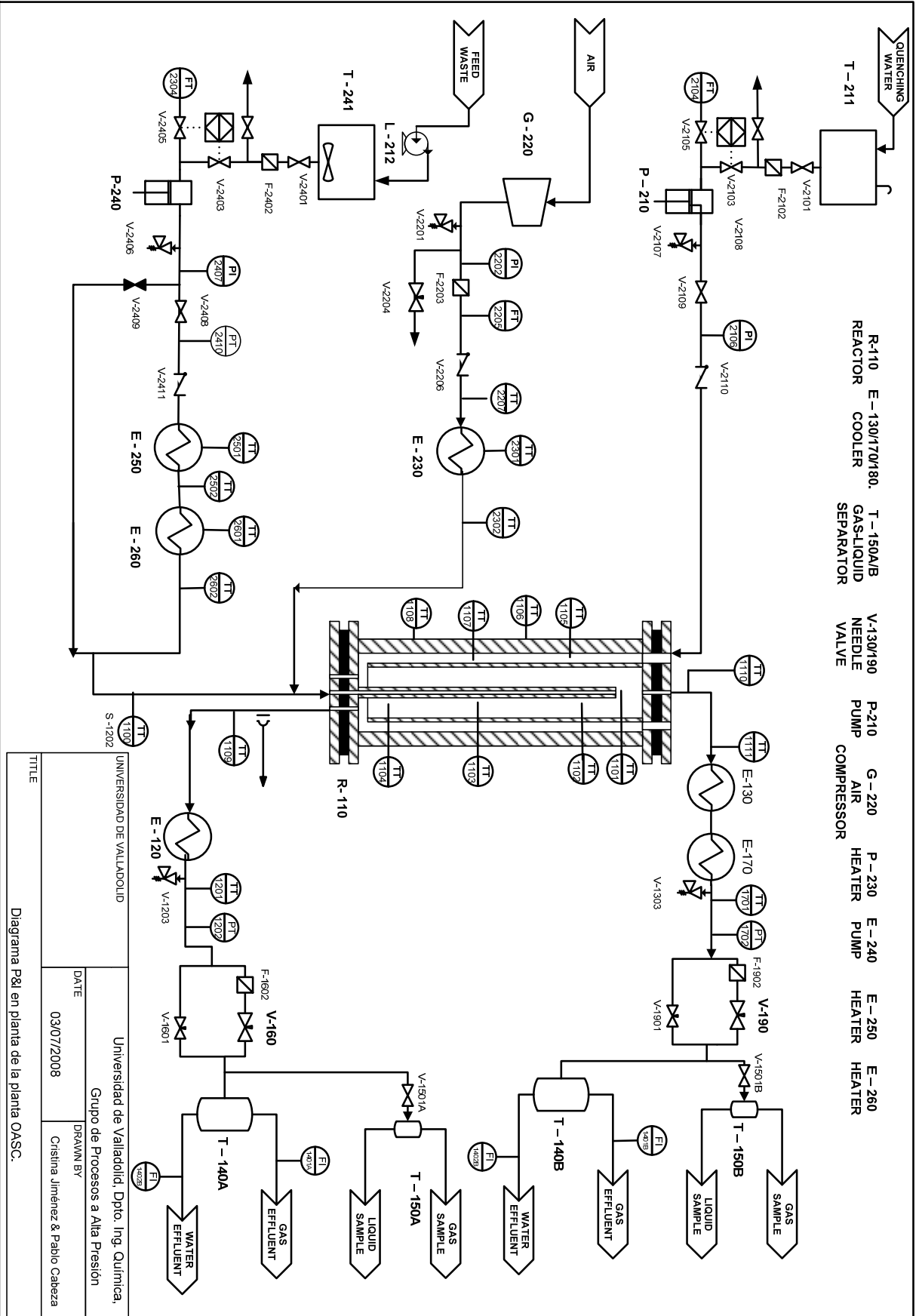
EQUIPMENT
T-110 WATER TANK
P-120 DIAPHRAGM PUMP
T-210 CO2 TANK
P-220 CRYOGENIC PUMP
E-220 EVAPORATOR
T-240 CO2 GAS VESSELS
T-310 RECEPTION TANK
P-320 WASTE PUMP
P-330 FEED PUMP
T-340 FEED TANK
P-350 DIAPHRAGM PUMP
E-360 HEAT EXCHANGER
E-370 FEED PREHEATER
R-410 TRANSPARENT WALL REACTOR
E-420 COOLER
D-430 COOLING TOWER
P-440 WATER PUMP
V-450 GAS (WASTE)
V-460 LIQUID (WASTE)
V-470 GAS (WASTE)
V-480 LIQUID (WASTE)
V-490 LIQUID (WASTE)
V-500 LIQUID (WASTE)
V-510 LIQUID (WASTE)
V-520 LIQUID (WASTE)
V-530 LIQUID (WASTE)
V-540 LIQUID (WASTE)
V-550 LIQUID (WASTE)
V-560 LIQUID (WASTE)
V-570 LIQUID (WASTE)
V-580 LIQUID (WASTE)
V-590 LIQUID (WASTE)
V-600 LIQUID (WASTE)
V-610 LIQUID (WASTE)
V-620 LIQUID (WASTE)
V-630 LIQUID (WASTE)
V-640 LIQUID (WASTE)
V-650 LIQUID (WASTE)
V-660 LIQUID (WASTE)
V-670 LIQUID (WASTE)
V-680 LIQUID (WASTE)
V-690 LIQUID (WASTE)
V-700 LIQUID (WASTE)
V-710 LIQUID (WASTE)
V-720 LIQUID (WASTE)
V-730 LIQUID (WASTE)
V-740 LIQUID (WASTE)
V-750 LIQUID (WASTE)
V-760 LIQUID (WASTE)
V-770 LIQUID (WASTE)
V-780 LIQUID (WASTE)
V-790 LIQUID (WASTE)
V-800 LIQUID (WASTE)
V-810 LIQUID (WASTE)
V-820 LIQUID (WASTE)
V-830 LIQUID (WASTE)
V-840 LIQUID (WASTE)
V-850 LIQUID (WASTE)
V-860 LIQUID (WASTE)
V-870 LIQUID (WASTE)
V-880 LIQUID (WASTE)
V-890 LIQUID (WASTE)
V-900 LIQUID (WASTE)
V-910 LIQUID (WASTE)
V-920 LIQUID (WASTE)
V-930 LIQUID (WASTE)
V-940 LIQUID (WASTE)
V-950 LIQUID (WASTE)
V-960 LIQUID (WASTE)
V-970 LIQUID (WASTE)
V-980 LIQUID (WASTE)
V-990 LIQUID (WASTE)
V-1000 LIQUID (WASTE)

NOTES:



UNIVERSIDAD DE VALLADOLID		Universidad de Valladolid, Dpto. Ing. Química,	
GRUPO DE PROCESOS A ALTA PRESIÓN		Grupo de Procesos a Alta Presión	
DATE	31/03/2008	DRAWN BY	Lola Bermejo & Rosa Fdez
TITLE Diagrama P&I en planta de la planta OASC. Estudio mezcladores			





UNIVERSIDAD DE VALLADOLID		Universidad de Valladolid, Dpto. Ing. Química, Grupo de Procesos a Alta Presión	
DATE	03/07/2008	DRAWN BY	Cristina Jiménez & Pablo Cabeza
TITLE Diagrama P&I en planta de la planta OASC.			

CHAPTER 4

TUBULAR REACTORS

CHAPTER 4

TUBULAR REACTORS

TABLE OF CONTENTS

4.1 EXPERIMENTAL STUDY OF HYDROTHERMAL FLAMES INITIATION USING DIFFERENT STATIC MIXER CONFIGURATIONS.....	119
4.1.1 INTRODUCTION	120
4.1.2 EXPERIMENTAL.....	122
4.1.2.1 Experimental set up.....	122
4.1.3. RESULTS AND DISCUSSION.....	127
4.1.3.1 Description of the results	127
4.1.3.2 Modeling.....	128
4.1.3.3 Determination of autoignition temperatures	129
4.1.3.4 Influence of the operation parameters.....	131
4.1.3.5 Comparison of the performance of the different mixers.....	134
4.1.3.6 TOC removal	137
4.1.4. CONCLUSIONS.....	138
4.1.5. REFERENCES	139
4.2.EXPERIMENTAL STUDY OF THE SUPERCRITICAL WATER OXIDATION OF RECALCITRANT COMPOUNDS UNDER HYDROTHERMAL FLAMES USING TUBULAR REACTORS.....	145
4.2.1. INTRODUCTION	145
4.2.2. EXPERIMENTAL.....	147
4.2.2.1 Experimental set up.....	147
4.2.2.2 Experimental procedure	149
4.2.2.3 Materials	149
4.2.3. RESULTS AND DISCUSSION.....	151
4.2.3.1 Influence of IPA concentration on the hydrothermal flame formation.....	151
4.2.3.2 Oxidation of an industrial waste containing Acetic Acid	153
4.2.3.3 Oxidation of aqueous mixtures of NH ₃ -IPA.....	155
4.2.4. CONCLUSIONS.....	162
4.2.5. REFERENCES	165

4.1. EXPERIMENTAL STUDY OF HYDROTHERMAL FLAMES INITIATION USING DIFFERENT STATIC MIXER CONFIGURATIONS

ABSTRACT

The object of this work is to study by experiments the initiation of the SCWO reaction of concentrated IPA solutions, by mixing a water + IPA stream and an air stream in different static mixers at different operational conditions (temperature, fuel concentration, velocity). The start of the reaction was monitored experimentally measuring the temperature inside the mixer and by TOC determination in liquid samples. The experimental facility was modeled to assume plug flow and using different kinetic models in order to represent accurately the experimental data. It was found that at temperatures lower than 450-500°C, depending on the mixer design, the reaction proceeded slowly, and when reaching higher temperatures the sharp increase indicated a much faster reaction mechanism. The description of the phenomenon is similar to the ignition of hydrothermal flames described in literature. In these cases TOC removals higher than 99% were reached in residence as low as 0.4 s. Ignition temperatures and minimum ignition injection temperatures were determined for the different mixer and experimental conditions.

4.1.1. INTRODUCTION

Supercritical water oxidation (SCWO) technology presents important environmental advantages for the treatment of industrial wastes [1, 2]. With the appropriate reaction temperatures almost any pollutant can be completely destroyed by SCWO, with residence times of a few seconds [3, 4]. The SCWO technology also presents some challenges related with the harsh operational conditions: salt deposition and corrosion. But these difficulties can be overcome by the use of appropriate construction materials and the development of new reactor designs [3-6].

Injection of the wastes at subcritical temperature has become an important aspect in the design of new SCWO reactors. In our group's previous work [7] it was found that using a transpiring wall reactor with a tubular mixer and back mixing area in the top, reaction can be initiated injecting the feed at temperatures as low as 150°C. We found very different results when working with different mixers. Oh et al reported the performance of a MODAR reactor with a down flow tubular injector and a reaction chamber with a recirculation area working with injection temperatures of 25°C for the feed and 200°C for the air flow. The mixing of the oxidant and the waste aqueous stream previous to the reaction, and the way the reaction starts, seem to be key aspects when designing a new reactor. Despite its importance, there is very little work done in this subject [8-11].

In the ETH of Zurich, the direct injection of the waste into a hydrothermal flame generated inside the reactor was developed as a solution to avoid the external preheating of the wastes up to supercritical conditions [12-15]. Hydrothermal flames were first described by Franck and coworkers [16-18]. The presence of a flame in a SCWO system would be expected to enhance the destructive abilities of the SCW medium [19, 20]. However, only a few works about hydrothermal flames have been published, among them the works of Steeper et al [21]; Serikawa et al [22] and Sobhy et al [20]. Also some works treating the modeling of hydrothermal flames has been published [23, 24]. The subject has been thoroughly revised by Augustine & Tester [19]. In general, most of the researchers used reaction chambers in which an oxidant stream (air, or pure oxygen) was introduced into a chamber containing a mixture of a fuel (generally methane, methanol or isopropyl alcohol) with supercritical water. In general, flames ignited spontaneously beyond a certain temperature, normally between 400 and 500°C. This autoignition temperature was higher for lower fuel

concentrations. There was a minimum temperature and a concentration under which flames were not produced. As the fuel concentration decreased the flame lost temperature and luminosity, but even when the luminosity was gone, the flame structure was maintained. In general, the conditions of the flame ignition depended on the fuel, the oxidant, the ratio of fuel/oxidant and the geometry of the injection system.

The object of this work was the study of the start of the reaction of supercritical water oxidation and hydrothermal flame formation. Vessel reactors usually need of a tubular mixer or injectors for the internal flame. The importance of mixer choice was made evident in our previous experiments. We suspect that initiation of the reaction and ignition of hydrothermal flames is produced inside of the mixers as a premixed flame (the hydrothermal flames described so far are non premixed or diffusion flames). Thus, in this work the reaction initiation will be studied in different isolated tubular mixers, that is, the mixers will be working outside a reaction chamber. In order to do this the temperature profile inside the tubes was monitored. The small volume of the mixer will allow the observation of effects difficult to appreciate when the hydrothermal flame is produced inside of a reaction chamber. The small residence times inside of the mixers and the elevated number of temperature measurements to allow having a more detailed vision of the insight of the flame initiation and made possible to find a kinetic model that reproduce accurately the data. When the reaction happens in a much bigger reaction chamber the temperature increases are absorbed by the mass contained in the big volume and the elevated residence times difficult to make evident the high reaction rates. It was observed that at lower temperatures the reaction proceeded at a lower rate and could be reproduced using literature kinetic reaction rates. When reaching a certain temperature a rapid increase of temperature was observed, much faster than the reaction rates described in literature. This phenomenon can be associated to the ignition of a hydrothermal flame inside of the mixers. Different ignition conditions were found using different mixer configurations, but the phenomenon is associated with higher inlet temperatures of the mixture.

4.1.2. EXPERIMENTAL

4.1.2.1. Experimental set up

All the experiments were carried out in the pilot plant of the University of Valladolid. It has a maximum capacity of 20 kg/h feed and uses air as an oxidant compressed by a four staged reciprocating compressor. Both air and feed are electrically preheated before being introduced in the tubular mixers. Temperatures in the mixing point and in several points of the mixers are monitored. After leaving the mixer the reaction mixture is quenched. The products of the reactor are cooled in the intercoolers after leaving the reactor, and afterwards depressurization samples of the liquid and gas effluents can be taken. A flow diagram of the pilot plant is shown in figure 4.1.1.

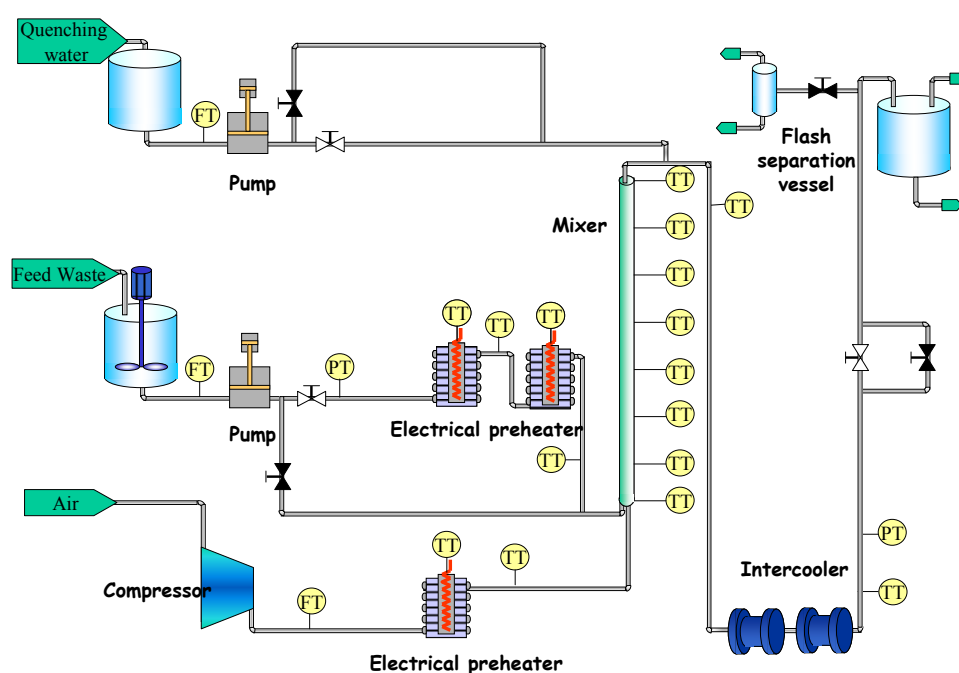
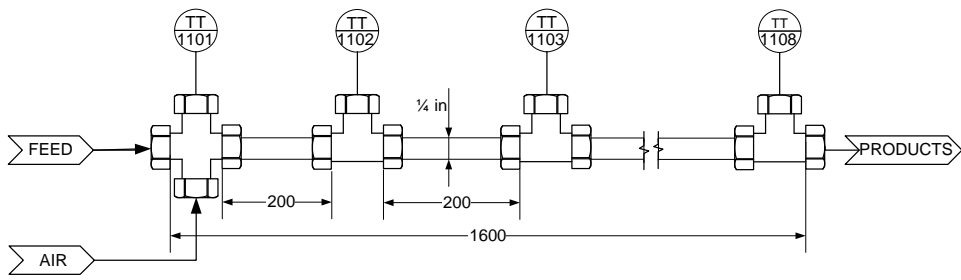
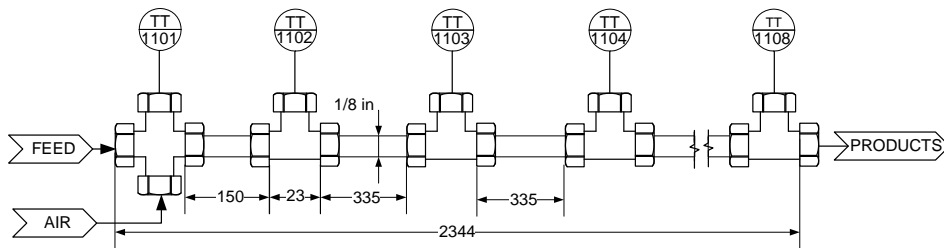


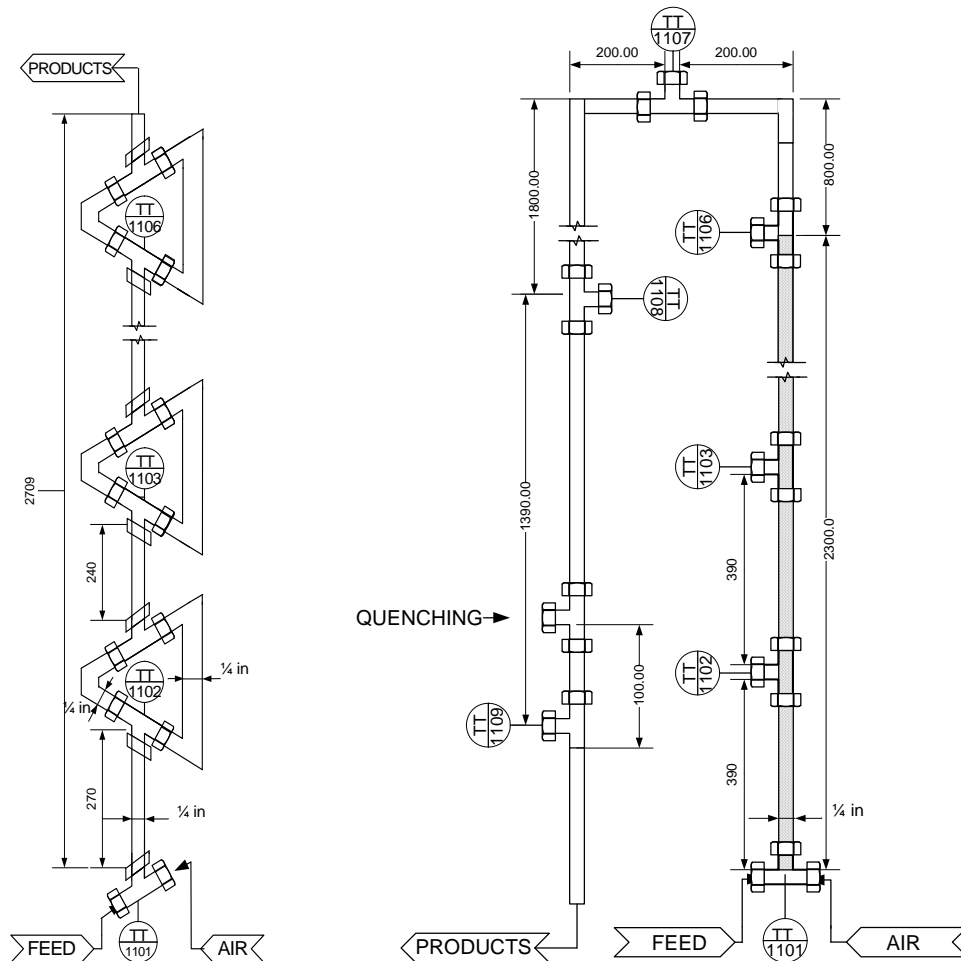
Figure 4.1.1: Flow diagram of the facility



Mixer 1



Mixer 2



Mixer 3

Mixer 4

Figure 4.1.2: Schemes of the mixers used in this study

Four mixers were studied. All the mixers were constructed with commercial Ni alloy C-276 tubing of $\frac{1}{4}$ " (i.d. 3.86 mm) and $\frac{1}{8}$ " (i.d. 1.75 mm). All of them were thermally isolated. Temperatures were measured with thermocouples type K (temperature range from 0 to 1000°C) with an accuracy of 1%. Their disposition and dimensions are represented in figure 4.1.2

· *Mixer 1* consisted of an $\frac{1}{4}$ " straight and empty tube with a length of 1584 mm and an internal volume of 18.5 mL. The flow inside the tube was upwards. Temperature was monitored using 8 thermocouples. Feed was injected to the bottom while air is injected perpendicularly.

· *Mixer 2* consisted of an $\frac{1}{8}$ " straight and empty tube with a length of 2344 mm and an internal volume of 5.63 mL. The flow inside the tube was upwards. Temperature was monitored using 8 thermocouples. Feed was injected to the bottom while air is injected perpendicularly.

· *Mixer 3* consisted of $\frac{1}{4}$ " straight and empty tube portions connected by portions where the flow is bifurcated and reversed, before being mixed again, producing a general upward flow. In this way the fluid elements containing air and feed are cut and mixed as shown in figure 4.1.3. The mixer had an internal volume of 31.75 mL. Temperature was monitored with 6 thermocouples. In this design feed and air inlets are opposite each other.

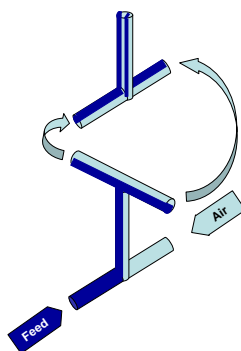


Figure 4.1.3: Scheme of how mixer 3 has worked

· *Mixer 4* consisted of four sections constructed using $\frac{1}{4}$ " straight tube. The first one has an upward flow and was filled with 2-3 mm AISI 316 rings giving a porosity of 50% and an internal volume of 12.2 mL. In this section temperature was monitored by 6 thermocouples. After this section there was an upflow empty tube of the same dimensions followed by a horizontal section, where temperature was also monitored and a downflow section where temperature was monitored as well. In this way it was

possible to monitor if the reaction ignited after the filled tube. The total internal volume was 47.3 L. Again, feed and air inlets are opposite each other.

All the feed used for the experiments consisted of synthetic solutions of isopropyl alcohol (IPA) (Technical 99% mass supplied by COFARCAS, Spain). Tap water was used without further purification, except in experiments performed in mixer 2, where distilled water was used to avoid plugging. All the TOC analyses of the samples were performed with a TOC5050 SHIMADZU Total Organic Carbon Analyzer. Air flow was measured with a Coriolis gas flow meter to a precision of 0.2%. To determine liquid flows, the time needed to fill a fixed volume was measured. IPA solutions were prepared volumetrically, measuring water volume to a precision of 1 L and IPA volume to a precision of 1 mL, resulting in an experimental error of 0.2% mass for a 4% mass and 5% mass IPA solutions.

4.1.2.2. Experimental procedure

At the beginning of a new experiment, the mixer was preheated by passing a supercritical water flow until all the thermocouples indicated temperatures higher than 400°C. Air flow was then introduced at 0-10% of the stoichiometry amount. When ignition occurred, the temperature increased sharply inside the mixer and in that moment quenching water was connected. Apart from the electrical preheating of the reagents no more heat was supplied to the system, the mixer being autothermal. That means that all the temperature rises produced inside of the mixer were due to the release of the heat of reaction during the oxidation of IPA. The system was maintained in stationary state and samples were taken. Temperature profiles were registered automatically. After sample taking, experimental conditions were changed, by reducing the temperature or by modifying feed flow. Samples were taken again when a new stationary state was reached. When no apparent increase of temperature over the mixer inlet temperature (registered by thermocouple TT1101 in the figure 4.1.2) was detected, samples were taken and after that, the experiment was finished. In every experiment a number of 1-4 stationary states could be evaluated depending on experimental conditions.

In all the experimental data, the investigated reagent mixtures (water + air) investigated were injected into the mixer, forming a homogeneous phase. That means that when the T-x conditions of the mixtures at the inlet of the mixer are represented in a Liquid-vapor diagram of the water-air mixture, all of them were situated in the vapor phase area. Figure 4.1.4 shows the experimental temperature vs composition conditions of the experimental data, plotted together with the bubble points line calculated using the Anderko-Pitzer EoS [25, 26] and using the parameters fixed for the water-air system [27].

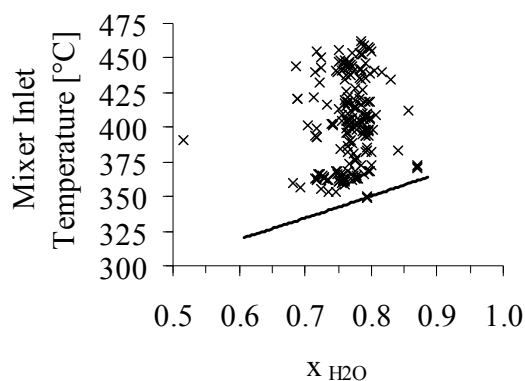


Figure 4.1.4: Experimental mixer inlet temperature vs water molar fraction of the mixture. They are plotted with the bubble point line calculated with the Anderko-Pitzer EoS. All the experimental points are found in the one phase area.

4.1.3. RESULTS AND DISCUSSION

4.1.3.1. Description of the results

Experiments with different feed flow rates, mixer injection temperatures and isopropanol concentrations were performed as displayed table 4.1.1.

Table 4.1.1: Operational conditions of the experiments

Mixer	% mass IPA	Feed Mass Flow [kg/h]	Injection temperature Range [°C]	
			Min	max
1	4	5.9	349	394
		7.4	353	415
		12.9	416	424
		18.0	401	422
	5	12.0	402	428
2	4	7.3	356	403
3	4	5.6	382	408
		7.4	386	420
		8.8	382	419
		9.7	396	407
4	4	5.8	434	444
		7.4	434	456
		8.6	443	463
		10.0	432	453

Three types of temperature profiles were obtained working with mixer 1 depending on the operational conditions. Examples are shown in figure 4.1.5. In the type a) profiles the temperature increased sharply from the mixing point. In the type b) profiles the temperature of the reaction mixture increased slowly until reaching a temperature in which a rapid increase of temperature was observed. In the type c) profiles the mixture gained temperature very slowly along the mixer. Similar temperature profiles were obtained working with the other mixers.

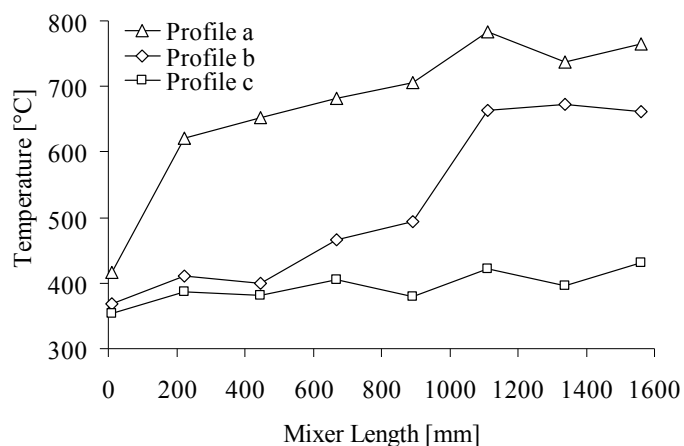


Figure 4.1.5: Examples of temperature profiles found in mixer 1. Profile a) Feed Flow: 12.9 kg/h; Mixer inlet temperature: 417°C; profile b) Feed Flow: 7.51 kg/h; Mixer inlet temperature: 368°C; profile c) Feed Flow: 7.51 kg/h; Mixer inlet temperature: 353°C

4.1.3.2. Modeling

The temperature profiles were compared to the predictions of a model that considered a plug flow reactor in steady state. The model had the characteristics of other models developed by the High Pressure Process Group of the University of Valladolid [28, 29]. In this model, only mass and energy balances were considered. Densities and enthalpies were calculated as a function of composition and temperature using the PR EoS with the translated volume correction [30]. The predictions of two kinetics models were compared to the experimental temperature profiles: the model by Li et al. [31] and the model by Hunter et al [32]. Li et al. [31] suggested that the oxidation kinetics involved the direct oxidation of the IPA and the formation and destruction of rate controlling intermediates. In our case acetic acid was considered as the only intermediate. The reaction rate constants were taken from Wightman [33]. The model of Hunter et al [32] considered that all the IPA was converted into acetone that oxidized to CO₂.

Type c) profiles were reproduced using the kinetic model developed by Li et al [31]. The slow temperature rise of type b) profiles was also reproduced using the same kinetic model. The model of Hunter et al [32] predicted even slower temperature increases than these of type c) profiles. Comparisons of some predictions to the experimental temperature profiles are shown in figure 4.1.6.

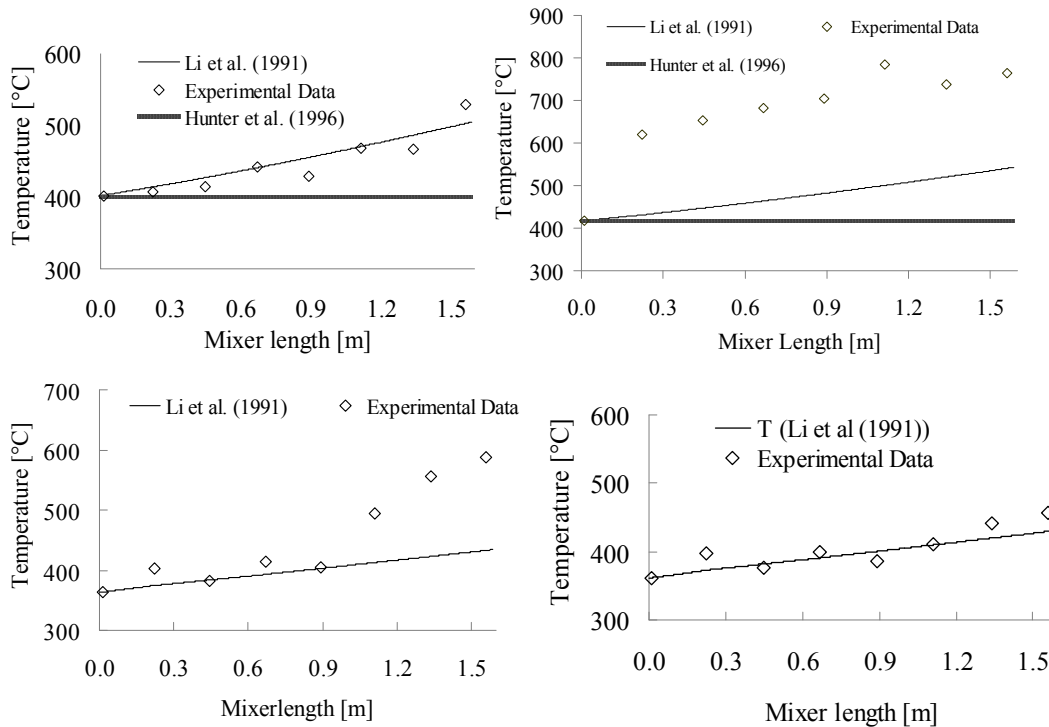


Figure 4.1.6: Comparison of the experimental temperature profile to the predictions of the kinetic models.

4.1.3.3. Determination of autoignition temperatures

All the mixers used were autothermal. This means that the temperature increases were due to the heat released by the almost instantaneous oxidation of the IPA. Thus, the rapid increases of temperature were associated with a change in the reaction mechanism favored by the high temperatures. The phenomenon observed was very similar to the formation of hydrothermal flames described in literature [19-22]. Serikawa et al [22] described the formation of hydrothermal flames using IPA as a fuel and air as an oxidant. They found that working at temperatures higher than 470°C spontaneous ignition was produced. If the mixture was injected at lower temperatures the reaction proceeded without flame until reaching the temperature at which the flames ignited. Flames were obtained with concentrations higher than 10000 ppm and flameless oxidation was impossible at concentrations higher than 24000 ppm (4% mass IPA).

We observed that ignition began with a rapid increase in temperature in one point, normally at the end of the mixer. Immediately the high temperature propagated along the mixer towards the injection points of the reagents, as shown in figure 4.1.7. This

behavior is similar to the description of the ignition of a premixed flame and the displacement of the flame front.

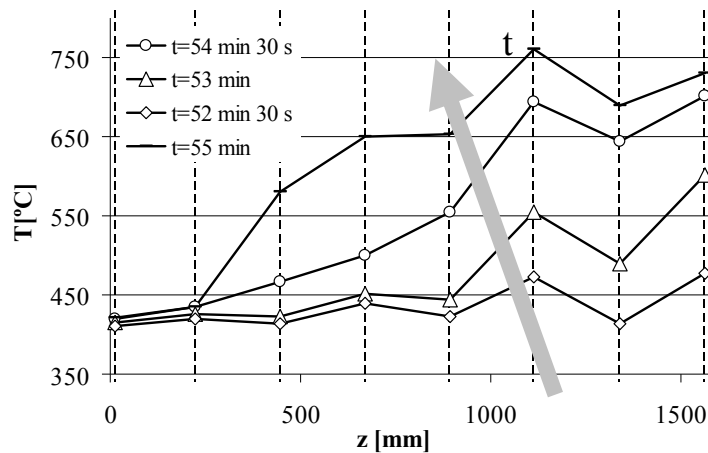


Figure 4.1.7: Ignition process. Evolution of the temperature profile with time. Feed flow: 13 kg/h, 5% mass IPA, Mixer inlet temperature= 410°C

Since inside of the mixer ignition was produced without any external energy source, we can describe the temperature immediately before the sharp increase as the autoignition temperature. Even when ignition is essentially a non-stationary phenomenon, we can consider that our change of reaction mechanism is due to an ignition. As our mixers are working in turbulent regime, it is well known that they operate with plug flow. Therefore, it is accepted that every new element fluid element does not mix with the preceding or the following elements. Thus, every new fluid element is ignited spontaneously when reaching a certain temperature. That means that the temperature at which the sharp temperature increase along the length of the reactor is produced can also be considered an autoignition temperature.

We determine this temperature as the point beyond which the majority of the data ignited. This temperature was determined for each mixer as showed in Table 4.1.2. Lowest autoignition temperature was observed working with mixer one.

Table 4.1.2: Autoignition temperature for the different mixers and general

Mixer	$T_{\text{autoig}} [^{\circ}\text{C}]$
1	450
2	486
3	482
4	505
Average	492

4.1.3.4. Influence of the operation parameters

The residence time that the reagents spent in the mixer before the ignition (*starting residence time*) was studied as a function of the mixer inlet temperature. The minimum mixer inlet temperature at which the flame was maintained in the monitored volume is called *limiting temperature*. The influences of the mixer, the feed flow and the fuel concentration were also studied.

4.1.3.4.1. Influence of the mixer. Figure 4.1.8 (a) shows starting residence times represented versus mixer inlet temperatures for different mixer configurations at a constant feed flow of 7.5 kg/h and 4% mass IPA. Only the data where a flame was produced inside of the mixer were considered, that is, in type (a) and (b) temperature profiles. It was observed that the lowest injection temperature at which oxidation with flame was produced was of about 360°C. At this temperature the reagents spent a residence time of 0.7 s in the mixer before reaching the flame front. When the mixer inlet temperature was increased higher than 375°C ignition was produced almost in the inlet of the mixer. Working with mixer 2 ignition happened within the same range of injection temperatures. In mixer 3 an injection temperature higher than 390°C and a residence time of 1.4 s were necessary for ignition, but at higher temperatures, residence time before ignition was reduced to 0.2 s. For mixer 4 minimum inlet temperatures of 430°C and residence times of 1.2 s were necessary. At temperatures higher than 450°C ignition occurred almost straight away in the mixer.

4.1.3.4.2. Influence of the feed flow. Figure 4.1.8 (b) shows the limiting inlet temperature for each mixer as a function of the feed flow. It was found that the highest limiting inlet temperatures were in mixer 4, while the lowest limiting temperatures were in mixer 1. In mixer 2 flames were only flames at flows of 7.5 kg/h. At higher flows the flame was probably blown out of the mixer. In mixers 3 and 4 the feed flow only slightly influenced the limiting temperature. In mixer 1 the influence of the feed flow was important, especially at low feed flows. At low feed flows (6 kg/h), that is, low velocities, the limiting injection temperature was as low as 350°C. Figure 4.1.8 (c) depicts starting residence time vs mixer inlet temperature for different feed flows using mixer 1 at a constant IPA concentration of 4% mass. It was observed that ignition occurred at lower temperatures with lower feed flows. For very low temperatures the residence time necessary for producing the ignition of the reagents was of 0.5 s for feed flows of 6 kg/h and 0.7 s for feed flows of 7.5 kg/h. At

higher temperatures, ignition occurred just at the beginning of the mixer. For higher feed flows (13 kg/h and 18 kg/h) ignition was only possible at injection temperatures higher than 400°C and it always occurred at the beginning of the mixer. In the magnification of the figure 4.1.8 (c) for $T > 380^\circ\text{C}$, it can be observed that residence times for ignition with flows of 18 kg/h were slightly lower than for feed flows of 13 kg/h and that of 7.5 kg/h at the same conditions, but this influence is almost negligible.

4.1.3.4.3. Influence of the fuel concentration. In figure 4.1.8 (d) data of starting residence time vs mixer inlet temperature in mixer 1 are depicted for different IPA concentrations and a feed flow of 12 kg/h. Only a very slight reduction in starting residence time was appreciated when increasing IPA concentration by 1% mass.

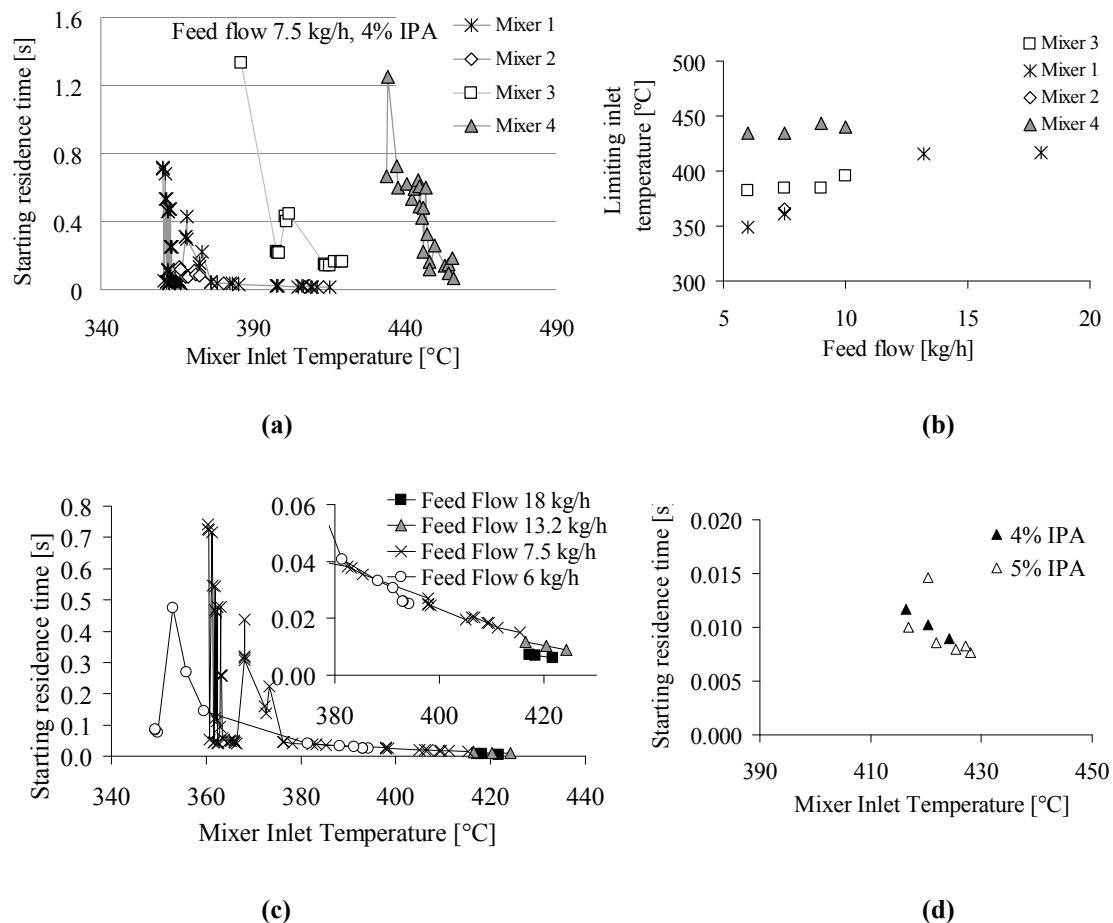


Figure 4.1.8: Study of the influence of the mixer inlet temperature on the residence time before ignition (starting residence time). **(a)** Starting residence time vs mixer inlet temperature for different mixer configurations at a constant feed flow of 7.5 kg/h and 4% mass IPA. **(b)** Limiting inlet temperature for ignition as a function of the feed flow for different mixers. **(c)** Starting residence time vs mixer inlet temperature for different feed flows using mixer 1 at a constant IPA concentration of 4% mass. **(d)** Starting residence time vs mixer inlet temperature for different IPA concentrations using mixer 1 and a feed flow of 12 kg/h.

4.1.3.4.4. Influence of the air excess and air temperature. The influences of the air temperature and the amount of air in excess over the stoichiometric were experimentally studied. It was found that temperature had only little effect in the starting residence time, while the air excess had a significant influence. To illustrate this effect several temperature profiles have been depicted in figure 4.1.9. The feed flow and feed temperature were kept constant for different air temperatures and excesses. In figure 4.1.9 a) and b) it is evident that the air excess has a strongest influence in delaying the ignition than air temperature. When the air temperature is very low in comparison with the feed temperature the temperature decreased forming a minimum just before ignition. In figure 4.1.9 c) two data with similar air excess and different air temperature are depicted. Ignition was almost simultaneous even with temperature differences of 40°C. For higher air temperature differences (almost 100°C) the ignition process was slower when air temperature was lower as illustrated in figure 4.1.9 d).

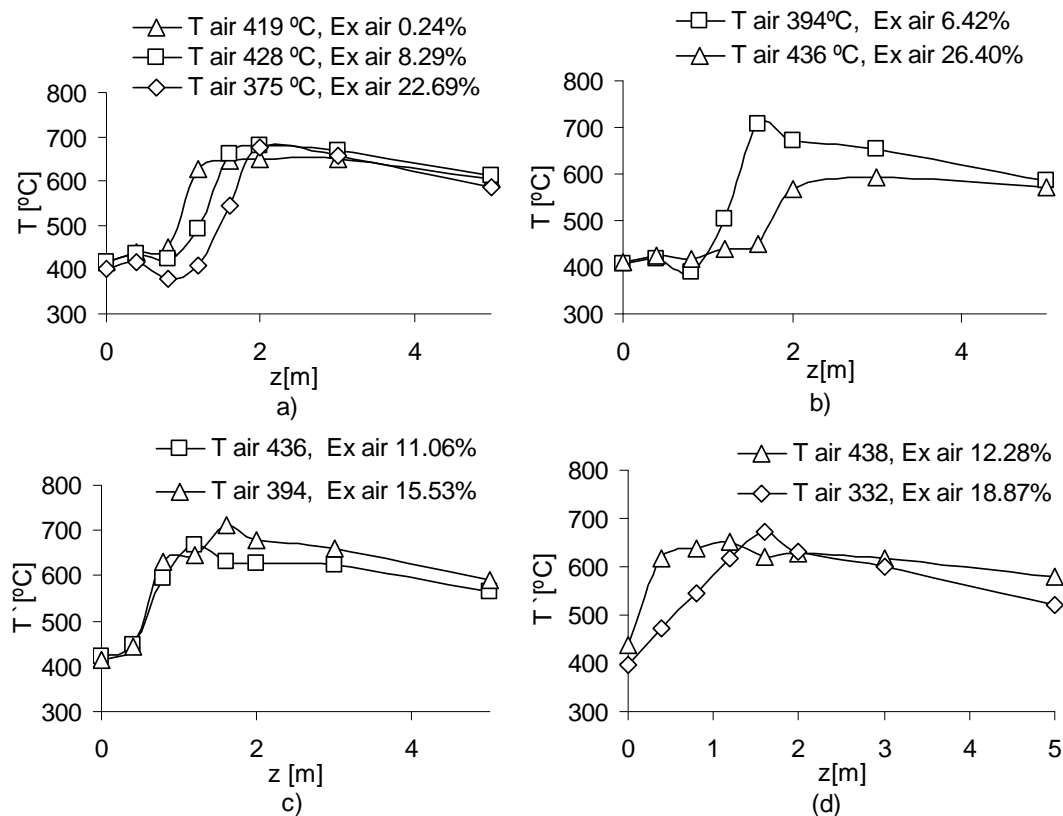


Figure 4.1.9: Temperature profile of several experimental data at a constant feed flow and feed temperature, changing air temperature and air excess over the stoichiometric amount for an IPA concentration of 4% mass **a)** Feed flow= 7.5 kg/h, $T_{\text{Feed}}=477^{\circ}\text{C}$; **b)** Feed flow= 7.4 kg/h, $T_{\text{Feed}}=462^{\circ}\text{C}$; **c)** Feed flow= 7.5 kg/h, $T_{\text{Feed}}=485^{\circ}\text{C}$; **d)** Feed flow= 7.5 kg/h, $T_{\text{Feed}}=510^{\circ}\text{C}$.

4.1.3.5. Comparison of the performance of the different mixers

In figure 4.1.10, comparisons of the temperature profiles obtained in the same operational conditions for different mixers are shown. In all the examples it was observed that ignition proceeded faster in mixer 1. It was observed that in mixer 2, temperature increase was slower, while in mixer 3, an elapsed residence time was necessary to produce the ignition.

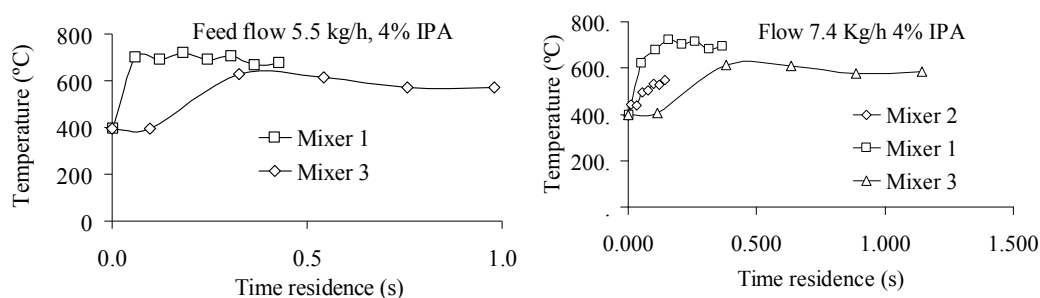


Figure 4.1.10: Comparison of the temperature profiles obtained under the same operational conditions for different mixers

4.1.3.5.1. Mixer 1. 60 experiments were performed using mixer 1. In general, the most favorable ignition data were obtained working with this mixer. It presented the lowest autoignition temperatures and limiting inlet temperatures. Also the residence time necessary for achieving ignition was the lowest. Plugging problems did not occur.

4.1.3.5.2. Mixer 2. Only 8 experimental stationary states were obtained using mixer 2. It was designed in order to increase the velocity of the reagents inside of the mixer, considering that, with a higher velocity and turbulence, the mixing process would be improved and ignition would occur at lower temperatures. However the ignition temperature resulted higher than in mixer 1. In addition, it was found that it was difficult to achieve ignition in this mixer. When ignition was produced, the elevated reaction temperatures could not be maintained steadily, and the temperature reduced straight away. This behavior is shown in figure 4.1.11 (a).

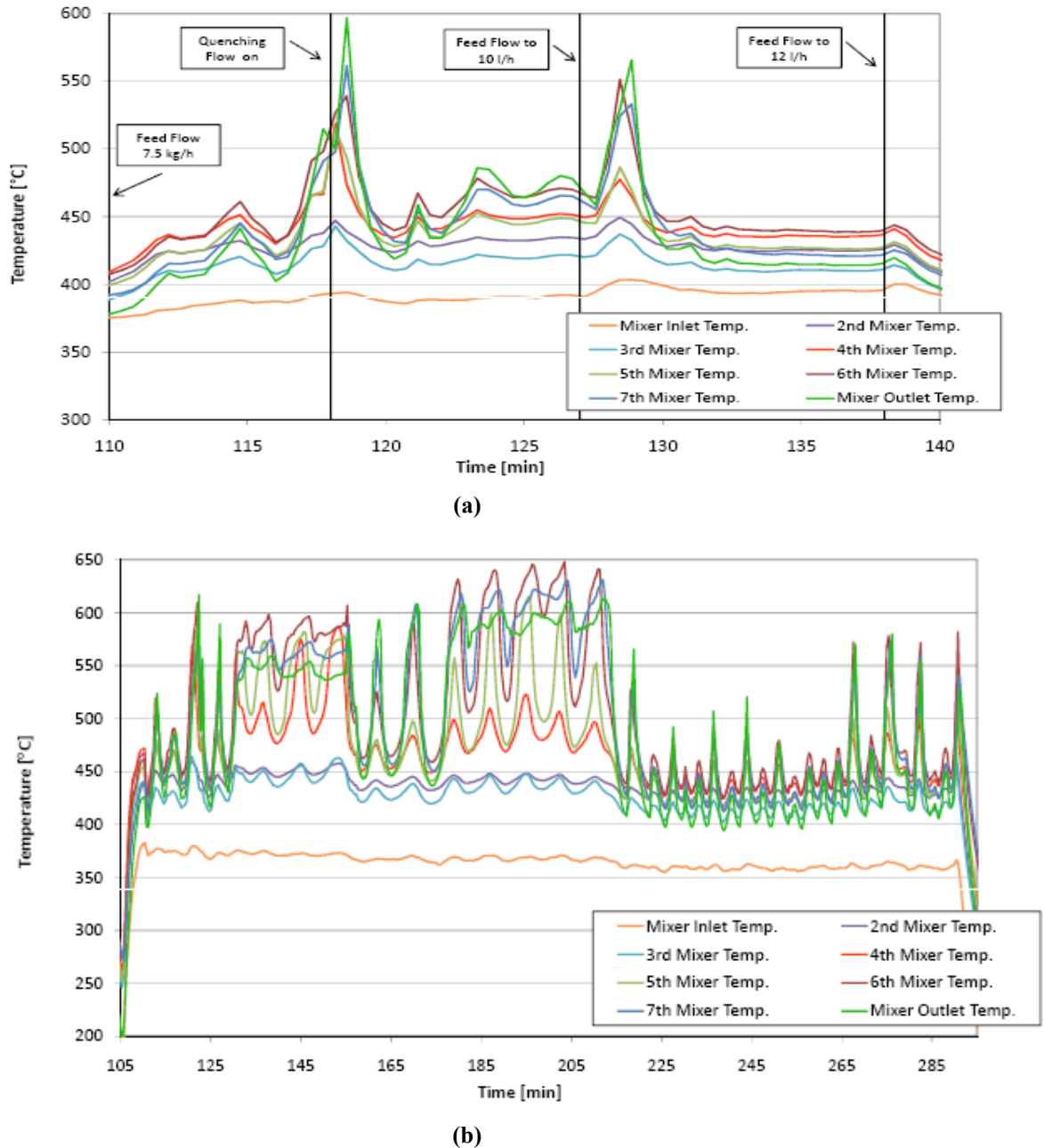


Figure 4.1.11: Evolution of temperature profile in two experiments with mixer 2

Figure 4.1.11 displays the temperature sequence of the eight thermocouples of the mixer during two different experiments. The experiments were carried out with an IPA concentration of 4% mass and a feed flow of 7.5 kg/h at the beginning of the experiment. Changes in the operational conditions are indicated by vertical lines in the diagram. It was observed that, in experiment a) for only two short periods of time during the experiment, the temperature increased in such a way as to indicate a flame oxidation. In experiment b), even though the operational conditions were very similar to the previous experiment, a different temperature sequence was obtained. Strong oscillations of the temperatures were observed at the first six measuring points inside

the mixer, but high temperatures were maintained for longer than 30 minutes in the last two thermocouples. The two temperature sequences also showed that there is a random component in ignition phenomenon, as the system responded differently at similar operation conditions. A possible explanation is that the formation of the flame flow pattern was hindered by the smaller diameter of the mixer, and the recirculation or back mixing of heated fluid elements to the inflowing colder ones, was not as intense as in mixer 1. Another explanation could be that the residence time was not sufficient and the system would have reached stable conditions if the mixer had been longer. A third explanation proposed was that the flame front was blown out of the mixer by the high velocity of the fluid.

This mixer caused a number of operational plugging problems related to salt deposition due to its reduced diameter. Further experiments with this mixer were performed using distilled water.

4.1.3.5.3. Mixer 3. 46 experiments were performed with mixer 3. It was designed to improve the mixing process between the air and the aqueous feed. The flow was separated into two branches that were joined later changing their disposition and permitting the different feed and air elements to mix, as shown in the figure 4.1.3. The strategy was not successful, as it was observed that higher ignition temperatures and residence times than those obtained in mixer 1 were necessary for ignition. A typical delay in ignition was observed in the temperature profiles shown in figure 4.1.9 that correspond to mixer 3. A very simple explanation is that the design of the mixer dissipated heat faster to the environment, so the time necessary for reaching the ignition temperature by flameless oxidation was longer. Another possible explanation is that the bifurcations of the flow made it difficult to form a flame flow pattern.

4.1.3.5.4. Mixer 4. 27 experiments were performed using mixer 4. It was filled with rings in order to permit the separation of the elements of the flow, increasing velocity and turbulence and improving the mixing process. This time, the temperature was monitored also in the empty tube after the mixer, and before the quenching flow inlet to check if ignition was produced after the mixer. Again it was found that improving the mixing process was unsuccessful. Very high ignition temperatures, higher than 505°C, were necessary to achieve flame oxidation in the filled area. The bad performance of mixer 4 can be explained as in the case of mixer 2 by the flame front

being blown out of the mixer by the high fluid velocity, or by the difficulty of forming a flame front due to the flow pattern produced by the filling of the tube.

4.1.3.6. TOC removal

Even though the object of this work was to study the reaction initiation and not to obtain total TOC removal, liquid samples were taken and TOC was analyzed. The results presented in figure 4.1.12 show that, TOC removals higher than 99% were obtained at residence times as low as 0.4 s when ignition occurred. It is remarkable that even when the configurations of the mixers were not optimized for producing or sustaining a flame, almost total TOC removal was obtained at residence times always lower than 1.1 s.

Oxidation by means of a hydrothermal flame makes possible to design very small vessels for the SCWO process, which is an important advantage in the industrial development of SCWO process.

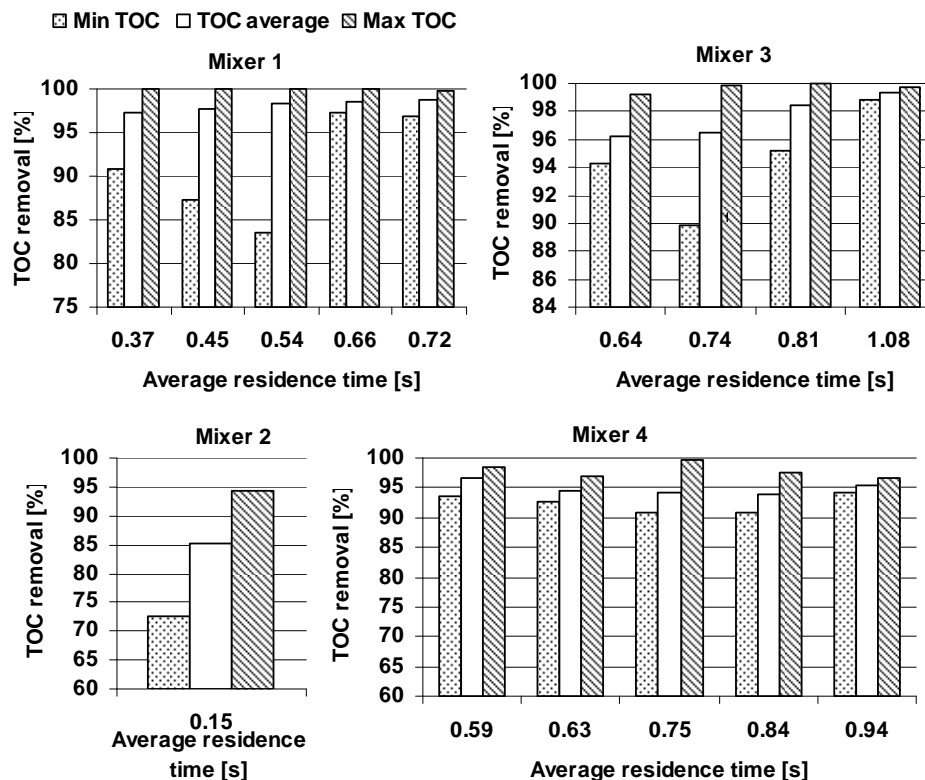


Figure 4.1.12: Maximum, minimum and average TOC removals at different residence times for the mixers studied

4.1.4. CONCLUSIONS

An experimental study of the mixing process and reaction initiation was carried out. The conclusions obtained were the following:

- The reaction initiation was studied using four different tubular mixers at different feed flows, IPA concentrations and inlet temperatures. All the experiments were performed in the one phase region. Temperature profiles inside the mixer were used as the main indicating parameter.
- When the reacting mixture reached a certain temperature (autoignition temperature) more rapid temperature increases were observed showing evidence of a faster reaction rate. These observations are consistent with the description of the behavior of hydrothermal flames.
- Flameless experimental temperature profiles were reproduced using the kinetic model developed by Li et al. Reaction rates when a flame was present were much faster than the ones predicted by the models described in literature.
- Autoignition temperatures were fixed for every mixer. The limiting inlet temperature and the residence time necessary for ignition were also determined. The empty ¼” tubular mixer presented the lowest autoignition temperature (450°C), and ignition occurred faster inside it. The other mixers, designed for improving the turbulence, resulted in poorer ignition conditions.
- TOC removals higher than 99% were obtained in residence times lower than 1.7 s when ignition was produced.
- An empty tube with low feed flows and residence times between 0.5-1 s seems to be the optimal configuration for flame formation. The results showed that in the conditions evaluated, the mixing process was not the limiting factor.

4.1.5. REFERENCES

- [1] P.A. Marrone, G.T. Hong, Supercritical Water Oxidation, in: M. Kutz (Ed.), Environmentally Conscious Materials and Chemicals Processing, John Wiley & Sons, Inc., Hoboken (NJ), 2007. p. 385
- [2] P. Kritzer, E. Dinjus, An assessment of supercritical water oxidation (SCWO): existing problems, possible solutions and new reactor concepts, Chemical Engineering Journal, 83 (2001) 207–214
- [3] M.D. Bermejo, M.J. Cocero, Supercritical water oxidation: A technical review, AIChE Journal, 52 (2006) 3933-3951
- [4] G. Brunner, Near and supercritical water. Part II: Oxidative processes, Journal of supercritical Fluids, 47 (2009) 382-390
- [5] P.A. Marrone, M. Hodes, K.A. Smith, J.W. Tester, Salt precipitation and scale control in supercritical water oxidation-part b: commercial/full-scale applications, Journal of supercritical Fluids, 29 (2004) 289-312
- [6] H. Schmieder, J. Abeln, Supercritical water oxidation: State of the art, Chemical Engineering & Technology, 22 (1999) 903-908
- [7] M.D. Bermejo, F. Fdez-Polanco, M.J. Cocero, Experimental study of the operational parameters of a transpiring wall reactor for supercritical water oxidation, Journal of supercritical Fluids, 39 (2006) 70-79
- [8] B.D. Phenix, J.L. DiNaro, J.W. Tester, J.B. Howard, K.A. Smith, The effects of mixing and oxidant choice on laboratory-scale measurements of supercritical water oxidation kinetics, Industrial & Engineering Chemistry Research, 41 (2002) 624-631
- [9] F. Vogel, J.L. DiNaro Blanchard, P.A. Marrone, S.F. Rice SF, P.A. Webley, W.A. Peters, K.A. Smith, J.W. Tester, Critical review of kinetic data for the oxidation of methanol in supercritical water, Journal of supercritical Fluids, 34 (2005) 249-286
- [10] T. Aizawa, Y. Masuda, K. Minami, M. Kanakubo, H. Nanjo, R.L. Smith, Direct observation of channel-tee mixing of high-temperature and high-pressure water, Journal of supercritical Fluids, 43 (2007) 222-227

- [11] J.P. Serin, J. Mercandier, F. Marias, P. Cezac, and F. Cansell, Use of cfd for the design of injectors for supercritical water oxidation, in: M. Perrut (Ed), Proceedings of the 10th European Meeting on Supercritical Fluids: Reactions, Materials and Natural Products Processing, Colmar, France, Dec 12 - 14, 2005.
- [12] H.L. LaRoche, M.Weber, C. Trepp, Design rules for the wall cooled hydrothermal burner (WHB), *Chemical Engineering & Technology*, 20 (3) (1997) 208–211.
- [13] B. Welling, K. Lieball, Ph. Rudolf von Rohr, Operating characteristics of a transpiring-wall scwo reactor with a hydrothermal flame as internal heat source, *Journal of supercritical Fluids*, 34 (2005) 35-50
- [14] K. Prikopsky, B. Wellig, Ph.Rudolf von Rohr, SCWO of salt containing artificial wastewater using a transpiring-wall reactor: Experimental results, *Journal of supercritical Fluids*, 40 (2007) 246–257
- [15] B. Wellig, M. Weber, K. Lieball, K. Prikopsky, Ph. Rudolf von Rohr, Hydrothermal methanol diffusion flame as internal heat source in a SCWO reactor, *Journal of Supercritical Fluids*, 49 (2009) 59–70
- [16] W. Schilling, E. U. Franck, Combustion and Diffusion Flames at High Pressures to 2000 bar, *Berichte Der Bunsen-Gesellschaft-Physical Chemistry Chemical Physics*, 92 (1988) 631-636
- [17] T. Hirth, E.U. Franck, Oxidation and Hydrothermolysis of Hydrocarbons in Supercritical Water at High Pressures *Berichte Der Bunsen-Gesellschaft-Physical Chemistry Chemical Physics*, 97 (1993) 1091-1098
- [18] G. M. Pohnsner, E.U. Franck, Spectra and Temperatures of Diffusion Flames at High Pressures to 1000 bar, *Berichte Der Bunsen-Gesellschaft-Physical Chemistry Chemical Physics*, 98 (1994) 1082-1090
- [19] C. Augustine, J. W. Tester, Hydrothermal flames: From phenomenological experimental demonstrations to quantitative understanding, *Journal of supercritical Fluids*, 47 (2009) 415–430

- [20] A. Sobhy, I.S. Butler, J.A. Kozinski, Selected profiles of high-pressure methanol–air flames in supercritical water, *Proceedings of the Combustion Institute.*, 31 (2007) 3369–3376
- [21] R. R. Steeper, S.F. Rice, M. S. Brown, S.C. Johnston, Methane and Methanol Diffusion Flames in Supercritical Water, *Journal of supercritical Fluids*, 5 (1992) 262-268
- [22] R.M. Serikawa, T. Usui, T. Nishimura, H. Sato, S. Hamada, H. Sekino, Hydrothermal flames in supercritical water oxidation: investigation in a pilot scale continuous reactor, *Fuel*, 81 (2002) 1147-1159
- [23] C. Narayanan, C. Frouzakis, K. Boulouchos, K. Prikopsky, B. Wellig, P. Rudolf von Rohr, Numerical modelling of a supercritical water oxidation reactor containing a hydrothermal flame. *Journal of supercritical Fluids*, 46 (2008) 149–155
- [24] J. Sierra-Pallares; M.T. Parra-Santos; J. García-Serna, F. Castro, M. J. Cocero, Numerical modelling of hydrothermal flames. Micromixing effects over turbulent reaction rates, *Journal of supercritical Fluids*, 50 (2009) 146–154
- [25] A. Anderko, K.S. Pitzer, EOS representation of phase equilibria and volumetric properties of the system NaCl–H₂O above 573 K, *Geochimica et Cosmochimica Acta*, 57 (1993) 1657-1680
- [26] J.J. Kosinski, A. Anderko, EOS for high-temperature aqueous electrolyte and nonelectrolyte systems, *Fluid Phase Equilibria*, 183-184 (2001) 75-86
- [27] M.D. Bermejo, A. Martín, M.J. Cocero, Application of the Anderko–Pitzer EoS to the calculation of thermodynamical properties of systems involved in the supercritical water oxidation process, *Journal of supercritical Fluids*, 42 (2007) 27–35
- [28] M.D Bermejo, F. Fdz.-Polanco, M.J. Cocero, Modeling of a transpiring wall reactor for the supercritical water oxidation using simple flow patterns: Comparison to experimental results, *Industrial & Engineering Chemistry Research*, 44 (2005) 3835-3845
- [29] M.J. Cocero, J.L. Martínez, Cool wall reactor for supercritical water oxidation: Modeling and operation results, *Journal of supercritical Fluids*, 31 (2004) 41-55
- [30] C. Magoulas, D. Tassios, Thermophysical properties of n-alkanes from C1 to C26 and their prediction for higher ones, *Fluid Phase Equilibria*, 56 (1990) 119-140

[31] L. Li, P. Chen, E.F. Gloyna, Generalized kinetic model for wet oxidation of organic compounds, *AICHE journal*, 37 (1991) 1687-1697

[32] T.B. Hunter, S.F. Rice, R.G. Hanush, Raman spectroscopic measurement of oxidation in supercritical water 2. Conversion of isopropyl alcohol to acetone, *Industrial & Engineering Chemistry Research*, 35 (1996) 3984-3990

[33] T.J. Wightman, Studies in supercritical wet air oxidation. Master's thesis, Chem. Eng. Dept., MIT, Cambridge,MA, 1981.

4.2. EXPERIMENTAL STUDY OF THE SUPERCRITICAL WATER OXIDATION OF RECALCITRANT COMPOUNDS UNDER HYDROTHERMAL FLAMES USING TUBULAR REACTORS

ABSTRACT

The hydrothermal flame is a new method of combustion that takes place in supercritical water oxidation reactions when the temperature is higher than the autoignition temperature. In these conditions, waste can be completely mineralized in residence times of milliseconds without the formation of by-products typical of conventional combustion. The object of this work is to study the hydrothermal flame formation in aqueous streams with high concentrations of recalcitrant compounds: an industrial waste with a high concentration of acetic acid and various concentrated solutions of ammonia. A tubular reactor with a residence time of 0.7 seconds was used. Oxygen was used as the oxidant and isopropyl-alcohol (IPA) as co-fuel to reach the operation temperature required. The increase of IPA concentrations in the feeds resulted in a better TOC removal. For mixtures containing acetic acid, 99% elimination of TOC was achieved at temperatures higher than 750°C. In the case of mixtures containing ammonia, TOC removals reached 99% while maximum total nitrogen removals were never higher than 94%, even for reaction temperatures higher than 710°C. Ignition was observed at concentrations as high as 6% wt NH₃ with 2% wt IPA while at IPA concentrations below 2% wt IPA, the ammonia did not ignite.

4.2.1. INTRODUCTION

In conditions above its critical point ($T=374^{\circ}\text{C}$ and $P= 22.1 \text{ MPa}$), water is completely miscible with organic substances and gases. Oxidation reactions can be carried out in this medium in the homogeneous phase, without mass transport limitations. The process using supercritical water most developed at the industrial scale is called supercritical water oxidation (SCWO). It consists of the total oxidation of compounds in a homogenous aqueous medium using air or oxygen as the oxidant. Due to the high temperatures, kinetics are very fast and total waste mineralization can be achieved using the appropriate combination of temperature and residence time. [1, 2]. At temperatures near the critical point of water ($400 - 450^{\circ}\text{C}$), residence times of about one minute are needed. When organic waste concentrations are high enough and temperatures are above the autoignition temperatures of the compounds, it is possible to form flames called hydrothermal flames. This phenomenon is due to the reduction of the autoignition temperature at high pressures. For inflammable compounds such as methane or methanol, hydrothermal flame can occur at temperatures as low as 400°C [3]. Supercritical water oxidation in the presence of hydrothermal flames can reduce residence times to the order of milliseconds [4] without the production of sub-products typical of conventional combustion such as NO_x [5] or dioxins [6].

SCWO with a hydrothermal flame has a number of advantages over the flameless process. Some of these advantages permit overcoming the traditional challenges that make the successful and profitable commercialization of SCWO technology difficult. The advantages include the following [4]:

- It allows the destruction of the pollutants in residence times of a few milliseconds, which permits the construction of smaller reactors.
- It is possible to initiate the reaction with feed injection temperatures near to room temperature when using vessel reactors [7-9]. This avoids problems such as plugging and corrosion in a preheating system, having an advantage from the operational and energy integration perspective.
- Higher operation temperatures improve the energy recovery

Tubular reactors are the optimal device for kinetic determination at high pressures, as well as for studying the ignition process of hydrothermal flames of different compounds, as it allows an accurate monitoring of the evolution of the temperature along different positions in the reactors, making it possible to obtain more accurate

experimental data than those obtained in vessel reactors. In a previous investigation by our research group [10], conditions for the formation of hydrothermal flames of isopropyl alcohol in tubular reactors were studied. It was determined that feed temperature and organic concentration are the most critical variables in hydrothermal flame formation. When working with gases, alcohols and other inflammable compounds, ignition is easily produced, [3, 4, 6, 11], but when working with other compounds that are more difficult to oxidize, a co-fuel may be needed to obtain the hydrothermal flame [12]. Ammonia (NH_3) and acetic acid (HAc) are considered the most recalcitrant compounds for the chemical oxidation processes, including, SCWO, as they are already partially oxidized compounds, frequently acting as reaction intermediates [13]. For this reason, they are considered to be key compounds for the study of the SCWO process.

The destruction of HAc has been reported by several authors [14-16]. In these investigations, different kinds of reactors were used at temperatures between 400-600°C in a flameless regime obtaining conversions over 90% in residence times of 4 - 30 s. The main products of acetic acid oxidation were CO_2 and water. Minor products included CO and trace amounts of methane, the main radical species in the mechanism are formic acid and methanol, a detailed mechanism for the oxidation of Acetic Acid was published by Boock and Klein, [17]

The final oxidation product of nitrogen compounds in supercritical water is N_2 [18]. Even though the complete oxidation product of nitrogen is NO_3^- , in the SCWO process the oxidation to N_2 is favored thermodynamically. It is known that ammonia is the main reaction intermediate and that the oxidation of ammonia is the rate-limiting step in the overall oxidation of nitrogen-containing organic waste [19]. This makes the study of ammonia oxidation an essential step in order to improve the process design in SCWO technology. In addition, the oxidation of ammonia is one of the slowest reactions in SCWO and it can be used for testing the performance of a new reactor design. Numerous difficulties for completely destroying ammonia in SCWO have been reported in literature, with important divergences: while some authors did not eliminate NH_3 , others, in similar conditions, obtained significant removals [20-22]. Our group's results showed complete destruction of nitrogen compounds and ammonia using IPA as a co-fuel in a vessel cooled wall reactor working at flame regime with residence times in the reactor of about 1 minute [5].

In this study, hydrothermal flame ignition of two different wastes was performed:

- A real industrial waste composed mainly of acetic acid, and containing also crotonaldehyde, a carcinogenic compound.
- Synthetic waste consisting of different aqueous solutions of the recalcitrant compound ammonia

A simple tubular reactor with residence times of less than 0.7 s was used in this study. Isopropyl alcohol (IPA) was used as a co-fuel to provide the enthalpy of combustion needed to obtain the flame ignition. The concentrations of recalcitrant compounds were increased while the concentrations of the co-fuel were decreased in order to observe how the ratio of waste to co-fuel can affect flame ignition and waste destruction. Previous to this investigation, the ignition of IPA solutions at several concentrations using oxygen as the oxidant were studied.

4.2.2. EXPERIMENTAL

4.2.2.1. Experimental set up

All the experiments described in this study were carried out in the demonstration plant owned by the University of Valladolid and located at the industrial site of the company CETRANSA in Santovenia de Pisuerga (Valladolid, Spain). The demonstration plant can work at temperatures up to 750°C and pressures up to 30 MPa. Feed flows of 9 kg/h were used for these experiments. Feed was electrically preheated before being introduced in the tubular reactor. The oxidant (oxygen) is injected into the feed at the inlet of the tubular reactor. Temperatures in the mixing point and in several points of the tubular reactor were monitored. After leaving the reactor, the reaction mixture was quenched. Then products were cooled in the intercoolers and finally depressurized. Samples of the liquid were taken, and the concentrations of NH_3 and NO_x in the gaseous stream were checked for selected experiments. A flow diagram of the pilot plant is shown in figure 4.2.1. The main elements of the facility are the following:

- A tank where the feed is prepared, with special attention given to the concentration of organic matter, because this concentration determines the operating temperature of the reactor.
- Metering diaphragm pump (DOSAPRO MAX ROYAL C) to drive the feed from the feed tank to the tubular reactor. Its maximum work pressure is of 23 MPa

- Two electrical preheaters in the feed line, They consist of cylinders in which four resistance of 2500 W each are embedded. A coil is surrounding the cylinder. The whole device is thermally isolated.
- The oxygen supply facility. Liquid oxygen is stored in a cryogenic deposit, from where it is pumped by a cryogenic metering pump until work pressure. The pump supplies a constant flow. After pumping, oxygen is vaporized in a finned tube heat exchanger. Then, the pressurized gaseous oxygen is stored in four reservoirs before it is mixed with the aqueous waste stream. The flow of oxygen withdrawn from these reservoirs can be controlled with a control valve
- The reactor consisted of a straight and empty tube made of Ni alloy C-276 with a length of 2000 mm and a diameter of $\frac{1}{4}$ " (i.d. 3.86 mm) giving an internal volume of 18.5 mL. The flow inside the tube was upwards
- Cooling systems. They consist of two coolers, in which the hot product of reaction flows inside a titanium alloy (Ti- 3Al-2.5V) coil, and is refrigerated by cooling water.
- The back pressure regulator valve consisting of a needle valve, SENTRY VREL11, is used. For security reasons, a second valve is placed in parallel to this valve.
- Flash chamber separator and sampling device that allows taking samples of the liquid and gaseous effluents.

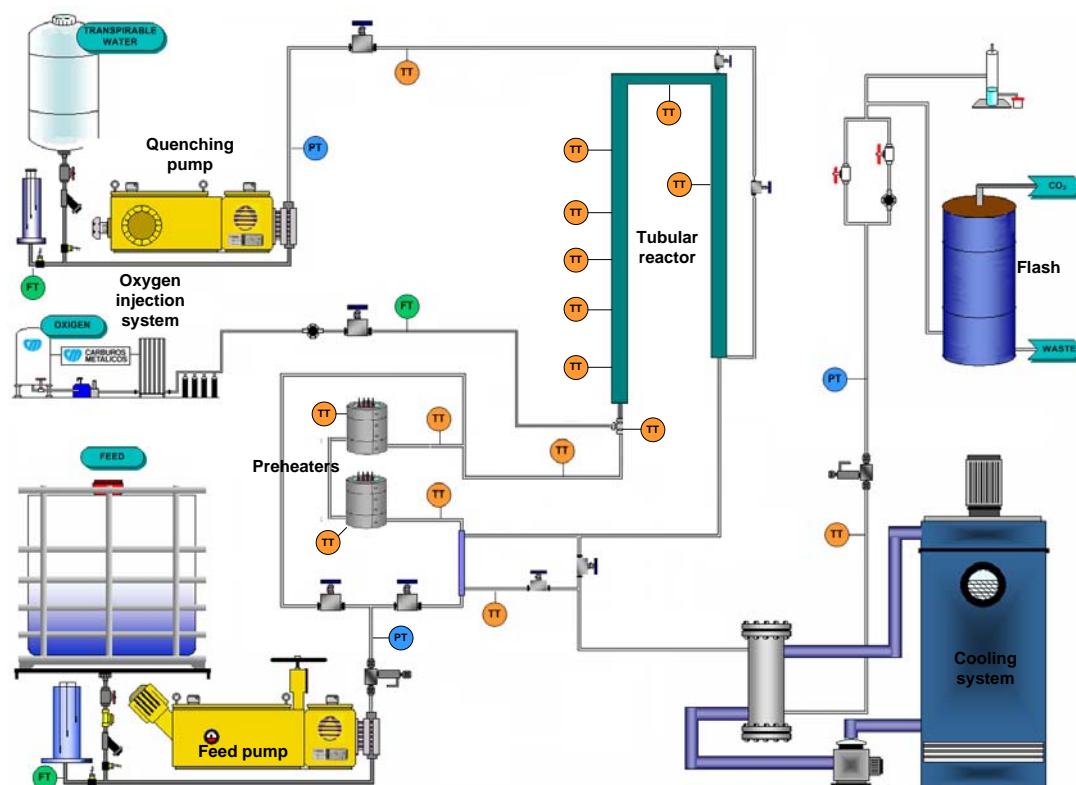


Figure 4.2.1 : Flow diagram of the facility

4.2.2.2. Experimental procedure

At the beginning of a new experiment, the reactor was preheated by pumping an initial feed of water and IPA (4% of IPA) through it until all the thermocouples indicated temperatures higher than 400°C. Once preheated the reactor, oxygen flow was introduced at 0-10% of the stoichiometric amount in order to start the ignition.

When a sharp increase in the temperature occurred, it indicates that the hydrothermal flame was ignited, and in that moment, quenching water was connected. Apart from the electrical preheating of the reagents, no more heat was supplied to the system, the reactor being auto-thermal

Even when the flame could not visually be observed, it is known that hydrothermal flames are formed at these temperatures and IPA concentrations [6]. On the other hand the sharp increase of temperature happens in a stretch of reactor shorter than 40 cm of reactor. This implies the oxidation of IPA in a residence time of 100 mS, being this residence time typical of SCWO at flame regime, while flameless SCWO requires higher residence times.

This indicates that all the rises in temperature produced inside of the reactor were due to the release of the heat of reaction during the oxidation of IPA. The system was maintained in a stationary state and samples were taken at the outlet of the system. Temperature profiles along the reactor were registered automatically when a sample was taken. After sample taking, experimental conditions were altered by changing the concentration of IPA and the one of waste or ammonia (depending on the experiment carried out), the flow of feed is maintained constant at 9 kg/h for all the experiments. All the experiments were monitored through temperature profiles in the reactor and TOC concentrations in the effluent.

4.2.2.3. Materials

Isopropanol (99% in mass) and Ammonia (25% in mass) were supplied by COFARCAS (Spain).

Experiments using a real industrial waste, mainly composed of acetic acid, were performed. The composition of the waste is shown in table 4.2.1.

Table 4.2.1: Composition of the industrial waste

Compound	Composition%
Acetic Acid	83.53
Acetaldehyde	8.95
Crotonaldehyde	1.79
Methanol	0.95
Cl ⁻	4.77

Experiments were performed using different dilutions of the waste in order to obtain different concentrations of acetic acid.

4.2.2.4. Analysis

All the Total Organic Carbon (TOC) analysis and Total Nitrogen (Total N) analysis of the samples were performed with a TOC 5050 SHIMADZU Total Organic Carbon Analyzer which uses combustion and IR analysis. The detection limit is 1 ppm.

NH₃ and NO_x in the gas effluent were analyzed with Dräger tubes detectors Lab Safety Supply CH29401 and CH31001. The NO_x detection limits for these tubes ranged from 0.5 to 100 ppm and the NH₃ detection limits for these tubes ranged from 5 to 70 ppm (standard deviation for both tubes are between 10 and 15%)

Nitrates and nitrites were characterized in the liquid effluent by ionic chromatography with an IC PAK A column of Waters. The detection limit is 1 ppm.

4.2.3. RESULTS AND DISCUSSION

4.2.3.1. Influence of IPA concentration on the hydrothermal flame formation

A study was conducted examining the influence of IPA concentrations on hydrothermal flame ignition when IPA was the only fuel present in the aqueous mixture. The experiments performed are summarized in table 4.2.2. Each experiment was repeated at least three times. Standard deviations were calculated and shown in table 4.2.2.

Table 4.2.2: Summary of the experiments performed with IPA as the only fuel in the mixture. Average values and standard deviations are shown.

C_{IPA0} (% wt)	TOC_0 (ppm C)	T_{Inj} (°C)	T_{max} (°C)	TOC Removal (%)	$\text{TOC}_{\text{outlet}}$ (ppm C)
4.5	27000	406 ± 3	708 ± 4	99.7 ± 0.1	77 ± 23
4.0	24000	404 ± 4	676 ± 1	99.3 ± 0.2	172 ± 37
3.5	21000	415 ± 2	631 ± 1	98.5 ± 0.3	323 ± 68
2.5	15000	416 ± 8	600 ± 1	96 ± 2	494 ± 252
2.0	12000	407 ± 3	566 ± 17	97 ± 2	344 ± 294
1.5	9000	407 ± 4	516 ± 10	94 ± 1	575 ± 97
1.0	6000	390 ± 8	440 ± 9	62 ± 5	2300 ± 331

The experimental temperature profiles obtained are depicted in figure 4.2.2. It is observed that when decreasing fuel concentration, the ignition and the point where the highest temperature is reached are delayed. Even when most of the IPA has reacted at that point, complete conversion is not obtained. As expected, increasing the concentration of IPA, the maximum temperature registered in the reactor is higher and the obtained conversion is higher as well. The observations of Vogel et al, [23] can explain this phenomenon. According to these authors, the SCWO reaction mechanism of methanol yields a S-shaped conversion vs. time curve. At the beginning of the reaction an induction time is observed; then in a second stage, the methanol is consumed rapidly in a quasi-steady propagation phase. When most of the reagent has been converted, termination reactions between radicals, which yield stable products, start to dominate and methanol conversion is slowed down (termination phase). Thus, even though the flame is generated and most of the TOC is eliminated, the termination step is slower and the reaction needs additional residence time to be

completed; this necessary residence time decreases when reaction temperature is higher.

The experimental temperature profiles are compared to the flameless temperature profile predicted by a mathematical model described in a previous work by our research work group, [10]. The model consists of a tubular reactor in which plug flow is considered. The reactor works in stationary state. Only mass and energy balances are solved. Runge Kutta method of the 4th order was used to solve the model. Densities and enthalpies were calculated as a function of composition and temperature using the PR EoS with the translated volume correction [24]. The kinetic of Wightman, [25] published by Li et al [13] was used. This kinetics was developed for phenol oxidation but, in a previous research [10] several kinetic models were tested and it was the best reproducing the experimental flameless temperature profile of IPA. It is shown that experimental temperature profiles are faster than the flameless temperature profiles predicted by the model even for the experimental data with 1% in mass, in which only 62% is removed. Nevertheless, a maximum temperature is reached, and even though there is more IPA to be oxidized, it is not, and no further temperature increase is registered. Results indicate that upon reaching a concentration low enough, flame regime is no longer possible, and for low IPA concentrations the TOC removal is lower than for higher TOC removals.

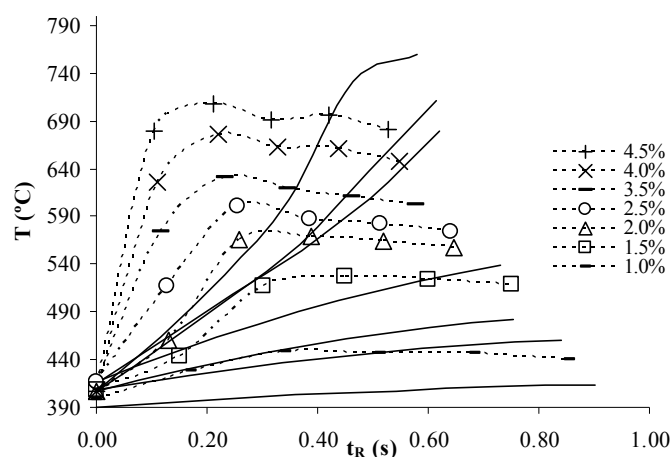


Figure 4.2.2: Temperature profile registered in experiments with different IPA concentrations. Comparison to predicted temperature profiles in flameless SCWO. Symbols linked by discontinuous line represent experimental data and solid lines represent prediction of the model for flameless oxidation

4.2.3.2. Oxidation of an industrial waste containing Acetic Acid

Experiments for the oxidation of the industrial waste were performed using different dilutions of waste with concentrations of acetic acid from 1.4 to 4% in mass. IPA was used as the co-fuel, thereby increasing the calorific power of the aqueous solutions in order to work at temperatures between 600 and 700°C. When waste concentration was increased, IPA concentration was decreased in order to keep the temperature value in this range. If TOC removal was not complete, IPA concentration was increased in order to increase the reaction temperature. All the experiments were performed with a fixed flow of 9 kg/h, injection temperatures between 390 - 410°C, and a pressure of 23 MPa, using oxygen as oxidant in concentrations above the stoichiometric proportion to achieve complete conversion to CO₂. Every experiment was repeated at least 3 times. The average values and the standard deviation of the data are showed in Table 4.2.3. Note that the uncertainties of experimental data are higher in a pilot scale plant than in a laboratory scale plant.

Table 4.2.3: Experiments performed with a highly acetic acid concentrated industrial waste

C_{HAcO}	C_{IPA0}	TOC_0		$\text{TOC}_{\text{outlet}}$	T_{Inj}	T_{max}	TOC Removal
(% wt)	(% wt)	(ppm C)		(ppm C)	(°C)	(°C)	(%)
		HAc	IPA				
1.4	3.5	5600	21000	1574 ± 689	409 ± 8	670 ± 21	94 ± 2
1.4	4.0	5600	24000	257 ± 137	409 ± 16	709 ± 20	98 ± 2
1.4	4.5	5600	27000	57 ± 28	396 ± 8	766 ± 10	99.8 ± 0.1
2.0	3.3	8000	19800	1082 ± 195	398 ± 4	690 ± 15	96.1 ± 0.7
3.0	3.5	12000	21000	135 ± 31	396 ± 8	745 ± 12	99.6 ± 0.1
4.0	2.5	16000	15000	1335 ± 473	387 ± 4	703 ± 10	95.7 ± 1.5
4.0	3.0	16000	18000	139 ± 23	403 ± 4	744 ± 4	99.6 ± 0.1

As expected, by increasing the amount of organic material in the feed, the maximum temperature reached in the reactor is higher and, consequently, the conversion of TOC increases as well. This behaviour is shown in figure 4.2.3 (a) where the TOC removals versus the maximum temperatures registered in the reactor are shown for several waste concentrations.

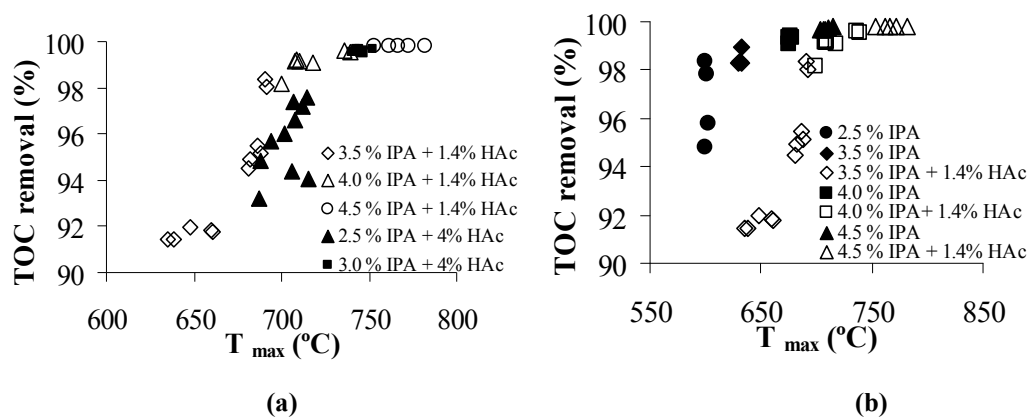


Figure 4.2.3.a: TOC removal versus maximum reaction temperature for mixtures with 1.4% and 4% acetic acid. Experimental conditions of the experiments: feed flow 9.5 kg/h flow. Oxygen excess over the stoichiometric concentration for complete oxidation to CO_2 and water $P=23\text{MPa}$.

Figure 4.2.3.b: TOC removal versus maximum reaction temperature for mixtures of different IPA concentrations and IPA+ 1.4 wt% acetic acid.

Figure 4.2.3 (b) compares the TOC removal versus maximum reaction temperature in feeds with different IPA concentrations, and in feeds with the same IPA concentrations and 1.4% acetic acid. Higher TOC removals were observed for mixtures not containing acetic acid. Almost total TOC removals ($>99.8\%$) were obtained at temperatures around 708°C for feeds containing only IPA, while those containing IPA+1% HAc needed a temperature higher than 750°C to obtain 99% TOC removal.

Despite good results of TOC removal of mixtures of waste-IPA, higher waste concentrations could not be tested due to significant corrosion problems detected in the preheating area. It was found that samples contained Ni concentrations as high as 232 ppm, originated in the corrosion of the Ni alloy tube. Cr concentrations of 23 ppm and Fe concentrations of 42 ppm were also found. This can be explained by the high chloride concentration of the waste.

Figure 4.2.4 shows the temperature profile along the reactor. It can be observed that the maximum residence time in the reactor is around 0.7 s. The sharp temperature increase, indicating the ignition of the hydrothermal flame, occurs at the beginning of the reactor with residence times between 100 and 150 ms, meaning that most of the TOC is eliminated in that point; but if reaction temperature is not high enough, complete TOC removal is not achieved. Again, extra residence time is needed to finish the termination step of the reaction [23].

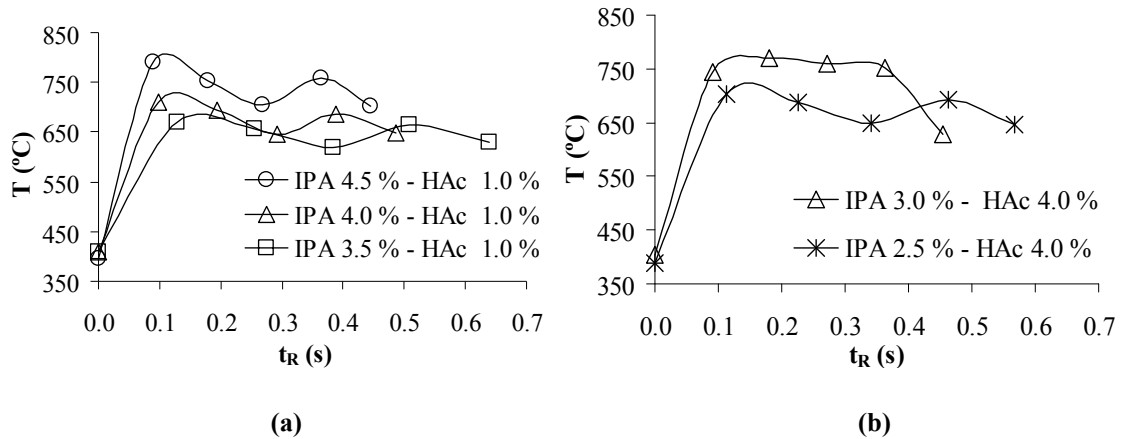


Figure 4.2.4 : Profile temperature for different experiments with acetic acid and IPA. **(a)** 1% acetic acid in mass; **(b)** 4% Acetic acid in mass

4.2.3.3. Oxidation of aqueous mixtures of NH_3 -IPA

In order to understand hydrothermal flame behaviour when dealing with nitrogen-containing compounds, experiments with concentrations from 2 to 8% of ammonia in mass were performed. IPA was used as a co-fuel in order to reach temperatures between 600 and 750°C. To improve the TOC removal, IPA concentrations were increased to elevate the reaction temperature. All of the experiments were performed with a fixed flow of 9 kg/h, injection temperatures between 400 and 430°C and a pressure of 23 MPa using oxygen as the oxidant for the total oxidation of the feed to CO_2 and N_2 . Each experiment was repeated at least 3 times. The average values and the standard deviation of the data are showed in Table 4.2.4.

Table 4.2.4: Experiments performed with NH_3 -IPA mixtures

C_{IPA0}	C_{NH_30}	TOC_0	TN_0	T_{inj}	T_{max}	TOC Outlet	TOC Removal	TN Outlet	TN removal
(% wt)	(% wt)	(ppm C)	(ppm N)	(°C)	(°C)	(ppm C)	(%)	(ppm N)	(%)
3.2	2.0	19200	16470	428 ± 21	710 ± 17	157 ± 48	96 ± 3	1033 ± 99	93.7 ± 0.6
3.8	2.0	22800	16470	408 ± 2	727 ± 1	106 ± 37	99.5 ± 0.2	1101 ± 60	93.3 ± 0.4
2.5	4.0	15000	32941	418 ± 3	709 ± 2	156 ± 922	98.6 ± 0.5	3032 ± 555	90.8 ± 1.7
3.0	4.0	18000	32941	412 ± 1	762 ± 2	186 ± 226	99.0 ± 1.2	2754 ± 208	91.6 ± 0.6
1.7	6.0	10200	49412	421 ± 2	609 ± 2	422 ± 80	95.9 ± 0.8	12360 ± 593	75.0 ± 1.2
2.0	6.0	12000	49412	414 ± 1	744 ± 3	103 ± 72	97 ± 3	3412 ± 261	93.1 ± 0.5
1.1	8.0	6000	65882	405 ± 1	574 ± 2	476 ± 3	92.1 ± 0.1	612714 ± 18	7.0 ± 0.6

As shown in table 4.2.4, it is possible to obtain TOC removal over 99% for mixtures of NH₃-IPA. However, in the case of the elimination of ammonia, the maximum removal was 94% at temperatures of approximately 750°C.

In general, TOC removal and Total N are improved with high temperatures. It is observed that, typically, when TOC removal is higher, N removal increases as well. Higher enthalpies content, that is, higher reaction temperatures, were needed to achieve TOC removals of over 99% when ammonia concentration was higher in the mixture. The improvements in N removal for temperatures higher than 710°C were relatively small. In our previous work [5], it was possible to get more than 99% removal of ammonia with temperatures close to 800°C in a cooled-wall reactor with a total residence time of 1 minute. Thus, it can be inferred that for the total destruction of ammonia, longer residence times or higher reaction temperatures are needed than those for which the facility was designed.

The temperature profiles registered along the reactor for different experiments with increasing NH₃ concentration and decreasing IPA concentration are shown in figure 4.2.5

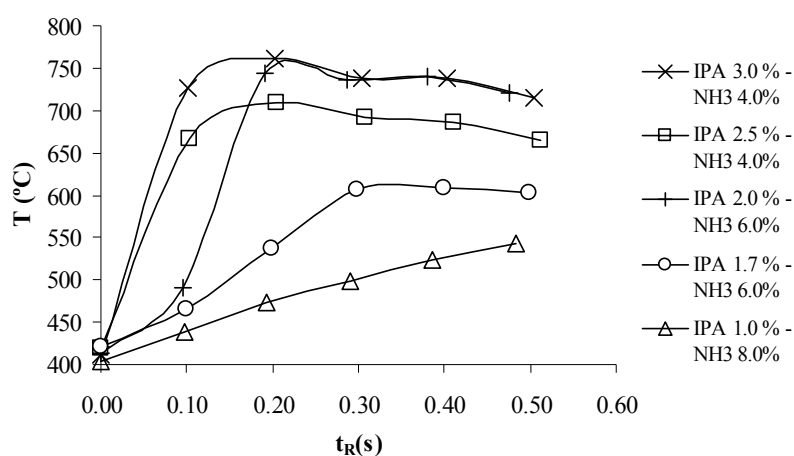


Figure 4.2.5 : Influence of Ammonia concentration for the hydrothermal flame formation

It is observed that with an ammonia concentration of 4% in mass and IPA concentrations of 3 and 2.5% in mass, ignition is produced at the beginning of the reactor. In this case, the IPA auto-ignites rapidly, and with the heat released, a sharp increase in temperature is produced, the autoignition temperature of ammonia is surpassed and it also reacts in flame regime, observing only one temperature increase. Even when the ignition was registered at 0.1s, at which point most of the pollutants were consumed, the TOC and N removal were not complete. As occurred in the case

of HAc, the last step of ammonia elimination is probably slower, as in the case of methanol [23], and the reaction could not be completed in the 0.7 s residence time.

For higher NH_3/IPA ratios the reaction proceeded more slowly, and the temperature profiles have been compared to the flameless temperature profiles predicted by the model. These comparisons are shown in figure 4.2.6.

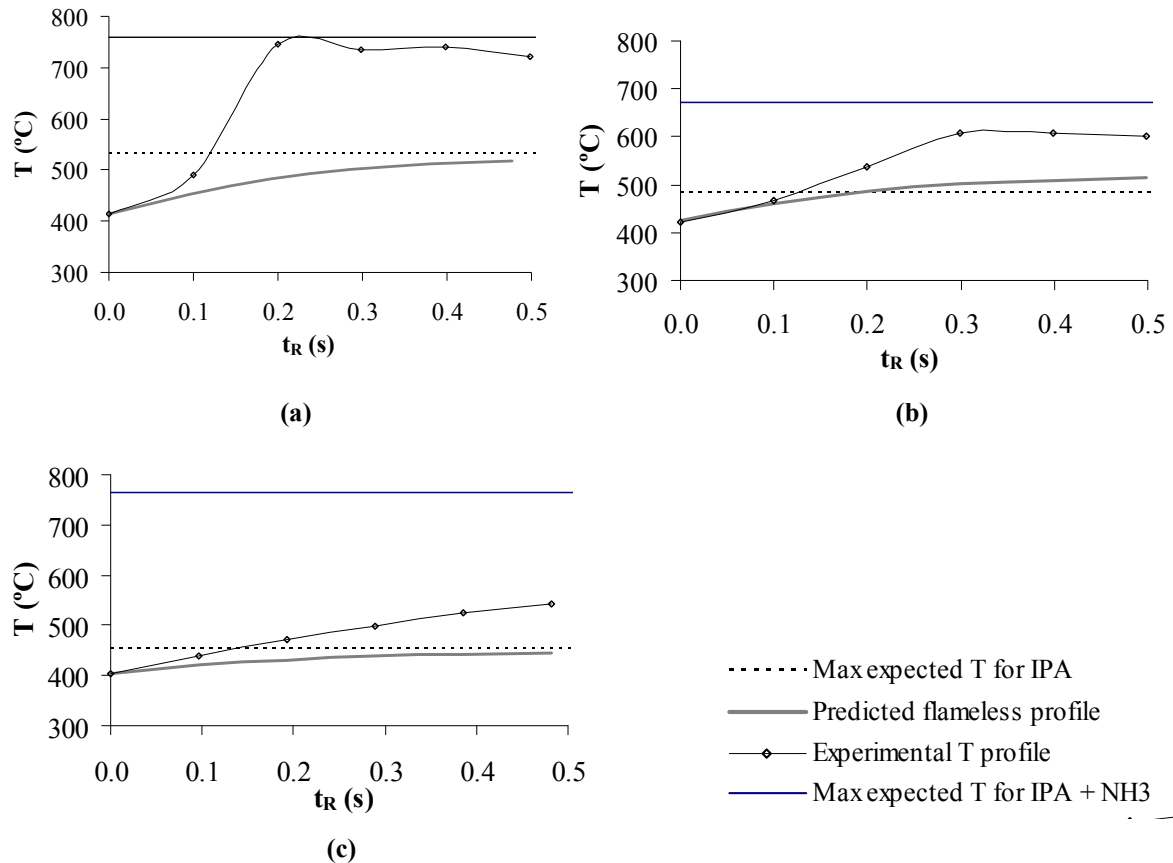


Figure 4.2.6 a: Comparison of the experimental temperature profile to the predictions of the kinetic models for a mixture of 2% of IPA and 6% of NH_3 , **(b):** for a mixture of 1.7% of IPA and 6% of NH_3 , **(c):** For a mixture of 1% of IPA and 8% of NH_3

When the concentration of ammonia increased to 6% and that of IPA decreased to 2%, the position of the flame moved away from the injection point, reaching the maximum temperature only at residence times of 0.2 s. The temperature profile in the first 0.05 s coincided with the flameless temperature profile predicted by the model, as shown in figure 4.2.6 a). Because the concentration of IPA was lower, it took longer for the mixture to be oxidized and release the heat necessary to reach the autoignition temperature, first of IPA and later of NH_3 , as occurred in the previous case.

When NH_3 concentration was 6% and IPA concentration was 1.7%, the reaction proceeded even more slowly. But a maximum temperature is reached that is not

further increased. The maximum temperature was reached only at 0.3 s, and only 95.9% IPA removal and 75% Total N removal were obtained. When compared with the flameless temperature profile predicted by the model, we observe that in the first 0.1 s residence time the temperature profile is equal to the flameless temperature profile as indicated in figure 4.2.7 b). This occurs just before reaching the adiabatic flame temperature, which is calculated by considering only the oxidation of IPA. At longer residence times, the reaction proceeded faster, which indicates that ammonia begin to react at that point. Even though the temperature increase was less sharp, IPA removal was near to 96%. Thus, apparently IPA ignition took place. The residence time at which maximum temperature occurs coincides with the maximum temperature in ignition with 1 and 2% IPA in mass. Thus, ammonia is not delaying the ignition of IPA as observed in figure 4.2.7. Ammonia removal was only 75%, reaching a maximum temperature of 600°C. But even with the 25% of the initial NH_3 content unreacted, no further temperature increase was registered, indicating that ammonia is not reacting beyond 75% conversion, at least in its propagation step at this ratio of IPA/ NH_3 .

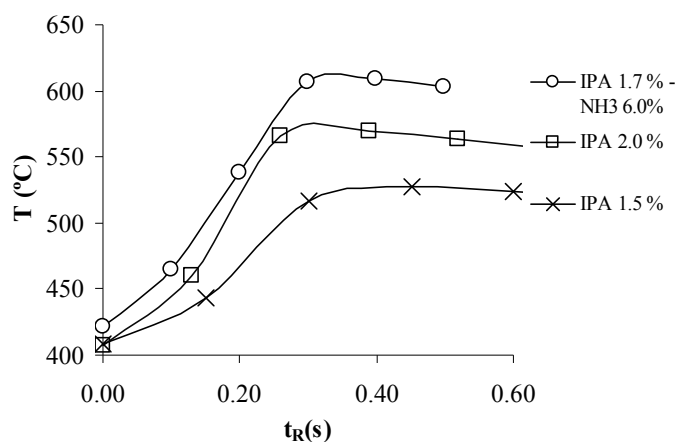


Figure 4.2.7: Comparison of the ignition of mixtures 6% NH_3 , 1.7% IPA to the ignition of IPA mixtures with 1.5 and 2% wt IPA.

With NH_3 concentration at 8% in mass and IPA concentration at 1% in mass, there was no sharp changes in the experimental temperature profile. Nevertheless, the temperature increased faster than indicated by the predicted flameless temperature profile showed in figure 4.2.7 c). Surprisingly, under those conditions a 93% of TOC removal was obtained while elimination in pure 1% IPA solution was only at 63%. Only 7% of the Total N was removed, but apparently the heat released by this oxidation contributed to a higher IPA elimination due to the temperature increase.

When ammonia was oxidized without IPA, no temperature increase was detected even at NH_3 concentrations as high as 10% NH_3 in mass.

Based on these results, it is believed that the ignition temperature of ammonia may be much higher than that of IPA. Thus, when high concentrations of IPA are used, ignition of IPA is produced and high temperatures lead to ammonia ignition and consequently to high ammonia removals, but the termination phase of the oxidation of NH_3 is too slow to reach a complete N elimination. When the concentration of IPA is too low for flame ignition, ammonia ignition is not reached, Total N removal is even slower and neither TOC nor N are completely eliminated.

Experimental temperature profiles of the oxidation of mixtures of 2.5% IPA only, 2.5% of IPA with 4% NH_3 and 2.5% IPA with 4% HAc, are compared with the flameless temperature profile calculated with the model in figure 4.2.8. Ignition is produced from the beginning of the reactor in all cases. When HAc or NH_3 are present in the mixture, temperature profiles are very similar. Only one sharp temperature increase can be observed indicating that the ignition of IPA readily leads to the ignition of the most recalcitrant compounds. Moreover, when IPA is reacting with other components, the temperature increase is faster than when it is reacting alone in the same concentration. Thus, the heat released by the oxidation of other compounds is accelerating the oxidation of IPA.

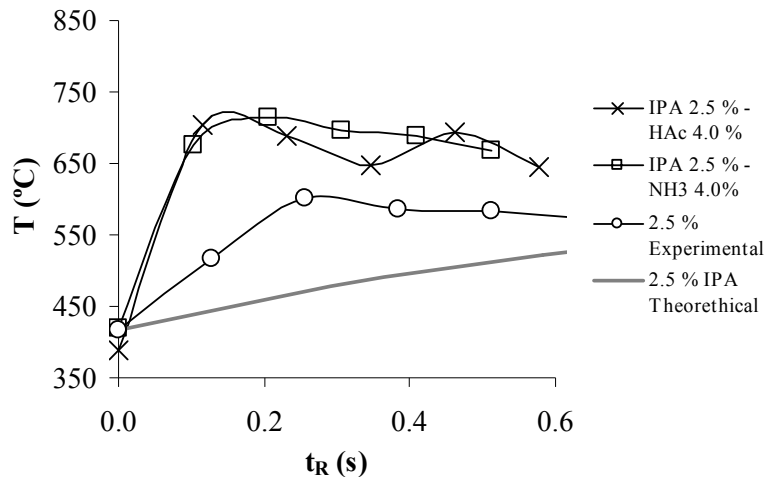


Figure 4.2.8: Profile temperatures for experiment of mixtures with IPA and HAc and NH_3

In the experiments with the highest concentration of IPA, for each ammonia concentration the presence of NO_x and NH_3 was investigated in the gas effluent and the concentration of NO_3^- in liquid effluent. The average results are shown in Table

4.2.5. It is observed that for higher NH_3/IPA ratios the Total N is increased in the liquid effluent. Concentrations of NH_3 between 4 and 60 ppm were found in the gas effluent. This concentration is increased when NH_3 concentrations are higher in the feed. Nevertheless, concentrations of NO_x in the gas effluent were below of the detection limit of 5 ppm.

Table 4.2.5: Average results of the total nitrogen, ammonia and nitrates present in samples taken from the gas effluent and liquid effluent flow.

C_{NH_30}	$C_{\text{IPA}0}$	TN (liquid)	NH_3 in Gas effluent	NO_x in Gas effluent	C_{NO_3} (liquid)	X_{NH_3}	N Converted to NO_3
(%)	(%)	(ppm N)	(ppm NH_3)	(ppm NO_x)	(ppm NO_3)	(%)	(%)
2.0	3.8	1101 ± 61	<5	<0.5	2012 ± 349	96.1 ± 0.7	2.7 ± 0.5
4.0	3.0	2754 ± 208	20	<0.5	1767 ± 115	92.9 ± 0.6	1.2 ± 0.1
6.0	2.0	3412 ± 262	60	<0.5	371 ± 67	93.3 ± 0.5	0.2 ± 0.1

Concentrations of nitrates and nitrites (NO_3^-) between 300 and 2000 ppm were found in the liquid effluents. The highest overall N removal was obtained in these samples. In figure 4.2.9, the NO_3^- concentration is represented versus excess of O_2 with respect to the stoichiometric value and versus maximum reaction temperatures for samples with different initial ammonia concentrations. In general, NO_3^- concentration increases with higher reaction temperature and higher oxygen excesses, as was observed our group's previous studies [5, 26].

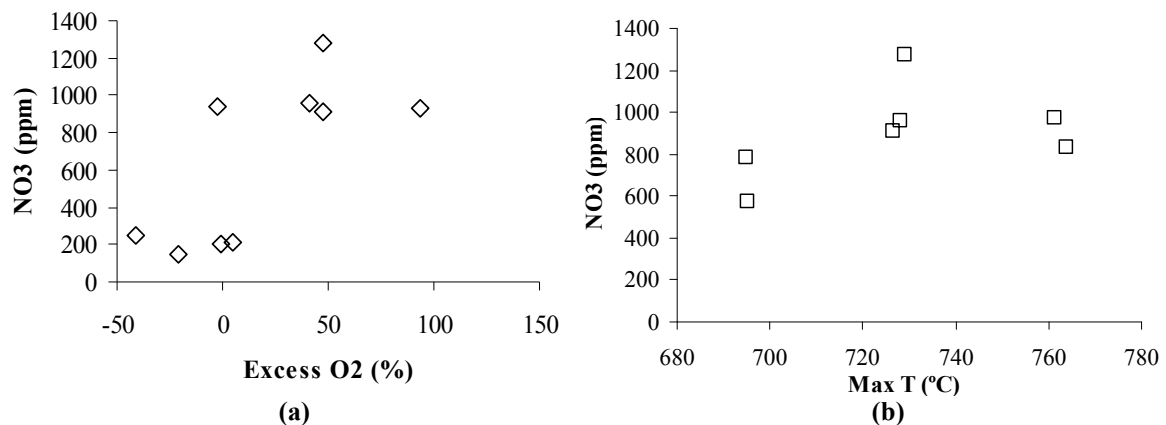


Figure 4.2.9: (a): Nitrates concentration present in the liquid effluent versus the O_2 in excess used for samples in a range of temperature of 720 – 750°C for samples with different ammonia concentrations, (b): Nitrates concentration present in the liquid effluent versus the maximum temperature registered in the reactor for samples with a flow in excess of O_2 between 30 and 50% for samples with different ammonia concentration

Temperature was monitored in 6 internal points of the reactor using 6 thermocouples type K. Feed and oxygen inlets are opposite each other. It is similar to the experimental set-up denominated as “mixer 1” described in a previous work, [10]

So far, the flameless SCWO has been commercially applied to several waste such as sludge, Chemicals weapons etc [1], sometimes using tubular reactors as long as 1 km long [27].

The results show in this work prove that the SCWO technology using hydrothermal flame as a heat source is able to destroy high amounts of recalcitrant compounds in residence times of around a seconds, using very compact reactors. The commercialization of this technology can be promising for the treatment of waste with elevated ammonia content such as sludge (with ammonia containing around 1%) or for waste derived from electronic industry, with elevated ammonia contents.

Nevertheless, previous to its commercialization the reactor design should still be optimize in order to find the appropriate residence time/temperature combination to completely destroy ammonia without generating NO_3^- , and to be able to inject cold waste into the flame to avoid corrosion in the preheating area.

4.2.4. CONCLUSIONS

The destruction of waste containing high concentrations of the recalcitrant compounds acetic acid and ammonia by supercritical water oxidation in the presence of a hydrothermal flame using isopropyl-alcohol as a co-fuel and oxygen as the oxidant was experimentally studied using a tubular reactor with a residence time of 0.7 s. In addition, as a preliminary step, the ignition of IPA solutions of different concentrations was studied.

Extremely high TOC and nitrogen conversions were obtained at the present operational conditions. Conversions increased with temperature up to a certain point:

- TOC removals were as high as 99.7% at temperatures higher than 700°C when working with IPA solution..
- 99% mineralization at temperatures as high as 750°C in concentrations up to 4% in mass of acetic acid: TOC removal was more difficult than in the oxidation of equivalent IPA solutions.
- Maximum 99% removals of TOC and 94% of N were obtained. No significant improvement in N removal was found at temperatures higher than 710°C.
- Concentrations of NH₃ between 4 and 60 ppm found in the gas effluent.
- Concentrations of NO_x in the gas effluent were below 0.5 ppm.
- Concentrations of nitrates and nitrites between 300 and 2000 ppm were found. The amount of NO₃⁻ is favoured by higher temperatures and oxygen excesses

When using IPA as a fuel and a recalcitrant compound, only one ignition point was observed, meaning that the increase of temperature produced by IPA ignition makes it possible to reach the autoignition conditions of the recalcitrant compounds as well.

- Impossible to obtain ignition using exclusively ammonia as fuel. A minimum concentration of 2% IPA in the ammonia-IPA-water mixture was necessary to obtain more than 90% ammonia elimination.

Most of the TOC and Total N were eliminated at the moment of the ignition, in a rapid temperature increase for forming the flame, but a remaining fraction of the

pollutant could not be eliminated using this tubular reactor. Very high temperatures or additional residence time seem are necessary. This is due to the low rate of oxidation reaction during the termination phase. This was especially remarkable in the case of ammonia, where eliminations higher than 93% were not possible in the operational conditions of our reactor.

Even though tubular reactors are entirely appropriate for the study of the ignition process of different compounds, the reactor design must be optimize to get a compact apparatus able to work with the appropriate residence time/temperature combination to completely destroy ammonia without generating NO_3^- , and to be able to inject cold waste into the flame to avoid corrosion in the preheating area.

· Future work:

- Study of the elimination of recalcitrant compounds using a hydrothermal flame in a vessel reactor with longer residence times and lower temperatures in order to avoid NO_3 formation.
- Avoiding corrosion problems in the preheating area by injection of the feed at room temperature into a hydrothermal flame.

LIST OF SYMBOLS

$C_{\text{HAc}0}$	Initial concentration of acetic acid	% wt
C_{HAc}	Concentration of acetic acid	% wt
$C_{\text{IPA}0}$	Initial concentration of isopropyl alcohol	% wt
C_{IPA}	Concentration of isopropyl alcohol	% wt
$C_{\text{NH}30}$	Initial concentration of ammonia	% wt
$C_{\text{NH}3}$	Concentration of ammonia	% wt
Exc O_2	Excess O_2 over the stoichiometric amount	%
P	Pressure	MPa
T	Temperature	$^{\circ}\text{C}$
t_{R}	Residence time	s
TOC	Total Organic Carbon	ppm
TN	Total Nitrogen	ppm
T_{max}	Maximum temperature in the reactor	$^{\circ}\text{C}$
T_{inj}	Injection temperature in the reactor	$^{\circ}\text{C}$
$X_{\text{NH}3}$	Ammonia conversion	
z	Reactor length	m

4.2.5. REFERENCES

- [1] M.D. Bermejo, M.J. Cocero, Supercritical water oxidation: A technical review, *AICHE Journal*, 52 (2006) 3933-3951.
- [2] G. Brunner, Near and supercritical water. Part II: Oxidative processes, *Journal of Supercritical Fluids*, 47 (2009) 382-390.
- [3] G.M. Pohsner, E.U. Franck, Spectra and temperatures of diffusion flames at high-pressures to 1000 bar, *Berichte Der Bunsen-Gesellschaft-Physical Chemistry Chemical Physics*, 98 (1994) 1082-1090.
- [4] C. Augustine, J.W. Tester, Hydrothermal flames: From phenomenological experimental demonstrations to quantitative understanding, *Journal of Supercritical Fluids*, 47 (2009) 415-430.
- [5] M.D. Bermejo, F. Cantero, M.J. Cocero, Supercritical water oxidation of feeds with high ammonia concentrations Pilot plant experimental results and modeling, *Chemical Engineering Journal*, 137 (2008) 542-549.
- [6] R.M. Serikawa, T. Usui, T. Nishimura, H. Sato, S. Hamada, H. Sekino, Hydrothermal flames in supercritical water oxidation: investigation in a pilot scale continuous reactor, *Fuel*, 81 (2002) 1147-1159.
- [7] M.D. Bermejo, E. Fdez-Polanco, M.J. Cocero, Experimental study of the operational parameters of a transpiring wall reactor for supercritical water oxidation, *Journal of Supercritical Fluids*, 39 (2006) 70-79.
- [8] C.H. Oh, R.J. Kochan, T.R. Charlton, A.L. Bourhis, Thermal-hydraulic modeling of supercritical water oxidation of ethanol, *Energy & Fuels*, 10 (1996) 326-332.
- [9] M.D. Bermejo, P. Cabeza, J.P.S. Queiroz, C. Jiménez, M.J. Cocero, Analysis of the scale up of a transpiring wall reactor with a hydrothermal flame as a heat source for the supercritical water oxidation, *Journal of Supercritical Fluids*, 56 (2011) 21-32.
- [10] M.D. Bermejo, P. Cabeza, M. Bahr, R. Fernández, V. Ríos, C. Jiménez, M.J. Cocero, Experimental study of hydrothermal flames initiation using different static mixer configurations, *Journal of Supercritical Fluids*, 50 (2009) 240-249.
- [11] B. Wellig, M. Weber, K. Lieball, K. Prikopsky, P.R. von Rohr, Hydrothermal methanol diffusion flame as internal heat source in a SCWO reactor, *Journal of Supercritical Fluids*, 49 (2009) 59-70.

- [12] A. Leybros, A. Roubaud, P. Guichardon, O. Boutin, Ion exchange resins destruction in a stirred supercritical water oxidation reactor, *Journal of Supercritical Fluids*, 51 (2010) 369-375.
- [13] L.X.C. Li, P. S. Gloyna, E. F., Generalized kinetic-model for wet oxidation of organic-compounds, *AIChE Journal*, 37 (1991) 1687-1697.
- [14] D. Mateos, J.R. Portela, J. Mercadier, F. Marias, C. Marraud, F. Cansell, New approach for kinetic parameters determination for hydrothermal oxidation reaction, *Journal of Supercritical Fluids*, 34 (2005) 63-70.
- [15] J.C. Meyer, P.A. Marrone, J.W. Tester, Acetic-acid oxidation and hydrolysis in supercritical water, *AIChE Journal*, 41 (1995) 2108-2121.
- [16] P.E. Savage, M.A. Smith, Kinetics of acetic-acid oxidation in supercritical water, *Environmental Science & Technology*, 29 (1995) 216-221.
- [17] J. Honga, J. Hongb, M. Otakic, O. Jollieta, Environmental and economic life cycle assessment for sewage sludge treatment processes in Japan, *Waste Management*, 29 (2009) 696-703.
- [18] W.R. Killilea, K.C. Swallow, G.T. Hong, The fate of nitrogen in supercritical water oxidation, *Journal of Supercritical Fluids*, 5 (1992) 72-78.
- [19] B. Al-Duri, L. Pinto, N.H. Ashraf-Ball, R.C.D. Santos, Thermal abatement of nitrogen-containing hydrocarbons by non-catalytic supercritical water oxidation (SCWO), *Journal of Materials Science*, 43 (2008) 1421-1428.
- [20] M. Goto, T. Nada, A. Kodama, T. Hirose, Kinetic analysis for destruction of municipal sewage sludge and alcohol distillery wastewater by supercritical water oxidation, *Industrial & Engineering Chemistry Research*, 38 (1999) 1863-1865.
- [21] J.M. Ploeger, A.C. Madlinger, J.W. Tester, Revised global kinetic measurements of ammonia oxidation in supercritical water, *Industrial & Engineering Chemistry Research*, 45 (2006) 6842-6845.
- [22] N. Segond, Y. Matsumura, K. Yamamoto, Determination of ammonia oxidation rate in sub- and supercritical water, *Industrial & Engineering Chemistry Research*, 41 (2002) 6020-6027.
- [23] F. Vogel, J.L.D. Blanchard, P.A. Marrone, S.F. Rice, P.A. Webley, W.A. Peters, K.A. Smith, J.W. Tester, Critical review of kinetic data for the oxidation of methanol in supercritical water, *Journal of Supercritical Fluids*, 34 (2005) 249-286.

[24] D.T.C. Magoulas, Thermophysical properties of n-alkanes from C1 to C26 and their prediction for higher ones, *Fluid Phase Equilibria*, 56 (1990) 119-140.

[25] T.J. Wightman, Studies in supercritical air oxidation,, in: *Chem. Eng. Dept.*, MIT, Berkeley, CA, , 1981.

[26] M.J. Cocero, E. Alonso, R. Torio, D. Vallelado, F. Fdz-Polanco, Supercritical water oxidation in a pilot plant of nitrogenous compounds: 2-propanol mixtures in the temperature range 500-750 degrees C, *Industrial & Engineering Chemistry Research*, 39 (2000) 3707-3716.

[27] European Commission, Nitrate Directive 91/676/EEC in, 1991.

CHAPTER 5

TRANSPIRING WALL REACTOR

CHAPTER 5

TRANSPIRING WALL REACTOR

TABLE OF CONTENTS

5.1. ANALYSIS OF THE SCALE UP OF A TRANSPIRING WALL REACTOR WITH A HYDROTHERMAL FLAME AS A HEAT SOURCE FOR THE SUPERCRITICAL WATER OXIDATION	173
5.1.1. INTRODUCTION	175
5.1.2. EXPERIMENTAL	177
5.1.2.1 Experimental facilities	177
5.1.2.2 Experimental procedure.....	181
5.1.3. RESULTS AND DISCUSSION.....	182
5.1.3.1 Analysis of the hydrothermal flame initiation in a tubular reactor using oxygen as the oxidant	182
5.1.3.2 Analysis of the operating parameters of the scaled up transpiring hydrothermal flame initiation in a tubular reactor using oxygen as the oxidant ..	185
5.1.3.3 Operational problems	190
5.1.3.4 Estimation of the flame front velocities	191
5.1.3.5 Modeling.....	193
5.1.4. CONCLUSIONS	200
5.1.5. REFERENCES	203

5.1. ANALYSIS OF THE SCALE UP OF A TRANSPIRING WALL REACTOR WITH A HYDROTHERMAL FLAME AS A HEAT SOURCE FOR THE SUPERCRITICAL WATER OXIDATION

ABSTRACT

Experimental data from a tubular reactor and from a transpiring wall reactor (TWR) are used to analyze the scaling up of SCWO reactors operating with a hydrothermal flame as a heat source. Results obtained with the tubular reactor show that fluid velocity inside the reactor determines the minimum injection temperature at which a stable hydrothermal flame is formed. When the fluid velocity inside of the reactor is lower, the extinction temperature of the hydrothermal flame in that reactor is also lower. Using this reactor, extinction temperatures are always near or above the critical temperature of water. Total TOC removals are possible working with isopropyl-alcohol at temperatures between 650 and 700°C and residence times of 0.5 s. Results of the TWR show that steady operation with a hydrothermal flame inside is possible even when reagents are injected at subcritical conditions as low as 170°C. Temperature measurements show that reaction is not initiated in the injector but in the reaction chamber, where fluid velocity is lower than 0.1 s. This was explained by estimating that the flame front velocity of a hydrothermal flame is of the order of 0.1 m/s. Thus, it is expected that the flame is stabilized in the reaction chamber and not in the injector, where fluid velocities are higher than 2 m/s. A previously developed model of the TWR was modified in order to describe the ignition in the reaction chamber and not in the injector. The model reproduces satisfactorily experimental data and it was used to propose the design of scaled up reactors for SCWO with a hydrothermal flame inside.

5.1.1. INTRODUCTION

Supercritical water oxidation (SCWO) takes advantage of the special solvation properties of water above its critical point (374°C, 22.1 MPa) to achieve the complete destruction of organic waste. Oxidation of organics dissolved in the supercritical water (SCW) proceeds in a homogeneous phase due to the complete miscibility of oxygen with SCW. The industrial development of the process has been delayed due to the main challenges of this technology: corrosion, salt deposition and high energetic demand [1, 2]. Corrosion and salt deposition problems, as well as heat recovery optimization, can be overcome by an appropriate reactor design able to isolate and reduce the areas with harsher reaction conditions, and by selection of appropriate construction materials. At the same time the reactor must allow maximizing the energy recovery to produce heat and electricity when possible.

When temperature is higher than the autoignition temperature, oxidation in SCW takes place in the form of flames, called hydrothermal flames. Hydrothermal flames were discovered by Franck and co-workers in the late 80's [3]. They have been applied in several SCWO reactors designs [4-6] showing a number of advantages over the flameless SCWO process [7]. The advantages include the following

- Reaction can be completed within milliseconds, which permits the construction of smaller reactors.
- It is possible to inject reagents in the flame at room temperature avoiding the external preheating. This avoids problems such as plugging and corrosion in a preheating system, having an advantage over the operational and energy integration perspective, because all the energy produced can be devoted to energy production.
- Higher temperatures (600 - 700°C) improve energy recovery from the heat of reaction of the waste.

The High Pressure Processes Group of the University of Valladolid (UVa) (Spain) recently showed the formation of hydrothermal flames in tubular reactors [8] with velocities between 2-20 m/s. In these experiments, solutions with IPA concentrations of 4-5% in mass were used. A sharp increase in temperature was registered inside the tubular reactors, indicating the ignition of the hydrothermal flame. It was proved that the kinetics described in literature were too slow to describe the fast temperature rise registered inside the reactors. Total TOC removals could be obtained in residence times lower than 0.5 s. This behavior was only observed when the injection temperatures (T_{inj})

were higher than 370°C. Narrower or filled reactors presented worse results than a simple empty ¼" tube.

Vessel reactors have demonstrated to be more successful in maintaining steady stable hydrothermal flames with injection temperatures near to room temperature [4-6]. Within the vessel reactors, the Transpiring Wall Reactor (TWR) is a reactor design developed for the Supercritical Water Oxidation (SCWO) process in order to overcome salt deposition and corrosion problems. It consists of a reaction chamber surrounded by a wall through which clean water circulates, forming a cool, protective film against corrosive agents, salt and high temperatures. In the last years several proposals of TWR have been patented and a number of reactor has been tested, developing different technical solutions [9] like alumina transpiring walls able to withstand corrosion and high temperatures [10], treating different waste even with high salt contents [9, 11] and using different preheating systems. The ETH Zurich has developed a transpiring wall reactor that allows maintaining a hydrothermal diffusion flame formed by mixing a concentrated aqueous stream of methanol at temperatures between 200 - 350°C with oxygen, and, in a posterior position of the device, injecting the cold waste into the flame [12]. Using the same facility, the inlet temperature of the fuel stream could be lowered below 100°C with 27 wt% methanol [5]. In the High Pressure Process Group of the University of Valladolid it was possible to form a premixed flame by injecting a feed consisting of an isopropanol (IPA) aqueous solution with a concentration as low as 6.5% wt IPA at temperatures above 420°C. Once the flame was ignited, it could be kept steady while the injection temperatures were reduced down to a temperature of 110°C [6].

In this work a scaled up transpiring wall reactor is tested at feed flows as high as 60 kg/h using both oxygen and air as the oxidants. Its behavior is analyzed paying special attention to the ignition process of the hydrothermal flame. To test further, ignition experiments in a tubular reactor were performed. The model previously developed for describing the behavior of this reactor [13] was modified in order to reproduce the hydrothermal flame reaction and used to propose an ideal scaled up of the reactor.

5.1.2. EXPERIMENTAL

5.1.2.1. Experimental facilities

Two reactors were used in this work: a tubular reactor and transpiring wall reactor. They are described below.

The **tubular reactor** consists of a ¼” Ni-alloy 625 tube with an internal diameter of 3.86 mm and 2 m long, similar to the one described in a previous work of the group [8] under the name of mixer 1, but with a higher length. The length was increased, with respect to the previous reactor, in order to detect when ignition was produced at longer residence times. Temperatures were registered at 6 points along the tube at distances of 0, 40, 80, 120, 160 and 200 mm from the mixing point. The diameter of the tubular reactor was chosen to be similar to that of the mixer used in the transpiring wall reactor described below. In its end, a quenching water stream is introduced in the reactor in order to stop the oxidation reactor.

The **transpiring wall reactor** of the University of Valladolid (UVa) consists of a stainless steel pressure shell with a volume of 6.3 L. It contains a reaction chamber surrounded by a porous wall through which clean water circulates. The feed and the oxidant are introduced into the reactor through its lower part, and they are fed through a tubular static mixer up to the upper part of the reaction chamber where the hydrothermal flame is ignited. After passing through the flame, the products of the reaction flow down mixing with the clean water that enters the reactor through the transpiring wall, and decontaminated water leaves the reactor through its lower part, as shown in figure 5.1.1 a).

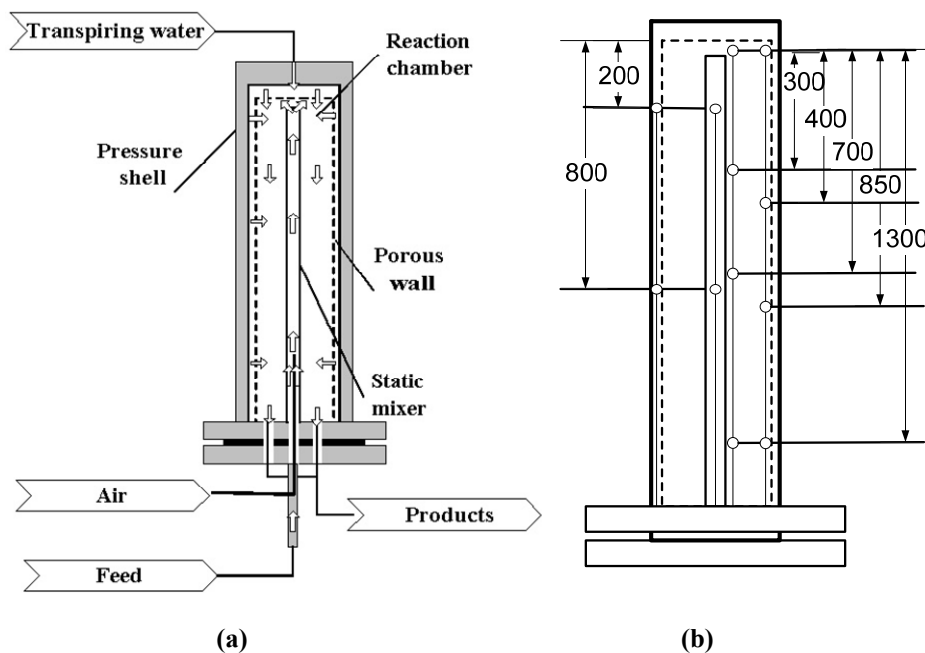


Figure 5.1.1: a) Scheme of the operation of the transpiring wall reactor, b) Temperature measurement points inside the transpiring wall reactor.

Experiments presented in this work were performed using the reactor design described as reactor design 3 in Bermejo et al [9]. It consists of a transpiring wall whose upper and lower sections are made of non-transpiring Ni alloy 625. It is porous only the central section of the reactor, that is made of porous sintered Ni alloy 600. The mixer was designed in such a way that the ignition was produced in the reaction chamber and not in the mixer. In a previous investigation of the research group it was demonstrated that much higher injection temperatures were necessary to have ignition in a filled tube than in an empty one [8]. Thus, the injector was constructed as a tube with an internal diameter of 9 mm filled with alloy 625 particles of different size, placing the smallest in the higher part of the mixer. Then, the feed enters at subcritical conditions into the reaction chamber, where it becomes supercritical when injected into the hydrothermal flame. In such a way, the salts dissolved in the feed precipitates in the chamber where it is less likely to produce blockage than in the tubular mixer. There are temperature measurements outside of the transpiring wall, inside the reaction chamber and also there are two temperature measurements inside the mixer to monitorize the reaction initiation. The temperature measurement points are shown in figure 5.1.1 b).

For analyzing the behaviour of the transpiring wall reactor some parameters are defined. These parameters and definitions were described in detail in previous works [6, 9].

· Transpiring flow ratio R , is the ratio of the transpiring flow divided by the total flow (feed + oxidant) as defined in equation 1.

$$R = \frac{\text{Transpiring_Flow}}{\text{Feed} + \text{Oxidant}} \quad (1)$$

• TOC removal (TOC Rem). TOC removal is defined as the mass of organic carbon eliminated divided by the initial mass of organic carbon introduced into the reactor in equation 2.

$$\text{TOC Rem} = \frac{\text{Feed} \cdot \text{TOC}_0 - (\text{Feed} + \text{Transpiring_Flow}) \cdot \text{TOC}_{ef}}{\text{Feed} \cdot \text{TOC}_0} \quad (2)$$

Where TOC_{ef} is the TOC in the effluent and TOC_0 is the initial TOC of the Feed.

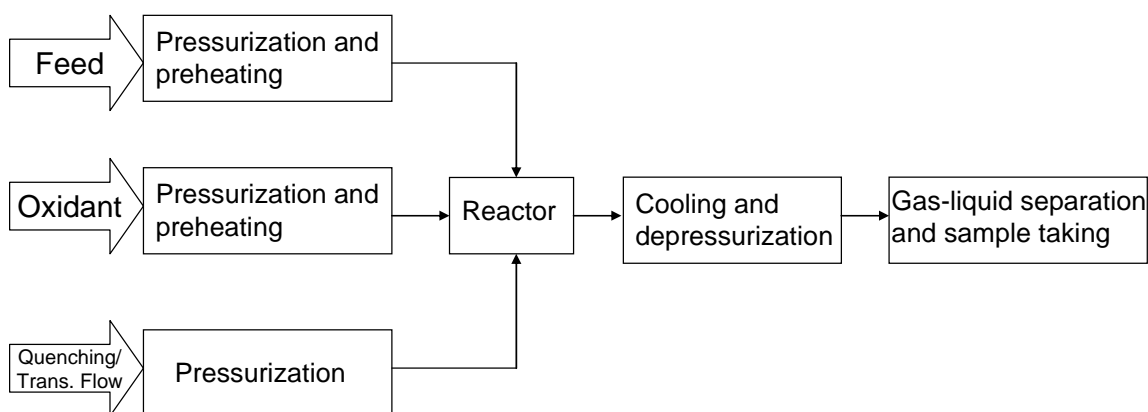
• Useful Residence Time (t_R) is defined as the time that the reagents spend in the reactor at conditions of flame regime. We consider that ignition happens when the temperature increases sharply. In our previous work we could estimate that ignition of IPA at happened more or less around a certain temperature that was different for each tubular reactor [8]. In conventional combustion it is known that autoignition temperature depends on the geometric factors as they influence fluid velocity and heat transmission. As determining the fraction of reactor at flame regime it is not a simple task, in order to make the parameters analysis the autoignition temperature of 470°C found by Serikawa and co-workers [14] is accepted. Thus, 470°C will be the minimum temperature for having flame regime, in order to make an estimation of the volume of reactor at which reaction proceeds at a elevated reaction rate. At higher temperatures reagents will oxidize in flame regime at faster reaction rates than those found in flameless oxidation. As they flow down the reactor and become mixed with the transpiring flow, reagents temperature decreases. When the temperature is lower than 470°C the reaction would proceed at flameless regime, with a much lower rate. Thus, only the residence time at temperatures higher than 470°C is considered “useful residence time”. The length of the reactor at temperatures higher than 470°C can be interpolated using the temperature profiles. With this length, the volume of the reactor at $T > 470^\circ\text{C}$ can be calculated. The residence time is evaluated by dividing this volume by the volumetric flow of reagents + transpiring flow determined using the density of the mixture at the average reaction temperature.

The reactors have been tested in two experimental facilities: a SCWO pilot plant and a SCWO demonstration plant. The main characteristics of each plant are summarized in table 5.1.1.

Table 5.1.1: Main characteristics of the experimental facilities used in this work

	Pilot plant	Demonstration plant
Oxidant	Air	Oxygen
Maximum feed flow capacity	40 kg/h	200 kg/h
Preheating	Electrical preheating	Electrical preheating and heat recovery from the hot products of the reactor in a concentric heat exchanger
Location	Premises of the University of Valladolid (Valladolid, Spain)	Premises of the Company CETRANSA (Santovenia de Pisuerga, Valladolid, Spain)
References	[6], [8],[9]	[15]

Both plants can be described according to the simplified scheme shown in figure 5.1.2. Further details of the plants can be found in literature [6, 8, 9, 15].

**Figure 5.1.2:** Block diagram of the SCWO plant

Temperatures were measured with type K thermocouples (temperature range from 0 to 1000°C) with an accuracy of 1% of the measurement. Air and oxygen flows were measured with Coriolis gas flow meters with a precision of 0.2%. Liquid flows were determined by measuring the time required to pump a certain liquid volume. The feeds of the reactors were prepared using net water and different concentrations of isopropyl alcohol (Technical isopropyl alcohol, 99% wt, supplied by COFARCAS (Spain)). IPA solutions were prepared volumetrically, measuring water volume with a precision of 1 L and IPA volume with a precision of 1 mL, resulting in an experimental error 0.4% of the concentration of the solution. Total organic carbon (TOC) was characterized using a Shimadzu 5050 TOC analyzer (detection limit: 1 ppm).

5.1.2.2. Experimental procedure

The transpiring wall reactor was tested first in the pilot plant using air as the oxidant and feed flows between 20 and 40 kg/h. Later on, the reactor was tested in the demonstration plant using oxygen as the oxidant with feed flows as high as 60 kg/h of feed. An extensive number of experiments were performed in order to obtain a total number of 22 pieces of experimental data performed in the pilot plant and 12 in the demonstration plant. The objective was to study the influence of the main operational parameters: feed flow, feed injection temperature, transpiring flow ratio and fuel concentration on the hydrothermal flame and on the residence time in the reactor.

In every experiment performed with the transpiring wall reactor, the reactor was first preheated electrically until the thermocouples situated at the walls of the pressure vessel indicated a temperature of 400°C. Then, the reaction was ignited using feeds with IPA concentrations as high as 8% wt IPA and injection temperatures higher than 400°C. Once the reaction was initiated the electrical heating of the wall of the reactor was turned off and transpiring flow was connected. Once reached the stationary state, reaction conditions were changed. Several stationary states were reached and samples were taken.

In the experiments using the tubular reactor, at the beginning of a new experiment, the reactor was preheated by passing a supercritical water flow through it until all the thermocouples indicated temperatures higher than 400°C. Oxidant flow was then introduced at 0-10% excess over the stoichiometric amount. When ignition occurred, the temperature increased sharply inside the tubular reactor and at that moment quenching water was connected. Apart from the electrical preheating of the reagents no more heat was supplied to the system, the reactor being autothermal. The system was maintained in a stationary state and samples were taken. After sample taking, experimental conditions were altered by reducing the temperature or by modifying feed flow or injection temperature. Samples were taken again when a new stationary state was reached. When no apparent increase in temperature compared to the temperature at the inlet of the tubular reactor was detected, samples were taken and after that, the experiment was finished. In every experiment a number of 1-4 stationary states could be evaluated depending on experimental conditions.

During the experiments, temperature profiles were registered automatically.

5.1.3. RESULTS AND DISCUSSION

5.1.3.1. Analysis of the hydrothermal flame initiation in a tubular reactor using oxygen as the oxidant

For the present work, new experiment using both oxygen and air as an oxidant were described using the tubular reactor described in section 5.1.2.1 Every experiment was repeated a minimum of three times. The average results obtained using air and oxygen as the oxidant are presented in table 5.1.2. It is observed that at residence times between 1.2 s and 0.3 s TOC removal higher than 99.0% were obtained with maximum temperatures around 700°C.

Table 5.1.2: Experimental data using the tubular reactor with both air and oxygen as the oxidant performed at C= 4% wt IPA and different feed flows. Average standard deviations are Oxidant flow: 0.2 kg/h; T_{inj} : 8°C; T_{max} : 15°C; TOC_{ef} =207 ppm; TOC_{rem} :0.8%; t_R : 0.03 s

Feed (kg/h)	O ₂ (kg/h)	T _{inj} (°C)	T _{max} (°C)	TOC Rem (%)	TOC _{ef} (ppm C)	t _R (s)
6.01	0.5	354	620	99.4	152	1.19
8.22	0.9	364	643	99.6	98	0.81
11.07	1.2	381	645	99.3	162	0.55
13.98	1.4	388	644	99.1	226	0.44
8.22	0.7	425	685	99.7	63	0.76
8.22	0.9	379	623	98.7	301	0.74
8.22	1.0	313	334	49.1	12,209	1.20

Feed (kg/h)	Air (kg/h)	T _{inj} (°C)	T _{max} (°C)	TOC rem (%)	TOC _{ef} (ppm C)	t _R (s)
6.00	2.8	370	697	99.7	72	0.59
7.50	3.7	373	703	99.9	31	0.50
9.00	4.1	381	653	99.7	71	0.34
10.00	5.1	383	686	98.7	306	0.31

In table 5.1.2 the experiments performed at the minimum injection temperature at which ignition occurred, that is extinction temperatures, at each feed flow are presented using both air and oxygen as the oxidant.

These data are plotted in figure 5.1.3 (a) showing the extinction temperatures represented versus the feed flows using air and oxygen as the oxidant. It can be observed that extinction temperatures were reduced when the feed flow was decreased, and that the extinction temperatures were lower when using oxygen as the oxidant.

In figure 5.1.3 (b), the same data were represented to show the extinction temperatures versus the total inlet flow (feed + oxidant). It is observed that, independently of the type of oxidant used, the extinction temperature of a hydrothermal flame in a tubular reactor was a function of the total flow inside of the reactor, that is, velocity inside of the tube. Consequently, for treating the same feed flow extinction temperature was lower using O_2 as the oxidant because the total flow was lower. In our previous work [8] it was observed that when working with air as the oxidant, ignition was only possible with homogeneous mixtures, at P, x conditions over the bubble point line. In the experiments performed in this work using oxygen as the oxidant, the reduction in the total flow allows the ignition of some mixtures injected below the bubble point temperature that is of liquid vapour mixtures.

In figure 5.1.3 (c) the bubble temperature line versus water composition, calculated using the Anderko-Pitzer EoS [16-18] is represented together with the T, x inlet conditions of the data using O_2 as oxidant. In table 5.1.3 experiments performed using oxygen as the oxidant at a fixed feed flow of 8.2 kg/h and different injection temperatures are presented as well. These data are represented in figure 5.1.3 (d) where the temperature profiles along the tubular reactor are shown. As described in our previous research [8], here it is observed as well that, when increasing injection temperature, the ignition happened at a shorter distance from the inlet of the tube. If the injection temperature was too low, ignition was not observed.

In table 5.1.3 it is observed that even when ignition is delayed TOC removals near 99% are obtained. If ignition is not registered in the reactor, as observed in the piece of data of injection temperature 313°C , the maximum registered temperature was of 334°C and conversion was of 49%.

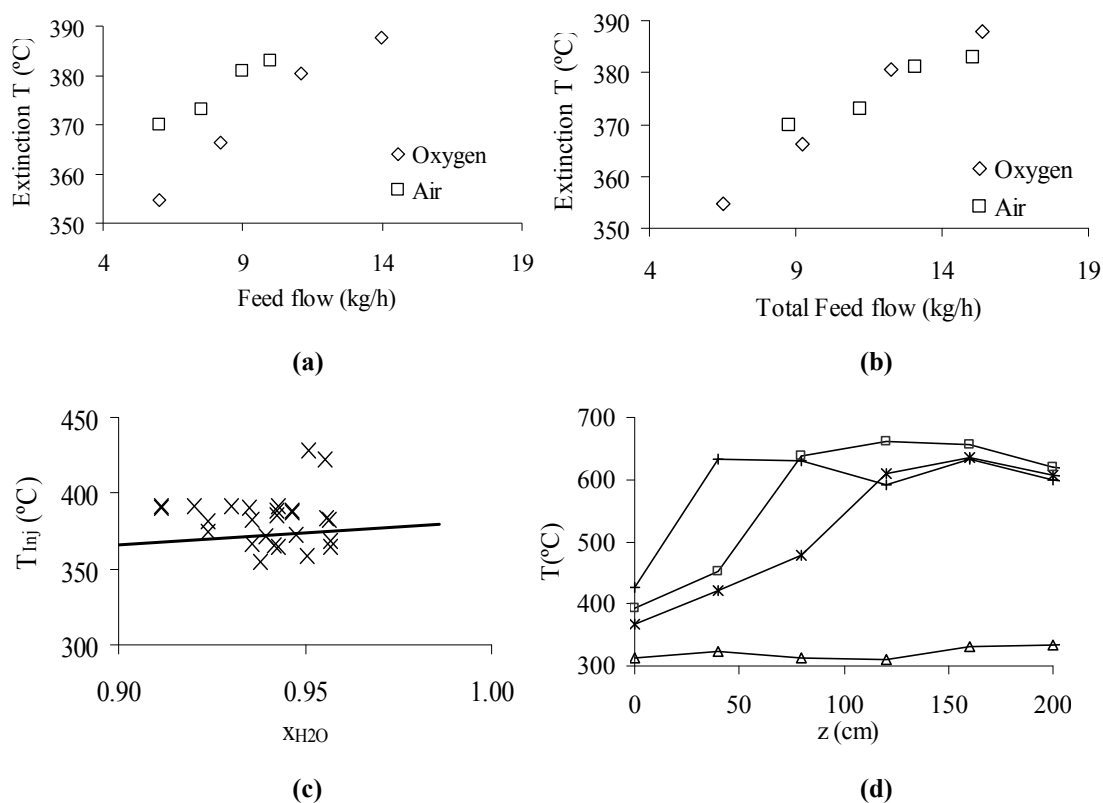


Figure 5.1.3 : Experiments with $\frac{1}{4}$ " empty tubular reactor. (a) Extinction at different feed flows using air and oxygen as oxidants working with 4% wt IPA; (b) Extinction at different total flows (feed+oxidant) using air and oxygen as the oxidants working with 4% wt IPA; (c) Temperature versus composition of the data at the inlet of the reactor represented together with the bubble point line calculated by the Anderko-Pitzer EoS; (d) Temperature profiles inside of the tubular reactor at different injections temperatures for a feed flow of 8 kg/h and $C=4\%$ wt IPA.

Results showed that injection temperature and fluid velocity are the main parameters involved in the ignition of hydrothermal flames in tubular reactors. Fluid velocity inside of the reactor determined the minimum injection temperature at which a stable hydrothermal flame was possible. Therefore, when the velocity in the reactor is lower, the extinction temperature is also lower. In general, TOC removals higher than 99% were possible working with IPA at temperatures between 650 and 700°C and residence times of 0.3 -1.2 s. Results indicated that tubular reactors are very simple and convenient device for performing SCWO reactors, in which total TOC removal can be obtained in very short residence time. But operating at steady hydrothermal flame regime is not possible if the feed is injected at low temperatures. This can be an inconvenience when working with feed containing salts that would precipitate in the preheating system producing plugging problems.

5.1.3.2. Analysis of the operating parameters of the scaled up transpiring hydrothermal flame initiation in a tubular reactor using oxygen as the oxidant

Several experiments using both air and oxygen as the oxidants were performed with the scaled up transpiring wall reactor. The main results of the experiments performed using air as the oxidant are listed in table 5.1.3, while the experiments performed using O₂ as the oxidant are presented in table 5.1.4.

The reactor design was tested for several feed flows, transpiring flows and feed injection temperatures in the pilot plant. TOC removals higher than 99% were obtained with feed flows from 7.5 to 31.8 kg/h at different feed temperatures and IPA concentrations. Reaction with a steady hydrothermal flame was possible with injection temperatures as low as 170°C and increasing the fuel concentration up to 10% wt IPA in order to reach reaction temperatures between 650-700°C.

Table 5.1.3: Average results of the experiments performed with the scaled up transpiring wall reactor working with air as the oxidant in the pilot plant. C_{IPA}: concentration of isopropanol in% in mass; R ratio: Transpiring Flow/Total Flow; T_{max}: maximum temperature registered in the reactor; TOC_{ef}: total organic carbon (TOC) in the effluent of the reactor; TOC Rem: TOC removal; T_{inj}: temperature of injection; t_R: useful residence times. Average standard deviations are Feed flow: 0.1 kg/h; T_{max} 3°C; TOC_{ef}=30 ppm; TOC_{rem}:0.1%; T_{inj}=2°C; t_R: 0.1s

TOTAL FLOW (kg/h)	C _{IPA} (% wt)	Feed (kg/h)	R	T _{max} (°C)	TOC _{ef} (ppm)	TOC Rem (%)	T _{inj} (°C)	t _R (s)
14.5	8.0%	7.4	0.50	665	90	99.6	350	16.7
23.3	8.0%	11.9	0.37	716	224	99.2	354	12.4
30.5	6.5%	17.9	0.49	682	165	99.2	346	9.7
33.9	8.0%	18.3	0.36	701	298	99.0	349	9.2
33.9	8.0%	17.8	0.36	694	352	98.8	311	8.7
41.2	6.5%	23.7	0.36	655	85	99.6	340	8.3
41.2	6.5%	23.1	0.49	650	126	99.4	323	7.6
41.4	8.0%	22.0	0.37	697	311	98.9	364	8.9
44.1	8.0%	23.9	0.32	687	429	98.6	326	7.6
42.2	8.0%	22.6	0.42	655	587	97.8	241	7.4
41.3	8.0%	21.7	0.31	657	679	97.8	253	7.8
42.1	8.0%	22.4	0.19	670	652	98.2	246	8.7
51.5	8.0%	27.7	0.33	694	298	99.0	321	8.1
53.4	8.0%	28.6	0.30	685	492	98.4	304	7.5
53.9	8.0%	27.2	0.33	659	129	99.6	214	7.5
58.0	9.0%	28.9	0.33	749	138	99.6	296	8.4
62.2	8.0%	31.8	0.33	611	254	99.1	189	6.2
63.9	8.5%	31.8	0.33	617	220	99.3	185	6.8
69.6	8.5%	36.7	0.33	613	847	97.3	170	4.3
69.5	9.0%	35.7	0.33	636	777	97.6	169	4.5
68.8	9.5%	34.4	0.34	655	833	97.5	169	5.1
68.5	10.0%	34.1	0.33	668	739	97.9	173	5.5

Using oxygen as the oxidant, experiments were performed with feed flows up to 61 kg/h. It was not possible to perform experiments at higher feed flows because the head loss in the static mixer was too high. In general, maximum temperatures between 600 and 800°C were reached. It was observed that oxygen excesses of 20% over the stoichiometric amount led to very high reaction temperatures, indicating a higher rate of reaction with respect to data with lower O₂ excess.

Table 5.1.4: Average values of the experiments performed with the scaled up transpiring wall reactor using oxygen as the oxidant in the demonstration plant. C_{IPA}: concentration of isopropanol in% wt; R ratio: Transpiring Flow/Total Flow; T_{max}: maximum temperature registered in the reactor; TOC_{ef}: total organic carbon (TOC) in the effluent of the reactor; TOC Rem: TOC removal; T_{inj}: temperature of injection; t_R: useful residence times. Average standard deviations are Feed flow: 0.8 kg/h; T_{max} 4°C; Excess O₂: 0.3%; TOC_{ef}=115 ppm; TOC_{rem}:0. 2%; T_{inj}=3°C; t_R: 0.2s

TOTAL FLOW (kg/h)	C _{IPA} (% wt)	Excess O ₂ (%)	Feed (kg/h)	R	T _{max} (°C)	TOC _{ef} (ppm)	TOC Rem (%)	T _{inj} (°C)	t _R (s)
26.1	8%	12%	21.5	0.39	758	4561	90.5	377	9.0
25.8	8%	14%	21.2	0.60	620	5259	89.0	380	7.7
39.5	8%	1%	33.1	0.39	618	4587	90.4	376	6.4
54.2	8%	10%	44.7	0.27	616	4639	90.3	343	7.3
52.5	8%	25%	42.4	0.35	783	3227	90.4	352	7.4
63.0	8%	6%	52.4	0.23	596	4154	91.3	316	8.2
66.1	8%	22%	53.6	0.34	818	2355	93.0	338	7.2
79.7	8%	12%	65.6	0.20	800	3729	90.4	304	7.6
79.8	8%	12%	65.7	0.29	778	3576	90.0	301	7.0
71.6	9%	-2%	59.1	0.20	710	4349	91.9	296	7.3
72.0	9%	4%	58.8	0.34	702	4989	90.8	296	5.9

In order to evaluate how the excess in oxygen concentration can explain the high increase in temperature we use a typical kinetic model depending on the oxidant concentration. The kinetic model selected was that of Webley and Tester [19]. An ideal adiabatic CSTR reactor was assumed. Feed (methane + water) and pure oxygen entered at 400°C and 23 MPa. Changing the air flow, but maintaining constant feed flow and a residence time of 0.1 s, it is possible to evaluate the effect of oxidant excess on reaction temperature and conversion. The results are presented in figure 5.1.4. It was obtained that when increasing air flow to have an excess from 0 to 500% the conversion first is decreasing up to and oxygen excess of 100% over stoichiometric amount and after that point is increasing from 55 to 65%. At the same time temperature is decreasing about 40°C due to the dilution effect of the oxidant effect. Thus, the increment of temperature of more than 100°C when increasing the excess of oxidant from 10 to 25% cannot be explained by a kinetic effect. We must accept that the increment of the reaction rate due to the oxygen excess is due to a bad mixing of the oxidant and the feed.

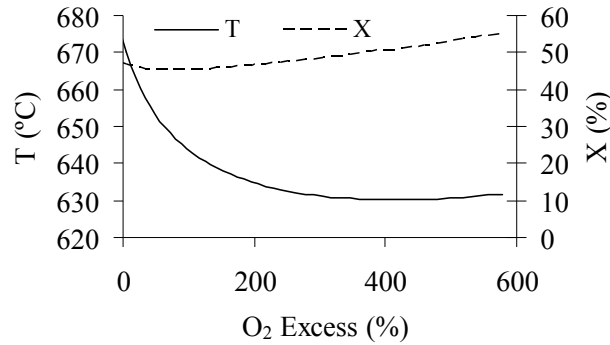


Figure 5.1.4: Influence of the oxygen excess over the stoichiometric in a SCWO CSTR reactor, with a residence time of 0.1 s, $T_{inj}=400^{\circ}\text{C}$ and $P=23\text{ MPa}$ for the oxidation of methane using the kinetic model of Webley and Tester [19].

Even when the performance of the reactor was good, and typical hydrothermal flame reaction temperatures were reached, the TOC removals were around 90%, with TOC contents of around 4000 ppm. These TOC concentrations are too high for the typical effluents obtained with the SCWO technology. With the tubular reactors it was demonstrated that complete conversion could be obtained in 0.3-1.2 s while the reactor presented useful residence times between 5-20 s. Thus, it was suspected that it was a leaking in the base of the injector and that in the last experiments a maximum of 9% of the feed was shortcut leaving directly the reactor without passing through the hydrothermal flame formed in the top of the injector. When the reactor was dismantled this theory was confirmed.

Useful residence times found in the reactor are much higher than the reaction time needed for the complete oxidation of IPA, nevertheless the study performed here about the influence of the different operational parameters in the useful residence time is useful when considering the destruction of more recalcitrant compounds such as ammonia in which the residence times necessary for complete oxidation can be longer.

Figure 5.1.5 (a) shows temperature profiles inside the reactor working at different conditions. Again, as in the experiments performed with the previous TWR [6], ignition was possible at subcritical injection temperatures as low as 170°C as shown in figure 5.1.5 (a). An increase in the temperature of the reagents from 150 to 250°C was observed in the injector. As the kinetic rate at those temperatures is very low for being responsible of such a temperature increase in this short residence time, it is inferred that the increase in temperature is due to heat transmission through the wall of the injector. No ignition in the injector was observed even at injection temperatures as high as 380°C

using O_2 as the oxidant, as observed figure 5.1.5 (b). High temperatures were exclusively registered at the top of the reaction chamber, just as the outlet of the mixer. This implies that the reaction mixture becomes supercritical only at the outlet of the injection chamber. Thus, salt precipitation will occur there, where plugging problems are less likely to occur than inside of the narrow static mixer.

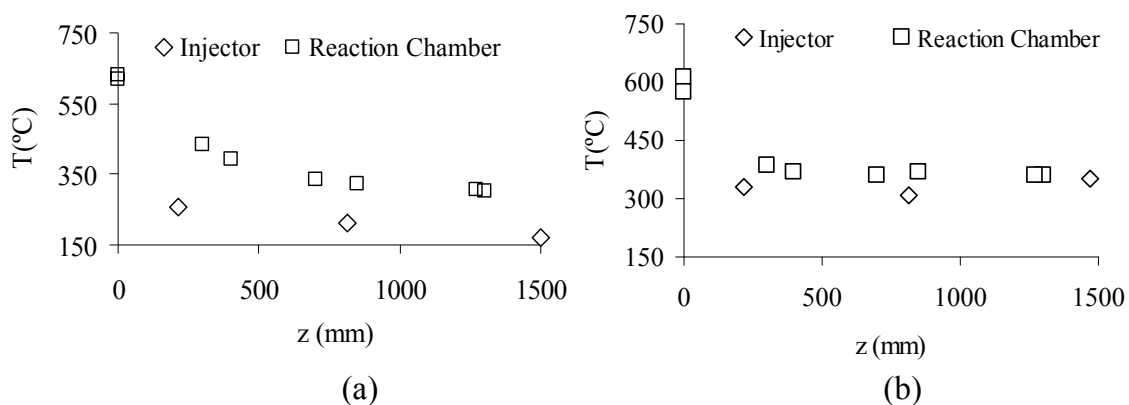


Figure 5.1.5: Temperature profiles in experiments in the scaled up transpiring wall reactor. (a) Feed flow= 36.7 kg/h; Oxidant: air; C=8.5% wt IPA; $T_{\text{Feed}}= 170^{\circ}\text{C}$; $T_{\text{Air}}=334^{\circ}\text{C}$; (b) Feed flow= 21.2 kg/h; Oxidant: O_2 ; C=8% wt IPA; $T_{\text{Feed}}=380^{\circ}\text{C}$

The influence of the operational parameters in the behavior of the reactor was studied by comparing the temperature profile along the reactor for different operational conditions. Figure 5.1.6 (a) shows the temperature profiles along the reactor for different feed flows, for a constant IPA concentration and transpiring flow. It was observed that for higher flows temperatures over the autoignition temperatures are kept longer along the reactor. This means that there was a bigger portion of the reactor at conditions above the ignition temperature of IPA (470°C). These results are in agreement with previous observations with TWRs made by our research group [6, 9]. Figure 5.1.6 (b) shows useful residence times represented as a function of the total flow (feed + oxidant) for data with a transpiring ratio between 0.3-0.4. At high flows, even when a longer portion of the reactor was operating in hydrothermal flame conditions, the useful residence time decreased faster with total feed flow.

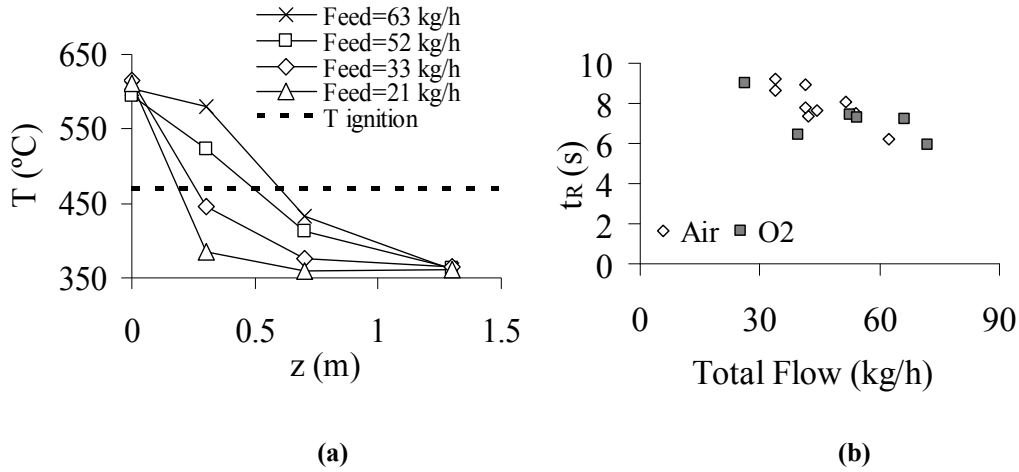


Figure 5.1.6 (a): Temperature profiles along the reactor for different feed flows using O₂ as an oxidant, Transpiring flow: 14 kg/h; **(b):** Useful residence times as a function of the total flow for experiments with transpiring flow/total flow ratios between 0.3 and 0.4

Figure 5.1.7 (a) shows the temperature profiles in the reactor for a feed flow of 21 kg/h and for a feed flow of 59 kg/h, with two transpiring flows in each case. It is observed that for lower feed flows the cooling effect of the transpiring wall was more remarkable and decreasing the transpiring flow increases the useful length of the reactor. These results are consistent with previous observations with TWRs made by our research group [6, 9]. Figure 5.1.7 (b) shows the useful residence times in the reactor as a function of the transpiring ratio R. Increasing of the transpiring flow ratio strongly reduced the useful residence time in the reactor, this reduction is similar for different feed flows. We consider that the optimum transpiring flow ratio is the minimum one able to cool down the effluent of the reactor to subcritical temperatures for the salts to leave the reactor dissolved into it.

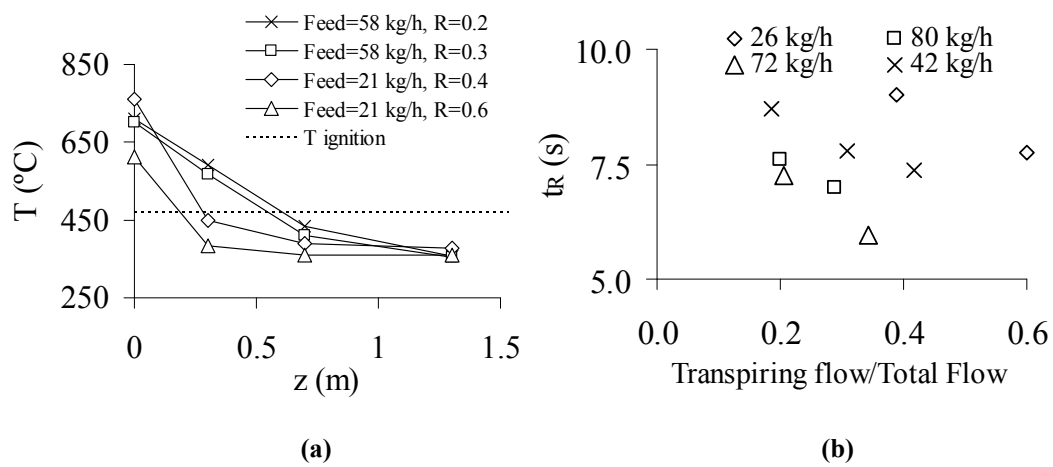


Figure 5.1.7: Temperature profiles along the reactor for different feed flows using O₂ as an oxidant, **(a)** Feed=58 kg/h, C=9% wt IPA; **(b)** Feed=21 kg/h, C=8% wt IPA

Figure 5.1.8 shows the temperature profiles in two experiments performed with a feed flow of 60 kg/h for 8 and 9% in weight of IPA are represented. An increase of only 1% in IPA concentration could produce an increase in the maximum temperature of around 150°C. Due to the different heat transmissions phenomena occurring in the reactor, the optimal fuel content of the feed to reach a reaction temperature between 650-700°C is different depending on the feed flow.

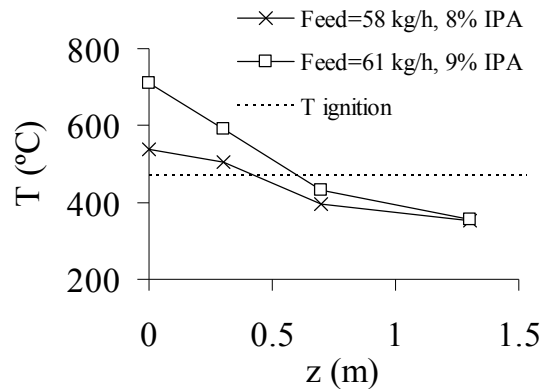


Figure 5.1.8: Temperature profiles along the reactor for different feed flows using O_2 as an oxidant, Transpiring Flow= 14 kg/h

Results using this transpiring wall reactor show that steady operation at flame regime is possible at subcritical injection temperature and that the ignition will never occur in the injector, making it a very convenient design for the injection of feeds with high salt contents, as it was proved in a previous study of the group [9]. Results also show as well that the performance of the reactor is highly dependent on the total flow, independently of the oxidant used, air or oxygen. At higher flows despite the fact that the fraction of the reactor at flame conditions increases, the useful residence time decreased. Transpiring flow has a strong influence both in reaction temperature and residence times.

5.1.3.3. Operational problems

The reactor was dismantled in order to check the possible leaking in the base of the mixer previously described. The leakage in the base of the injector was confirmed. In addition, during the dismantling procedure, the transpiring wall was broken in several pieces because the sintered transpiring materials were fragilized due to the high temperatures. Even when the warmer point of the reactor was constructed in metallic Ni-Alloy more resistant to high temperatures, the temperatures withstood by the

sintered transpiring materials were still too high and it fragilized and broke, as happened with previous transpiring walls [10]. The transpiring wall also showed signs of corrosion.

5.1.3.4. Estimation of the flame front velocities

The previous results presented for both the tubular reactor and the transpiring wall reactor showed that fluid flow velocity determines the extinction temperature of the hydrothermal flame. It was observed that hydrothermal flames are stabilized in vessels in which the flow sections are large enough to keep a low fluid flow velocity making possible the feed injection at subcritical temperatures. If the fluid flow velocity was higher, the injection temperature necessary to keep a steady flame was also higher. In order to go deep into this phenomenon the flame front velocity was estimated.

A flame is defined as the surface where the combustion reaction is happening. In the case of a premixed flame, this surface separates the cold reagents from the hot combustion products. This surface is moving towards the inlet reagents at the velocity of the flame front. The flame is stabilized when the velocity of the flame is equal to the velocity of the flow. If the flame front velocity is lower than the fluid flow velocity the flame would be blown out. If it is higher the flame front will move till the point where the oxidant and the fuel are mixed. The flame front velocity can be estimated using the expression shown in equation (3) and developed by Semenov [20]:

$$v = \sqrt{\frac{2\lambda c_{pf}^2 A_0 w_0 \left(\frac{T_0}{T_f}\right)^2 \left(\frac{n_r}{n_p}\right)^2 Le^2 \left(\frac{RT_f^2}{E_a}\right)^3 e^{-E_a/RT_f}}{\left(\bar{c}_p\right)^3 (T_f - T_0)^3}} \quad (3)$$

Where,

T_0 is the temperature of unburned mixture just before the ignition; T_f is the flame temperature; λ the thermal conductivity of unburned mixture; c_{pf} the specific heat capacity of the mixture at T_f ; \bar{c}_p the average specific heat capacity between T_0 and T_f ; A_0 , the Arrhenius pre-exponential factor; w_0 the mass fraction of fuel; (n_r/n_p) number of moles of reactant to product; Le is the Lewis number of unburned mixture; E_a the energy of activation; and R , the gas constant.

The Lewis (Le) number is the ratio of thermal to mass diffusivities, as shown in equation (4):

$$Le = \frac{\lambda}{\rho c_p D} \quad (4)$$

Where,

ρ is the mixture's density; and D is the mass diffusivity of fuel in the mixture.

Properties were calculated assuming a constant temperature of 700°C for the flame. Density and specific heat capacity were calculated using the Peng-Robinson EoS with the translated volume correction [22], considering the composition of the fluid before combustion. Mixture thermal conductivity was estimated using TRAPP method, for gas mixtures at high pressures, with Wassiljeva equation for low pressure estimation [23]. Mass diffusivity was calculated with the method described by He [24]. Kinetic parameters were experimentally determined from the data taken from previous works of our group [8, 25] using a first order reaction with respect the fuel and the oxygen, where the constant k is dependent on the temperature following an Arrhenius type equation $k = A_0 \cdot \exp(-E_a/RT)$ where $A_0 = 223872.1 \text{ m}^3\text{kmol}^{-1}\text{s}^{-1}$ and $E_a = 45016 \text{ J/mol}$.

Figure 5.1.9 shows the flame front velocity as a function of the temperature of the mixture before the reaction for a hydrothermal flame at 23 MPa and 700°C. Flame front velocities vary between 0.01 and 0.1 m/s, much lower than the typical flame front velocities in air combustion (0.4-3 m/s). It is observed that when the temperature of the mixture before ignition is higher, the flame front velocity is also higher. This behavior is qualitatively consistent with our observations of the results in the tubular reactors, where at lower feed flows lower injection temperatures were necessary to have ignition.

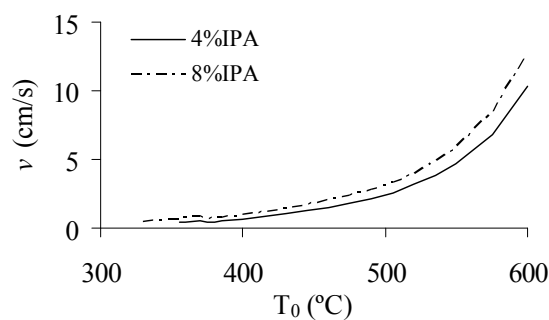


Figure 5.1.9: Flame Front Velocity, in cm/s, as function of temperature of the unburned mixture just before the flame, in°C, with the flame temperature fixed at 700°C.

These calculated flame front velocity values can only be considered estimative because for supercritical aqueous mixture properties cannot be calculated with precision and in some cases they only can be estimated. Nevertheless, they can help to understand why is possible to inject feeds at subcritical temperatures in a hydrothermal flame when

using a vessel reactor and not when using a tubular reactor, and why the hydrothermal flames are not formed in the injectors. The velocities inside of the injector are around 3-24 m/s while the maximum velocities in the reaction chamber are around 0.04 m/s. Thus, it is expected that the flame front is maintained in a fixed position of the reaction chamber, where the flame front velocities are of the same order of magnitude as the estimated flame front velocity. Then, the reagents at subcritical temperatures can be preheated when injected into the flame till reaching the ignition temperature. When working with the tubular reactor, as the velocities were between than 2 and 12 m/s, the flame front was blown out of the tube. Thus, each fluid element must reach the ignition temperature and form a new flame front.

As an indicative rule for the design of vessel reactor with a flame inside it can be established that the velocity of the fluid inside of the reaction chamber has to be between 0.1-0.01 m/s while the velocity in the injector must be higher than 1 m/s. Using this rule it can be estimated that a reactor for treating a feed flow of 200 kg/h (the maximum flow of our demonstration plant), must have a minimum reaction chamber diameter of 85 mm and an internal injector diameter lower than 10 mm. For an industrial plant with a treatment capacity of 3000 kg/h, such as the SCWO plant that Chematur AB constructed in the site of Johnson Matthey [1, 26, 27], a reactor with a reaction chamber of a minimum of 330 mm of diameter and an injector lower than 40 mm would be needed.

5.1.3.5. Modelling

A model previously developed for describing the behaviour of the transpiring wall reactor [13] was modified in order to describe the performance of the reactor with a hydrothermal flame inside, incorporating the results obtained in this work and in the study of the reaction initiation of SCWO of IPA using tubular reactors [8]. The model takes into account stationary conditions considering only mass and energy balances, resolved by the Runge-Kutta method of 4th order, while the momentum equation was neglected. The pressure along the reactor was considered constant and equal to 23 MPa. The heats of reaction were calculated for different temperatures using the Peng-Robinson EoS with Boston-Mathias alpha function. Heat capacities and densities were calculated using the Peng-Robinson EoS (PR EoS) with the translated volume correction considering the exact composition of the mixture [22] as described in a

previous work of our research group [16]. Global heat transmission coefficients were calculated as a function of the total mass flow. The coefficient for the heat transmission of the outer wall with the environment was taken as $0.5 \text{ W/m}^2 \text{ K}$.

The kinetics pathways used are those reported by Li et al. [28]. These authors suggest that the oxidation kinetics involve the formation and destruction of rate controlling intermediates, while some organics compounds are directly transformed into the final oxidation products. Acetic acid is the only intermediate reagent considered in the simulation. Kinetics is assumed to be first order. Values of the kinetic constants are given in table 5.1.5.

Table 5.1.5: Kinetic Parameters in the Arrhenius equation used to simulate the IPA oxidation

	A (s⁻¹)	E_a (J/mol)
k ₁ (IPA to CO ₂)	$2.61 \cdot 10^5$	64000
k ₂ (IPA to HAc)	$2.61 \cdot 10^5$	64000
k ₃ (HAc to CO ₂)	$2.55 \cdot 10^{11}$	172700

For modeling the reactor is divided into three consecutive areas:

- The injector, where chemical reaction is not occurring according to our experimental results and only heat transmission is considered.
- The top part of the reaction chamber, where the flame takes place can be modeled as a CSTR because of the recirculation flows produced in the area. Reaction and heat transfer with the wall of the reaction chamber are both considered.
- The lower part of the reaction chamber, where plug flow is considered. Reaction, heat transfer and mixing with the transpiring flow are considered in this area.

The equations governing the behavior of these areas are the following:

1) The energy balance of the injector is calculated as shown in Eq. 5.

$$c_p \cdot m_0 \left(\frac{dT_m}{dz} \right) = -U \cdot \pi \cdot D \cdot (T_m - T_R) \quad (5)$$

Where, c_p is the specific heat of the mixture, m_0 is the inlet mass flow, D is the external diameter of the injector, T_R is the temperature in the reaction chamber, T_m is the temperature in the injector and U is the global heat transfer coefficient between the reaction chamber and the injector.

2) The equations considered for the CSTR area are the following:

- Mass balance for the isopropyl alcohol (A) and to the acetic acid (B) is shown in

Eqs. 6 and 7.

$$C_{A,CSTR} = \frac{F_{A0}}{m_0 / \rho_{CSTR} + (k_1(T_{CSTR}) + k_2(T_{CSTR})) \cdot V \cdot 3600} \quad (6)$$

$$C_{B,CSTR} = \frac{3/2 \cdot k_3(T_{CSTR}) \cdot C_{A,CSTR} \cdot V \cdot 3600}{m_0 / \rho_{CSTR} + k_3(T_{CSTR}) \cdot V \cdot 3600} \quad (7)$$

Where, C are concentrations in mol/L, the subindex CSTR refers to the values inside the top part of the reactor, F_{A0} is the initial molar flow of IPA, ρ_{CSTR} is the density inside the CSTR, T_{CSTR} is the temperature at the top part of the reactor and V is volume of the CSTR in m^3 . It can be calculated by Eq. 8:

$$V = S \cdot L_{CSTR} \quad (8)$$

Where S is the section of the reactor and L_{CSTR} is the length of the top part of the reactor considered as a CSTR. Experimentally, the CSTR length was fixed at 40 mm [14].

The energy balance of the CSTR is shown in Eq. 9:

$$[m_0 \cdot (\Delta H_T)_{in} + V(\sum k_{ij}(T_{CSTR}) \cdot C_{iCSTR} \cdot (-\Delta H_R)_{ij})] = [m_0 \cdot (\Delta H_T)_{out} + q_T] \quad (9)$$

Where, ΔH_T is the enthalpy of the mixture at the inlet conditions (in) and at the outlet condition (out) in J/kg, q_T is the heat flow transmitted by convection through the wall of the reaction chamber in J/h.

3) Equations considered in the plug flow part of the reaction chamber are the following: The global mass balance in the reaction chamber (m), and the species mass balances for reagents IPA (A) and acetic acid (B) are calculated in every integration step using Eqs 10 to 12.

$$\frac{dm}{dz} = \pi \cdot D_i \cdot m_{Transp} / A_{Transp} \quad (10)$$

$$-F_{A0} \frac{dX_A}{dz} = S(\alpha \cdot r_1 + \beta \cdot r_2) \quad (11)$$

$$\frac{dF_B}{dz} = S(\beta \cdot r_2 - \gamma \cdot r_3) \quad (12)$$

Where D_i is the internal diameter of the reaction chamber, m_{Transp} is the total transpiring flow in kg/h, A_{Transp} is the transpiring surface of the reactor; α , β , γ are the stoichiometric coefficients of the reactions 1, 2 and 3 respectively, r_i is the reaction rate of reaction 1, 2 and 3 respectively, F_B is the molar flow of acetic acid, X is the conversion, z is the height of the reactor, where $z=0$ is the top part.

The energy balance is expressed in Eq. 14.

$$c_p \left(m \frac{dT_R}{dz} + T_R \frac{dm}{dz} \right) = \pi \cdot D_i \cdot m_{Transp} / A_{Transp} \cdot h_{H_2O}(T_{Transp}) + S \cdot \Sigma(-\Delta H r_{ij}) \cdot r_i \quad (13)$$

$$- U_{transp} \pi \cdot D_i \cdot (T_R - T_{transp}) + U \cdot \pi \cdot D \cdot (T_m - T_R)$$

Where T_R is the temperature in the reaction chamber, h_{H_2O} is the specific enthalpy of water, S is the internal section of the reaction chamber, U_{transp} is the heat transmission coefficient through the transpiring wall, T_{transp} is the temperature of the transpiring flow.

Results of the modeling

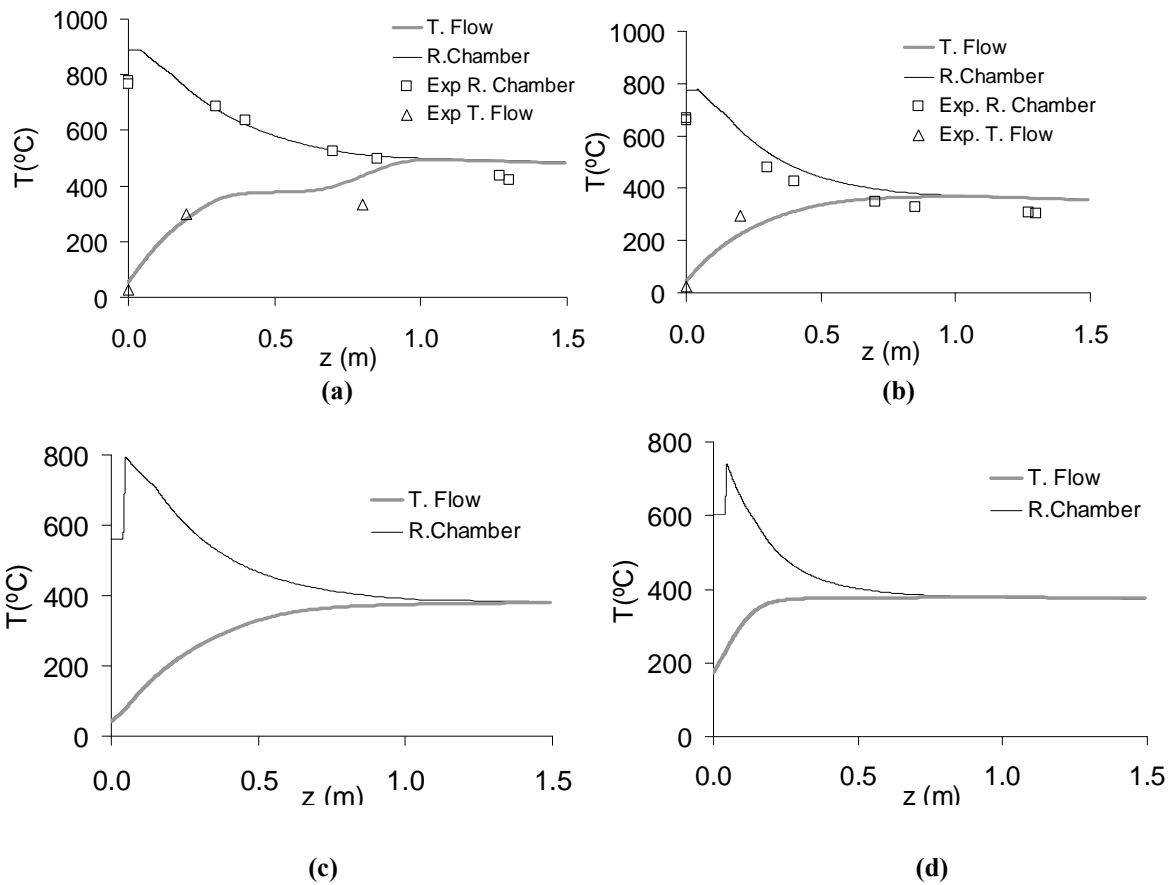
In first place, the model was tested by reproducing the experimental temperature profile of two experiments. Figure 5.1.10 (a) shows the comparison of the experimental and predicted temperature profile in the experiment with the highest feed flow using O_2 as the oxidant, while in the figure 5.1.10 (b) the experimental and predicted temperature profiles of a data with a subcritical temperature using air as the oxidant are represented. It is observed that the model gives a good prediction of the temperature profile, with the exception of the maximum temperature that is overpredicted. PR EoS normally overpredicts temperature in SCW systems as observed in a previous work of the group [16]. The concentration profiles are not represented as most of the organic matter is eliminated in the top of the reaction chamber. Accurate elimination predicted cannot be expected of first order kinetic model, as it cannot represent the termination step of the reaction [29]. Nevertheless a first order model can give an idea of when most organic matter is eliminated.

In a second step, the model was used to predict the SCWO of feeds 200 and 3000 kg/h, in reactors with injectors and reaction chamber diameters as proposed in section 5.1.3.4 according to the estimated flame front velocities.

Figure 5.1.10 (c) shows the prediction of the temperature profile for a transpiring wall reactor of $D_i=85$ mm, $D_{injector}=10$ mm and $L=1470$ mm for a feed flow of 200 kg/h, $C_A=12.5\%$ wt, $R=0.4$ and $T_{inj}=25^\circ C$ using O_2 as the oxidant. Figure 5.1.10 (d) shows the prediction of the temperature profile for a transpiring wall reactor of $D_i=330$ mm, $D_{injector}=40$ mm and $L=1470$ mm, for a feed flow of 3000 kg/h, $C_A=13.5\%$ wt; $R=0.6$;

$T_{inj}=25^{\circ}\text{C}$ using O_2 as the oxidant. It is observed that the scaled-up reactors present similar temperature profiles to that of the experimental data. Most of the fuel is consumed in the CSTR part of the reactor reaching a temperature near to 600°C , and the fuel is completely removed in the first few centimetres of the plug flow area of the reactor reaching temperatures higher than 700°C . Fuel concentrations are higher than those used in the experiments in order to achieve reactions temperatures between $700\text{--}800^{\circ}\text{C}$ at injection temperatures of 25°C . Transpiring flow relations R have to be elevated to 0.4 for feed flows of 200 kg/h and to 0.6 in the case of 3000 kg/h in order to obtain subcritical outlet temperatures.

This can be explained because in wider reactors the ratio transpiring surface/reaction volume is lower. According to the model total TOC removal is obtained in residence times of less than 0.4 s , in agreement to the results shown in the tubular reactors. Thus, reaction is finished in the first 50 mm of the reactor, but longer residence time is needed to reach subcritical temperatures at the outlet of the reactor.



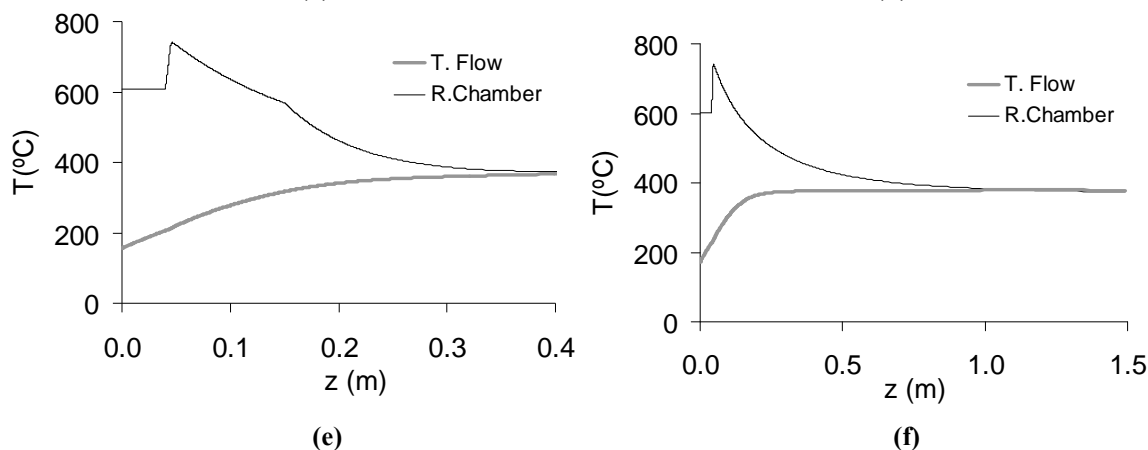


Figure 5.1.10: (a) Comparison of the temperature profile predicted by the model to the experimental temperatures for a experimental data with a Feed=65.7 kg/h; $C_A=8\%$ wt; $R=0.29$; $T_{inj}=301^\circ\text{C}$ using O_2 as the oxidant; (b) Comparison of the temperature profile predicted by the model to the experimental temperatures for a experimental data with a Feed=34.1 kg/h; $C_A=10\%$ wt; $R=0.33$; $T_{inj}=173^\circ\text{C}$ using air as the oxidant; (c) Prediction of the temperature profile for a transpiring wall reactor of $D_i=85$ mm; $D_{injector}=10$ mm, $L=1470$ mm, Feed= 200 kg/h; $C_A=12.5\%$ wt; $R=0.4$; $T_{inj}=25^\circ\text{C}$ using O_2 as the oxidant; (d) Prediction of the temperature profile for a transpiring wall reactor of $D_i=330$ mm; $D_{injector}=40$ mm, $L=1470$ mm, Feed= 3000 kg/h; $C_A=13.5\%$ wt; $R=0.6$; $T_{inj}=25^\circ\text{C}$ using O_2 as the oxidant; (e) Prediction of the temperature profile for a transpiring wall reactor of $D_i=330$ mm; $D_{injector}=40$ mm, $L=400$ mm, Feed= 3000 kg/h; $C_A=14\%$ wt; $R=0.7$; $T_{feed}=25^\circ\text{C}$ using O_2 as the oxidant; (f) Prediction of the temperature profile for a non-transpiring wall reactor of $D_i=330$ mm; $d_{injector}=40$ mm, $L=1470$ mm, Feed= 3000 kg/h; $C_A=13.5\%$ wt; $R=0.6$; $T_{feed}=25^\circ\text{C}$ using O_2 as the oxidant;

In a third step the model was used to propose substantial changes in the design of the reactors for a feed flow of 3000 kg/h. The first change proposed was the reduction of the length of a transpiring wall reactor. The simulation shown in figure 5.1.10 (d) shows that the reaction is finished in the first 50 mm of the reactor. A certain additional length is necessary to cool down the products to subcritical temperatures. A transpiring wall reactor of a shorter length is proposed.

Figure 5.1.10 (e) shows the temperature profile of a transpiring wall reactor of diameters $D_i=330$ mm; $D_{injector}=40$ mm, but with a length of only 400 mm for a feed flow of 3000 kg/h. The first 150 mm of the reactor are considered non-transpiring while the rest is a transpiring wall. Total TOC removal is predicted to happen at 0.4 s, and a subcritical outlet temperature can be obtained. As the transpiring flow has to enter in the reactor in a shorter space, a faster cool down of the products down to subcritical temperatures is obtained, but transpiring flow ratio must be higher than in the case (d), where the reactor is longer. Also a slightly higher concentration of IPA is necessary because the preheating of the reagent in the injector is reduced when reducing the length of the reactor.

As the resistance of the transpiring material to the high temperatures has been found to be low in the experiments, the second change proposed is to construct a cooled wall reactor [1, 15] with similar dimensions and performance as the transpiring wall reactor but in which the reaction chamber wall is not transpiring. This can be an appropriate reactor design to avoid the poorly resistant sintered transpiring Ni-alloys.

Figure 5.1.10 (f) shows the temperature profile predicted for such a reactor, with similar dimensions of case (d) for a flow of 3000 kg/h when the wall of reactor is not transpiring. It is observed that temperature profiles are similar in cases, (d) and (f); with the difference that cooling in transpiring reactor is somewhat faster.

5.1.4. CONCLUSIONS

In this work, data from a tubular reactor and from a transpiring wall reactor were used in order to analyze the scaling up process of SCWO reactors with a hydrothermal flame inside.

Results shows that fluid velocity inside of the reactor determines the minimum injection temperature at which a stable hydrothermal flame is possible. When the velocity in the reactor is lower, the extinction temperature is also lower, being possible the injection at temperatures as low as 170°C when working with the transpiring wall reactor in which the fluid flow velocity was below 0.04 m/s.

These results could be explained by estimating the hydrothermal flame front velocity. At conditions of 23 MPa and 700°C these values are between 0.1 and 0.01 m/s, much lower than typical flame front velocities in conventional combustion, and decrease with decreasing temperature before ignition. These velocities are lower than the velocity inside the injector (3-24 m/s) and of the tubular reactors, and of the same order of magnitude as those in the reaction chamber (0.04 m/s). Thus, it is expected that the flame is stabilized in the reaction chamber and not in the injector, as it has been experimentally observed.

When designing a reactor consisting of an injector and a reaction chamber and it is necessary that the reaction begin in the reaction chamber, an indicative rule for calculating the diameter of reaction chamber and injector is proposed. Fluid velocity must be kept higher than 1 m/s in the injector and lower than 0.1 m/s in the reaction chamber.

The scaling of SCWO vessel reactors was studied using a previously developed model of the reactor that was modified in order to describe the ignition in the reaction chamber and not in the injector. The model reproduces satisfactorily experimental data and was used to predict the behavior of scaled up reactors for SCWO with a hydrothermal flame inside. According to the predictions of the model, a transpiring wall vessel reactor of reduced size can be used to treat feed flows as high as 3000 kg/h, injecting the reagents at 25°C. Two partially transpiring wall reactors, as the one used in this work, of lengths 400 and 1500 present a similar performance. A cooled wall reactor 1500 mm can achieve a similar performance as a transpiring wall reactor of the same dimensions.

LIST OF SYMBOLS

A_0	Pre-exponential factor Arrhenius equation	s^{-1}
A_{Transp}	Total transpiring area	m^2
C	Concentration	mol/L
c_p	Specific heat capacity	J/kgK
D	External diameter of the injector	m
D_i	Internal diameter of the reaction chamber	m
$D_{injector}$	Internal diameter of the injector	m
E_a	Energy of activation	J/kmol
Feed	Feed flow	kg/h
F	Molar flow	mol/h
H	Enthalpy	J
ΔH_R	Heat of reaction	J/mol
ΔH_T	Total enthalpy of the mixture	J
k	Kinetic reaction constant	s^{-1}
L	Length	m
Le	Lewis number	
m	Reagents flow	kg/h
m_0	Inlet reagents flow	kg/h
m_{Transp}	Transpiring flow	kg/h
$m_{TranspT}$	Total transpiring flow	kg/h
n	Number of mols of reagents/products	
P	Pressure	MPa
q	Heat flow	W
R	Transpiring flow ratio	
r_i	Reaction rate	$mol \cdot m^{-3} s^{-1}$
S	Reaction chamber section	m^2
t_R	Useful residence time	s
T	Temperature	$^{\circ}C$
T_{inj}	Temperature of injection of reagents	$^{\circ}C$
T_{max}	Maximum temperature registered in the reactor	$^{\circ}C$
TOC	Total organic carbon	ppm C
TOC_0	Initial TOC concentration	ppm C

TOC _{ef}	TOC in the effluent of the reactor	ppm C
TOC Rem	TOC removal	
U _{Transp}	Global heat transfer coefficient reaction chamber-transpiring flow	
	W/m ² K	
U	Global heat transfer coefficient injector-reactor chamber	W/m ² K
V	Volume	m ³
w	Mass fraction of fuel	
X	Conversion	
X _{H2O}	Molar fraction of water	
z	Position	m

Subindex

0	Referred to initial condition
A	Referred to IPA in the model
B	Referred to Acetic Acid
CSTR	Referred to the top of the reaction chamber (CSTR)
f	Referred to the flame conditions
H ₂ O	Referred to water
m	Referred to the injector
p	Referred to reaction products
R	Referred to the reaction chamber
r	Referred to reagents
Transp	Referred to the transpiring water

Greeks

α	Stoichiometric coefficient of reaction 1	
β	Stoichiometric coefficient of reaction 2	
γ	Stoichiometric coefficient of reaction 3	
λ	Thermal conductivity	W/mK
v	Flame front velocity	m/s
ρ	Density	kg/m ³
τ	Characteristic kinetics time	s

5.1.5. REFERENCES

- [1] M.D. Bermejo, M.J. Cocero, Supercritical water oxidation: A technical review, *AICHE Journal*, 52 (2006) 3933-3951
- [2] G. Brunner, Near and supercritical water. Part II: Oxidative processes, *Journal of supercritical Fluids*, 47 (2009) 382-390
- [3] W. Schilling, E. U. Franck, Combustion and Diffusion Flames at High Pressures to 2000 bar, *Berichte Der Bunsen-Gesellschaft-Physical Chemistry Chemical Physics*, 92 (1988) 631-636
- [4] C.H. Oh, R.J. Kochan, T.R. Charlton, A.L. Bourhis, Thermal-hydraulic modeling of supercritical water oxidation of ethanol, *Energy Fuels*, 10 (1996) 326-332.
- [5] B. Wellig, M. Weber, K. Lieball, K. Prikopsky, Ph. Rudolf von Rohr, Hydrothermal methanol diffusion flame as internal heat source in a SCWO reactor, *Journal of Supercritical Fluids*, 49 (2009) 59–70
- [6] M.D. Bermejo, F. Fdez-Polanco, M.J. Cocero, Experimental study of the operational parameters of a transpiring wall reactor for supercritical water oxidation, *Journal of supercritical Fluids*, 39 (2006) 70-79
- [7] C. Augustine, J. W. Tester, Hydrothermal flames: From phenomenological experimental demonstrations to quantitative understanding, *Journal of supercritical Fluids*, 47 (2009) 415–430
- [8] M.D. Bermejo, P. Cabeza, M. Bahr, R. Fernández, V. Ríos, C. Jiménez, M.J. Cocero, Experimental study of hydrothermal flames initiation using different static mixer configurations, *Journal of Supercritical. Fluids*, 50 (2009) 240-249.
- [9] M. D. Bermejo, F. Fdez-Polanco, M. J. Cocero, Effect of the Transpiring Wall on the Behavior of a Supercritical Water Oxidation Reactor: Modeling and Experimental Results, *Industrial & Engineering Chemistry Research*, 45 (2006) 3438–3446
- [10] E. Fauvel, C. Jousot-Dubien, P. Guichardon, G. Charbit, F. Charbit, S. Sarrade, S, A double-wall reactor for hydrothermal oxidation with supercritical water flow across the inner porous tube, *Journal of supercritical Fluids*, 28 (2004) 47-56
- [11] K. Prikopsky, B. Wellig, Ph.Rudolf von Rohr, SCWO of salt containing artificial wastewater using a transpiring-wall reactor: Experimental results, *Journal of supercritical Fluids*, 40 (2007) 246–257

- [12] B. Wellig, K. Lieball, Ph. Rudolf von Rohr, Operating characteristics of a transpiring-wall SCWO reactor with a hydrothermal flame as internal heat source. *Journal of supercritical Fluids*, 34 (2005) 35-50
- [13] M.D. Bermejo, F. Fdez-Polanco, M. J. Cocero, Modeling of a Transpiring Wall Reactor for the Supercritical Water Oxidation Using Simple Flow Patterns: Comparison to Experimental Results, *Industrial & Engineering Chemistry Research*, 44 (2005) 3835-3845
- [14] R.M. Serikawa, T. Usui, T. Nishimura, H. Sato, S. Hamada, H. Sekino, Hydrothermal flames in supercritical water oxidation: investigation in a pilot scale continuous reactor, *Fuel*, 81 (2002) 1147-1159
- [15] M.D. Bermejo, D. Rincon, A. Martin, M.J. Cocero, Experimental Performance and Modeling of a New Cooled-Wall Reactor for the Supercritical Water Oxidation, *Industrial & Engineering Chemistry Research*, 48 (2009) 6262–6272
- [16] A. Anderko, K.S. Pitzer, EOS representation of phase equilibria and volumetric properties of the system NaCl–H₂O above 573 K, *Geochimica et Cosmochimica Acta*, 57 (1993) 1657-1680
- [17] J.J. Kosinski, A. Anderko, EOS for high-temperature aqueous electrolyte and nonelectrolyte systems, *Fluid Phase Equilibria*, 183-184 (2001) 75-86
- [18] M.D. Bermejo, A. Martín, M.J. Cocero, Application of the Anderko–Pitzer EoS to the calculation of thermodynamical properties of systems involved in the supercritical water oxidation process, *Journal of supercritical Fluids*, 42 (2007) 27–35
- [19] P.A. Webley, J.W. Tester, Fundamental kinetics of methane oxidation in supercritical water, *Energy Fuels*, 5 (1991) 411–419.
- [21] I. Glassman, R. A. Yetter, *Combustion*, 4th ed., Elsevier, San Diego, 2008, pp. 161-168
- [22] C. Magoulas, D. Tassios, Thermophysical properties of n-alkanes from C1 to C20 and their prediction for higher ones, *Fluid Phase Equilibria*. 56 (1990) 119–140
- [23] B.E. Poling, J. M. Prausnitz, J. P. O’Connell, *The Properties of Gases and Liquids*, 5th ed., McGraw-Hill, New York, 2004, pp.10.1-10.7
- [24] Chao-Hong He, Prediction of Binary Diffusion Coefficients of Solutes in Supercritical Solvents, *AIChE Journal*, 43 (1997) 2944-2947
- [25] J.P.S. Queiroz, M.D. Bermejo, P. Cabeza, C. Jiménez, M.J. Cocero, Behavior of SCWO vessel reactors with a hydrothermal flame: analysis with CFD model.

Proceedings of “II Iberoamerican Conference on Supercritical Fluids. PROSCIBA 2010” Natal (Brazil)5-9th April 2010

[26] <http://www.scfi.eu/products/precious-metal-catalyst-recovery/> (last accessed 9th August 2010)

[27] S. Collard, S. Phillips, A. Burgess, L. Stenmark, A. Gidner. The Aquacat ® Process for precious metal recovery. Presented at the 7th International Symposium on Supercritical Fluids, Orlando, FL, 2005.

[28] L. Li, P. Chen, E.F. Gloyna, Generalized kinetic-model for wet oxidation of organic-compounds, AICHE Journal,. 37 (1991) 1687-1697

[29] F. Vogel, J. L. D. Blanchard, P. A. Marrone, S. F. Rice, P. A. Webley, W. A. Peters, K. A. Smith and J. W. Tester, Critical review of kinetic data for the oxidation of methanol in supercritical water, Journal of supercritical Fluids, 34 (2005) 249-286

CHAPTER 6

NEW COOLED WALL REACTOR DESIGN

CHAPTER 6

NEW COOLED WALL REACTOR DESIGN

TABLE OF CONTENTS

6.1 EXPERIMENTAL STUDY OF HYDROTHERMAL FLAMES FORMATION USING A TUBULAR INJECTOR IN A REFRIGERATED REACTION CHAMBER. INFLUENCE OF THE OPERATIONAL AND GEOMETRICAL PARAMETERS .	211
6.1.1. INTRODUCTION	213
6.1.2. EXPERIMENTAL	216
6.1.3. RESULTS	219
6.1.3.1. Experimental performance	219
6.1.3.2. Stability of the flame and TOC Removal	220
6.1.3.3. Energy balances in the reactor	222
6.1.3.4. Influence of the fluid flow velocity in the position of the flame front	223
6.1.3.5. Influence of the length of the injector	225
6.1.3.6. Influence of inorganic salts	227
6.1.4. CONCLUSIONS	232
6.1.5. REFERENCES	234
6.2. SLUDGE DESTRUCTION BY MEANS OF A HYDROTHERMAL FLAME. OPTIMIZATION OF AMMONIA DESTRUCTION CONDITIONS	237
6.2.1. INTRODUCTION	239
6.2.2. EXPERIMENTAL	242
6.2.2.1 Experimental set up	242
6.2.2.2 Experimental procedure	243
6.2.2.3 Materials	244
6.2.3. RESULTS AND DISCUSSION	245
6.2.3.1 Ammonia destruction	245
6.2.3.2. Control of nitrate formation	251

6.2.3.3 Oxidation of synthetic sludge	253
6.2.3.4 Oxidation of sludge	255
6.2.3.5 energy production by scwo of sludge	256
6.2.4. CONCLUSIONS	261
6.2.5. REFERENCES	263
6.3. ANALYSIS OF THE BEHAVIOR OF A SCWO COOLED WALL REACTOR WORKING WITH TWO OUTLETS. EXPERIMENTAL RESULTS AND ENERGETIC STUDY	269
6.3.1. INTRODUCTION	269
6.3.2. EXPERIMENTAL	272
6.3.2. EXPERIMENTAL	272
6.3.2.1 Experimental setup	272
6.3.2.2 Experimental procedure.....	274
6.3.2.3 Materials	275
6.3.2.4 Parameter calculations.....	275
6.3.3. RESULTS.....	277
6.3.3.1 Influence of the upper effluent fraction.....	277
6.3.3.2 Influence of the IPA concentration.....	278
6.3.3 Influence of the cooling water	279
6.3.3.4 Ammonia removal	280
6.3.3.5 Behaviour of the reactor working with feeds with high content in salts..	281
6.3.3.6 Energy recovery.....	282
6.3.4. CONCLUSIONS	285
6.3.5. REFERENCES	287

6.1. EXPERIMENTAL STUDY OF HYDROTHERMAL FLAMES FORMATION USING A TUBULAR INJECTOR IN A REFRIGERATED REACTION CHAMBER. INFLUENCE OF THE OPERATIONAL AND GEOMETRICAL PARAMETERS

ABSTRACT

Experimental results using three different empty tubular injectors into a refrigerated reaction chamber containing a hydrothermal flame as an internal heat source are presented. In the supercritical water oxidation process if the feed is injected into a hydrothermal flame, its external pre-heating is not necessary. Due to this, plugging and corrosion problems produced during transition from subcritical to supercritical conditions in the preheating system can be avoided. The influence of feed flow, injection temperature and diameter and length of the injector has been evaluated by studying the temperature profiles along the reactor, the Total Organic Carbon (TOC) removal and the extinction temperatures at different conditions. It was possible to inject reactants at temperatures below 50°C into the hydrothermal flame with organic destruction efficiencies higher than 99.9%, presenting better operational results than other reactors constructed by our research work. The effect of salt addition under sub critical conditions in a hydrothermal flame was also studied. Feeds containing up to 2.5% wt Na₂SO₄ could be injected in the reactor without plugging problems and a TOC removal of 99.7% was achieved in these conditions. However, only about 10% of the salt introduced in the reactor could be recovered.

6.1.1. INTRODUCTION

Above its critical point (374°C and 22.1 MPa), water acts as a non-polar solvent completely miscible with organics. Besides, supercritical water (SCW) presents complete miscibility with permanent gases such as nitrogen, oxygen, and carbon dioxide, creating a homogeneous reaction medium for oxidation reactions in which oxidation takes place in residence times between several seconds and one minute. At a temperature higher than the autoignition temperature of reagents, this oxidation proceeds in the form of flames. These flames generated in an aqueous medium are called hydrothermal flames. They were discovered by Franck in 1988 [1]. In these conditions, total mineralization of the fuel can be carried out even in residence times between 10-100 ms [2], without producing subproducts typical of incinerations process such as dioxins or NO_x or dioxins [3,4]. Therefore, the main application of SCW is the treatment of wastewaters, especially those containing recalcitrant, xenobiotic, and non-biodegradable pollutants, by homogeneous oxidation in a process known as Supercritical Water Oxidation (SCWO). The lack of interfacial mass transfer resistances in a single-phase mixture, combined with high reaction temperatures allows almost any pollutant to be completely mineralized [5].

SCWO technology also presents some challenges related to the harsh operational conditions: salt deposition and corrosion. Corrosion of reaction vessels and process equipment with SCW combined with reactive ion such as Cl^- , F^- , H_3O^+ , and oxygen, and, more important, equipment fouling and plugging due to precipitation of salt particles in SCW are the most severe problems than SCWO processes face nowadays [6, 7, 8].

The solubility of inorganic salts in SCW decreases sharply when exceeding the critical point of water. Therefore the salts that are soluble in room-temperature water precipitate in supercritical conditions. Precipitated salts often form agglomerates and incrustations on internal surfaces, thereby inhibiting heat transfer from/to exterior surfaces [9, 10]. In the literature, different examples of deposition studies of various mixtures of salts can be found: Armellini and coworkers [11] used sodium sulfate for the investigations of the rapid “shock like” precipitation in binary salt-water systems. Rogak and Teshima [12] performed solubility and deposition studies of sodium sulfate in a tube with full turbulent flow and developed a heat-transfer model. Kawasaki and

coworkers [13] studied the feasibility of flowing salt concentrated streams at supercritical conditions through high pressures tubes. A number of solubility studies of different salts in SCWO can be found in the literature [14-18].

SCWO limitations can be overcome by the use of appropriate construction materials and the development of new reactor designs [6, 7, 8]. Different solutions have been proposed to solve the salt deposition problem [10]. One of them is the injection of the reagents at subcritical temperatures over a hydrothermal flame, in order to avoid salt precipitation, plugging and also corrosion, in the preheating system, due to the slow transition from subcritical to supercritical conditions in this equipment. If the feed is rapidly preheated by directly injecting it into a flame, the salts can precipitate in areas where plugging is less likely to occur, such as in a wide reaction chamber. At the same time the slow transition from subcritical to supercritical water, where corrosion is more problematic, is avoided.

Since hydrothermal flames were discovered, several research groups have developed reactors working with a hydrothermal flame as a heat source. The MODAR reactor was able to work with injection temperatures of 25°C and injecting the air at 220°C [19]. In the ETH of Zurich, the direct injection of the waste into a diffusion hydrothermal flame generated inside the reactor was developed as a solution to avoid the external preheating of the wastes up to supercritical conditions [20, 21]. Příkopský and coworkers [22] investigated the feasibility of injecting feeds with a 3%wt of sodium sulfate (Na_2SO_4) in the transpiring wall reactor with a diffusion hydrothermal flame as internal heat source. No plugging was observed during the experiments, but salt deposits were detected in the upper hot zone of the reactor. In a previous investigation of our research group [23], it was found that using a transpiring wall reactor, a premixed hydrothermal flame inside the reaction chamber could be maintained when injecting the feed at a temperature as low as 110°C. Using a similar reactor, feeds with up to 4.74% wt Na_2SO_4 could be injected [24]. The reactor worked without plugging, but the recovery of salts was only between 5% and 50%. Both research groups reported an increase in the temperature when salt was injected in the reactor [22, 24].

It has been proved that injection of cold products over a hydrothermal flame is only possible when working with vessel reactors and it is not possible when working with tubular reactors. Flame formation in different tubular reactors was studied by the High Pressure Process Group of the University of Valladolid [25]. For none of these reactors the flame could be kept steady at injection temperatures lower than 370°C. No

enhancement was found by improving the mixing or the turbulence. Thus, it was proved that a vessel reactor was more favorable for the formation and stabilization of hydrothermal flames, especially at low injection temperatures. In a former investigation by our group it was proposed that this better behavior was due to the low flame front velocities in hydrothermal flames that is lower than 0.1 m/s, in comparison to the higher flame front velocities in atmospheric conditions (0.4- 3 m/s). This is the reason why flow velocities lower than 0.1 m/s are necessary to keep a stable hydrothermal flame where cold reagents can be injected [26].

The objective of this research was the study of the formation and stabilization of a premixed hydrothermal flame in a refrigerated reaction chamber with a tubular injector using isopropyl-alcohol (IPA) as fuel. The influence of operational parameters such as feed flow, injection temperature and fuel concentration as well as geometrical factors such as the diameter and length of the injector were studied. To keep a flame regime during the experiments concentration and temperature were kept above the conditions for maintaining a stable flame found by Serikawa (4% wt IPA and 470°C) [3]. Finally the system was tested by introducing feeds containing salts in the reactor.

6.1.2. EXPERIMENTAL

All the experiments presented in this work were carried out in the SCWO pilot plant of the University of Valladolid. Its maximum treatment capacity is 24 kg/h and it uses air as oxidant which is compressed by a four-stage reciprocating compressor. Aqueous feed and air are pressurized and preheated electrically before being introduced in the reactor where the flame is produced. Refrigerating water is also pressurized and introduced in the reactor. At the outlet of the reactor the effluent and the refrigerating water are cooled down and depressurized. The flow diagram of the facility is shown in Figure 6.1.1. More information about the facility can be found elsewhere [23- 25].

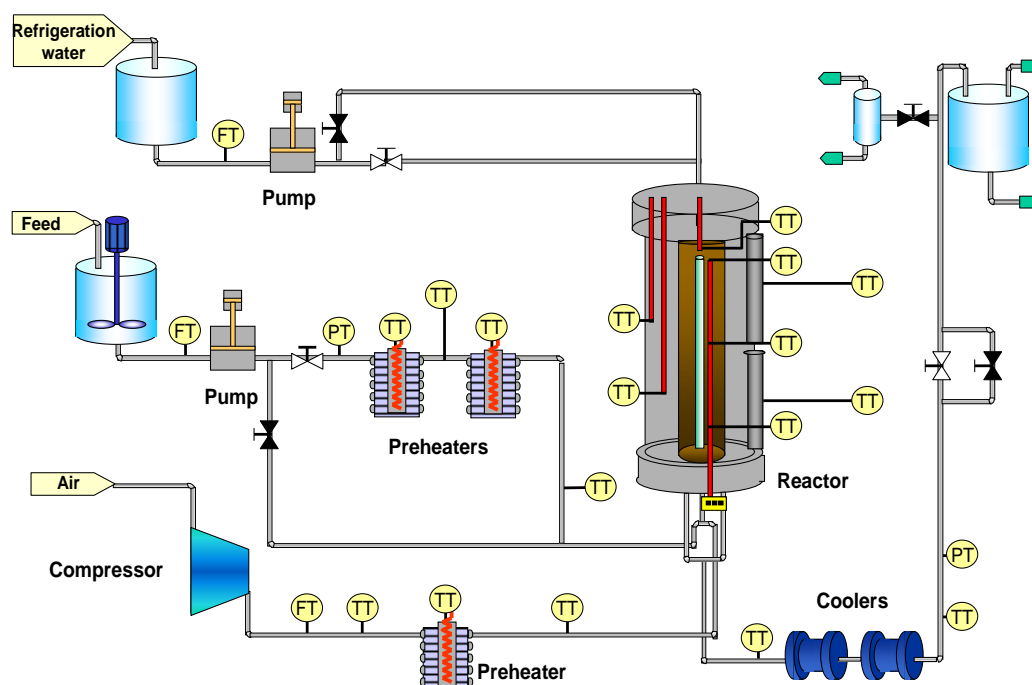


Figure 6.1.1: Diagram of the SCWO pilot plant

The reactor consisted of a vertical Ni-alloy empty reaction chamber of 53.4 mm of internal diameter and 1 m high. It is inside a reaction vessel made of AISI 316 stainless steel able to stand a maximum pressure of 30 MPa and a maximum temperature at 400°C. The reaction chamber was refrigerated by passing pressurized water at room temperature through the space between the reaction chamber and the pressure vessel. The reagents (feed and air) were introduced to the lower part of the reactor through a tubular injector to the top of the reaction chamber. The flame was produced near the outlet of the injector, where the maximum temperature was registered. Three injectors

constructed with empty tubes were tested. Characteristics of those injectors are summarized in Table 3.1.1

Table 6.1.1: Characteristics of the three injectors studied in this work

Injector	Injector 1	Injector 2	Injector 3
Material	Ni-alloy 625	Ni-alloy 625	Ni-alloy 625
External Diameter (in)	1/4	1/8	1/4
Internal Diameter (mm)	3.86	2.16	3.86
Length (mm)	950	950	550

A simple design with empty reaction chamber and empty injector was used because they proved to be more efficient in the SCWO process compared to other reactor designs tested by our research group [4, 23, 25, 26].

Figure 6.1.2 shows a scheme of the top of the reactor chamber with the different position of thermocouples and injectors. The position of the thermocouples was not the same for all the experiments. Thermocouple T1 was situated at 30 mm from the top of the reaction chamber and 20 mm from the exit of the injector exit when working with injectors 1 and 2. When working with injector 3 experiments with T1 in three different positions were performed. They are indicated as positions 1 to 3 in the part b of figure 6.1.2.

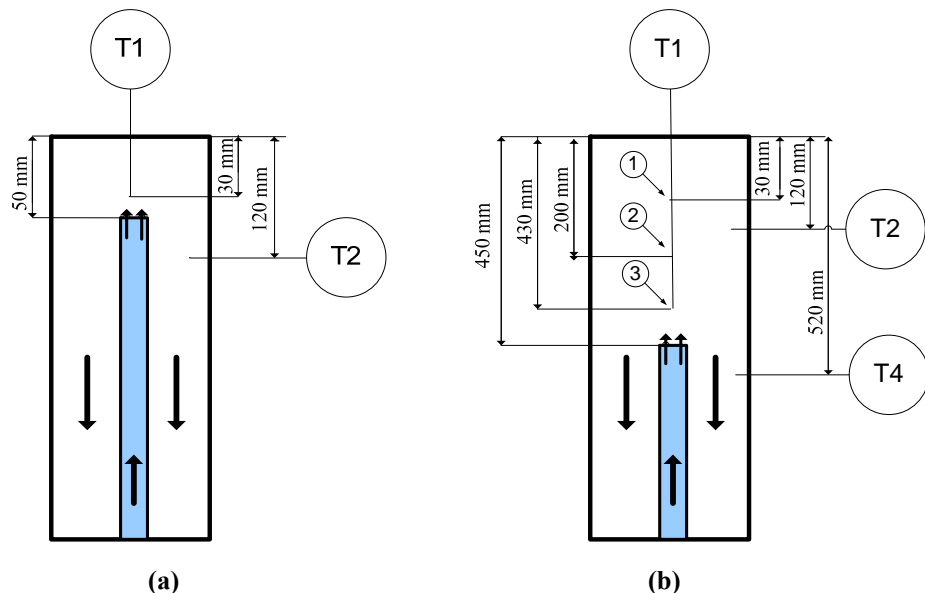


Figure 6.1. 2: (a) Scheme of the top of the reaction chamber, with the positions of the temperature measurement for injectors 950mm long. (b) Scheme of the top of the reaction chamber with the position of the temperature measurements when working with the injector of 550mm long, showing the different positions of thermocouple T1 in the different experiments.

The experiments described in this work were performed using synthetic feeds prepared with isopropyl alcohol (IPA, 99% purity) supplied by COFARCAS (Spain) and water from the tap without further purification. Synthetic wastes containing salts were prepared using Na_2SO_4 supplied by COFARCAS (Purity > 98%) (Spain).

The Total Organic Carbon (TOC) of the samples was determined using a SHIMADZU TOC Analyzer model TOC-VCSH. Salt concentration was measured using a conductivimeter Basic 30 provided by Crison. For doing this, conductivities of solutions of known Na_2SO_4 concentration were measured obtaining a lineal calibration line between conductivity and Na_2SO_4 concentration.

Temperatures were measured in several points of the reactor, as indicated in the scheme of the reactor shown in figure 6.1.2, with type K thermocouples (temperature range from 0 to 1000°C) with accuracy of 1% of the measurement.

Air flow was measured with a Coriolis gas flow meter with a precision of 0.2%. To determine liquid flows, the time needed to pump a fixed volume was measured by the computer.

IPA solutions were prepared volumetrically, measuring water volume with a precision of 1 L and IPA volume with a precision of 1 mL, resulting in an experimental error of 0.3-0.6% for a 6.5-12.5% IPA solution.

6.1.3. RESULTS

6.1.3.1. Experimental performance

The evolution of the main operational variables in a typical experiment is shown in Figure 6.1.3. At the beginning of each experiment, the reactor was first preheated electrically until the walls of the pressure vessel reached a temperature of 400°C (This part is not shown in figure 6.1.3. Then the reaction was initiated injecting IPA solutions 8-9.5% wt IPA and air preheated electrically at temperatures higher than 400°C. The flame was ignited after 10 minutes of the beginning of the experiment, observing a sharp increase in the temperature as shown in figure 6.1.3. In that moment, the electrical heating of the wall of the reactor was turned off. Several stationary states were reached by lowering the injection temperatures and samples were taken. For keeping the maximum temperature in values between 600 - 700°C, IPA concentration was increased as the injection temperature was decreased.

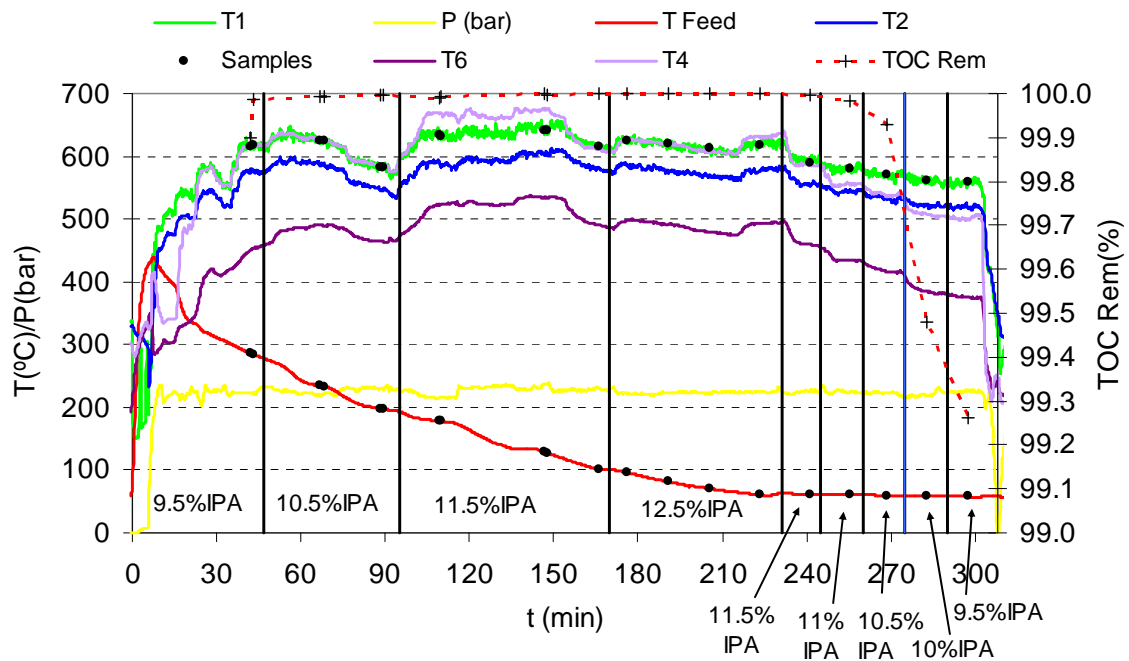
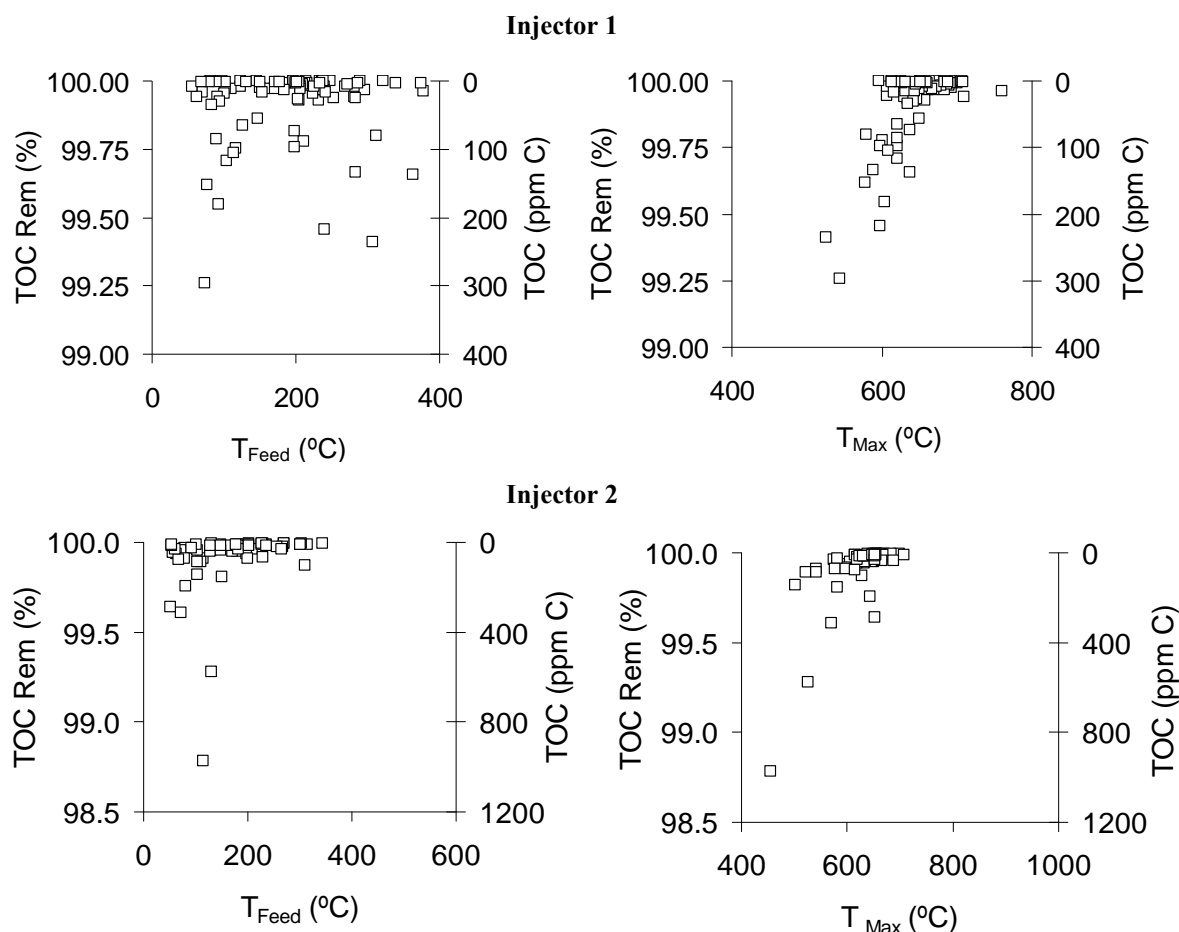


Figure 6.1.3: Temperature, pressure and TOC removal profiles evolution during a typical experiment carried out with the injector 3, with the thermocouple T1 situated in position 3

6.1.3.2. Stability of the flame and TOC Removal

A total of 24 experiments with three different feed flows: 13, 20 and 25 kg/h, were performed using feeds not containing salts in order to study the influence of the operational and geometrical parameters in the formation and stabilization of the hydrothermal flame. Each experiment lasted between 85 and 300 minutes and several stationary states were reached at decreasing injection temperatures from 375 to 50 °C. These experiments are summarized in Table S.6.1.1 in the Supporting Information Appendix I.

Experiments showed that, using the three injector configurations, steady operation under hydrothermal flame regime was possible even with injection temperatures as low as 50°C, as observed in figure 6.1.3 TOC removals and TOC concentrations in the effluent are plotted as a function of feed injection temperature and maximum temperature registered in the reactor chamber in figure 6.1.4.



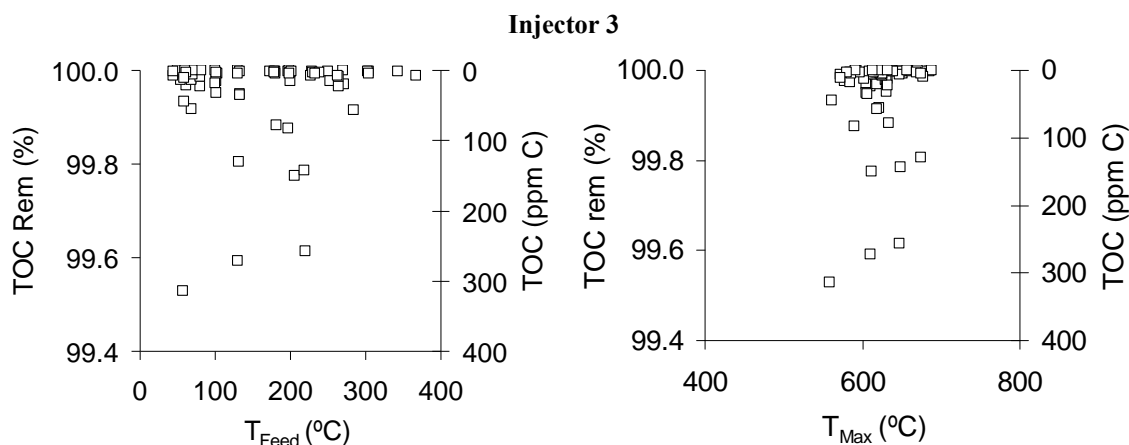


Figure 6.1.4: TOC removal (TOC Rem.) and TOC concentration in the effluent as a function of maximum temperature (T_{Max}) and feed injection temperatures (T_{Feed}) for the three injectors.

In most experiments TOC removal was higher than 99.95%, with concentration in the effluent lower than 20 ppm. When feed injection temperatures were below 100°C, it was possible to reach TOC removals as high as working with higher feed temperatures. Some isolated samples contained TOC concentrations of up to 400 ppm (injector 1), 800 ppm (injector 2), and 350 ppm (injector 3) were obtained. Those high TOC concentrations were mostly coincident with instabilities in the reactor, and when maximum reaction temperatures were lower than 650°C.

In general results obtained with the present design are better than the ones obtained with other reactors tested by our research groups. Even when the empty wide reaction chamber was tested successfully with the transpiring wall reactor [23], injection temperatures are lower using the present design and TOC removal are higher. In addition, using empty injectors avoid plugging problems caused by filled injectors. The smaller diameter and lower volume of the new reactor make it faster in reaching new steady state when changing operating conditions.

The figure S.6.1.1 in the Supporting Information (Appendix I) shows the maximum temperatures reached in the reaction chamber using the different injectors with different feed temperatures and IPA concentrations. It is observed that when feed injection temperatures were decreased, IPA concentrations were increased in order to have reaction temperature between 600 and 700°C. For keeping those reactions temperatures IPA concentrations of 6.5 to 9% wt IPA were necessary in injector 1. Injector 2 needed IPA concentrations between 7.5 and 12.5% wt IPA and injector 3 from 8.5 to 12.5% wt IPA.

Reaction temperature decreased quickly with feed temperature when these are lower than 100°C, but reactor could work in steady state in that conditions as observed in Figure 6.1.3. Temperatures at which flame was extinguished spontaneously for different feed flows and IPA concentration are shown in figure 6.1.5. There was a quasi-linear relationship between extinction temperature and concentration of organic matter, that it is different for each injector having the flow only a slight influence. For the same IPA concentration, extinction temperatures were lower for injector 1, implying that more stable hydrothermal flame were formed using this injector.

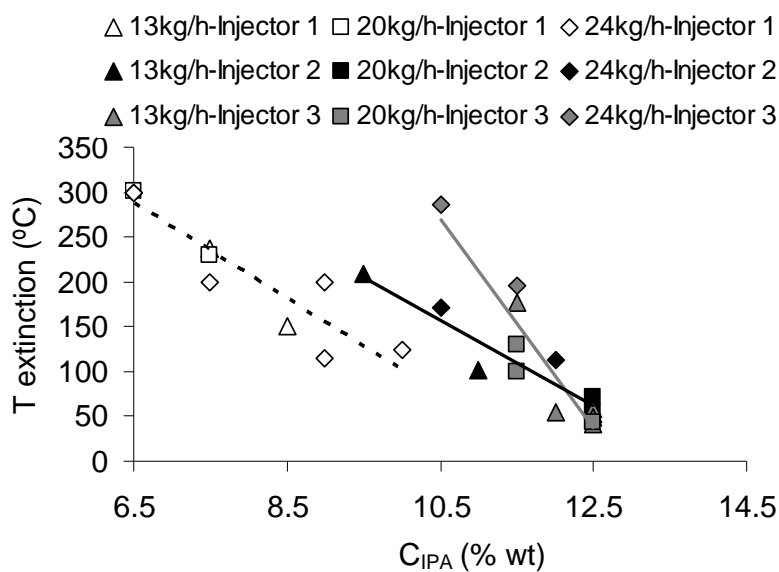


Figure 6.1.5: Extinction temperatures registered in injector 1, 2 and 3 for different feed flows as a function of IPA concentrations.

6.1.3.3. Energy balances in the reactor

In section 6.1.3.2 it was observed that IPA concentrations necessary to reach the maximum temperatures between 600-700°C were higher using injectors 2 and 3 than with injector 1. To better understand this discrepancy the balances of energy in the reactor were calculated. It was considered that reactants, feed and air entered in the reactor at temperatures measured by thermocouples. The adiabatic flame temperatures were calculated assuming that IPA was totally burnt and that the reactor was adiabatic. For calculating the enthalpy of the mixture the properties of the pure compounds were balanced as a function of the composition of the mixture. The adiabatic flame temperatures were compared to the maximum temperatures registered in the reactor in the figure S.6.1.2 in the Appendix I. It was found that when injection temperatures were lower than 200°C, calculated adiabatic flame temperatures were lower than maximum

experimental temperatures measured in the reactor. This discrepancy was more than 30% in the case of injector 1 while it was much lower in the case of injectors 2 and 3 (less than 10 and 20% respectively).

The injection temperatures needed to reach the experimental maximum reaction temperatures were calculated, and plotted in figure 6.1.6. In general, for injector 1 calculated temperatures were up to 200°C higher than the experimental ones, being these discrepancies higher for lower injection temperatures. The discrepancies between the calculated and experimental injection temperatures for injector 2 and 3 were much lower.

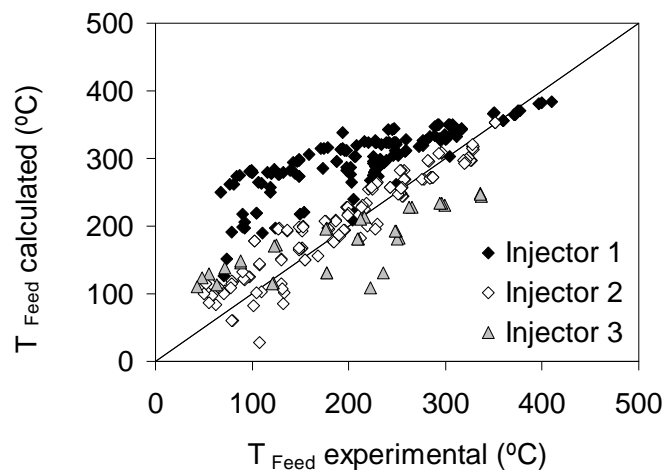


Figure 6.1.6: Experimental injection temperatures versus calculated inlet temperatures for reaching maximum experimental temperatures using balanced properties method.

These different results between injector 1 and the other may be explained by supposing that reactants got into flame zone at a higher temperature than at the entrance of the injector due to heat exchange between hot products and reactants through the wall of the injector.

6.1.3.4. Influence of the fluid flow velocity in the position of the flame front

When injectors 1 and 2 were analyzed it was observed that the maximum temperature was displaced from position T1 to position T2 when the feed temperature was decreased and the difference between these two temperatures become smaller again when IPA concentration is increased, as showed in figure 6.1.7

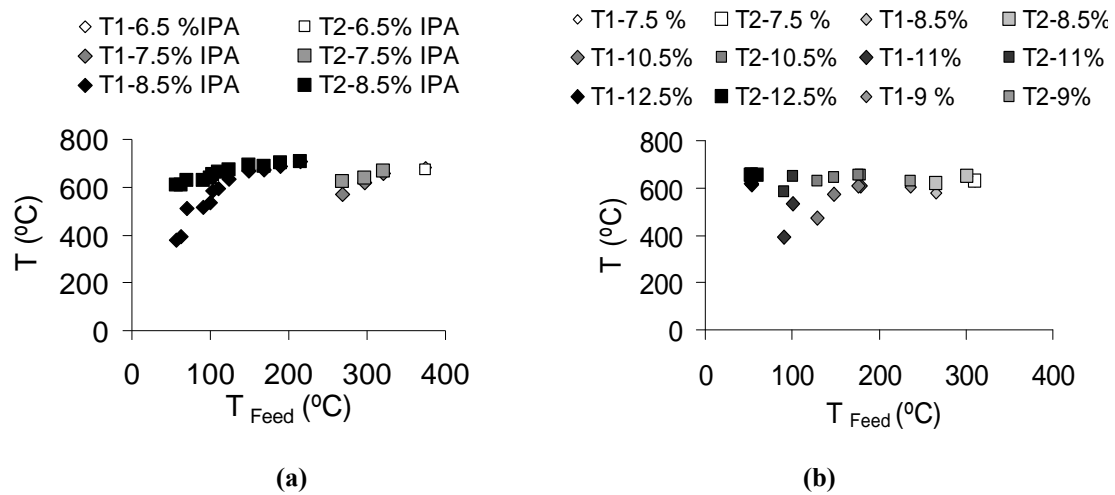


Figure 6.1.7: Temperatures T_1 and T_2 versus injection temperature for increasing IPA concentrations.
a) Feed= 20 kg/h; injector 1 **b)** Feed= 13 kg/h; injector 2

The difference between temperatures T_1 and T_2 was also influenced by the velocity at the exit of the injector. The influence of the velocity at the exit of the injector is made evident in figure 6.1.8. The temperature difference $T_2 - T_1$ was calculated for different fluid flow velocities and plotted against feed inlet temperature. As a simplification, the velocities were calculated by fixing a temperature of 350°C for the mixture at the outlet of the injector.

The data present high degree of dispersion because of this assumption and because data of different IPA concentrations were plotted together though the concentration was demonstrated to have some influence as shown in figure 6.1.7.

We noticed that the difference between T_1 and T_2 was increased with decreasing feed inlet temperatures, and it is substantially higher when increasing the fluid velocity at the outlet of the injector. This can be interpreted as a delay of the position of the flame, that is the position with the higher temperature, with respect to the injection point. Thus higher injection velocities and lower injection temperatures delay the position of the flame, while high fuel concentrations bring the flame near the injector.

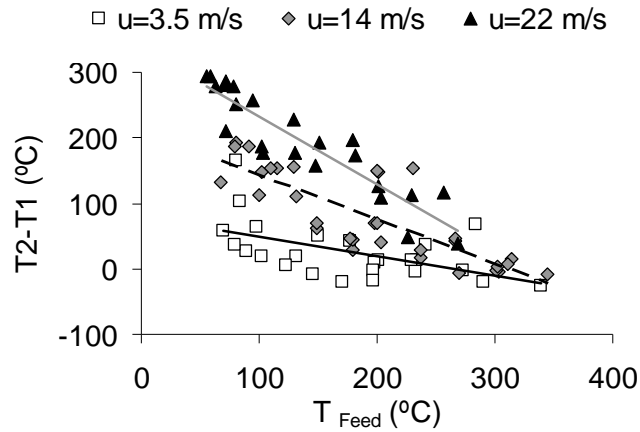


Figure 6.1.8: Temperatures difference (T_1-T_2) versus injection temperature for different velocities at the outlet of the injector

6.1.3.5. Influence of the length of the injector

For studying the influence of the length of the injector the experiments performed with injectors 1 and 3 were analyzed. Apart from the difference in the heat transmitted through the wall of the injector, the main difference for the flame formation and stabilization using different lengths of injectors has to do with the different distances from the outlet of the injector to the top end of the reactor. It is expected that the position of the injector with respect to the top end of the reactor would change the position of the flame inside the reaction chamber.

When using injector 3, experiments using temperature measurement positions at three different distances from the outlet of the injector were carried out. The temperature profiles of three equivalent experiments, performed with the same operational conditions, at three different positions of the thermocouple are represented in Figure 6.1.9. It was observed that the maximum temperature was always registered in temperature measurement position 3, that is, at 20 mm from the outlet of the injector in the central position of the reactor. Thus, the maximum temperature was in the middle of the reactor, and the temperature was decreasing from this point up-flow and down-flow. In figure 6.1.9, the temperature profiles of experimental data with injectors 1 are also represented together with the temperature profiles of injector 3. When using injector 1 the maximum temperature was registered in the position T2, at the top of the reactor, slightly below and in the side of the outlet of the injector, and not just at the outlet of the injector as in the case of injector 3. Then, the temperature was decreasing down flow the reactor, being the temperature at the outlet in the reactor much lower than in the case of injector 3.

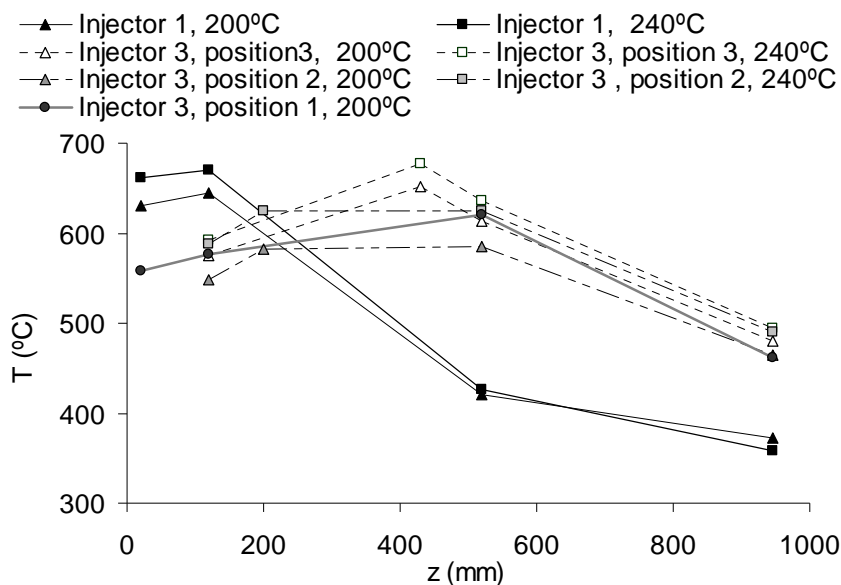


Figure 6.1.9: Temperature profile in the reactor for injectors 1 and 3 working with a feed flow of 13 kg/h and feed injection temperatures of 200 and 240°C

For making a better comparison of the temperature profile using both injectors, these temperature profiles are represented along the length of the reactor taking as origin the outlet of the injectors in figure 6.1.10. The ceiling position with respect to the outlet of the injector is represented as a discontinuous blue and red line for injectors 1 and 3 respectively. It is observed that, when working with injector 1 at 50 mm from the ceiling the maximum reaction temperature that is the position of the flame is situated in the side of injectors. The reagents leave the injector, and hit against the ceiling of the reactor producing a recirculation in the side of the reaction chamber as the top, as shown in the CFD simulation performed by our group of a reactor with a similar injection system [27]. Thus, the maximum temperature is produced when the reagents are in their way down. Using injector 3, where there is nothing to interrupt the flow up of the reagents, the flame will be formed at a few millimeters from the outlet of the injector.

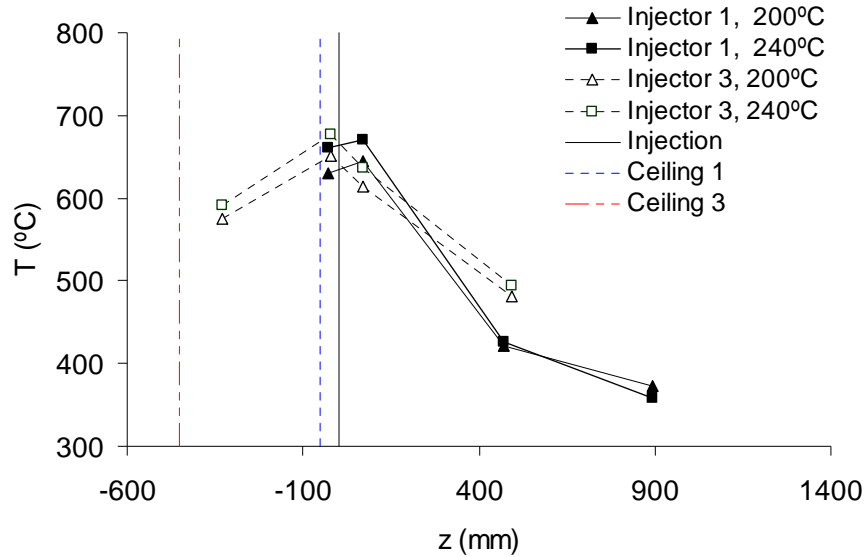


Figure 6.1.10: Temperature profile versus relative position of the thermocouples in the injectors 1 and 3 with respect to the injection points.

Using both configurations almost total TOC removals were obtained using IPA as fuel, and steady operation with the hydrothermal flame was possible with injection temperatures lower than 100°C. Injector 3 has the advantage that the flame when situated at the exit of the injector is farther from the top end of the reactor and also the walls are kept at a lower temperature enhancing its resistance and durability of the construction materials. In addition, higher fuel concentrations must be higher when using this configuration as the heat transfer surface is lower.

Using injector 1, the lower part of the reactor is at colder. This lower temperature in the bottom of the reactor is beneficial for the salt recovery, because precipitated inorganic salts can leave the reactor dissolved in the effluent without producing plugging in the outlet lines and coolers.

6.1.3.6. Influence of inorganic salts

In order to check the performance of the injection system when it is dealing with feeds with high salt concentrations, several experiments were performed with feeds containing different concentration of sodium sulfate (Na_2SO_4). This salt was selected because, according to the classification of salt–water systems by solubility behavior of Marshall this salt corresponds to type 2, that is, it precipitates directly as a solid without an intermediate liquid stage [7]. In addition, Na_2SO_4 is less corrosive than NaCl with materials forming as chromium oxide protecting film such as Ni-Alloy and stainless steel.

Injector 1 was selected to perform these experiments because lower temperatures in the bottom of the reactor were obtained with respect to injector 3. This can make salt removal easier because they can leave the reactor dissolved in the effluent. Furthermore, plugging is less likely in the 1/4" tube used in injector 1 than in the narrower 1/8" tube of injector 2. The experiments performed with feed containing salts are summarized in table 6.1.2

Table 6.1.2: Summary of the experiments performed with feeds containing Na₂SO₄

Experiment	C_{Na2SO4} (% wt)	C_{IPA} (% wt)	t_{operation} (min)	t_{salt injection} (min)	Feed flow (kg/h)	Number Samples
O	1	10	110	40	24	14
P	0.5	9	115	49	24	13
Q	1	8.5-9.5	85	35	24	8
R	1	9.5-10	135	68	24	15
S	2.5	9.5	118	40	24	8
T	1	9.5-10	117	45	20	6
U	1	9.5-10.5	150	88	24	10

Figure 6.1.11 shows the evolution of temperature, pressure, TOC removal and salt recovery in a typical experiment performed with a feed containing 2.5%wt Na₂SO₄. Feeds containing salts could be injected without producing plugging in the reactor, as indicated by the stable pressure observed in figure 6.1.11. In these experiments TOC removals continued being higher than 99.7% even after the injection of the feed containing Na₂SO₄. This is an improvement over the result obtained in experiments performed formerly with the transpiring wall reactor working with feeds containing Na₂SO₄ [24]. Nevertheless, it was possible to recover only a 10% in average of the diluted salt with the products. This means that there was an accumulation of salts into the reactor. The future research must be focused in solving this salt accumulation problem.

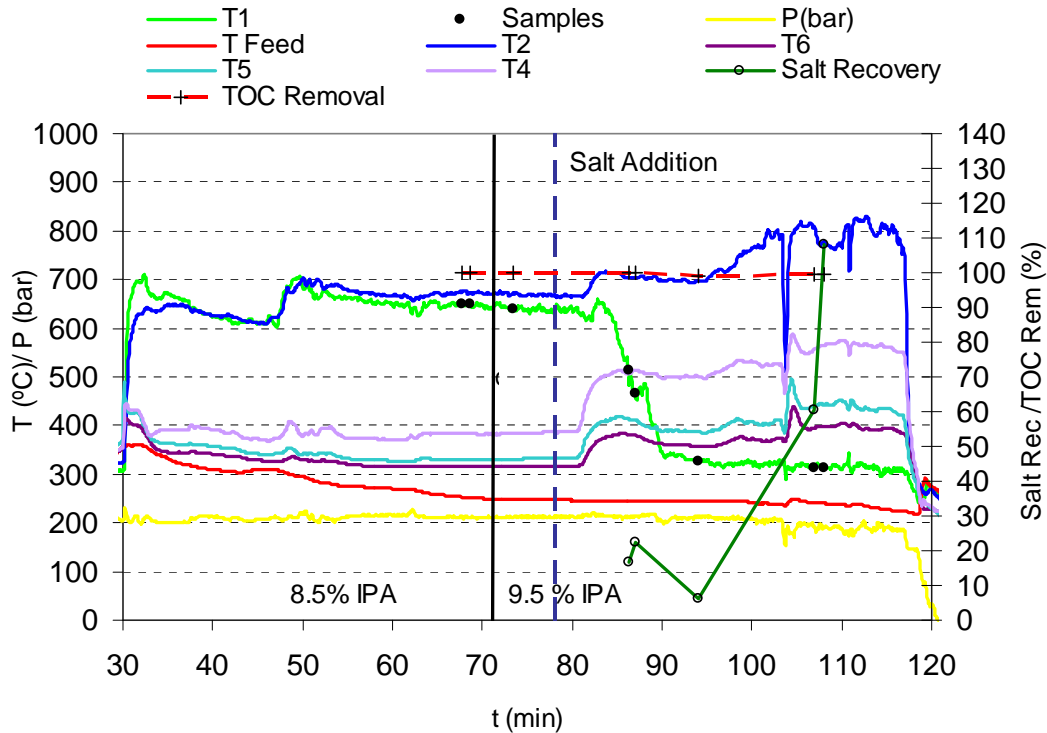


Figure 6.1.11: Temperature, pressure, TOC removal, and salt recovery profile of an experiment performed with a feed flow of 24kg/h, 9.5% IPA and 2.5% Na_2SO_4 .

Salt recovery is related to the temperature at the bottom of the reactor. When this temperature decreased, the liquid fraction in the bottom of the reactor increased, and therefore the amount of diluted salt is increased and the salt recovery increased. Increase the turbulence in the lower part of the reactor can be beneficial for faster salt redissolution on the effluent.

Salt recovery in some points was very high exceeding 100%, as observed in figure 6.1.11 in $t=110$ min. This fact can be interpreted as solid clusters of salts swept away by the outlet streams and dissolved in the cooling systems.

When a feed containing Na_2SO_4 was introduced into the reactor, the temperature in position T1, just at the outlet of the injector, decreased, indicating that the position of the flame is delayed with respect to the injector outlet. It is also observed that the other temperatures in the reactor increased. This temperature increase is proportional to the salt concentration in the feed as observed in figure 6.1.12. An increase in temperature when salts were injected was observed previously by other authors [22, 24]. Příkopský and coworkers [22] associated it to the formation of hot points in the thermocouples due to salt deposition.

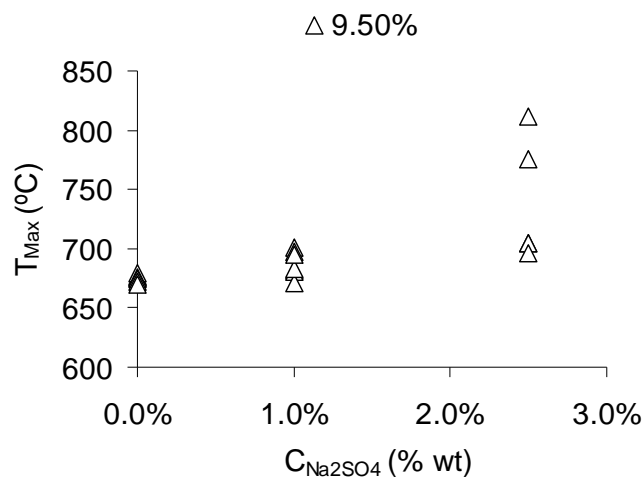


Figure 6.1.12: Maximum temperatures reached in the reactor at Na_2SO_4 concentrations in the feed for IPA concentration of 9.5% wt

It is known that the presence of salts have an influence in the liquid fraction. This fraction increases when the salt concentration increases under the same pressure and temperature conditions. The Anderko-Pitzer EoS, developed specifically for aqueous systems containing salts at high pressures and temperatures [28,29] and adapted by our group to be used in SCWO systems [30], was used to calculate the percentage of liquid water at different temperatures as a function of NaCl concentration, as shown in figure 6.1.13. It is observed that the percentage of liquid water in the reaction mixture increases with salt concentration. This increase is more pronounced at higher temperatures.

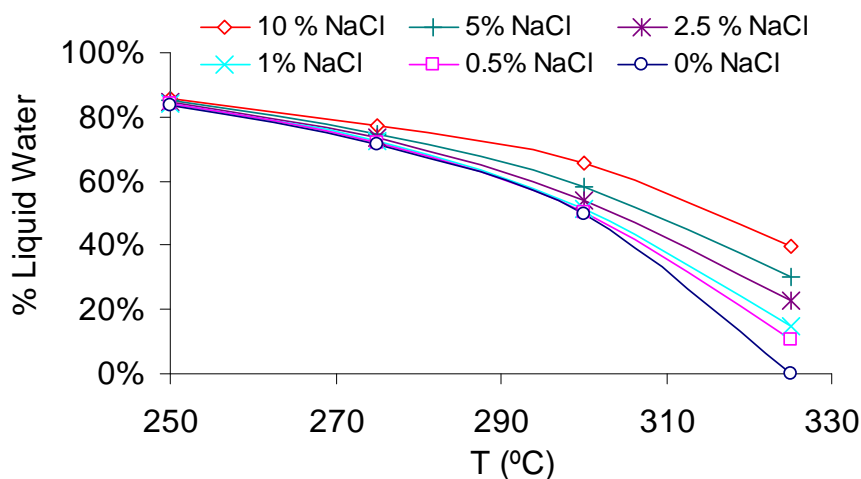


Figure 6.1.13: Proportion of water liquefied as a function of temperature and NaCl concentration for 60% mol water-air mixtures

Based on these calculations, energy balances of the reactor were performed. According to these calculations, for the same enthalpy values of the product mixture at

the outlet of the reactor, the higher the liquid fraction, the higher the temperature. Table 6.1.3 shows a comparison of the increase of temperature associated with an increase of the liquid fraction, calculated with the energy balances, and the increase in temperature observed in experiments. The temperature increases calculated are of the same order of magnitude of the experimental increments produced in the bottom (T6) of the reactor.

Table 6.1.3: Experimental and theoretical increase of temperature in the bottom of the reactor

Experiment	C_{Na2SO4} (% wt)	Fraction of liquefied water	$\Delta T_{\text{experimental}}$ (T6) (°C)	$\Delta T_{\text{theoretical}}$ (°C)
O	1	0.50	20	63
P	0.5	0.11	38	29
R	1	0.15	36	33
S	2.5	0.35	67	52
U	1	0.51	23	63

6.1.4. CONCLUSIONS

In this work, the behavior of hydrothermal flames in an empty reaction chamber using different empty tubular injectors inside a cooled reaction chamber was experimentally studied by using three injectors, two of 950 mm long and 1/4" and 1/8" of diameter, and one of 550 mm long and 1/4" of diameter.

Stable hydrothermal flames were maintained with feed flows between 13 kg/h and 25 kg/h and feed injection temperatures as low as 50°C. TOC removals higher than 99.95% were obtained with all the operational conditions tested with TOC concentrations of less than 20 ppm in the effluent. Showing better performance than other reactor configurations previously tested by our research group.

An important effect of heat transmission through the wall of the injector was observed. Due to this effect, reagents are preheated at the injector, reaching temperatures higher than the calculated adiabatic flame temperature.

When injection velocity was increased, feed injection temperature was decreased or fuel concentration was decreased, the maximum temperature in the reaction chamber was observed further from the outlet of the injector, indicating that the flame front was moving backwards when these changes in process conditions were applied.

It is observed that, when the outlet of the injector was farther from the top end of the reactor the flame is not deformed and the hydrothermal flame was formed just at the outlet of the injector, while if the outlet of injector is very near to the ceiling of the reactor the flame is formed in the recirculation area, down in the side of the injector. In the last case the products of the reactor are cooled as they flow down the reactor. When a shorter injector is used, higher temperature was achieved at the exit of the injector, in the centrum of the reactor and temperature decreased from the outlet of the injector to the upflow and downflow the reactor.

Feeds with salts concentration up to 2.5% wt Na_2SO_4 could be injected in the reactor without plugging. Nevertheless only an average of 10% of the salts could be recovered. In these experiments TOC removals higher than 99.7% could be achieved. In comparison to experiments without salts, flame formation was delayed with respect to the injector outlet. In addition, the injection of salts produced an increase of temperature into the reactor. The phase equilibrium calculations performed with the Anderko-Pitzer EoS show that at higher salt concentrations the fraction of liquid in the reactor is increased, conducting to higher temperatures at the same P,T conditions.

In general, a reactor design with a lot of advantages has been developed, allowing very high TOC removals, low extinction temperatures as well as injections of feeds with high salt contents. In a future work the design must be improved in order to recover the totality of the salts introduced in the reactor.

6.1.5. REFERENCES

- [1] W. Schilling, E. U. Franck, Combustion and Diffusion Flames at High Pressures to 2000 bar, *Berichte Der Bunsen-Gesellschaft-Physical Chemistry Chemical Physics*, 92 (1988) 631-636
- [2] C. Augustine, J.W. Tester, Hydrothermal flames: From phenomenological experimental demonstrations to quantitative understanding, *Journal of Supercritical Fluids*, 47 (2009) 415–430
- [3] R.M. Serikawa, T. Usui, T. Nishimura, H. Sato, S. Hamada, H. Sekino, Hydrothermal flames in supercritical water oxidation: investigation in a pilot scale continuous reactor, *Fuel*, 81 (2002) 1147-1159
- [4] M.D. Bermejo, F. Cantero, M.J. Cocero, Supercritical water oxidation of feeds with high ammonia concentrations: Pilot plant experimental results and modeling, *Chemical Engineering Journal*, 137 (2008) 542-549
- [5] G. Brunner, Near and supercritical water. Part II: Oxidative processes, *Journal of Supercritical Fluids*, 47 (2009) 382-390
- [6] M.D. Bermejo, M.J. Cocero, Supercritical water oxidation: A technical review, *AIChE Journal*, 52 (2006) 3933-3951
- [7] P.A. Marrone, G.T. Hong, Supercritical Water Oxidation, in: M. Kutz (Ed.), *Environmentally Conscious Materials and Chemicals Processing*, John Wiley & Sons Inc., Hoboken (NJ), 2007. pp. 385-453
- [8] P. Kritzer, E. Dinjus, An assessment of supercritical water oxidation (SCWO): existing problems, possible solutions and new reactor concepts, *Chemical Engineering Journal*, 83 (2001) 207–214
- [9] M. Hodes, P.A. Marrone, G.T. Hong, K.A. Smith, J.W. Tester, Salt precipitation and scale control in supercritical water oxidation—Part A: Fundamentals and research. *Journal of Supercritical Fluids*, 29 (2004) 265-288.
- [10] P. A. Marrone, M. Hodes, K. A. Smith, J. W. Tester, Salt precipitation and scale control in supercritical water oxidation—part B: commercial/full-scale applications, *Journal of Supercritical Fluids*, 29 (2004) 289–312
- [11] F.J. Armellini, J.W. Tester, G.T. Hong, Precipitation of sodium chloride and sodium sulfate in water from sub- to supercritical conditions—150 to 550°C, 100 to 300 bar, *Journal of Supercritical Fluids*, 7 (1994) 147–158.

- [12] S.N. Rogak, P. Teshima, Deposition of sodium sulfate in a heated flow of supercritical water, *AIChE Journal*, 45 (1999) 240–247.
- [13] S. Kawasaki, T. Oe, S. Itoh, A. Suzuki, K. Sue, K. Arai, Flow characteristics of aqueous salt solutions for applications in supercritical water oxidation, *Journal of Supercritical Fluids*, 42 (2007) 241-254
- [14] F.J. Armellini, J.W. Tester, Solubility of sodium chloride and sulphate in sub- and supercritical water vapour from 450–550°C and 100–250 bar, *Fluid Phase Equilibria*, 84 (1993) 123-142.
- [15] M.S. Khan, S.N. Rogak, Solubility of Na₂SO₄, Na₂CO₃ and their mixtures in supercritical water, *Journal of supercritical Fluids*, 30 (2004) 359-373.
- [16] M.M. DiPippo, K. Sako, J.W. Tester, Ternary phase equilibria for the sodium chloride–sodium sulfate–water system at 200 and 250 bar up to 400°C, *Fluid Phase Equilibria*, 157 (1999) 229-255.
- [17] I. Leusbrock, S.J. Metz, G. Rexwinkel, G.F. Versteeg, The solubilities of phosphate and sulfate salts in supercritical water, *Journal of Supercritical Fluids*, 54 (2010) 1-8
- [18] H. Higashi, Y. Iwai, K. Matsumoto, Y. Kitani, F. Okazaki, Y. Shimoyama, Y. Arai, Measurement and correlation for solubilities of alkali metal chlorides in water vapor at high temperature and pressure, *Fluid Phase Equilibria*, 228-229 (2005) 547-551.
- [19] C.H. Oh, R.L. Kochan, T.R. Charlton, Thermal-Hydraulic Modeling of Supercritical Water Oxidation of Ethanol, *Energy & Fuels*, 10 (1996) 326-332
- [20] B. Welling, K. Lieball, Ph. Rudolf von Rohr, Operating characteristics of a transpiring-wall SCWO reactor with a hydrothermal flame as internal heat source, *Journal of Supercritical Fluids*, 34 (2005) 35-50
- [21] B. Wellig, M. Weber, K. Lieball, K. Prikopsky, Ph. Rudolf von Rohr, Hydrothermal methanol diffusion flame as internal heat source in a SCWO reactor, *Journal of Supercritical Fluids*, 49 (2009) 59–70
- [22] K. Prikopsky, B. Wellig, Ph. Rudolf von Rohr, SCWO of salt containing artificial wastewater using a transpiring-wall reactor: Experimental results, *Journal of Supercritical Fluids*, 40 (2007) 246–257
- [23] M.D. Bermejo, F. Fdez-Polanco, M.J. Cocero, Experimental study of the operational parameters of a transpiring wall reactor for supercritical water oxidation, *Journal of Supercritical Fluids*, 39 (2006) 70-79

- [24] M.D. Bermejo, F. Fdez-Polanco, M. J. Cocero, Effect of the Transpiring Wall on the Behavior of a Supercritical Water Oxidation Reactor: Modeling and Experimental Results, *Industrial & Engineering Chemistry Research*, 45 (2006) 3438–3446
- [25] M.D. Bermejo, P. Cabeza, R. Fernández, V. Ríos, C. Jiménez, M.J. Cocero, Experimental study of hydrothermal flames initiation using different static injector configurations, *Journal of Supercritical Fluids*, 50 (2009) 240-249
- [26] M.D. Bermejo, P. Cabeza, J.P.S. Queiroz, C. Jiménez, M.J. Cocero, Analysis of the Scale up of a Transpiring Wall Reactor with a Hydrothermal Flame as a Heat Source for the Supercritical Water Oxidation, *Journal of Supercritical Fluids*, 56 (2011) 21-32
- [27] M.D. Bermejo, A. Martín, J.P.S. Queiroz, I. Bielsa, V. Ríos, M.J. Cocero. Computational fluid dynamics simulation of a transpiring wall reactor for supercritical water oxidation, *Chemical Engineering Journal*, 158 (2010) 431-440
- [28] A. Anderko, K.S. Pitzer, EOS representation of phase equilibria and volumetric properties of the system NaCl–H₂O above 573 K, *Geochimica et Cosmochimica Acta*, 57 (1993) 1657-1680
- [29] J.J. Kosinski, A. Anderko, EOS for high-temperature aqueous electrolyte and nonelectrolyte systems, *Fluid Phase Equilibria*, 183-184 (2001) 75-86
- [30] M.D. Bermejo, A. Martín, M.J. Cocero, Application of the Anderko–Pitzer EoS to the calculation of thermodynamical properties of systems involved in the supercritical water oxidation process, *Journal of Supercritical Fluids*, 42 (2007) 27-35

6.2. SLUDGE DESTRUCTION BY MEANS OF A HYDROTHERMAL FLAME. OPTIMIZATION OF AMMONIA DESTRUCTION CONDITIONS

ABSTRACT

Disposal of the sludge produced by wastewater treatment process has become in recent years an environmental concern. This sludge contains a remarkable amount of ammonium nitrogen (N-NH_4^+) that is one of the most important issues that difficult its disposal. Current technologies for ammonium treatment and sludge disposal present both technical and legal limitations. In recent years, Supercritical Water Oxidation process (SCWO) has been presented as a desirable breakthrough in such application field. In this work, the destruction of sludge by SCWO under hydrothermal flame regime was studied. Under these conditions, oxidation reaction is much faster and completes in terms of milliseconds instead of minutes as in conventional SCWO. The waste can be totally mineralized, converting N-NH_4^+ to N_2 without producing prejudicial subproducts as in the case of incineration. Due to the occurrence of the combustion in a watery environment, dewatering and drying problems related to classical incineration are not present but the possibility of energy generation from the sludge is still possible. In this study, firstly, the destruction of ammonia was studied by treating synthetic fuels with concentrations of ammonia as high as 8% wt using isopropyl alcohol as a co-fuel. Conversions higher than 99.99% for total organic carbon (TOC) and 99,90% for ammonia were reached, which means effluent concentrations lower than 10 ppm of TOC and 20 ppm or total nitrogen (TN). Excess nitrate formation was successfully reduced by controlling reaction temperature and oxidant excess over stoichiometric. Once optimized the reaction conditions for ammonium removal, successful operational tests were performed using synthetic and real sludge. Finally, the energy production capacity of the process at industrial scale is evaluated.

6.2.1. INTRODUCTION

Wastewater management is, nowadays, one of the most important and critical issues related to waste management. European Water Framework Directive (WFD) 2000/60/EC [1] establishes that all kind of wastewaters, must be treated before their final disposal. Nevertheless, almost all the processes used to treat wastewaters produce sludge as a byproduct. The disposal of this sludge creates another environmental problem. Main alternative for sludge disposal is land application, but sludge requires further treatments before their final disposal in order to reduce its biohazard potential and their nitrogen content as state in Sewage Sludge Directive 86/278/EEC [2] and Urban Waste-water Treatment Directive 91/271/EEC [3] . Anyway, even when land application of sludge is carried out according to the regulations in force, there are still concerns related to its human health and environmental impact [4].

Widely spread Anaerobic Digestion (AD) is not a final disposal for the sludge because produces a sludge with a high Ammonium Nitrogen (N-NH_4^+) content [5], that is one of the most important issues related to sludge disposal especially when destined to land application [6]. Current processes used for ammonium removal present limitations. For example, biological Nitrification/Denitrification process is not efficient for sludge with ammonium content higher than 1.0 kg/m^3 as N-NH_4^+ , because it causes inhibition of the microorganisms. On other hand, ammonia stripping presents huge energy costs for heating up the entire sludge stream.

Other processes that may be used as final sludge disposal strategy, such as composting, landfilling or incineration also present important limitations. Composting can not be applied to all kind of sludge and it is associated to greenhouse gases emissions [7] and problems related to incomplete inactivation of pathogen microorganism [8]. Landfilling produces leachates that needs further treatments as well as greenhouse gases emissions [9].

Incineration is an attractive strategy as final disposal strategy due to the energy production potential of sludge that present energy content, ranging from 4 to 14 MJ/kg. Nevertheless, dewatering and drying pre-treatment make it expensive both in economic

and energy terms. Moreover, it is associated to gaseous emission and ashes containing hazardous compounds. Thus, incineration is not desirable as a sludge treatment [10].

A less conventional process proposed for the treatment of sludge, especially industrial sludge is the wet air oxidation where sludge can be oxidized in liquid water at high pressure (2-20 MPa) and temperature (150 - 325°C). Nevertheless this process is not able to eliminate ammonia and high amount of organic acids generated, being necessary a post treatment of the effluent. [11]

In recent years, Supercritical Water Oxidation (SCWO) has been proposed, tested and applied successfully as an alternative sludge treatment even at a wide scale. It present evident advantages over incineration [12] when applied to sludge because drying of sludge is not required. What it is more, heteroatoms are converted to oxides, acids or salts, allowing the recovery of valuable compounds [13]. The first SCWO industrial plant for sludge treatment was constructed in Harlingen with the HydroSolids® in 2001 [14]. The plant had a treatment capacity up to 9.8 dry tons per day of sludge. The destruction for Chemical Oxygen Demand (COD) in the sludge ranged 99,93-99,96% while the ammonia destruction range was from 49,6 to 84,1%. The plants was in operation only till 2002 due to corrosion problems [15]

A full scale SCWO plant for sludge oxidation with a capacity of 5 t/day in dry basis was constructed in Iron Bridge Regional Water Treatment Facility (Florida, USA). The plant is in trials since 2009 and operating with sludge since February 2011 [16]. It is based on the design principles of the 1993 Modell patent WO/1993/000304 [17] (Now owned by SuperWater Systems [18]), with several new enhancements [19]. Recently, Donghai Xu et al [20] have developed the first SCWO pilot scale plant in China for the treatment of sludge with a maximum capacity of 125 kg/h. They obtained good preliminary results as 98.5% of TOC removal and 96.5% of ammonia removal.

At temperatures higher than autoignition temperature, SCWO reaction proceeds in the form of flames known as hydrothermal flames. High pressure (250- 300 bar) reduces ignition temperature down to 450-550°C using concentrations lower than those needed for combustion [21]. In addition, reaction times are reduced sometimes to the order of milliseconds, making it possible to construct more compact reactors. As in the flameless

SCWO process, in the presence of a hydrothermal flame nitrogen is converted to N_2 and pollutants such as NO_x and dioxins, are not produced [21, 22].

The effluent of the SCWO process (consisting of steam at high temperature and high pressure) can be used to produce energy by production of steam for using in a Rankine or a Brayton cycle or by direct expansion of the effluent on a turbine [23, 24]. When working under hydrothermal flame regime, the higher temperatures allows higher efficiency in energy production than in flameless process. In addition, feed preheating and all its associated problems of corrosion and salt deposition in this step can be avoided by injected the feed directly into the hydrothermal flame [25], [26].

Ammonia is the most recalcitrant compound to SCWO [27, 28] and, so far it has not been possible to generate hydrothermal flames using it exclusively as fuel. Nevertheless, it is known that together with organic compounds such as alcohols, high ammonia eliminations can be achieved [28] being even possible to work in hydrothermal flame regime [19]. In a previous works of our research group oxidation efficiencies as high as 99% were achieved in presence of hydrothermal flames using isopropyl-alcohol as a co-fuel in residence times as low as 0.5 s even with ammonia concentrations as high as 8% wt. Nevertheless complete ammonia removal was not possible and, high nitrate concentrations were produced. [22, 29]

The objective of this work is to study and optimize the SCWO destruction conditions of ammonia by using a hydrothermal flame in a new design of cooled wall vessel reactor followed by a short study of the destruction of a synthetic and a real sludge. Finally, a preliminary study of the energy production of an industrial process of SCWO of sludge is presented.

It is proved that the utilization of a vessel reactor and longer residence times of up to 30 seconds instead of milliseconds, led to improve the previous results of our group using a tubular reactor. It is due mainly to a better control of the flame. Ammonia conversions higher than 99.99% were achieved and nitrate control in the effluent is possible by thorough control of oxygen excess and reaction temperature.

6.2.2. EXPERIMENTAL

6.2.2.1. Experimental set up

The experiments were carried out in the pilot plant of the University of Valladolid. The maximum treatment capacity of the plant is of 24 kg/h of feed. Air was used as the oxidant supplied by a four-staged reciprocating compressor. Aqueous feed and air are pressurized and preheated electrically before being introduced in the reactor where the flame was produced. The reactor pressure shell was kept at temperatures lower than 400°C by using room temperature pressurized water. At the outlet of the reactor the effluent is cooled down and depressurized. The flow diagram of the facility is shown in figure 6.2.1

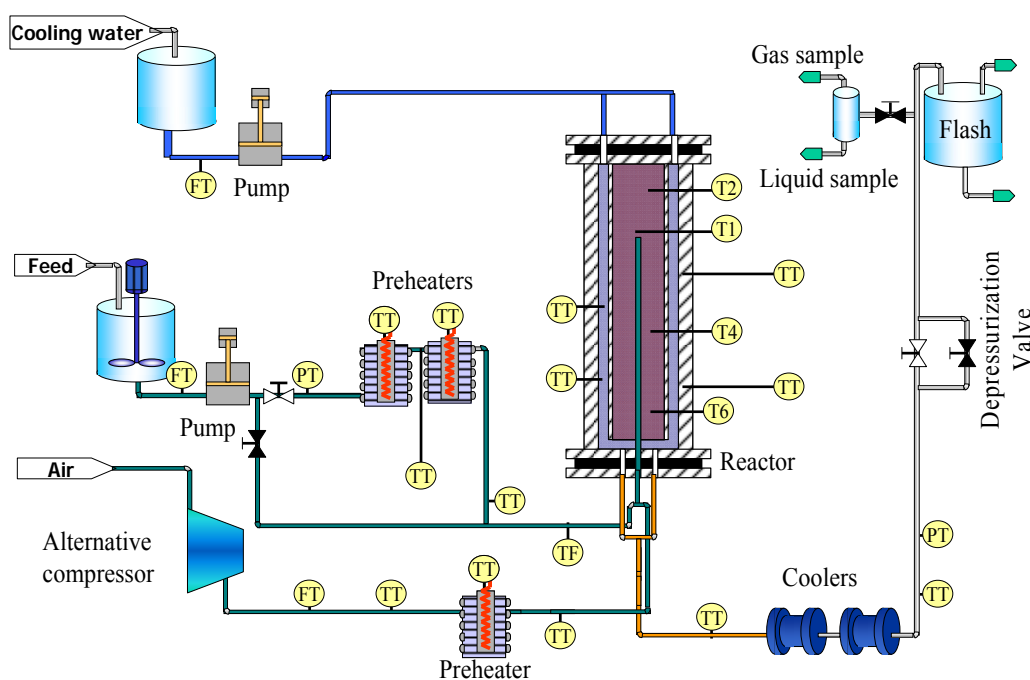


Figure 6.2.1: Diagram of the pilot plant used in SCWO.

The reactor consisted of a vertical Ni-alloy reaction chamber of 53.4 mm of internal diameter and 1 m high. It is contained in a pressure vessel made of AISI 316 able to stand a maximum pressure of 30 MPa and 400°C. The reagents (feed and air) were introduced in the reactor through a tubular injector up to the top of the reaction chamber. The flame was produced outside of the injector, where the maximum temperature was registered. Pressurized room temperature water flowed between the

reaction chamber wall and the pressure vessel inner wall, keeping it at temperatures below 400°C, making possible to use stainless steel for pressure vessel construction. The products flowed down the reactor leaving it by its lower part. Further information of the experimental facility and the reactor can be found elsewhere [30].

6.2.2.2. Experimental procedure

In each experiment, electrical resistances were used in order to preheat the reaction vessel to 400°C. Then, the reaction was initiated by injecting IPA solutions with concentrations as high as 7.0-8.5% IPA and air preheated electrically, both at temperatures higher than 400°C. Once the flame was ignited the electrical heating of the wall of the reactor was turned off. For keeping the maximum temperature constant in values around 600 - 700°C till the desired injection temperature is reached, IPA concentration was increased as the injection temperature was decreased. In almost all the experiments, ignition produced within the first 15 minutes and the steady state was reached in less than 30 minutes.

After the target injection temperature was reached (200°C or room temperature, around 20 - 30°C), feeds with different compositions were injected in the reactor.

Temperature is monitored in several points of the reactor using thermocouples type K. Liquid effluent is analyzed to determine Total Organic Carbon (TOC), Total Nitrogen (TN) and nitrate and nitrite concentration.

TOC analysis and Total Nitrogen (Total N) analysis of the samples were performed with a TOC 5050 SHIMADZU Total Organic Carbon Analyzer which uses combustion and IR analysis. The detection limit is 1 ppm.

Nitrates and nitrites were characterized in the liquid effluent by ionic chromatography with an IC PAK A column of Waters. The detection limit is 1 ppm.

N-NH_4^+ at the effluent is obtained from the difference of TN and the Nitrogen of N-NO_3 and N-NO_2

NH_3 and NO_x in the gas effluent were analysed with Dräger tubes detectors Lab Safety Supply CH29401 and CH31001. The NO_x detection limits for these tubes ranged from 0.5 to 100 ppm and the NH_3 detection limits for these tubes ranged from 5 to 70 ppm (standard deviation for both tubes are between 10 and 15%).

6.2.2.3. Materials

Feeds with ammonia and isopropanol were prepared using Isopropyl alcohol (99% in mass) and Ammonia (25% in mass) supplied by COFARCAS (Spain).

Feeds with Synthetic sludge were prepared using cellulose micro-crystalline (97%) supplied by VWR, Isopropanol (99% in mass) and Ammonia (25% in mass) supplied by COFARCAS (Spain). The components were mixed with tap water in the following proportion. IPA (9%), cellulose (6%) ammonia (1%) and a few grams of soluble coffee for simulate colour.

Feeds with real sludge from the second stage of the wastewater treatment plant of Valladolid (Spain). Properties: COD of 63000 ppm, volatile solids 6%, TOC of 10500 ppm and TN of 400 ppm. The sludge was diluted in order to be pumpable.

6.2.3. RESULTS AND DISCUSSION

6.2.3.1. Ammonia destruction

6.2.3.1.1. Influence of reaction and injection temperatures

Feeds with various concentrations of ammonia from 0.5 to 8% NH_4^+ were studied in order to observe the influence of the ammonia concentration in the hydrothermal flame formation and the minimum temperature necessary to completely oxidize ammonia into nitrogen.

In the experiments performed, it was not possible to sustain the flame using exclusively ammonia as the fuel, thus isopropanol was used as a co-fuel in order to supply the necessary heat to sustain the hydrothermal flame.

This is consistent with a previous work of the group in which it was not possible to sustain the flame using only ammonia as fuel using tubular reactors [22]. In this work the minimum concentration of co-fuel used was 8% of IPA for a 8% of ammonia, in comparison to 1,2% of IPA for a 8% of ammonia used in the previous work. The higher proportion is explained by the higher amount of heat necessary to release in the vessel reactor in which the feed is injected at much lower temperatures than in the case of the tubular reactor where the feed is injected at supercritical conditions.

Experiments at injection temperatures of 200°C and at room temperature (20 - 30°C) were performed. Figure 6.2.2 shows TOC and ammonia removal as a function of the maximum temperature registered in the reactor for various ammonia concentrations, at both injection temperatures. NH_4^+ oxidation with efficiencies higher than 99.9% was observed at temperatures higher than as low as 600°C and residence times between 20 - 30 s.

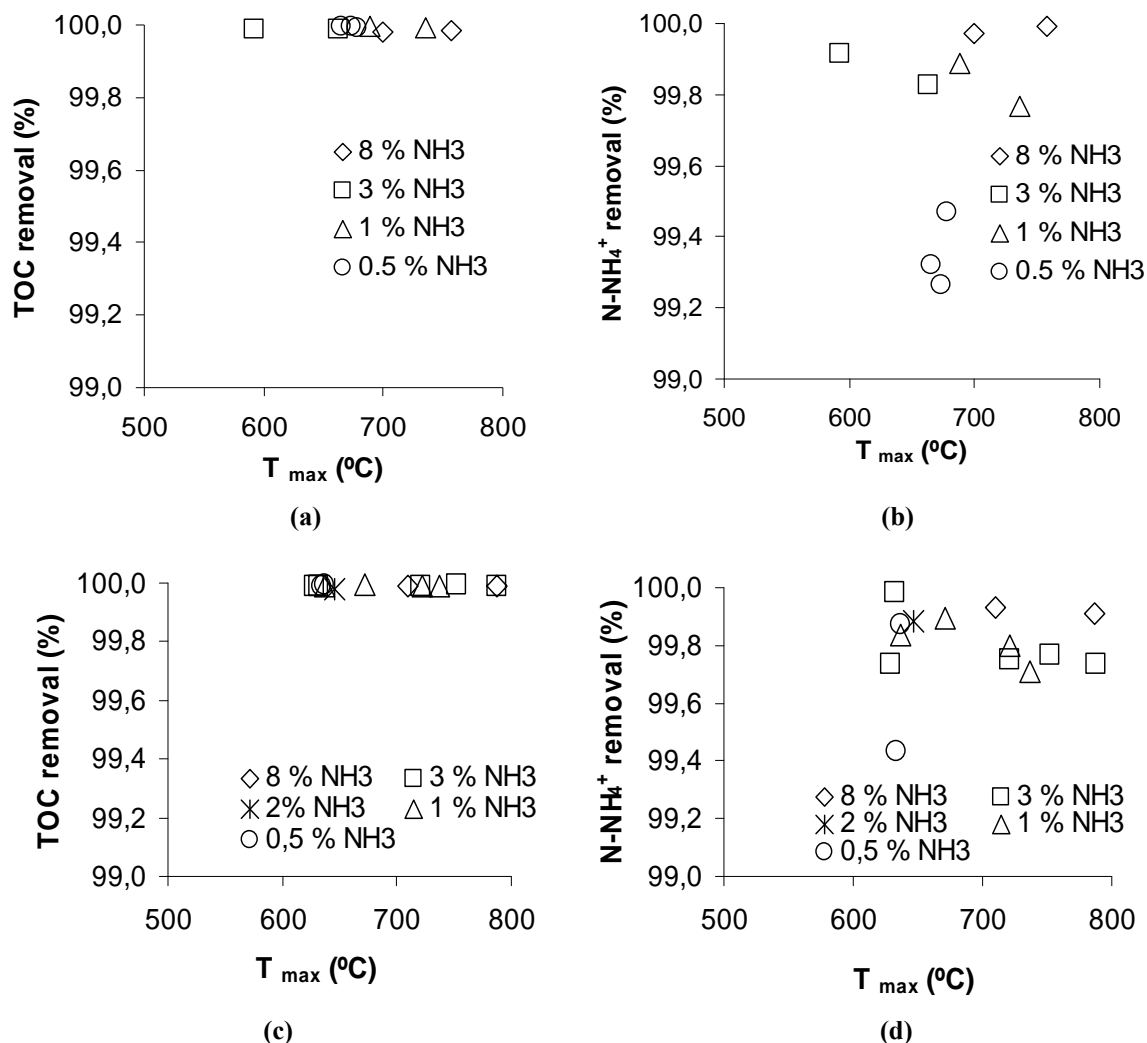


Figure 6.2.2 a & b: TOC removal (a) and N-NH₄⁺ removal (b) at different temperatures obtained with different concentration of ammonia and isopropanol with a injection temperature of 200°C. TOC removal (c) and NH₄⁺ removal (d) at different temperatures obtained with different concentration of ammonia and isopropanol with feed injected at room temperature with a injection temperature of room temperature (20 - 30°C)

According to the results presented in figure 6.2.2, there is no difference in TOC and TN removal when working at different injection temperatures, apart from the need of using a higher amount of cofuel to compensate the lower injection temperatures.

At lower temperatures the flame was not self-sustained and the process was not possible. Thus, while the flame is ignited, effluents with incomplete NH₄⁺ elimination are never produced.

As figure 6.2.3 shows, the minimum temperatures observed where stable flame was possible lay in the range 624 -676°C depending the ammonia concentration.

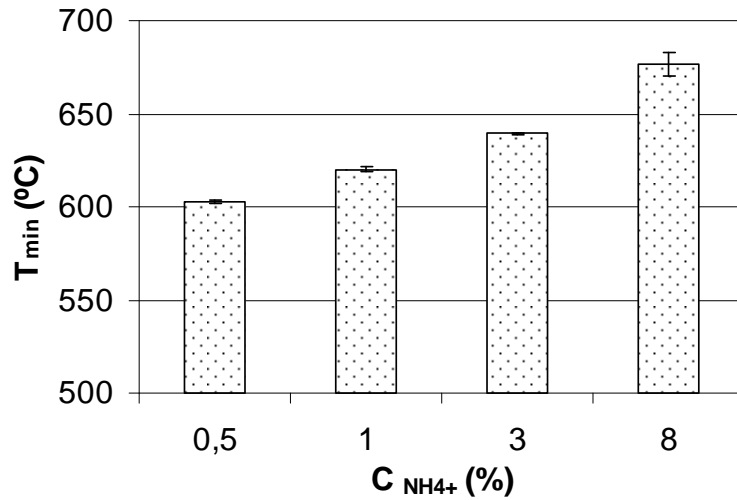


Figure 6.2.3: Minimum temperatures registered to maintain a stable flame depending on the ammonia concentration

Table 6.2.1 and table 6.2.2 collect all the average experimental at injection temperature of 200°C and room temperature respectively.

Table 6.2.1: Main results from the experiments made at injection feed of 200°C

$C_{NH_4^+}$ (%)	C_{IPA0} (%)	T_{Inj} (°C)	T_{Max} (°C)	Ex air (%)	TOC Removal (%)	N-NH ₄ ⁺ removal (%)	N-NH ₄ ⁺ outlet (ppm)	N-NO ₃ outlet (ppm)
8	8	178±2	699 ± 15	17± 4	99.98 ± 0.01	99.97 ± 0.03	10 ±5	114 ± 113
8	8.5	192 ± 5	757 ± 14	12 ± 1	99.98 ± 0.01	99.99 ± 0.01	3 ±2	62 ± 30
3	8.5	209 ± 3	592 ± 5	8 ± 1	99.99 ± 0.01	99.92 ± 0.06	11 ±9	64 ± 14
3	9	207 ± 3	663 ± 6	9 ± 2	99.99 ± 0.01	99.83 ± 0.03	25 ±4	281 ± 27
1	9.5	189 ± 9	689 ± 7	3 ± 1	99.99 ± 0.01	99.89 ± 0.09	7 ±6	49 ± 17
1	10.5	200 ± 10	736 ± 4	6 ± 1	99.99 ± 0.01	99.77 ± 0.10	15 ±9	146 ± 2
0.5	9.5	202 ± 7	678 ± 5	2 ± 1	99.99 ± 0.01	99.47 ± 0.07	18 ±2	48 ± 1
0.5	9.5	208 ± 2	665 ± 3	6 ± 1	99.99 ± 0.01	99.32 ± 0.01	23 ±1	97 ± 3
0.5	9.5	203 ± 6	673 ± 2	11 ± 1	99.99 ± 0.01	99.27 ± 0.02	25 ±1	109 ± 1

Table 6.2.2: Main results from the experiments made at injection temperature of 20°C

$C_{NH_4^+}$ (%)	C_{IPA0} (%)	T_{Inj} (°C)	T_{Max} (°C)	Ex air (%)	TOC Removal (%)	N-NH ₄ ⁺ Removal (%)	N-NH ₄ ⁺ outlet (ppm)	N-NO ₃ outlet (ppm)
8	10	34 ± 3	710 ± 20	10 ± 3	99.99 ± 0.01	99.93 ± 0.05	30 ±20	400 ± 200
8	11	29 ± 1	787 ± 4	10 ± 1	99.99 ± 0.01	99.91 ± 0.03	30 ±10	550 ± 30
3	10	34 ± 1	632 ± 1	3 ± 1	99.99 ± 0.01	99.98 ± 0.02	3 ±3	97 ± 1
3	11	34 ± 1	630 ± 40	11 ± 5	99.99 ± 0.01	99.74 ± 0.10	40 ±20	600 ± 200
3	12	30 ± 1	721 ± 9	6 ± 2	99.99 ± 0.01	99.75 ± 0.01	36 ±2	710 ± 110
3	12.5	32 ± 1	752 ± 4	3 ± 1	99.99 ± 0.01	99.77 ± 0.01	33 ±1	520 ± 40
3	13	31 ± 1	787 ± 6	5 ± 1	99.99 ± 0.01	99.73 ± 0.01	38 ±1	702 ± 1
2	10	34 ± 1	646 ± 9	2 ± 3	99.98 ± 0.02	99.88 ± 0.08	19 ±13	90 ± 30
1	11	37 ± 1	563 ± 1	4 ± 1	99.99 ± 0.01	99.84 ± 0.01	11 ±1	83 ± 8
1	12	36 ± 2	737 ± 4	7 ± 1	99.99 ± 0.01	99.71 ± 0.07	19 ±4	330 ± 20
0.5	11.5	26 ± 1	636 ± 5	7 ± 1	99.99 ± 0.01	99.87 ± 0.11	4 ±4	42 ± 4
0.5	11.5	25 ± 1	633 ± 9	1 ± 1	99.99 ± 0.01	99.43 ± 0.04	19 ±1	11 ± 3

The concentrations of NO_x and NH_4^+ in the gas effluent were under the detection limit of 0.5 ppm and 5 ppm respectively for all the experimental conditions tested.

As it can be observed in tables 6.2.1 and 6.2.2, the concentration of ammonia (N-NH_4^+) in the effluent is always lower than 50 ppm that is the limit of disposal dictated in the Water Framework Directive [1]. In the case of nitrates, the disposal limit is surpassed. Thus lower concentration of N-NO_3^- (below 20 ppm). To do so, further experiments controlling air in excess and reaction temperature were performed. These experiments are described in section 6.2.3.2.

6.2.3.1.2. Influence of the type of reactor used in the ammonia destruction with hydrothermal flames: Vessel reactor vs Tubular reactor

In a previous work it was studied the destruction of ammonia in a tubular reactor working with hydrothermal flames [22]. In this section, the performance of both reactors is compared and the main differences between them are determined as well as the advantages and disadvantages of both of them. For doing this, several operational parameters such as residence time, reaction temperature, ammonia removal or nitrate formation were studied. These results are summarized in table 6.2.4 and 6.2.5.

Table 6.2.4: Comparison of operational conditions studied in both reactors

Reactor type	$T_{\text{Inj}} (^{\circ}\text{C})$		$C_{\text{IPA0}} (\%)$		$C_{\text{NH}_4^+} (\%)$		$T_{\text{max}} (^{\circ}\text{C})$	
	Max	Min	Max	Min	Max	Min	Max	Min
Tubular [22]	428	405	3.8	1.7	8.0	2.0	762	575
New CWR [This work]	200	20	14	8	8.0	0.5	787	592

Using vessel reactors it is possible to work at lower injection temperatures but higher IPA concentrations are required to reach the necessary reactions temperatures. In both cases, the range of ammonia concentration studied was similar and the range of reaction temperatures registered inside the reactor was also similar.

For the case of TOC and ammonia removal and nitrate formation, table 6.2.5 shows the results of the samples taken for each reactor.

Table 6.2.5: Values obtained for different analysis for samples taken at the outlet of each reactor

Reactor type	TOC removal (%)		N-NH ₄ ⁺ removal (%)		N-NO ₃ (ppm)		N-NH ₄ ⁺ (ppm)		t _R (s)	
	Max	Min	Max	Min	Max	Min	Max	Min	Max	Min
Tubular [22]	99.50	75.00	96.10	92.90	2012	371	3412	1101	0.5	0.7
New CWR [This work]	99.997	99.98	99.99	99.27	1246	3	30	4	30	20

Even when most of the TOC and ammonia can be eliminated in tubular reactors in residence times between 0.5- 0.7 s, total removal cannot be achieved in such short residence times. Nevertheless, when using the vessel reactor, with residence times between 20 and 30 s elimination is complete. Vogel and coworkers [31] proposed that SCWO kinetics consisted of three main steps: initiation, propagation in which most elimination occurs and termination step that proceeds at a lower reaction rate. The uncompleted elimination of ammonia in residence times as short as 0.7 s can be explained by the slow occurrence of that termination step, that it especially slow due to the recalcitrant character of ammonia. Nevertheless, when the residence time is increased the reaction can be completed even at relatively low temperatures. This residence time limitation of the tubular reactor could be solved by using longer tubular reactors.

Another advantage of vessel reactor is the possibility of initiating the reaction and completing it with a very high elimination injecting feeds at low temperatures, even at room temperature, what allow avoiding corrosion and salt deposition problems in the preheating system.

6.2.3.1.3. Improvements provide by the new cooled wall reactor design for feeds containing ammonia

In table 6.2.6 the present results are compared to the results presented by our group using a previous design of the cooled wall reactor in which, the reaction vessel consisted in a bed of alumina spheres of diameters .[29] .

Table 6.2.6: Comparison of results obtained with both reactors.

Reactor type	T _{Inj} (°C)		C _{IPA0} (%)		C _{NH₄⁺} (%)		T _{max} (°C)	
	Max	Min	Max	Min	Max	Min	Max	Min
CWR [29]	381	284	7.5	2.5	7	1	844	597
New CWR [this work]	200	20	14	8	8	0.5	787	592

The results with the new design are better than those previously obtained in which temperatures as high as 800 - 850°C were necessary to completely eliminate NH_4^+ from the effluent. In addition, as table 6.2.7 shows, these better results were obtained with lower residence times and injection temperatures

Table 6.2.7: Values obtained for different analysis for samples taken at the outlet of each reactor

Reactor type	TOC removal (%)		N- NH_4^+ removal (%)		N- NO_3 (ppm)		N- NH_4 (ppm)		t_R (s)	
	Max	Min	Max	Min	Max	Min	Max	Min	Max	Min
CWR [29]	99.99	82.00	99.99	71.00	6650	5	1650	4	48	32
New CWR [this work]	99.99	99.98	99.99	99.27	1246	3	30	4	30	20

One of the major differences of this reactor can be observed in figure 6.2.4 where is plotted the minimal temperature required to achieve the maximum N- NH_4^+ removal: In the new reactor high destruction efficiencies were possible even at reactions temperatures as low as 600°C.

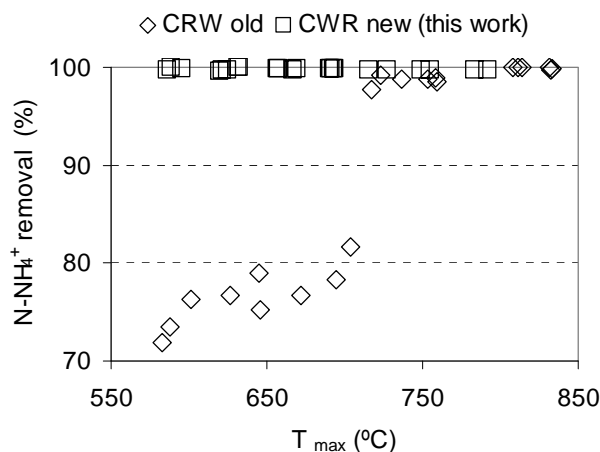


Figure 6.2.4: N- NH_4^+ removal obtained in both reactors with feeds containing 3% of NH_4^+

Using the new reactor NO_x and NH_3 in the gas effluent were below the detection limit in all the studied conditions, while in the CWR it was found NO_x in a range of 5 – 30 ppm at the gas outlet when the reaction temperature reached was over 730°C. This can be explained by the higher temperature together with longer residence times. The better results of the new device can be explained by the use of an empty reactor vessel that better stabilizes the hydrothermal flame as was proved in a previous work of the group [32]

6.2.3.2. Control of nitrate formation

According to the results presented in section 6.2.3.1, the main limitation of the process is the formation of nitrates. It is known that nitrate concentration is increased when working at high temperatures and high oxidant excesses [29, 33, 34]. Several experiments paying attention to these two parameters were performed in order to find the best operational conditions for the ammonia removal and to prove the viability of using SCWO under hydrothermal flame conditions without producing nitrate as a subproduct.

6.2.3.2.1. Influence of Air excess

In first place, the influence of air excess was studied. For doing this, experiments with 0.5%, 1% and 3% of NH_4^+ and different air flow (0.5-15% in excess) were made. Main results are presented in figure 6.2.5 where TOC removal, N-NH_4^+ removal and nitrogen converted to nitrates in the liquid samples taken at the outlet of the reactor are represented as a function of the air excess.

It was observed that air excess is not improving ammonia or TOC destruction. Nevertheless, when the fraction of air excess over the stoichiometric amount is higher, the fraction of N-NH_4^+ converted into nitrates increased. For all the different mixtures of ammonia, when air excess is higher than 5%, the fraction of initial nitrogen converted to nitrates stabilized in maximum values around 3 - 2.5%. with peaks till 4% for the cases with feeds with the highest concentration (3 – 8%)

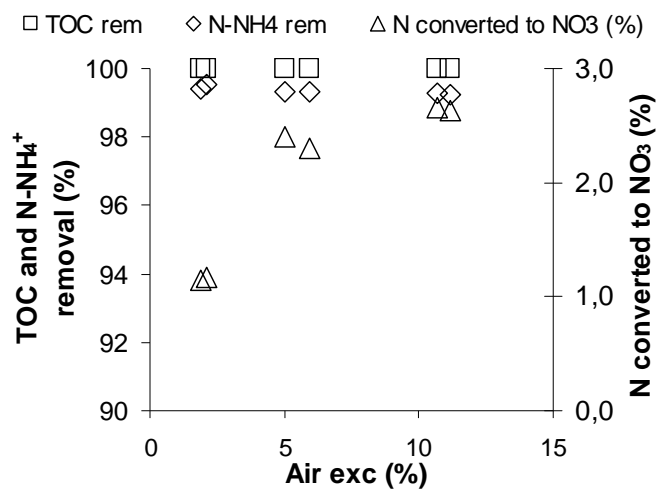


Figure 6.2.5: Influence of air excess in NH_4^+ removal and fraction of nitrogen transformed into nitrates with respect to the initial N-NH_4^+ concentration, experimental conditions 0,5% wt NH_4^+ , $T_{\text{inj}}=200^\circ\text{C}$, $T_{\text{max}}=680^\circ\text{C}$.

6.2.3.2.2. Influence reaction temperature and ammonia concentration

The reactor used in this work is working autothermally what means that the reaction temperature is determined by the heat content and depends on the feed concentration. Thus, for increasing or decreasing the reaction temperature, higher or lower co-fuel (IPA) concentrations are used.

In order to study the influence of the reaction temperature for a given ammonia concentration, several IPA concentrations must be used, keeping constant the rest of variables (injection temperature and air excess). Figure 6.2.6 shows the nitrate concentration in the effluent as a function of the reaction temperature for different initial ammonia concentration. It can be appreciated that at lower reaction temperatures the nitrate concentration in the effluent is also lower working with different feeds of ammonia, however when reaction temperatures are higher more nitrates are formed when the initial ammonia concentration injected is also higher.

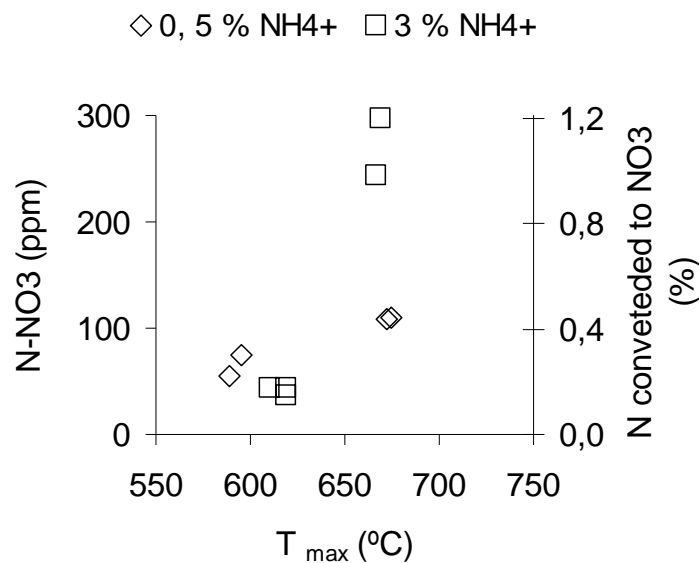


Figure 6.2.6: N-NO₃⁻ concentration in the effluent and fraction of nitrogen transformed into nitrates with respect to the initial N-NH₄⁺ concentration versus maximum reaction temperature., Experimental conditions of 0.5% and 3% wt NH₄⁺, T_{inje}=200°C, Air excess= 7-8%

6.2.3.3.3. Influence of Injection Temperature

For studying the influence of injection temperature, a series of experiments at the same reaction temperature and a similar air in excess were carried out at different injection temperatures in order to study the effect of this variable in the nitrate formation.

Figure 6.2.7 shows that a higher concentration of nitrates in the effluent is obtained with lower injection temperatures when the rest of the variables remain constant. This could be related to the higher proportion of isopropanol with respect to initial ammonia concentration, but with the facility used it is not possible to isolate the influence of the two variables.

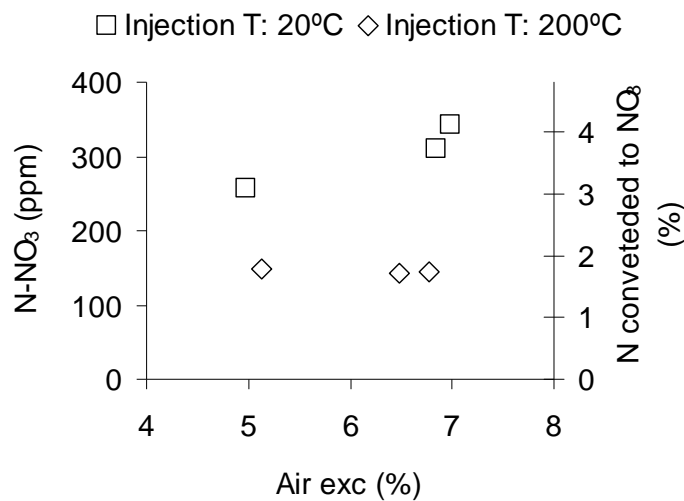


Figure 6.2.7: N-NO₃ concentration and fraction of nitrogen transformed into nitrates with respect to the initial N-NH₄⁺ concentration versus air in excess for different injection temperatures. Experimental conditions 1% wt NH₄⁺, T_{max}=730°C

Summarizing, total ammonia removal is obtained for reaction temperatures over 600°C being the main problem nitrate formation that can be controlled by working with air in excess lower than a 2-3% and reaction temperatures lower than 650°C.

6.2.3.3. Oxidation of synthetic sludge

The viability of injecting solid suspension in the reactor and its complete oxidation on the hydrothermal flame was proved by injecting a synthetic sludge with a homogeneous size distribution.

Despite of the injection of a solid suspension in the reactor, operations was stable without plugging problems or pressure instability.

The analysis of the liquid samples taken at the outlet of the reactor gave values of TOC removal between 99.90% and 99.99% what means values of TOC in the range 49 - 77 ppm. TN and nitrate concentration were also analyzed obtaining values between 80 and 17 ppm for N-NH₄⁺ and 75 to 14 for N-NO₃⁻ as shown in table 6.2.8. All the values obtained were below the disposal limits fixed in the Water Framework Directive [1] (50 ppm of NH₄⁺ and 20 ppm of N-NO₃). Optimal conditions were achieved by reducing the temperature down to 606°C to control nitrates even when the residence times where 10 s longer. A slight temperature increase from 606 to 626°C conducts to an increase of nitrate over the dumping limits, even when N-NH₄⁺ concentration was substantially reduced.

Table 6.2.8: Summary of the operational conditions and main results obtained working using a synthetic sludge as a feed

t_R (s)	Ex air (%)	T_{max} (°C)	TOC removal (%)	N-NH ₄ ⁺ removal (%)	TOC outlet (ppm)	N-NO ₃ ⁻ outlet (ppm)	N-NH ₄ ⁺ outlet (ppm)
25	2	637	99.92	99.57	61	75	35
25	3	641	99.94	99.63	52	54	31
35	3	606	99.90	99.33	77	15	50
35	4	626	99.93	99.79	60	32	17

As observed in figure 6.2.8, the colour of the feed was also eliminated.

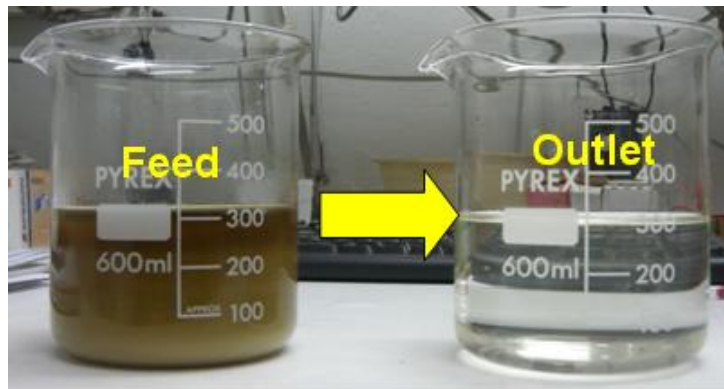


Figure 6.2.8: Samples of the feed and the effluent of the experiments made with synthetic sludge

In addition NO_x and NH₃ concentration in the gaseous effluent were below the detection limits of 0.5 ppm and 5 ppm respectively for all the experimental conditions tested.

6.2.3.4. Oxidation of sludge

In the last step a real sludge from the second stage of the wastewater treatment plant of Valladolid was injected in the reactor. An initial sludge of 6% volatile solids (main properties in experimental section) was diluted down to 1.3% in mass of volatile solids while 11% IPA in mass was added in order to provide the heat reaction necessary to reach temperatures high enough to reach flame regime. The feed flow was maintained at 13,60 kg/h. The characteristic of the feed are shown in Table 6.2.9.

Table 6.2.9: Feed properties for studying the oxidation of a real sludge

C_{IPA0} (%)	C_{Sludge} (%)	TOC (ppm)	TN (ppm)	VS (%)
11	22	73180	100	1.3

Main operational parameters and results of the experiments are summarized in Table 6.2.10. It is observed that successful operation was achieved at relatively low reaction temperatures from 553 to 512°C and residence times between 21 and 25 s. TOC removals higher than 99.82% were reached (TOC concentrations in the effluent between 54 and 78 ppm C). $N-NH_4^+$ concentrations in the effluent were below 36 ppm, while concentrations of $N-NO_3^-$ were between 11-6 ppm. All the results obtained were below the dumping limits, for the case of COD all the samples are lower than 500 ppm (Converting TOC to COD for IPA whose equivalence is 2.4 ppm COD for 1 ppm of TOC)

Table 6.2.10: Summary of the operational conditions and main results obtained working using a synthetic sludge as a feed

t_R (s)	Ex air (%)	T_{max} (°C)	TOC removal (%)	TOC outlet (ppm)	$N-NH_4^+$ outlet (ppm)	$N-NO_3^-$ outlet (ppm)
21	4	512	99.90	54	33	6
23	9	518	99.87	66	35	8
22	6	531	99.82	96	36	11
24	7	522	99.85	76	28	10
24	8	531	99.89	59	29	6
25	11	553	99.85	78	31	6

6.2.3.5. Energy production by SCWO of sludge

The application of SCWO technology to produce electricity was evaluated by theoretical energy balances.

Calculations have been made for a SCWO plant of sludge coming from urban sewage-disposal plant. Sludge calorific power was estimated through an empirical correlation [35] as 18 780 kJ/kg – dry basis. The concentration of the sludge was studied as function of inlet temperature, in order to achieve 600°C at reaction chamber, according to the results obtained experimentally for optimal ammonia removal minimizing nitrate production. The operating pressure is 230 bar.

Mass and energy balances were solved taking thermal and volumetric properties from Peng-Robinson Equation of State with volume translation (vtPR-EoS). It was assumed a mixture of water, oxygen, nitrogen and carbon dioxide. Sludge properties are assumed to be water properties.

Initially, air is used as oxidizing agent for all calculations. For a reference flow of 1 kg/h of solids, the amount of air needed to oxidize the organic material is 6.21 kg/h. Once these values are fixed, and the temperature of reaction is also prescribed, there are two variables of interest: injection temperature (independent variable) and water content i.e. sludge concentration (dependent variable). For lower injection temperatures, sludge must be concentrated in order to release the amount of energy not provided with preheating and reaching the same temperature. Thus, for higher injection temperatures, it must be diluted.

Figure 6.2.9 shows sludge concentration as function of inlet temperature. In order to reach 600°C at reaction chamber, feed must have 20.6% solids at an injection temperature of 25°C. If inlet temperature increases, concentration decreases down to 3.7% at 425°C. That means water content rises. Lower injection temperatures avoid corrosion and salt deposition issues. When the feed temperature increases, some source of heating should be used. This source could be an external heating, such as for example a natural gas boiler, or part of the heat contained in the products stream through energetic integration.

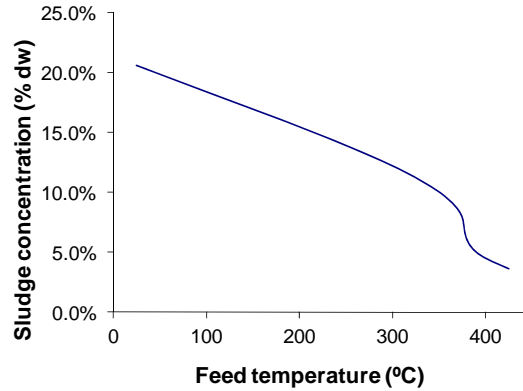


Figure 6.2.9: Sludge concentration, as mass fraction of dry material, in function of inlet temperature. Oxidation with air.

The conventional way for electric generation is using the products stream as heat source for a Rankine cycle. The products stream could generate steam at 400 °C and 46 bar, the usual conditions on medium size industrial process [36]. This process has been studied for different feed injection temperatures, using external preheating source. It was found that feed should be preheated over 325°C in order to achieve an electrical production equivalent to the plant consumption. Below this injection temperature, energetic consumption of compressor and pumps is greater than the power production at turbine. At injection temperature of 425°C the net efficiency of the process would be 10.5%. Nevertheless, at this condition, the heating source used for preheating feed could be used more efficiently for direct generation of steam.

Another option for the production of electricity by SCWO of sludge is by direct expansion of products stream through a turbine. The efficiency of this process was calculated using Peng-Robinson Equation of State with Boston-Mathias alpha function and considering an isentropic turbine.

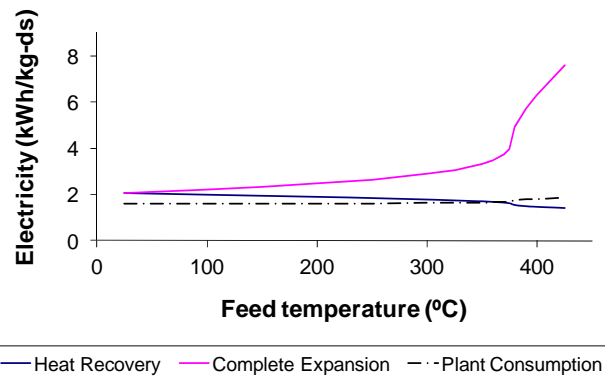


Figure 6.2.10: Electric energy produced and consumed by oxidation of 1 kg of dry sludge. Oxidation with air.

Figure 6.2.10 shows electric production, kWh per kilogram of dry sludge, for complete expansion of products stream (pink) and for its partial expansion (blue), where a fraction of the stream is used in preheating feed. Both alternatives supply the electric plant consumption if injection temperature is below 370°C. Above this point, the stream of products has not enough energy for preheating the feed and for generating the electricity demanded by the plant. The plant consumption was estimated by pumps and compressors power.

Complete expansion of the products produces more electricity but implies using some external heat for feed conditioning, which could increase the operational costs of the plant. The energetic efficiency of the process is the net electricity (i.e. kWh produced minus kWh consumed) divided by the heat released in the oxidation (plus the external heat in case of complete expansion). Efficiency of both alternatives is shown in figure 6.2.11.

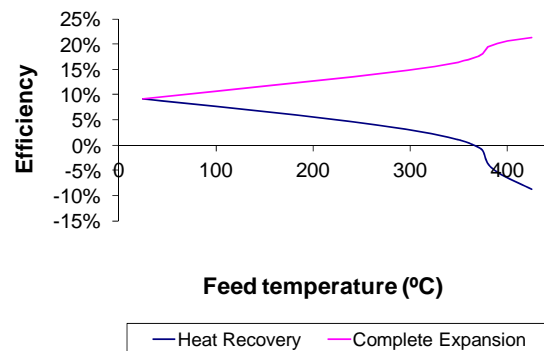


Figure 6.2.11- Efficiency of electric generation. Oxidation with air.

Currently, most large SCWO plants use oxygen as the oxidant [14, 19, 20]. The energetic efficiency of the process would be improved using pure oxygen instead of air. The high electrical consumption of air compressor could be replaced by low consumption cryogenic pumps. Also, the absence of nitrogen reduces the heat capacity of the system, and sludge can be diluted. Furthermore, pure oxygen does not need to be preheated up to feed injection temperature [9].

Using oxygen, in order to reach 600°C at reaction chamber, feed should have 17.4% solids at 25°C, and 3.5% at 425°C, as shown in figure 6.2.12.

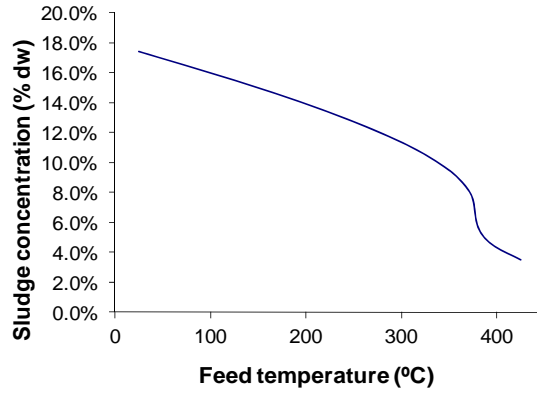


Figure 6.2.12: Sludge concentration, as mass fraction of dry material, in function of inlet temperature. Oxidation with pure oxygen.

Figure 6.2.13 shows electric production, kWh per kilogram of dry sludge, for complete expansion of products stream (pink) and for its partial expansion (blue), when using oxygen as the oxidant. Both alternatives supply the electric plant consumption with large excess.

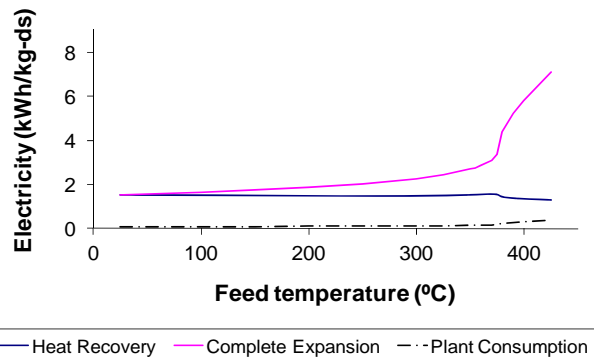


Figure 6.2.13: Electric energy produced and consumed by oxidation of 1 kg of dry sludge. Oxidation with pure oxygen.

Figure 6.2.14 shows that the use of pure oxygen increases the process efficiency, when compared with air (figure 6.2.11). In this case, efficiency remains practically constant if inlet temperature is below the critical temperature.

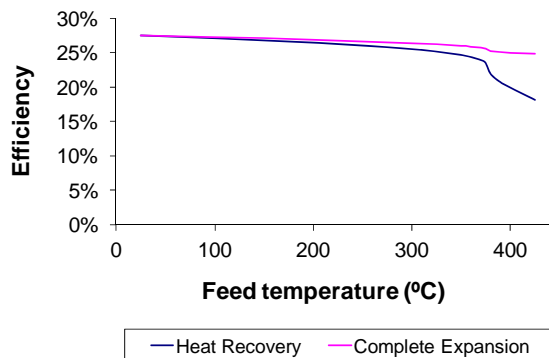


Figure 6.2.14: Efficiency of electric generation. Oxidation with pure oxygen.

However, the cost and energy consumption of producing pure oxygen could affect the viability of the process. Depending on the plant capacity, oxygen can be supplied by a provider or produced in situ. If oxygen is produced in situ by air distillation, the net electricity produced will be positive if the consumption at distillation process is lower than 0.99 kWh/kg-O₂. Simulation made by Kansha et al.[37] for a conventional cryogenic plant producing 31 000 Nm³/h of pure oxygen, gives an energetic consumption of 0.40 kWh/kg-O₂.

This analysis reveals that production of electricity from SCWO plant of sludge is only possible at high yields by directly expanding the products of the oxidation, and in this case it is more efficient when an external heating source is used for preheating. And this efficiency depends greatly on the injection temperature. Thus, oxidizing sludge in the conditions experimentally fixed in this work can lead to efficiencies in electricity production between 10 and 25% when the products are directly expanded in a turbine, if the feed is not preheated with the reaction effluent. The efficiency can be as high as 27% using oxygen as an oxidant, even when preheating the feed with the effluent, but in this case the economic or the energetic const of the oxidant must be considered.

6.2.4. CONCLUSIONS

In this work the viability of using the supercritical water oxidation process for the destruction of wastewater treatment plant sludge in the presence of a hydrothermal flame was studied using a new reactor design.

In first place, the oxidation of ammonia in presence of a hydrothermal flame using the new reactor was studied. Total ammonia oxidation was observed at temperatures higher than 600°C at residence times of 20-30 s. Below a certain temperature, that is function on ammonia concentration, the flame was not produced. This temperature varies from 600 to 700°C and it is increasing when the initial ammonia concentration is higher. Emissions of NH_3 and NO_x in the gas effluent were below the detection limits of 5 and 0.5 ppm respectively in all the experiments performed.

It was observed that in some operation conditions the effluent presented high nitrate concentration. Further experiments conducted to know that the fraction of ammonia converted to nitrate increased with oxidant excess, and reaction temperature and decreased with higher injection temperature and initial N-NH_4^+ concentration.

By controlling these parameters, keeping reaction temperature below 650°C and air excess below 2.5% effluent of the process accomplishing European Legislation were obtained in a single reaction step

Destruction of a synthetic and a real sludge were achieved obtaining TOC removals higher than 99.95% ($\text{TOC} < 80$ ppm), concentrations in the effluent of N-NH_4^+ and N-NO_3^- lower than 20 ppm without problems of plugging and no formation of NO_x^-

The production of energy by SCWO of sludge was theoretically studied. The energy produced by using the effluent as the heating source of a Rankine cycle it is lower than the energy consumed by the SCWO plant unless the feed is preheated at temperatures higher than 325°C with an external heat source. Direct expansion of the effluent can conduct to energy efficiencies as high as 25% (27% if oxygen is used as the oxidant). The efficiency of electricity production strongly depends on the injection temperature of the reagent and of the use fuel as external heating source.

LIST OF SYMBOLS

C_{IPA0}	Initial concentration of isopropyl alcohol	% wt
C_{IPA}	Concentration of isopropyl alcohol	% wt
$C_{NH_4^+0}$	Initial concentration of ammonia	% wt
$C_{NH_4^+}$	Concentration of ammonia	% wt
C_{sludge}	Initial concentration of sludges	% wt
P	Pressure	MPa
T	Temperature	°C
t_R	Residence time	s
TOC	Total Organic Carbon	ppm
TN	Total Nitrogen	ppm
COD	Chemical Oxygen demand	ppm
T_{max}	Maximum temperature in the reactor	°C
T_{inj}	Injection temperature in the reactor	°C
SV	Content of volatile solids of sludges	%

6.2.5. REFERENCES

- [1] European Commission, Water Framework Directive 2000/60/EC, in, 2000.
- [2] European Commission, Sewage Sludge Directive 86/278/EEC, in, 1986.
- [3] European Commission, Urban Waste-water Treatment Directive 91/271/EEC in, 1991.
- [4] Targeted National Sewage Sludge Survey Statistical Analysis Report U.S. , in, Environmental Protection Agency - Office of Water, 2009.
- [5] J. Honga, J. Hongb, M. Otakic, O. Jollieta, Environmental and economic life cycle assessment for sewage sludge treatment processes in Japan, *Waste Management*, 29 (2009) 696-703.
- [6] European Commission, Nitrate Directive 91/676/EEC in, 1991.
- [7] E. Cadena, J. Colón, A. Artola, A. Sánchez, X. Font, Environmental impact of two aerobic composting technologies using life cycle assessment., *International Journal of Life Cycle Assess*, 14 (2009) 401–410.
- [8] S.J. Pravinkumar, A cluster of legionnaires' disease caused by legionella longbeachae linked to potting compost in scotland, 2008-2009, *Eurosurveillance*, 15 (2010) 8.
- [9] X.F. Lou, J. Nair, The impact of landfilling and composting on greenhouse gas emissions – A review, *Bioresource Technology*, 100 (2009) 3792–3798.
- [10] Y.-J. Suh, P. Rousseaux, An LCA of alternative wastewater sludge treatment scenarios, *Resources, Conservation and Recycling*, 35 (2002) 191-200.
- [11] J. Chung, M. Lee, J. Ahn, W. Bae, Y.W. Lee, H. Shim, Effects of operational conditions on sludge degradation and organic acids formation in low-critical wet air oxidation, *Journal of Hazardous Materials*, 162 (2009) 10-16.
- [12] D. Fytili, A. Zabaniotou, Utilization of sewage sludge in EU application of old and new methods-A review, *Renewable and Sustainable Energy Reviews*, 12 (2008) 116-140.
- [13] B. Veriansyah, J.D. Kim, Y.W. Lee, Simultaneous recovery of chromium and destruction of organics from LCD manufacturing process wastewater by supercritical water oxidation, *Journal of Cleaner Production*, 15 (2007) 972-978.
- [14] J.W. Griffith, D.H. Raymond, The first commercial supercritical water oxidation sludge processing plant, *Waste Management*, 22 (2002) 453-459.

- [15] P.A. Marrone, G.T. Hong, Supercritical Water oxidation, in: M. Kutz (Ed.) Environmentally Conscious Materials and Chemicals Processing, John Wiley & Sons Inc, Hoboken (NJ), 2007, pp. 385-443
- [16] http://www.cityoforlando.net/cityclerk/citycouncil/workshop_files/presentations/2011-04-25_oxidation.pdf (last accessed 31th May 2012)
- [17] M. Modell, E. Kuharich, M.S. Rooney, Supercritical water oxidations process and apparatus of organics with inorganics, WO/1993/000304
- [18] <http://www.superwatersolutions.com/> (last accessed 31th May 2012)
- [19] D.S. Sloan, M. Modell, R.A. Pelletie, Sludge Management in the City of Orlando- It's Supercritical!, Florida water resources journal, 60 (2008) 46-54.
- [20] D. Xu, S. Wang, X. Tang, Y. Gong, Y. Guo, Y. Wang, J. Zhang, Design of the first pilot scale plant of China for supercritical water oxidation of sewage sludge, Chemical Engineering Research and Design, 90 (2012) 288–297.
- [21] R.M. Serikawa, T. Usui, T. Nishimura, H. Sato, S. Hamada, H. Sekino, Hydrothermal flames in supercritical water oxidation: investigation in a pilot scale continuous reactor, Fuel, 81 (2002) 1147-1159.
- [22] P. Cabeza, M.D. Bermejo, C. Jimenez, M.J. Cocero, Experimental study of the supercritical water oxidation of recalcitrant compounds under hydrothermal flames using tubular reactors, Water Research, 45 (2011) 2485-2495.
- [23] E.D. Lavric, H. Weyten, J. De Ruyck, V. Pleşu, V. Lavric, Supercritical water oxidation improvements through chemical reactors energy integration, Applied Thermal Engineering, 26 (2006) 1385-1392.
- [24] M.D. Bermejo, M.J. Cocero, F. Fernandez-Polanco, A process for generating power from the oxidation of coal in supercritical water, Fuel, 83 (2004) 195-204.
- [25] B. Wellig, M. Weber, K. Lieball, K. Prikopsky, P.R. von Rohr, Hydrothermal methanol diffusion flame as internal heat source in a SCWO reactor, Journal of Supercritical Fluids, 49 (2009) 59-70.
- [26] C. Augustine, J.W. Tester, Hydrothermal flames: From phenomenological experimental demonstrations to quantitative understanding, Journal of Supercritical Fluids, 47 (2009) 415-430.
- [27] B. Al-Duri, L. Pinto, N.H. Ashraf-Ball, R.C.D. Santos, Thermal abatement of nitrogen-containing hydrocarbons by non-catalytic supercritical water oxidation (SCWO), Journal of Materials Science, 43 (2008) 1421-1428.

- [28] P.A. Webley, J.W. Tester, H.R. Holgate, Oxidation kinetics of ammonia and ammonia-methanol mixtures in Supercritical Water in the Temperature range 530-700°C at 246 bar, *Chemical Engineering Research and Design*, 30 (1991) 1745-1754.
- [29] M.D. Bermejo, F. Cantero, M.J. Cocero, Supercritical water oxidation of feeds with high ammonia concentrations Pilot plant experimental results and modeling, *Chemical Engineering Journal*, 137 (2008) 542-549.
- [30] M.D. Bermejo, C. Jiménez, P. Cabeza, A. Matías-Gago, M.J. Cocero, Experimental study of hydrothermal flames formation using a tubular injector in a refrigerated reaction chamber. Influence of the operational and geometrical parameters, *Journal of Supercritical Fluids*, 59 (2011) 140-148.
- [31] F. Vogel, J.L.D. Blanchard, P.A. Marrone, S.F. Rice, P.A. Webley, W.A. Peters, K.A. Smith, J.W. Tester, Critical review of kinetic data for the oxidation of methanol in supercritical water, *Journal of Supercritical Fluids*, 34 (2005) 249-286.
- [32] M.D. Bermejo, P. Cabeza, M. Bahr, R. Fernández, V. Ríos, C. Jiménez, M.J. Cocero, Experimental study of hydrothermal flames initiation using different static mixer configurations, *Journal of Supercritical Fluids*, 50 (2009) 240-249.
- [33] M.J. Cocero, E. Alonso, R. Torio, D. Vallelado, F. Fdz-Polanco, Supercritical water oxidation in a pilot plant of nitrogenous compounds: 2-propanol mixtures in the temperature range 500-750 degrees C, *Industrial & Engineering Chemistry Research*, 39 (2000) 3707-3716.
- [34] N. Segond, Y. Matsumura, K. Yamamoto, Determination of ammonia oxidation rate in sub- and supercritical water, *Industrial & Engineering Chemistry Research*, 41 (2002) 6020-6027.
- [35] S.A. Channiwala, P.P. Parikh, A unified correlation for estimating HHV of solid, liquid and gaseous fuels, *Fuel*, 81 (2002) 1051-1063.
- [36] R.H. Perry, D.W. Green, *Perry's Chemical Engineers' Handbook* . (7th Edition). , 1997.
- [37] Y. Kansha, A. Kishimoto, T. Nakagawa, A. Tsutsumi, A novel cryogenic air separation process based on self-heat recuperation, *Separation and Purification Technology*, 77 (2011) 389-396.

6.3. ANALYSIS OF THE BEHAVIOR OF A SCWO COOLED WALL REACTOR WORKING WITH TWO OUTLETS. EXPERIMENTAL RESULTS AND ENERGETIC STUDY

ABSTRACT

This work presents experimental results obtained with a new configuration of a cooled wall reactor working with two outlets: an upper outlet through which a hot effluent (500 – 600°C) free of salts is obtained and lower outlet through which an effluent at subcritical temperature dissolving the precipitated salts is obtained. Different flow distributions were tested in order to find the optimal conditions. TOC removal over 99,99% were obtained at injection temperatures as low as room temperature, when the fraction of products leaving the reactor in the upper effluent is lower than 70% of the feed flow

The performance of the reactor was tested with the oxidation of a recalcitrant compound such as ammonia, using IPA as co-fuel. Removals higher than 99% of N-NH₄⁺ were achieved in both effluents, working with temperatures near 700°C. Slightly better eliminations were obtained in the bottom effluent because it remains for a longer residence time inside the reactor

The behaviour of the reactor working with feeds with a high concentration of salts was also tested. Feeds containing up to 2.5% wt Na₂SO₄ could be injected in the reactor without plugging problems and a TOC removal of 99.7% was achieved in these conditions. Upper effluent always presented a concentration of salt lower than 20 ppm

Finally, a theoretical analysis of the energy recovery of the reactor working with two outlets was made. It was found that direct expansion of the upper effluent would allow to produce enough energy for covering the energy requirements of the pumping equipments.

6.3.1. INTRODUCTION

Since Franck et al [1] discovered the hydrothermal flame and it could be applied to the Supercritical Water Oxidation (SCWO), new challenges came up to the study of SCWO. For flammable compounds such as methane or methanol, hydrothermal flame can occur at temperatures as low as 400°C [2]. SCWO in the presence of hydrothermal flames can reduce residence times to the order of milliseconds [3] without the production of sub-products typical of conventional combustion such as NO_x [4] or dioxins [5].

SCWO with a hydrothermal flame has a number of advantages over the flameless process. Some of these advantages permit overcoming the traditional challenges that make the successful and profitable commercialization of SCWO technology difficult. The advantages include the following [3]:

- The reduced residence times (in the order of milliseconds) allows the construction of smaller reactors.
- It is possible to carry out the reaction with feed injection temperatures near to room temperature when using vessel reactors [6, 7]. This avoids problems such as plugging and corrosion in a preheating system, having an advantage from the operational and energy integration perspective.
- Higher operation temperatures improve the energy recovery

The first reactor probably working with a hydrothermal flame inside was the MODAR reactor, working in conditions of concentration, temperature and pressure above the ignition conditions of methanol and being able to work with injection temperatures of 25°C and injecting the air at 220°C [7]. In the ETH of Zurich, the direct injection of the waste into a diffusion hydrothermal flame generated inside the reactor was developed as a solution to avoid the external preheating of the waste up to supercritical conditions [8, 9]. Příkopský and coworkers [10] investigated the feasibility of injecting feeds with a 3%wt of sodium sulfate (Na₂SO₄) in the transpiring wall reactor with a diffusion hydrothermal flame as internal heat source. No plugging was observed during the experiments, but salt deposits were detected in the upper hot zone of the reactor. In a previous investigation of our research group [6], it was found that using a transpiring wall reactor, a premixed hydrothermal flame inside the reaction chamber could be maintained when injecting the feed at a temperature as low as 110°C. Using a similar

reactor, feeds with up to 4.74% wt Na_2SO_4 could be injected [11]. The reactor worked without plugging, but the recovery of salts was only between 5% and 50%. Both research groups reported an increase in the temperature when salt was injected in the reactor [10, 11].

It has been proved that injection of cold feeds over a hydrothermal flame is only possible when working with vessel reactors [9-11] and it is not possible when working with tubular reactors [12]. This behavior was due to the low flame front velocities in hydrothermal flames that is lower than 0.1 m/s, in comparison to the higher flame front velocities at atmospheric conditions (0.4- 3 m/s). This is the reason why flow velocities lower than 0.1 m/s are necessary to keep a stable hydrothermal flame where cold reagents can be injected [13]. Recently our group has succeeded in keeping working continuously a vessel reactor injecting feeds at temperatures as low as 25°C [14].

Even though the most immediate application of hydrothermal flames is in the Supercritical Water Oxidation (SCWO) process for waste destruction, which is the most industrially developed hydrothermal process., it is possible to move from the idea of hydrothermal flame as a technology for the destruction of wastes to considering the hydrothermal flame as a technology for the generation of clean energy, which could eventually substitute the actual technologies based on atmospheric combustion. The efficiency in energy production from coal by SCWO of coal and direct expansion of the effluent was compared to the efficiencies of other conventional power plants [15]. If the steam was produced at 650°C and 30 MPa, efficiencies as high as 38% were obtained by SCWO. Efficiency was as high as 41% if the effluent was reheated and expanded a second time. The efficiencies at the same steam conditions for pulverized coal power plant and pressurized fluidized bed power plant were 32 and 34% respectively. Comparison is more favourable using oxygen enriched or even using pure oxygen as the oxidant. In this last option the cost of the oxidant must be assumed. Nevertheless it is known that the used of oxygen as an oxidant is investigated to improve the efficiency of combustion in power plants.

In his proposal for a sustainable society with a decentralized production based on renewable resources, Arai [16] proposed the supercritical oxidation of biomass wastes and other sustainable fuels with a hydrothermal flame as a clean energy source. Augustine and Tester [3] also propose its utilization with low grade fuels. In general,

this technology can be applied to the valorization of waste such as wastewater treatment plant sludge, biomass or plastic wastes and in general any kind of waste with high energetic content.

To form these flames it is necessary to use aqueous mixtures with a heat content of at least 1250 kJ/L. One important challenge about working with hydrothermal flames is the chance improving energy recovery in SCWO system [15]. Hydrothermal flames allow new reactor designs that not only are able to inject feeds without preheating because of the possibility of injecting reactants at room temperature but also use the heat released by the flame for other purposes as the energetic integration of the process [17] or for production of electricity by turbines. In the case of waste with high concentration of inorganic substances, new reactor designs able to separate these salts from the effluent must be developed in order to make it possible to directly expand the effluent in an electricity production turbine.

The main goal of this work is the study of the behaviour of new cooled wall reactor with the main particularity of having two outlets in order to try to keep the maximum heat released by the flame in a clean and high temperature flow leaving the reactor from the upper zone and other flow at subcritical conditions with the salts dissolved going out for the bottom of the reactor.

In this way the optimum upper/lower effluent relation was optimized taking into account the temperature profiles inside the reactor and the organic matter elimination in both streams. The performance of the reactor with recalcitrant pollutants such as ammonia was tested as well as the performance of the reactor with feeds containing salts. Finally, a theoretical energetic study of the process with the new reactor was performed.

6.3.2. EXPERIMENTAL

6.3.2.1. Experimental setup

All the experiments analyzed in this research have been carried out in the SCWO facility installed in the University of Valladolid. It consists of a continuous facility working with a feed flow of 22,5 L/h, and air supplied by a four stage compressor, with a maximum feed rate of 36 kg/h is used as the oxidant. The reactor consists of a pressure vessel made of AISI 316 stainless steel able to stand a maximum pressure of 30 MPa and a maximum wall temperature of 400°C, containing a reaction chamber made of Ni-alloy 625 where the temperature can be as high as 700°C.

Wastewater feed and air are previously pressurized and preheated up with electrical resistances to the desired temperature before being injected by the bottom of the reactor. The reagents are conducted to the top of the reactor chamber by means of a tubular injector. At the outlet of the injector the hydrothermal flame is formed. Cooling water, previously pressurized is circulating between the pressure vessel and the reaction chamber introduced by the top of the reactor in order to cool down the vessel at a temperature lower than 400°C. This cooling water is entering in the reaction chamber through its lower part and leaving the reactor by the bottom together with a fraction of the products. The rest of the products leave the reactor by another outlet situated in the top of the reactor chamber. After leaving the reactor, both effluents are cooled down in the intercoolers and depressurized. The flow diagram of the facility with two outlets is shown in figure 6.3.1. More information about the facility can be found elsewhere [6, 12].

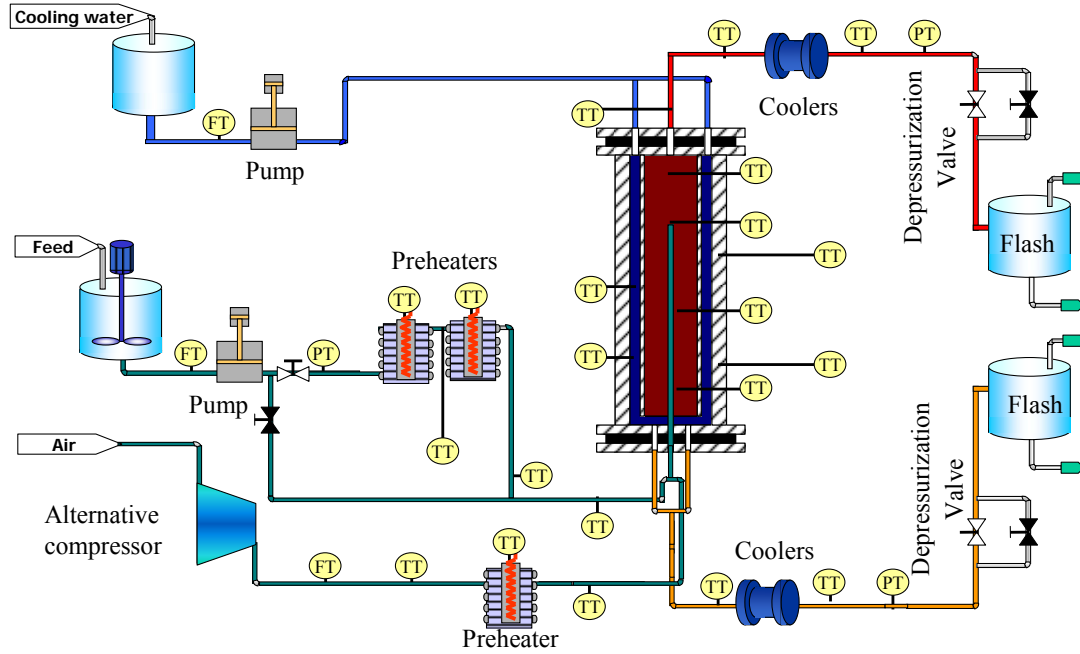


Figure 6.3.1: Diagram of SCWO facility with two outlets.

Figure 6.3.2 shows a scheme of the reactor with the different position of thermocouples inside the reaction chamber. The different temperature profiles are referred at the position of these four thermocouples. Each effluent (top and bottom flow) is measured with a rotameter in order to know the distribution of the feed flow respect the two outlets.

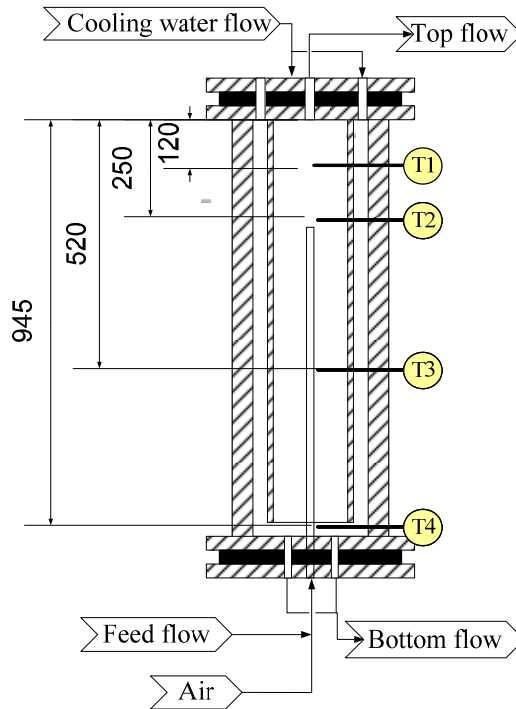


Figure 6.3.2: Scheme of the reactor with the positions of the temperature measurement inside the reaction chamber and the flow distribution

6.3.2.2. Experimental procedure

Previous to the beginning of the experiment the reactor must be preheated electrically to 400°C. The reaction is initiated by injected air and wastewater streams preheated electrically up to a temperature higher than 400°C. A few minutes after continuous injecting of IPA solution and air stream the hydrothermal flame is ignited. At that moment a sharp increase the temperatures at the top of the reactor (T1 and T2) is registered.

Then, the electrical heating of the wall of the reactor is turned off and the cooling water flow is connected. For keeping the maximum temperature constant in values around 600 - 700°C till the desired injection temperature is reached, IPA concentration was increased as the injection temperature was decreased down to the selected injection temperature.

After the target injection temperature is reached (From 300°C till room temperature, around 20 - 30°C), the upper flow and bottom flow are regulated opening or closing the decompression valves keeping the air and the pressure constant. Pressure must be stabilized around 23MPa. Several stationary states with different prepared feeds and different flow up/bottom ratio are reached and samples of the liquid effluent are taken.

Total Organic Carbon (TOC) and Total Nitrogen (TN) analysis of the samples were performed with a TOC 5050 SHIMADZU Total Organic Carbon Analyzer which uses combustion and IR analysis. The detection limit is 1 ppm.

Salt concentration is measured using a conductivimeter Basic 30 provided by Crison. For doing this, conductivities of solutions of known Na₂SO₄ concentration is measured obtaining a linear calibration line between conductivity and Na₂SO₄ concentration. The calibration line and the values obtained are shown in Appendix I.

Nitrates and nitrites were characterized in the liquid effluent by ionic chromatography with an IC PAK A column of Waters. The detection limit is 1 ppm.

N-NH₄⁺ concentration in the effluent is obtained from the difference of TN and the concentration nitric Nitrogen (N-NO₃ and N-NO₂).

NH₃ and NO_x in the gas effluent were analysed with Dräger tubes detectors Lab Safety Supply CH29401 and CH31001. The NO_x detection limits for these tubes ranged from 0.5 to 100 ppm and the NH₃ detection limits for these tubes ranged from 5 to 70 ppm (standard deviation for both tubes are between 10 and 15%).

6.3.2.3. Materials

The experiments analysed in this research were performed using feeds prepared with isopropyl alcohol (IPA, 99% purity) supplied by COFARCAS (Spain) and tap water without further purification,

For experiments made with ammonia it was used ammonia (25% in mass) supplied by COFARCAS (Spain).

Synthetic waste containing salts were prepared using Na_2SO_4 supplied by COFARCAS (purity > 98%) (Spain).

For the studies with feeds containing salts, distillate water was used to prepare the feed in order to analyze exclusively the model inorganic salts injected with the feed and avoid possible confusions with salt present in tap water.

6.3.2.4. Parameter calculations

In order to clarify some term used along the work, the next equations show how some new parameters not used in previous works have been calculated:

The fraction of Feed flow leaving the reactor by the top outlet is defined as the upper effluent fraction, as defined in eq.1

$$\text{Upper effluent fraction (\%)} = \frac{F_{\text{TOP}} \left(\frac{\text{kg}}{\text{h}} \right)}{F_{\text{FEED}} \left(\frac{\text{kg}}{\text{h}} \right)} \cdot 100 \quad (1)$$

Where F_{TOP} and F_{FEED} are the mass flow of top effluent and flow in kg/ respectively.

Due to cooling water is mixed with the feed flow that come out the reactor at the bottom outlet, the TOC of samples taken at the bottom flow have to be corrected in order to know the real concentration of TOC and TN at the bottom effluent. The concentration of top effluent do not have to be corrected because this flow is not mixed with the cooling water flow:

$$TOC_{\text{bottom}} = \frac{TOC_{\text{bottom measured}} \cdot x(F_{\text{FEED}} + F_{\text{COOLINGWATER}} - F_{\text{TOP}})}{(F_{\text{FEED}} - F_{\text{TOP}})} \quad (2)$$

$$TN_{\text{bottom}} = \frac{TOC_{\text{bottom measured}} \cdot x(F_{\text{FEED}} + F_{\text{COOLINGWATER}} - F_{\text{TOP}})}{(F_{\text{FEED}} - F_{\text{TOP}})} \quad (3)$$

Once the TOC and TN is corrected it can be calculated the removal for each effluent:

$$\text{TOCremoval top} = \left(1 - \frac{\text{TOC}_{\text{top}}}{\text{TOC}_0}\right) \times 100 \quad (4)$$

$$\text{TOCremoval bottom} = \left(1 - \frac{\text{TOC}_{\text{bottom}}}{\text{TOC}_0}\right) \times 100 \quad (5)$$

$$\text{N - NH}_4^+\text{removal top} = \left(1 - \frac{\text{N - NH}_4^{\text{TOP}}}{\text{N - NH}_4^{\text{FEED}}}\right) \times 100 \quad (6)$$

$$\text{N - NH}_4^+\text{removal bottom} = \left(1 - \frac{\text{N - NH}_4^{\text{bottom}}}{\text{N - NH}_4^{\text{FEED}}}\right) \times 100 \quad (7)$$

The fraction of Na_2SO_4 recovered in the top and bottom effluent are defined in eq. 8 and 9.

$$\text{Salt recovery top flow} = \frac{C_{\text{Na}_2\text{SO}_4, \text{TOP}} \cdot F_{\text{TOP}} \left(\frac{\text{kg}}{\text{h}}\right)}{C_{\text{Na}_2\text{SO}_4\text{FEED}} \cdot F_{\text{FEED}} \left(\frac{\text{kg}}{\text{h}}\right)} \cdot 100 \quad (8)$$

$$\text{Salt recovery bottom flow} = \frac{C_{\text{Na}_2\text{SO}_4, \text{BOTTOM}} \times F_{\text{BOTTOM}} \left(\frac{\text{kg}}{\text{h}}\right)}{C_{\text{Na}_2\text{SO}_4, \text{FEED}} \times F_{\text{FEED}} \left(\frac{\text{kg}}{\text{h}}\right)} \cdot 100 \quad (9)$$

Where $C_{\text{Na}_2\text{SO}_4, \text{TOP}}$, $C_{\text{Na}_2\text{SO}_4, \text{BOTTOM}}$ and $C_{\text{Na}_2\text{SO}_4, \text{FEED}}$ are the concentration of Na_2SO_4 in% wt in the top and bottom effluents and in the Feed respectively.

6.3.3. RESULTS AND DISCUSSION

6.3.3.1. Influence of the upper effluent fraction.

The flow distribution between the two outlets and how the flame is affected in terms of temperature was first studied. Attention was also paid to the IPA elimination in both effluents.

Temperature profiles inside the reactor

With the new configuration of the reactor, the first point was the study of the influence of upper flow fraction (equation 1) in order to check how the new outlet affects to the behaviour of the hydrothermal flame

Experiments were made at different injection temperatures of 200°C and at room temperature.

In order to analyse the results, the experimental temperature profiles registered along the reactor for the different flow distributions were compared in figure 6.3.3 a and b.

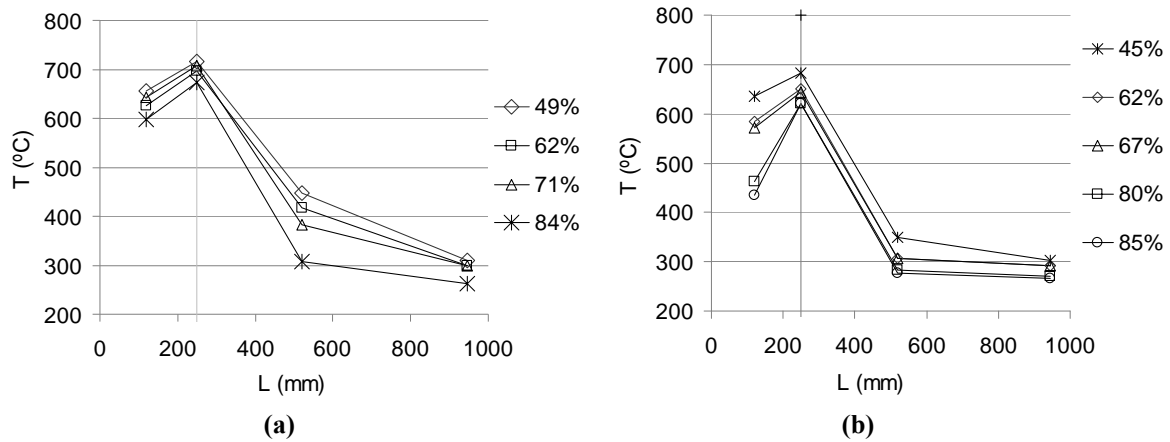


Figure 6.3.3 a: Temperature profiles for different upper effluent fraction at 20°C (a) and at 200°C (b). The vertical line indicates the position of the injector outlet

In both figures it can be observed that when the upper flow is increased, all the temperatures inside the reactor decrease. This is because the top outlet is closer to the injector outlet and when a higher fraction is leaving the reactor by the top a low amount of products is flowing down the reactor. Thus, the heat content of this flow fraction is not transmitted to the reaction chamber and to the reagents entering through the injector.

TOC Removal

In the figures 6.3.4 a & b the TOC concentration in both effluents was plotted as a function of the upper flow fraction. In figure 6.3.4 a the feed inlet temperature is 20°C (room T) and in figure 6.3.4 b the feed inlet temperature is 200°C.

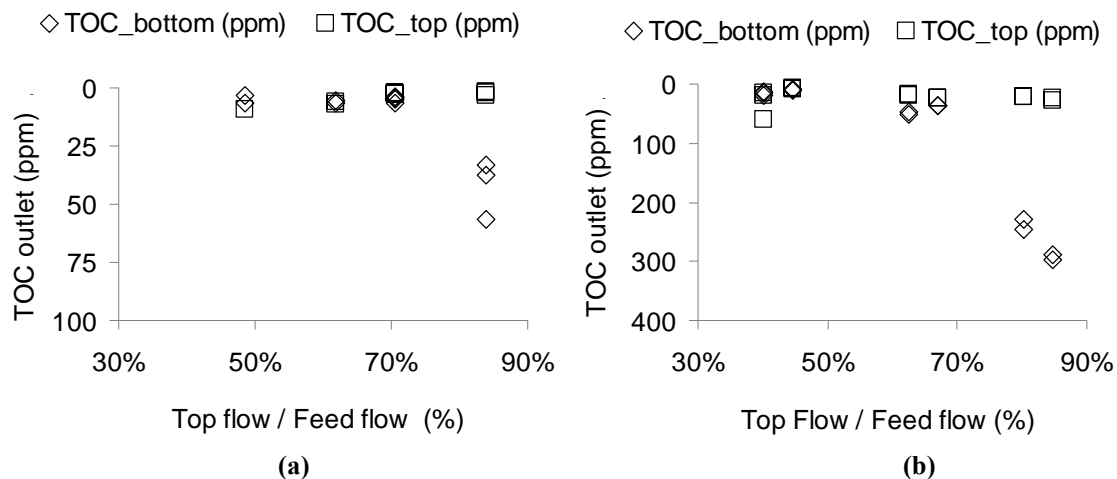


Figure 6.3.4 (a): Values of TOC in the top and bottom effluent as a function of the upper effluent fraction at injection temperature of 20°C and 13, 5% of IPA **(b)** at an injection temperature of 200°C and 10, 5% of IPA at different upper flow fractions.

In both experiments TOC removals higher than 99,99% were obtained in both effluent when the fraction of effluent leaving the reactor by its upper part is lower than 70%. Thus, the optimum upper effluent fraction is around this value. This behaviour could be explained because the increasing the upper flow fraction can elongate the flame and making that some bottom products do not react completely because they do not without pass through the flame.

6.3.3.2. Influence of the IPA concentration.

Temperature profiles inside the reactor

In order to analyse the influence of the IPA concentration in the temperatures profile along the reactor, Experiments at injection temperature of 20°C and at 85% upper effluent fraction condition were carried out in order to try to improve the removal of TOC at the bottom flow for the highest upper flow fractions. As it can be observed in the figure 6.3.5, higher IPA concentration generates higher temperatures in the top of the reactor. Meanwhile at the bottom of the reactor the temperatures are similar for both IPA concentrations when the upper effluent fraction remains constant. The values of TOC in both cases were lower than 10 ppm at the top flow and lower than 100 ppm at the bottom flow but no improves in the TOC bottom removal were observed.

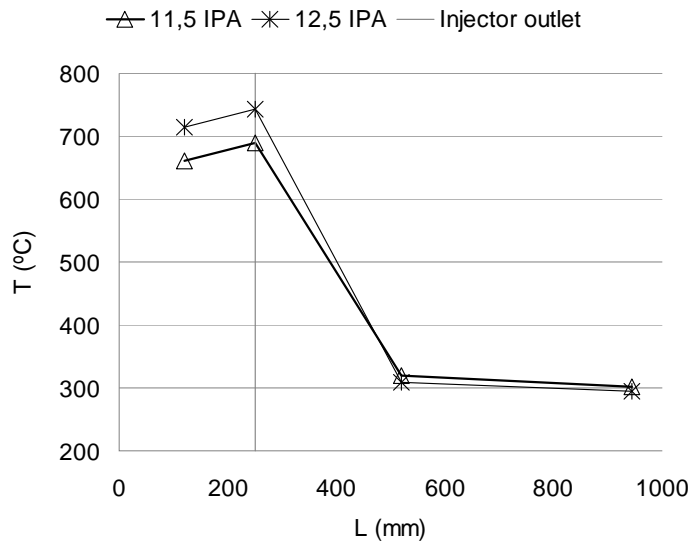


Figure 6.3.5: Temperature profile for different feed concentrations and with a relation of 85% of upper effluent fraction and an injection temperature of 20°C.

6.3.3. Influence of the cooling water

Temperature profiles inside the reactor

A study was performed trying to know the influence of the cooling water flow in the temperatures profiles along the reactor. The injection temperature of the experiment was 200°C and the ratio top flow / total flow was fixed at 48%. Three cooling water flows were studied: 5.2, 6.8 and 9.1 kg/h. (keeping the feed flow at 13,5 kg/h)

The evolution of the temperature profiles along the reactor is shown in the figure 6.3.6 a. The figure shows that temperatures along the whole reactor decrease when the cooling flow increases with a consequence reduction of the TOC removal in the bottom effluent as can be appreciated in figure 6.3.6 b where the values of TOC concentration are plotted as a function of the cooling flow. It is observed that from feed flows higher than 9,1 kg/h. TOC concentration increases as much as 500 ppm in the bottom effluent. With these results it can be noticed that with a flow of 5–6 kg/h of cooling water is enough to have good removals and keep the temperature at the bottom of the reactor below the supercritical temperature (374°C), and that if a lower bottom temperature is required, an increase of the cooling flow could be worth but taking care with not decrease the TOC removal

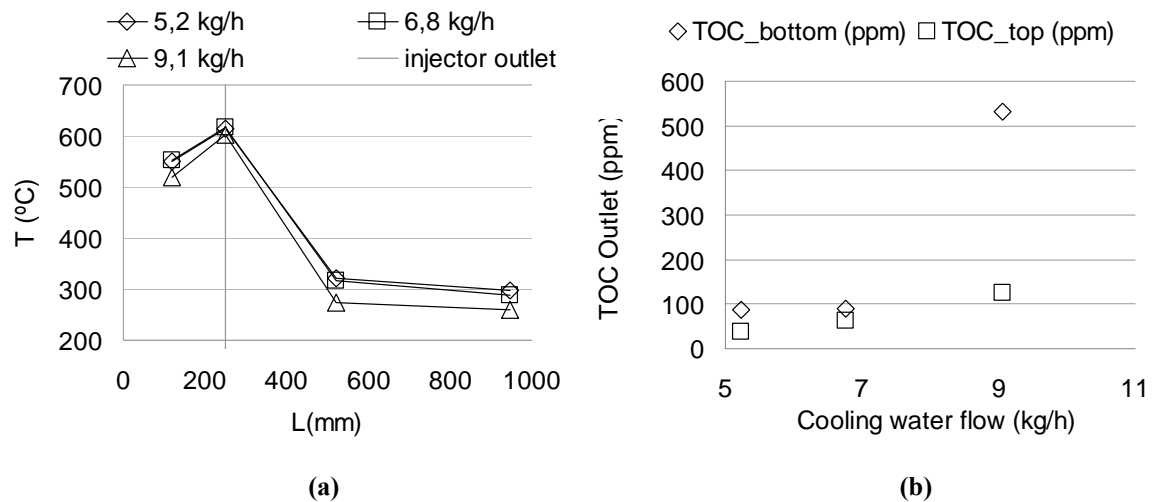


Figure 6.3.6 a: Temperature profiles for different cooling water flows.
Figure 6.3.6 b: TOC values in top and bottom effluents for different cooling water flows

6.3.3.4. Ammonia removal

Different mixtures of IPA and ammonia were tested with the new configuration of the reactor. In chapter 6.2, mixtures of ammonia and IPA were tested in the same reactor working with only the bottom outlet. The main results obtained with this new configuration, were compared with results obtained in section 6.2.3.1.

Figure 6.3.7 shows Ammonia and TOC removal represented versus maximum temperature registered inside the reactor. The upper effluent fraction was kept constant at values around 50% which means that the 50% of the feed injected has been taken out by the upper outlet.

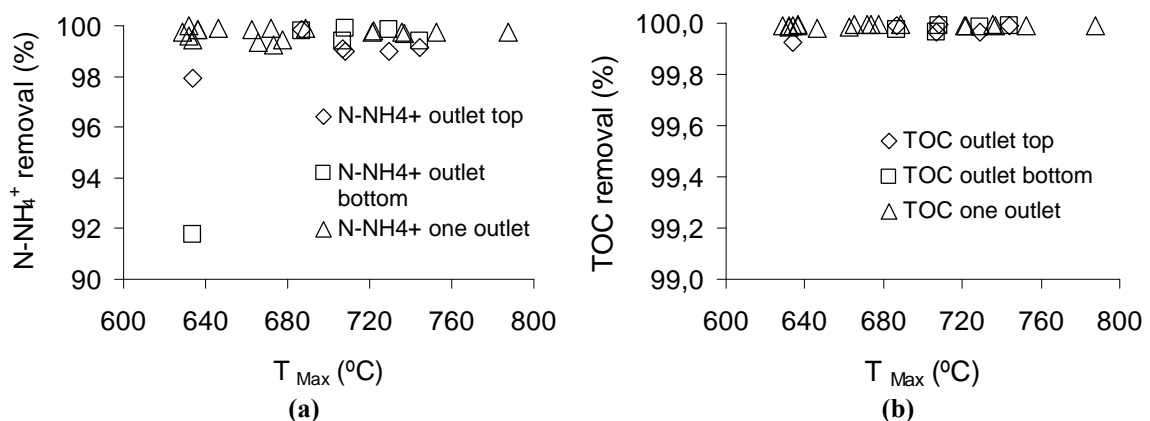


Figure 6.3.7 a: Ammonia removal (a) and TOC removal. (b) vs max temperature inside the reactor for feeds with ammonia concentration between 0,5 - 3% and IPA of 9 - 11,5% working with 100% bottom flow and with 50% top flow

It can be appreciated that temperatures higher than 700°C are required to achieve removals over 99%. These temperatures are higher than those needed to obtain the same removal with the reactor working with only one outlet

Table 6.3.1 summarises the average results for removal of the different experiments made with mixtures of ammonia and IPA:

Table 6.3.1: Removal results from the experiments made with different concentrations of ammonia

$C_{\text{NH}_4^+}$ (%)	C_{IPA0} (%)	T_{max} (°C)	TOC Removal top (%)	TOC Removal bottom (%)	N-NH ₄ ⁺ Removal top (%)	N-NH ₄ ⁺ Removal bottom (%)	N-NO ₃ ⁻ top (ppm)	N-NO ₃ ⁻ bottom (ppm)
0,5	11,5	744 ± 7	99,99 ± 0,01	99,99 ± 0,01	99,13 ± 0,06	99,41 ± 0,62	49 ± 2	38 ± 11
0,5	10,5	706 ± 9	99,97 ± 0,05	99,96 ± 0,02	99,07 ± 0,20	99,41 ± 0,06	47 ± 11	21 ± 1
0,5	10,0	634 ± 6	99,93 ± 0,05	94,71 ± 0,97	97,94 ± 0,52	91,77 ± 0,54	50 ± 14	14 ± 2
1,0	10,0	708 ± 3	99,99 ± 0,01	99,99 ± 0,01	98,99 ± 0,20	99,88 ± 0,40	36 ± 23	74 ± 16
3,0	9,0	686 ± 3	99,99 ± 0,01	99,97 ± 0,01	99,83 ± 0,14	99,79 ± 0,03	186 ± 21	78 ± 6
3,0	9,5	729 ± 5	99,97 ± 0,02	99,98 ± 0,02	99,29 ± 0,30	99,82 ± 0,10	26 ± 13	27 ± 15

Working with two outlets, it is observed that ammonia removal is slightly higher in the bottom effluent than in the top effluent, probably because the residence time for the products comprising the lower effluent is longer than the one of the top effluent, that it seems to be too short to have complete oxidation of ammonia [4].

6.3.3.5. Behaviour of the reactor working with feeds with high content in salts

The main goal of this new design of the reactor is to obtain a top effluent at high temperature and free of salts, becoming this way in a flow available to be used in systems to produce energy. To achieve that, salts contained in the feed must precipitate and fall, leaving the reactor dissolved in the bottom effluent while the top effluent is free of salts.

For this purpose feeds with Na₂SO₄ concentrations till 2,5% (25000 ppm) using with IPA as fuel to obtain reaction temperatures of 700°C, and feed flows of 13-14 kg/h, were injected in the reactor. In table 6.3.2 the main results of the experiments made with

feed containing salts are summarized. Equations (3) and (4) described in the experimental section explain how the salt recovery is calculated

Table 6.3.2: Main results for the experience made with feed containing 2,5% wt of Na₂SO₄

Sample	F _{TOP} (kg/h)	F _{BOTTOM} (kg/h)	TOC TOP (ppm)	TOC BOTTOM (ppm)	T max (°C)	T bottom (°C)	C _{Na2SO4} top (ppm)	Bottom Na ₂ SO ₄ recovery (%)
L3	7	10	2	164	723	291	<20	72
L4	7	10	2	164	749	297	<20	14
L5	7	10	1	277	712	301	<20	71
L6	7	10	1	471	740	302	<20	52
L7	7	10	1	18	742	303	<20	11
L8	7	10	1	55	683	302	<20	94
Average			3	192	725	299	20	43

As can be observed in table 6.3.2, it is possible to recover a top effluent free of salts (Concentrations of Na₂SO₄ lower than 20 ppm, with conductivities to values of the conductivity of distillate water, values in the supporting information of this chapter, table S.6.3.2) and at temperatures over 500°C, available to be expanded in a turbine or for the production of steam at high temperature that can be also expanded in a turbine.

Paying attention to the salt recovery at the bottom flow, it was possible to obtain an average of 43% of salt recovery.

This recovery is higher than the obtained with the reactor working with only one outlet (Average of 10%, section 6.1.3.6) but it was not possible to improve and stabilize it along the experiment with longer times. This fact could be interpreted as the possible formation of solid clusters of salts swept away by the outlet stream and dissolved in the cooling systems.

6.3.3.6. Energy recovery

The most conventional method for electric generation is using the products stream as heat source for a Rankine cycle. The products stream could generate steam at 400°C and 46 bar, the usual conditions on medium size industrial process [18].

A less conventional option, for the production of electricity by SCWO of a waste is by direct expansion of products stream through a turbine.

Figure 6.3.8 shows a scheme of the Rankine cycle for the production of steam with the top flow.

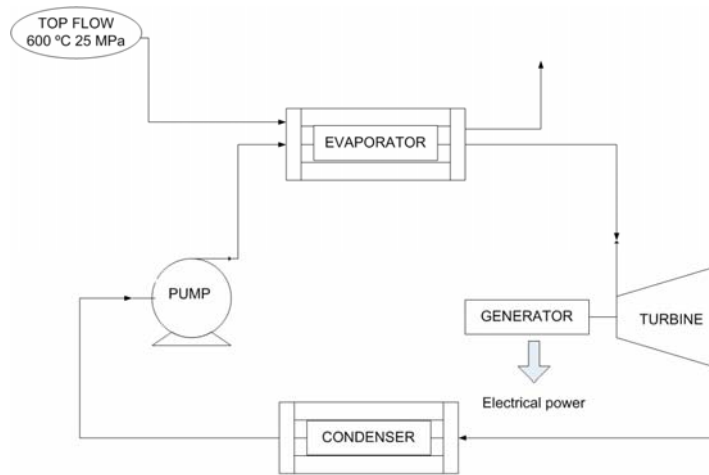


Figure 6.3.8: Rankine cycle example

In order to analyze the possibility of using the high temperature top effluent of the reactor to produce energy, a simple analysis of the options for generating energy was performed. For this study, the energy recovery from the bottom flow due to the work was not studied because its liquid state and its high salt content need complex energy recovery systems that go beyond the scope of this work.

The properties of the steam at 400°C and 4,6 MPa are taken from typical expansion turbines which works with steam at high temperature. Turbine expansion was calculated using Peng-Robinson Equation of State with Boston-Mathias alpha function and considering an isentropic turbine.

Mass and energy balances were solved taking thermal properties from Peng-Robinson Equation of State and volumetric properties from Peng-Robinson Equation of State with volume translation (vtPR-EoS). It was assumed that all the gases involved in the combustion leaves the reactor with the top effluent: gases produced in the reaction (CO_2), N_2 and O_2 (in excess) from the air mixed with the water flow, being the bottom effluent considered as pure water.

The amount of energy produced for kg/h of feed with a heat content of (3750 kJ/kg) by direct expansion for different upper flow fractions.

Table 6.3.3 shows the range of energy in kWh/kg of feed that could be produced with two different upper flow fractions at the temperature registered at the outlet of the reactor obtained in the experiments by direct expansion of the flow.

Table 6.3.3: Values for the energy recovery by direct expansion of the top effluent for a 3750 kJ/kg and an injection temperature of 200°C at different upper flow fractions

	F_{TOP} / F_{FEED} (%)	T top (°C)	Energy produced by Direct expansion (kWh / kg Feed)
Max	84	633	0,44
Min	35	510	0,30

Table 6.3.4 shows the energy produced by expansion of steam at 400°C and 46 bar in a Rankine cycle produced with the energy release by the top flow of the reactor.

Table 6.3.4: Values for the energy recovery by direct expansion of the top effluent for a 3750 kJ/kg and an injection temperature of 200°C at different upper flow fractions.

	F_{TOP} / F_{FEED} (%)	T top (°C)	Steam produced (kg/kg Feed)	Energy produced by Rankine Cycle (kWh / kg Feed)
Max	84	633	0,50	0,11
Min	35	510	0,20	0,05

As can be observed the energy produced by direct expansion of the flow from the reactor is bigger than the energy obtained by the production of steam that could be expanded afterwards

Taking a look to the total energy consumption of the pilot plant, table 6.3.5 shows the energy required for each electrical equipment.

Table 6.3.5: Main electrical consumes of the pilot plant

Pumping equipment		Heating equipment		TOTAL (kWh / kg Feed)
Compressor (kWh/kg Feed)	1,11	Flows Preheater (kWh/kg Feed)	1,48	
Liquid pumps (kWh/kg Feed)	0,20	Reactor Preheaters (kWh/kg Feed)	0,30	
Total	1,31	Total	1,78	3,10

Paying attention to these consumes and the results of the energy recovery from table 6.3.3 and 6.3.4, a total production of energy of 0,44 kWh/kg (14% of the total electrical consume of the plant) could be obtained by direct expansion of the top flow in turbine which could cover for example the electrical requirement of the both liquid pumps (0,20 kWh/kg)

In the case of the production of steam, with only 0,11 kWh produced (3% of the total electrical consume of the plant)

6.3.4. CONCLUSIONS

A new configuration of a cooled wall reactor working with hydrothermal flame was tested with the main characteristic of having two outlets one at the bottom and other at the top of the reactor in order to obtain two different effluents: one at high temperatures and free of inorganic solids to be used for energy production and other with all the inorganic solid dissolved for the goal of avoid any plugging in the process.

Using IPA as fuel TOC removal was higher than 99,9% in both effluents while the percentage of products leaving the reactor in the top effluent was lower than 70%. At higher top effluents total TOC removal is not achieves in the bottom effluent

Removal of ammonia higher than 99% were possible with intermediate upper flow fractions and temperatures over 700°C but the removal of ammonia in the upper flow was lower than in the bottom flow probably due to the necessity of higher residence times for the oxidation of products coming out the reactor trough the top outlet.

Experimental results using IPA as fuel and Na_2SO_4 as a model salt show that is possible to obtain a top effluent at 600°C, with a salt content lower than 20 ppm and a bottom effluent which allows recovering an average of 43% of salts at a temperature of 300°C.

An initial estimation about the possible energy production through the top flow was studied thanks to the new configuration of the reactor developed for this work. The results show that the upper flow, being expanded in a turbine, could produce 44 kWh/kg (14% of the total electrical consume of the plant), that could be enough energy for covering the consume of the pumping equipment.(0,20 kWh/kg)

LIST OF SYMBOLS

$C_{\text{IPA}0}$	Initial concentration of isopropyl alcohol	% wt
C_{IPA}	Concentration of isopropyl alcohol	% wt
$C_{\text{NH}_4^+0}$	Initial concentration of ammonia	% wt
$C_{\text{NH}_4^+}$	Concentration of ammonia	% wt
$C_{\text{Na}_2\text{SO}_4 \text{ BOTTOM}}$	Concentration of inorganic salt at the bottom outlet	ppm
$C_{\text{Na}_2\text{SO}_4 \text{ FED}}$	Concentration of inorganic salt at the inlet	ppm
$C_{\text{Na}_2\text{SO}_4 \text{ TOP}}$	Concentration of inorganic salt at the top outlet	ppm
F_{BOTTOM}	Flow from the bottom outlet of the reactor	kg/h
$F_{\text{COOLING WATER}}$	Flow from the bottom outlet of the reactor	kg/h
F_{FEED}	Flow pumped with the reactants	kg/h
F_{TOP}	Flow from the upper outlet of the reactor	kg/h
L	Position of the thermocouples inside the reactor	mm
$\text{Na}_2\text{SO}_4 \text{ recovery}$	Percent of salt recovery at the outlet of the reactor	%
$\text{N-NO}_3^- \text{ top}$	Concentration of nitrogen in nitrate way at the top	ppm
$\text{N-NO}_3^- \text{ bottom}$	Concentration of nitrogen in nitrate way at the bottom	ppm
P	Pressure	MPa
T	Temperature	°C
T_{TOP}	Temperature of the top effluent	°C
T_{max}	Maximum temperature in the reactor	°C
T_{bottom}	Temperature at the bottom of the reactor	°C
T_{inj}	Injection temperature in the reactor	°C
t_{R}	Residence time	s
$\text{TOC}_{\text{bottom}}$	Total Organic Carbon of bottom flow	ppm
TOC_{Top}	Total Organic Carbon of top flow	ppm
TN	Total Nitrogen	ppm

6.3.5. REFERENCES

- [1] W. Schilling, E.U. Franck, Combustion and diffusion flames at high-pressures to 2000 bar, *Berichte Der Bunsen-Gesellschaft-Physical Chemistry Chemical Physics*, 92 (1988) 631-636.
- [2] G.M. Pohsner, E.U. Franck, Spectra and temperatures of diffusion flames at high-pressures to 1000 bar, *Berichte Der Bunsen-Gesellschaft-Physical Chemistry Chemical Physics*, 98 (1994) 1082-1090.
- [3] C. Augustine, J.W. Tester, Hydrothermal flames: From phenomenological experimental demonstrations to quantitative understanding, *Journal of Supercritical Fluids*, 47 (2009) 415-430.
- [4] P. Cabeza, M.D. Bermejo, C. Jimenez, M.J. Cocero, Experimental study of the supercritical water oxidation of recalcitrant compounds under hydrothermal flames using tubular reactors, *Water Research*, 45 (2011) 2485-2495.
- [5] R.M. Serikawa, T. Usui, T. Nishimura, H. Sato, S. Hamada, H. Sekino, Hydrothermal flames in supercritical water oxidation: investigation in a pilot scale continuous reactor, *Fuel*, 81 (2002) 1147-1159.
- [6] M.D. Bermejo, E. Fdez-Polanco, M.J. Cocero, Experimental study of the operational parameters of a transpiring wall reactor for supercritical water oxidation, *Journal of Supercritical Fluids*, 39 (2006) 70-79.
- [7] C.H. Oh, R.J. Kochan, T.R. Charlton, A.L. Bourhis, Thermal-hydraulic modeling of supercritical water oxidation of ethanol, *Energy & Fuels*, 10 (1996) 326-332.
- [8] B. Wellig, K. Lieball, P. Rudolf von Rohr, Operating characteristics of a transpiring-wall SCWO reactor with a hydrothermal flame as internal heat source, *Journal of Supercritical Fluids*, 34 (2005) 35-50.
- [9] B. Wellig, M. Weber, K. Lieball, K. Prikopský, P. Rudolf von Rohr, Hydrothermal methanol diffusion flame as internal heat source in a SCWO reactor, *Journal of Supercritical Fluids*, 49 (2009) 59-70.
- [10] K. Prikopský, B. Wellig, P.R. von Rohr, SCWO of salt containing artificial wastewater using a transpiring-wall reactor: Experimental results, *Journal of Supercritical Fluids*, 40 (2007) 246-257.

- [11] M.D. Bermejo, F. Fdez-Polanco, M.J. Cocero, Effect of the transpiring wall on the behavior of a supercritical water oxidation reactor: Modeling and experimental results, *Industrial & Engineering Chemistry Research*, 45 (2006) 3438-3446.
- [12] M.D. Bermejo, P. Cabeza, M. Bahr, R. Fernández, V. Ríos, C. Jiménez, M.J. Cocero, Experimental study of hydrothermal flames initiation using different static mixer configurations, *Journal of Supercritical Fluids*, 50 (2009) 240-249.
- [13] M.D. Bermejo, P. Cabeza, J.P.S. Queiroz, C. Jiménez, M.J. Cocero, Analysis of the scale up of a transpiring wall reactor with a hydrothermal flame as a heat source for the supercritical water oxidation, *Journal of Supercritical Fluids*, 56 (2011) 21-32.
- [14] M.D. Bermejo, C. Jiménez, P. Cabeza, A. Matías-Gago, M.J. Cocero, Experimental study of hydrothermal flames formation using a tubular injector in a refrigerated reaction chamber. Influence of the operational and geometrical parameters, *Journal of Supercritical Fluids*, 59 (2011) 140-148.
- [15] M.D. Bermejo, M.J. Cocero, F. Fernandez-Polanco, A process for generating power from the oxidation of coal in supercritical water, *Fuel*, 83 (2004) 195-204.
- [16] K. Arai, R.L. Smith Jr, T.M. Aida, Decentralized chemical processes with supercritical fluid technology for sustainable society, *Journal of Supercritical Fluids*, 47 (2009) 628-636.
- [17] E.D. Lavric, H. Weyten, J. De Ruyck, V. Pleşu, V. Lavric, Supercritical water oxidation improvements through chemical reactors energy integration, *Applied Thermal Engineering*, 26 (2006) 1385-1392.
- [18] R.H. Perry, D.W. Green, *Perry's Chemical Engineers' Handbook* . (7th Edition). , 1997.

CHAPTER 7

CONCLUSIONS AND FUTURE WORK

CHAPTER 7

CONCLUSIONS AND FUTURE WORK

CONCLUSIONS

In this thesis the development and scale-up of vessel reactors for supercritical water oxidation working with a hydrothermal flame as an internal heat source was carried out. This allowed the development of a new cooled wall reactor design for supercritical water oxidation able to inject feeds at room temperature, to work with wastes containing some inorganic salt and to optimize the energetic use.

During the development of this thesis the following conclusions were obtained:

- 1) The initiation of hydrothermal flames in different tubular reactors was studied. The injection temperature was found to be decisive parameter in the hydrothermal flame ignition, requiring temperatures near or above ignition temperature of the mixtures.
- 2) The flame initiation of recalcitrant compounds such as acetic acid or ammonia in tubular reactors was studied. In the case of acetic acid, important problems of corrosion did not allow to work with concentrations higher than 4% in mass. In the case of ammonia, it was not possible to ignite or sustain hydrothermal flames exclusively of ammonia, and it was always necessary the addition of isopropanol as cofuel.
- 3) Total organic carbon removals higher than 99% were achieved with residence times lower than 1 s was achieved in the presence of hydrothermal flame working with flammable compounds, but when working with recalcitrant compounds such as ammonia, it was not possible to achieve total removals, even at temperatures over 750 °C at residence times lower than 1 s.

4) A transpiring wall reactor with a hydrothermal flame as a heat source was tested with feed flows up to 60 kg/h. Construction elements such as the nickel alloy transpiring wall and injectors filled with particles showed not be sturdy enough and they have been discarded for the final design.

5) A method for the scale up of vessel reactors with a hydrothermal flame as internal heat source based on the flame front velocity was proposed. The flame front velocity in supercritical conditions was estimated to be between 0.01 and 0.1 m/s, values one order of magnitude lower than those of typical atmospheric flame front velocities. The proposed method consists of the design of injectors with feed flow velocities higher than the flame front velocities in the injector to prevent the ignition occurs inside the while reaction chamber is designed to work with flow velocities of the order of magnitude of the flame front velocity to allow the flame remains stable in the reaction chamber allowing the injection of reagents at room temperature inside the flame.

6) The influence of geometrical parameters on the formation of hydrothermal flames was studied. The length of the injector plays an important role due to the flame is formed just outside of the injector and can determine the greatest distance to the walls of the reaction chamber favouring the preservation of materials.

7) A new cooled wall reactor was built set up and started up. The proposed design is composed by the following elements:

- a. Tubular injector
- b. Cooled reaction chamber, which allows the cooling water to enter through its lower part and mix with the reaction products.
- c. Pressure vessel with a lower and an upper flange that allows easy assembly and disassembly of the unit for maintenance.

The new reactor was successfully tested in the pilot plant at the University of Valladolid with feed flows up to 23 kg/h. It has proved to be easy to operate, versatile and sturdy.

The new reactor allows obtaining total organic carbon and ammonia removals up to 99.99% even injecting the feed at room temperature. Using the new reactor the injection of feeds with 2.5% of salts of Na_2SO_4 , is possible obtaining recoveries up to 20%

The energy recovery of the reactor was improved by adding to the original design an additional outlet on the top of the reactor for the hot products.. The optimum flow distribution working with this configuration happens when the 70% of the feed is recovered through the upper outlet. For higher upper outlet flows, total organic carbon removal is reduced. A top effluent at temperatures above 600 °C, with a salt content less than 20 ppm is obtained, being suitable for its use in energy Recovery of salts through the bottom outlet was lower than 40%.

The elimination of recalcitrant compounds such as ammonia is slightly lower in the upper effluent than in the lower effluent due to the low residence time of this flow in the reactor.

This new reactor was object of an European Patent Application (PCT/ES2011/070727).

FUTURE WORK

The new reactor design must be modified by increasing the distance between the injector and the top outlet in order to improve the elimination of recalcitrant compounds.

The next step for the reactor development is to test it with different industrial waste in order to check the applicability of the apparatus.

At a demonstration scale in a continuous facilities that allows to test the operation of the reactor for long operation times of various weeks or months in order to identify possible operational problems.

APPENDIX I

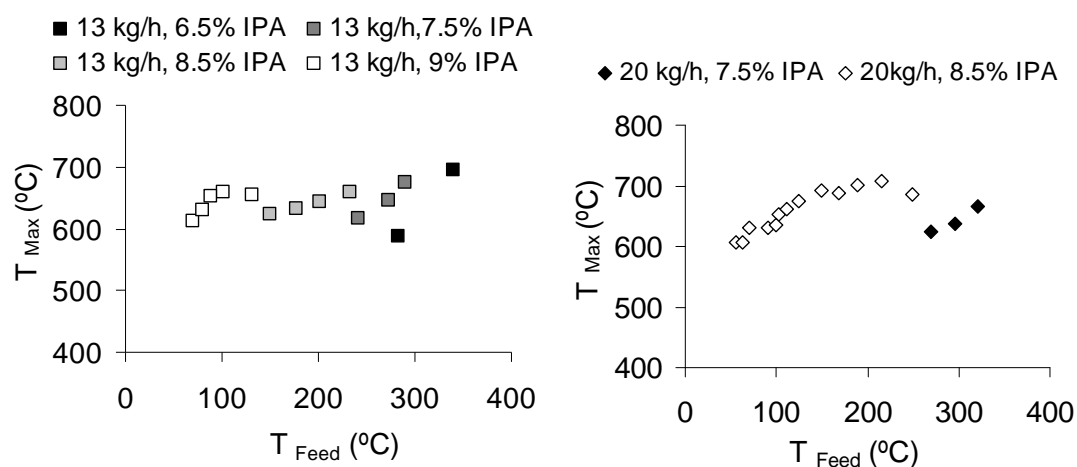
SUPPORTING INFORMATION CHAPTER 6

SUPPORTING INFORMATION SECTION 6.1

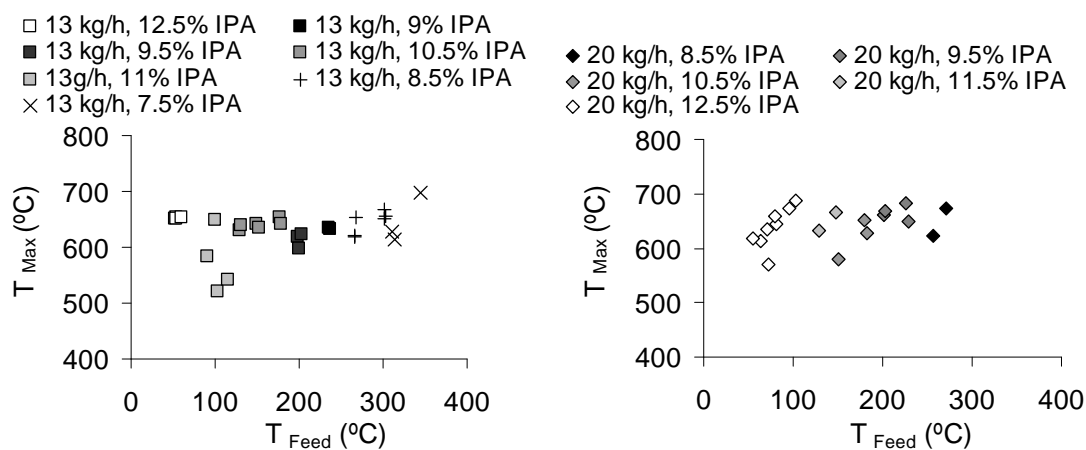
Table S.6.1.1. Summary of all experiments carried out in order to study the influence of all operational and geometrical parameters in a tubular injector into of a reaction chamber.

INJECTOR 1. 1/4" and 950 mm						
Experiment	Feed (kg/h)	t_{operation} (min)	Number Samples	T_{Feed Max} (°C)	T_{Feed Min} (°C)	C_{IPA} (% ww)
E	25	100	18	362	198	6.5-7.5
F	20	220	28	375	50	6.5-8.5
H	13	300	24	340	80	6.5-8.6
J	25	200	14	225	90	8.5-9.5
L	23	160	18	285	70	8.5-10.5
M	13	240	16	283	70	6.5-9
INJECTOR 2. 1/8" and 950 mm						
Experiment	Feed (kg/h)	t_{operation} (min)	Number Samples	T_{Feed Max} (°C)	T_{Feed Min} (°C)	C_{IPA} (% ww)
B	13.6	215	24	344	102	7.5-11
C	20	205	23	272	55	8.5-12.5
D	25	94	8	230	171	9.5-10.5
E	24	141	13	230	113	9.5-12
F	13.6	92	9	306	209	8.5-9.5
G	20	185	19	270	71	8.5-12.5
H	13.6	240	28	312	52	7.5-12.5
M	13	240	16	283	70	6.5-9
INJECTOR 3. 1/4" and 550 mm Thermocouple Position 1 z= 20mm						
Experiment	Feed (kg/h)	t_{operation} (min)	Number Samples	T_{Feed Max} (°C)	T_{Feed Min} (°C)	C_{IPA} (% ww)
B	13.6	245	16	368	54	8.5-12
C	24	100	8	380	286	9.5-10.5
D	13	140	14	357	176	9.5-11.5
E	13	250	24	306	40.8	9.5-12.5
F	20	215	13	265	100	9.5-11.5
INJECTOR 3. 1/4" and 550 mm Thermocouple Position 2 z= 200mm						
Experiment	Feed (kg/h)	t_{operation} (min)	N° Samples	T_{Feed Max} (°C)	T_{Feed Min} (°C)	%IPA
J	13.6	265	18	327	48.1	8.5-12.5
K	13	330	20	287	58	9.5-12.5
INJECTOR 3. 1/4" and 550 mm Thermocouple Position 3 z= 430mm						
Experiment	Feed (kg/h)	t_{operation} (min)	N° Samples	T_{Feed Max} (°C)	T_{Feed Min} (°C)	%IPA
G	13	135	11	268	130	9.5-11.5
H	20	260	18	306	44.2	9.5-12.5
I	24	130	4	220	195	10.5-11.5

Injector 1



Injector 2



Injector 3

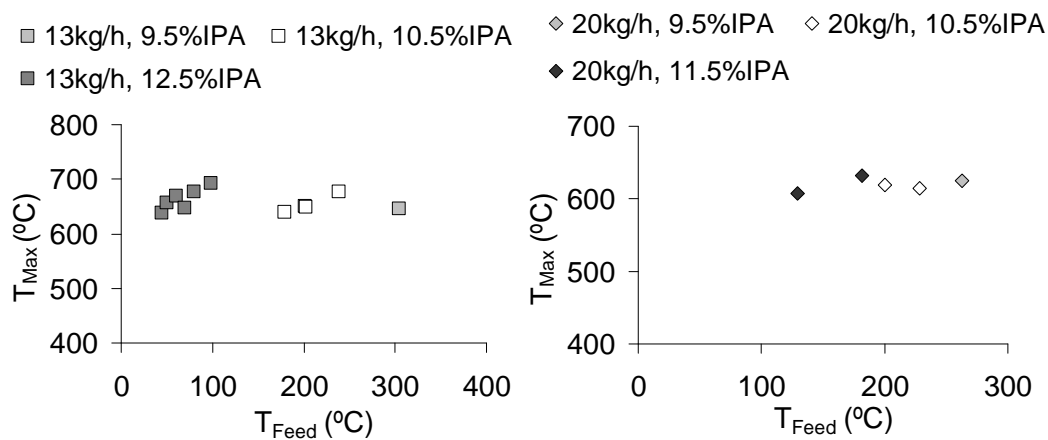
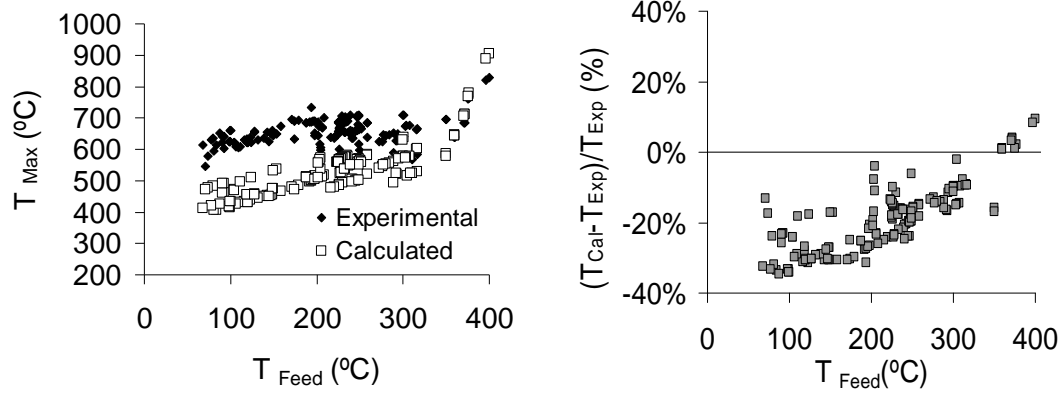
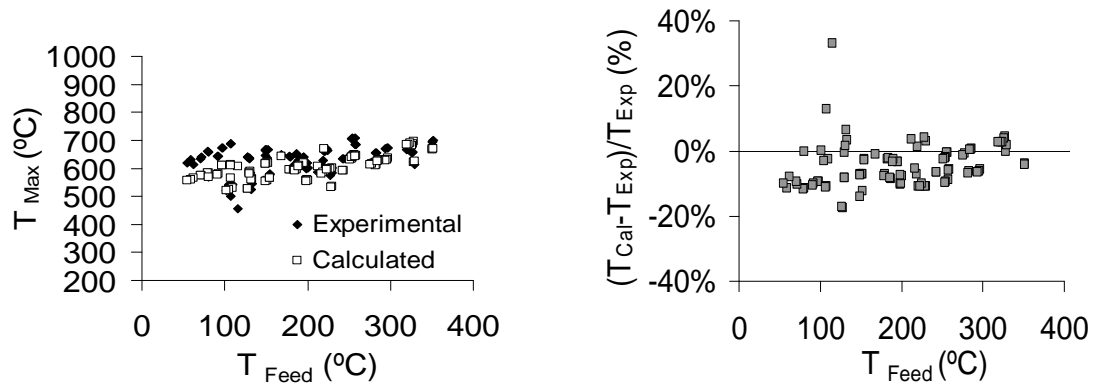


Figure S.6.1.1. Maximum temperatures reached in the reaction chamber at different feed flows and isopropyl alcohol (IPA) concentrations in injectors 1, 2 and 3

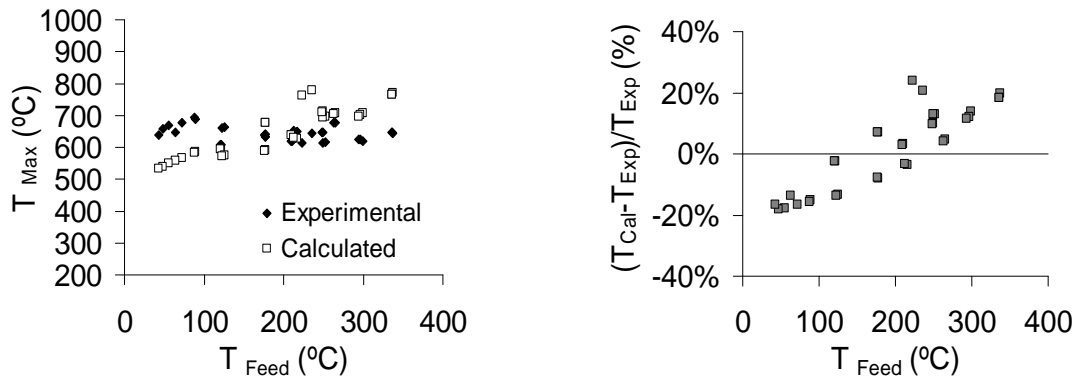
Injector 1



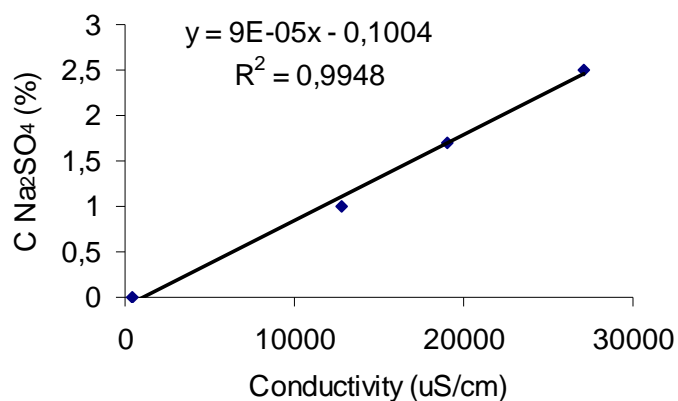
Injector 2



Injector 3

**Figure S.6.1.2.** Maximum temperatures experimental and calculated

SUPPORTING INFORMATION SECTION 6.3



FigureS.6.3.1: Calibration curve made to calculate the concentration of liquid samples taken in the experience with feeds containing inorganic salts

Table S.6.3.2. Values of conductivity of standards samples of Na₂SO₄

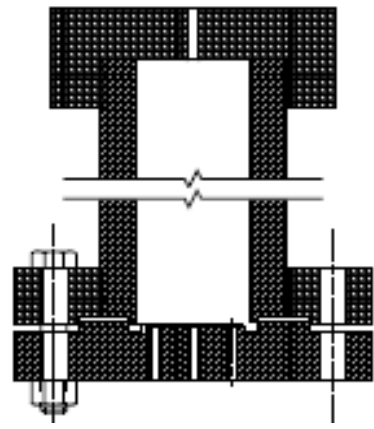
Concentración Na ₂ SO ₄ (%)	Conductivity (uS/cm)
0	442
0	469
0	460
1	12770
1	12740
1	12970
1,7	18860
1,7	18660
1,7	19620
2,5	26540
2,5	26400
2,5	28240

Table S.6.3.2. Values of conductivity of samples taken in experience L whose main results are shown in section 6.3.3.5

Sample	Conductivity top flow (uS/cm)	Conductivity bottom flow (uS/cm)
L1	190,50	357,20
L2	666,00	10630,00
L3	227,40	5410,00
L4	213,30	2080,00
L5	203,20	10520,00
L6	212,50	7740,00
L7	201,20	1585,10
L8	207,00	13900,00
L9	237,40	627,00

APPENDIX II

PROCESS DATA SHEETS

		TRANSPIRING WALL REACTOR PROCESS DATA SHEET					
Pilot plant: SCWO CETRANSA							
BY	M ^a Dolores Bermejo			REV	Pablo Cabeza		
1	Item number	R-110	3	Manufacturer	REPRESA		
2	Service		4	Type	Transpiring wall reactor		
OPERATIONAL AND CONSTRUCCION DATA							
5	Test pressure	450 bar	11	Position	Vertical		
6	Max work pressure	270 bar	12	Total Volume at pressure	3.08 dm ³		
7	Design pressure	300 bar	13	Total Volume	32.13 dm ³		
8	Service pressure	250 bar	14	Fluid	Agua, comps orgánicos		
9	External wall design temperature	400°C	15	External wall work temperature	350°C		
10	Internal wall design temperature	1000°C	16	internal wall work temperature	700°C		
External wall				Transpiring l wall			
17	Type	AISI 316L	21	Type	INCONEL®		
18	Length	1500 mm	22	Length	995 mm		
19	External diameter	145 mm	23	External diameter	80 mm		
20	Thickness	27,5 mm	24	Thickness	3 mm		
Top closed							
25	Type	AISI 316L					
26	Length						
27	External diameter	221 mm					
28	Internal diameter	145 mm					
29							
30							
31							
Bottom Flanges							
32	Type	AISI 316L					
33	Length	85 mm					
34	External diameter	217 mm					
35	Internal diameter	145 mm					
36	Closed flange						
37	Type	AISI 316L					
38	External diameter	217 mm					
39	Thickness	75 mm					
CONTROL EQUIPMENT							
	Manometer	0-600 bar					
	Burst disc	Ranged at 6750 psig					
	Relief valve	Ranged at 385 bar					
NOTES							
DATE		EDITED		VERIFIQUED		APPROBED	
22/03/11		Pablo Cabeza					

	<p>FEED PUMP PROCESS DATA SHEET</p> <p>Pilot plant: SCWO CETRANSA</p>	
---	---	---

BY	Daniel Rincón	REV	Pablo Cabeza
----	---------------	-----	--------------

1	Item number	P-350	3	Manufacturer	Dossapro-MiltonRoyal
2	Service	Waste pump	4	Type	Maxroyal C

OPERATIONAL AND CONSTRUCCION DATA

5	Liquid pumped	Waste
6	Temperature	20°C
7	Max Flow	200 kg/h
8	Max pressure	450 bar
9	Min pressure	9 bar
10	Discharge pressure	2000 to 2500 daN
11	Duty	4 KW
12	Location	Outdoors



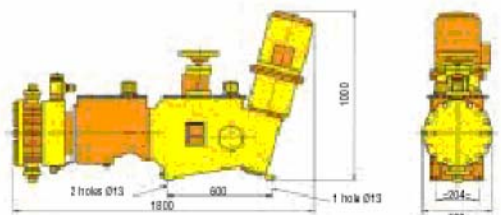
DRIVE

13	Electric drive	4 kW
14	Speed	142 r.p.m
15	Phases	3
16	Power factor	0.6

OTHER CHARACTERISITC

PLUNGER DOSING PUMP				DIAPHRAGM DOSING PUMP (D)			
ø Plunger (mm)	Speed (strokes/min)	Flow rate (Q) (l/h)	Max (bar) pressure	ø Plunger (mm)	Speed (strokes/min)	Flow rate (Q) (l/h)	Max (bar) pressure
20	140	201	450	25	140	313	300
25	140	314	400	32	140	513	248
32	140	518	243	40	140	801	159
40	140	812	155	50	140	1252	101
50	140	1270	98	55	140	1515	84
55	140	1537	81	63	140	1988	64
66	140	2022	61	70	140	2455	50
90	112	3299	29	90	140	4059	31
125	112	6361	14	125	112	6263	16
160	112	10430	9	145	112	8429	12
-	-	-	-	160	112	12234	10

Maxroyal C

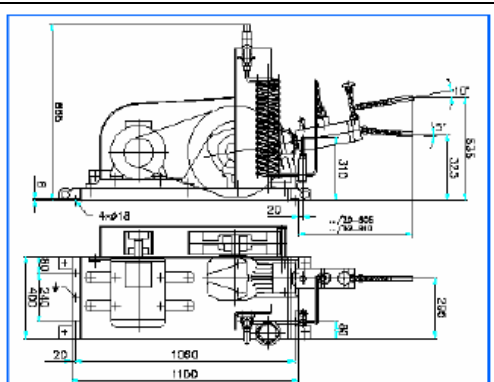


CONTROL EQUIPMENT

17	Rupture disc	Pressure rating set to 6750 psig
18	Relief valve	Pressure rating set to 6750 250 bar

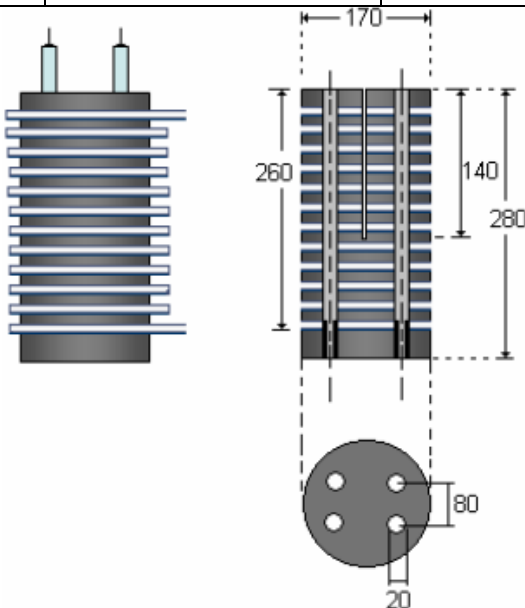
NOTES

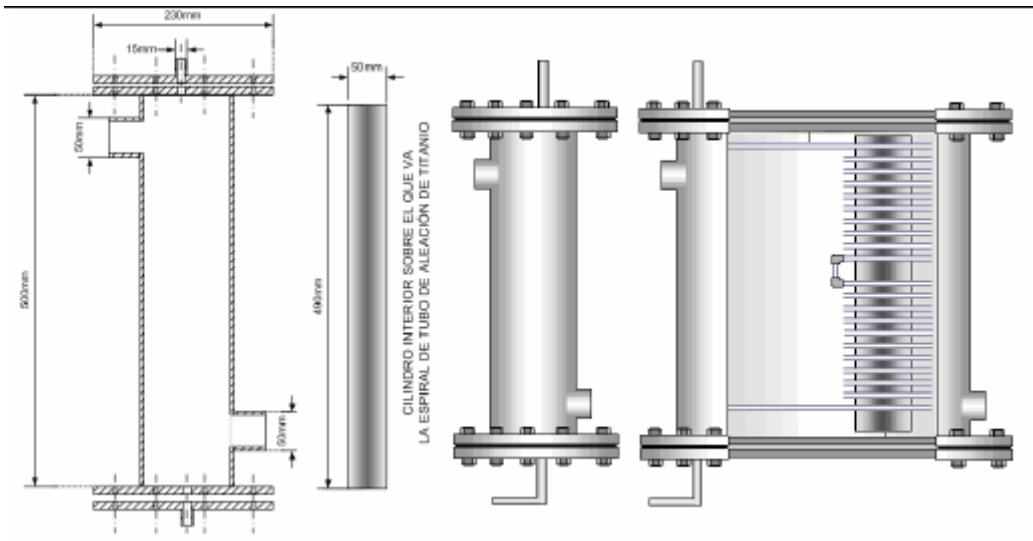
DATE	EDITED	VERIFIQUED	APPROBED
22/03/12	Pablo Cabeza		

		OXIGEN PUMP PROCESS DATA SHEET				
Pilot plant: SCWO CETRANSA						
BY	Daniel Rincón		REV	Pablo Cabeza		
1	Item number	P-220	4	Manufacturer	Cryostar-France SA	
2	Service	O ₂ Impulsion	5	Type	A-SDPD 2220-K	
3	Year manufacture	2000	6	S.N	99399.01	
OPERATIONAL AND CONSTRUCCION DATA						
7	Speed	144 r.p.m				
8	Operational Temperature	- 183°C				
9	Flow	1.4 l/min				
10	Capacity	67 Nm ³ /h				
11	Max pressure aspiration	15 bar				
12	Propel pressure	350 bar				
13	Min NPSH	0,15 bar				
14	Power consumption	1,1 kW				
DRIVE DATA						
15	Serial number	792602427				
16	Type	Ls 132 s				
17	Frequency	50 Hz				
18	Phases	3				
19	Protection	IP 55				
20	Isolation type	F/B				
21	Voltage	123/400V				
22	Power	3 kW				
23	Speed	945				
CONTROL EQUIPMENT						
24	Security valve	Pressure rating set at 350 bar				
NOTES						
DATE	EDITED	VERIFIQUED	APPROBED			
22/03/12	Pablo Cabeza					

		AIR COOLER / O₂ BOTTLES PROCESS DATA SHEET					
Pilot plant: SCWO CETRANSA							
BY	Daniel Rincón			REV	Pablo Cabeza		
AIR COOLER							
1	Item number	E-230	3	Manufacturer	Cryostar-France SA		
2	Service	Phase change O ₂	4	Type	CB-160 B-1198		
OPERATIONAL AND CONSTRUCCION DATA							
5	Test Pressure	45500 kPa					
6	Max Pressure	35000 kPa					
7	Max capacity	3.68 Litres					
8	Service Temperature	50°C					
9	Min Temperature	-196°C					
10	Max Flow	132 m ³ /h					
11	Weight	450 kg					
Service conditions							
12	Outlet O ₂ temperature	15 °C					
13	Outlet pressure	300 bar					
14	Pipe diameter	8/16 mm					
CONTROL EQUIPMENT							
15	Manometer	0 – 600 bar					
16	Thermostat	-30 to 50°C					
17	Security valve	Pressure rating set at 385 bar					
18	By pass valve						
19	Pressure switch for high pressure						
O ₂ BOTTLES							
1	Item number	T-	3	Manufacturer	Worthington Heiser		
2	Service	Phase change O ₂	4	Type	Cylinders GmbnH		
OPERATIONAL AND CONSTRUCCION DATA							
5	Volume	50 l	9	External diameter	229 mm		
6	Pressure	350 bar	10	Thickness	9,00 mm		
7	Test pressure	525 bar	11	Material	Steel Cr-Mo		
8	Gas	Oxygen	12	Fitting diameter	8/16 mm		
CONTROL EQUIPMENT							
13	Security valve	Pressure rating set at 300 bar					
14	Backstop valves						
NOTES							
DATE	EDITED	VERIFIQUED			APPROBED		
22/03/12	Pablo Cabeza						



		PREHEATER PROCESS DATA SHEET Pilot plant: SCWO CETRANSA					
BY	Daniel Rincón		REV	Pablo Cabeza			
1	Item number	E-370	3	Manufacturer	UVA		
2	Service	Preheat the waste	4	Type	Electric		
OPERATIONAL AND CONSTRUCCION DATA							
5	Support	Brass.-cass	12	Isolation support	Aluminum frame		
6	Electric resistances	4x2500W	13	Fluid	Water / waste		
7	Pipe length	6 m	14	Cp	4,3 kJ/kg		
8	Nominal diameter	¼ inch	15	Pressure	250 bar		
9	thickness	0,035 mm	16	Min Temperature	25°C		
10	Pipe material	Inconel 600	17	Max Temperature	550°C		
11	Isolation	Wool	18	U	3310 (W/m ²)		
CONTROL EQUIPMENT AND OTHER CHARACTERISTICS							
19	Rupture disc	Pressure rating set to 6750 psig					
20	Temperature control	Thermocouples type K					
 							
NOTES							
DATE		EDITED		VERIFIQUED		APPROBED	
22/03/12		Pablo Cabeza					

		COOLER PROCESS DATA SHEET Pilot plant: SCWO CETRANSA					
BY		Daniel Rincón		REV		Pablo Cabeza	
1	Item number	E-420		3	Manufacturer	UVA	
2	Service	Refrigeration of products		4	Type		
OPERATIONAL AND CONSTRUCCION DATA							
External wall				Interior			
6	Fitting diameter	50 mm		13	Fitting diameter	¾ in	
7	Fitting type	Plastic tube		14	Fitting type		
8	Material	Stainless steel		15	Material pipe	Titanium alloy	
9	lock	Bolts and joint		16	Length pipe	4.5 m	
10	Pressure	3 bar		17	Max pressure	250 bar	
11	Max Temperature	100°C		18	Max temperature	400°C	
12	Fluid	Water		19	Fluid	Outlet reactor	
OTHER CHARACTERISTICS							
 <p style="text-align: center;">CILINDRO INTERIOR SOBRE EL QUE VA LA ESPIRAL DE TUBO DE ALEACION DE TITANIO</p>							
CONTROL EQUIPMENT							
20	Temperature control			Thermocouples type K			
NOTES							
							
DATE		EDITED		VERIFIQUED		APPROBED	
22/03/12		Pablo Cabeza					

	<p>REFRIGERATION TOWER PROCESS DATA SHEET</p> <p>Pilot plant: SCWO CETRANSA</p>	
---	---	---

BY	Daniel Rincón	REV	Pablo Cabeza
----	---------------	-----	--------------

1	Item number	D-430	3	Manufacturer	Sulzer España S.A
2	Service	Refrigerate water	4	Type	EwK 064

OPERATIONAL AND CONSTRUCCION DATA

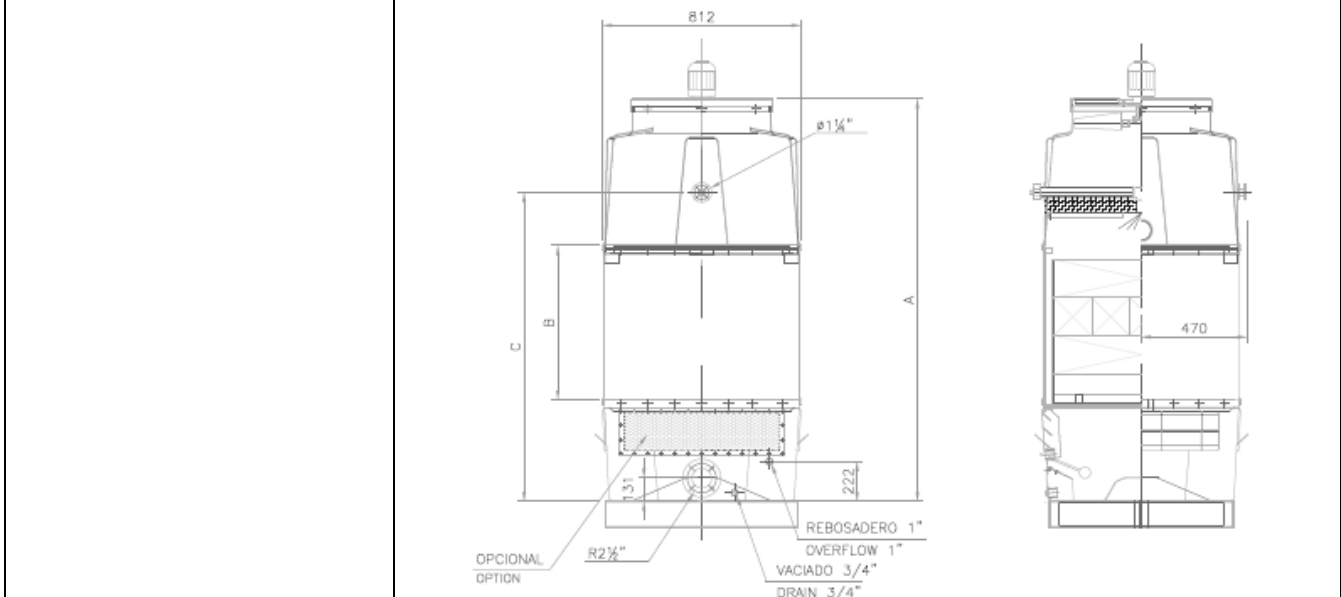
5	Power misspent	103 kW
6	Weight empty	130 kg
7	Weihgt in service	295 kg
8	Power ventilator	0.55 kW
9	lenght	812 mm
10	Height	2020 mm
11	wide	812 mm
12	Inlet temperature	35°C
13	Outlet temperature	30°C
14	Wet temperature	24°C
15	Wall material	Polyester
16	Interior	Plastic



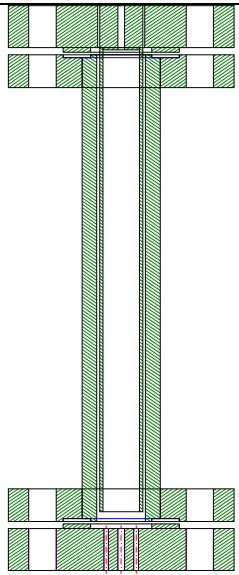
CONTROL EQUIPMENT

17	Temperature control	Thermocouples type K
18	Switch on	Manual button
19	Biocide for pools	

NOTES



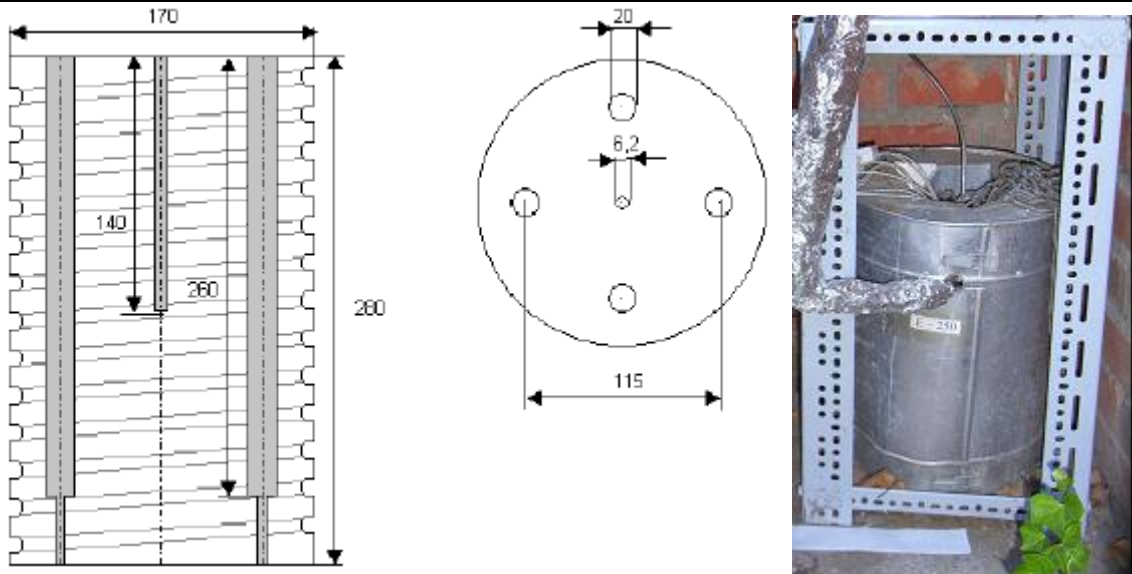
DATE	EDITED	VERIFIQUED	APPROBED
22/03/12	Pablo Cabeza		

		REACTOR PROCESS DATA SHEET					
		PILOT PLANT UNIVERSITY OF VALLADOLID					
BY	Pablo Cabeza Pérez		REV				
1	Item number	R-110	3	Manufacturer	UVA		
2	Service		4	Type	Cooled wall reactor		
OPERATIONAL AND CONSTRUCCION DATA							
5	Test pressure	429 bar	11	Position	Vertical		
6	Max work pressure	270 bar	12	Total Volume at pressure	3.08 dm ³		
7	Design pressure	300 bar	13	Total Volume	32.13 dm ³		
8	Service pressure	250 bar	14	Fluid	Agua, comps orgánicos		
9	External wall design temperature	400°C	15	External wall work temperature	350°C		
10	Internal wall design temperature	1000°C	16	internal wall work temperature	700°C		
External wall				Internal wall			
17	Type	AISI 316L	21	Type	INCONEL®		
18	Length	1000 mm	22	Length	995 mm		
19	External diameter	114 mm	23	External diameter	63 mm		
20	Thickness	21.5 mm	24	Thickness	4.8 mm		
Top Flanges							
25	Type	AISI 316L					
26	Length	70 mm					
27	External diameter	330 mm					
28	Internal diameter	114 mm					
29	Closed flange						
30	External diameter	330 mm					
31	Thickness	90 mm					
Bottom Flanges							
32	Type	AISI 316L					
33	Length	70 mm					
34	External diameter	330 mm					
35	Internal diameter	114 mm					
36	Closed flange						
37	Type	AISI 316L					
38	External diameter	330 mm					
39	Thickness	90 mm					
CONTROL EQUIPMENT							
	Manometer	0-600 bar					
	Burst disc	Ranged at 6750 psig					
	Relief valve	Ranged at 385 bar					
NOTES							
DATE		EDITED	VERIFIQUED		APPROBED		
22/03/11		Pablo Cabeza					

		AIR COMPRESSOR PROCESS DATA SHEET											
PILOT PLANT UNIVERSITY OF VALLADOLID													
BY	M ^a Dolores Bermejo	REV	Pablo Cabeza										
1	Item number	G-220	3	Manufacturer	Ingersoll-Rand								
2	Service	Air pump	4	Type	H15T4								
OPERATIONAL AND CONSTRUCCION DATA													
5	Fluid	Air											
6	Temperature	20°C											
7	Max Flow	36 kg/h											
8	Min pressure	1 bar											
9	Discharge pressure	300 bar											
10	Inlet temperature	20°C											
11	Outlet temperature	40°C											
12	Stages	4											
13	Cooler between stages	air											
DRIVE													
13	Electric drive	15 kW											
14	Speed	1445 r.p.m											
15	Phases	3											
16	Power factor	0.8											
17	Voltage	220 V											
18	Cycles	50											
													
							CONTROL EQUIPMENT						
							17	Backstop valve					
							18	Relief valve	Pressure rating set to 6750 280 bar				
19	Automatic switch off	Overpressures over 300 bar											
NOTES													
DATE	EDITED	VERIFIQUED	APPROBED										
22/03/12	Pablo Cabeza												

		FEED PUMP PROCESS DATA SHEET				
PILOT PLANT UNIVERSITY OF VALLADOLID						
BY	M ^a Dolores Bermejo	REV	Pablo Cabeza			
1	Item number	P-240	3	Manufacturer	Dossapro-MiltonRoyal	
2	Service	Waste pump	4	Type	MB. 112.S(L) 12.M 300/VV2	
OPERATIONAL AND CONSTRUCCION DATA						
5	Liquid pumped	Aqueous solutions				
6	Temperature	20°C				
7	Max Flow	25 kg/h				
8	Max pressure	450 bar				
9	Min pressure	1 bar				
10	Discharge pressure	300 bar				
11	Piston	Steel ASISI 316-L				
12	Frame	Cast iron				
						
DRIVE						
13	Electric drive	1.4 kW				
14	Speed	142 r.p.m				
15	Phases	3				
16	Power factor	0.8				
17	Voltage	220 V				
18	Cycles	50				
CONTROL EQUIPMENT						
17	Backstop valve					
18	Relief valve	Pressure rating set to 6750 280 bar				
NOTES						
DATE	EDITED	VERIFIQUED	APPROBED			
22/03/12	Pablo Cabeza					

		FEED PUMP PROCESS DATA SHEET			
PILOT PLANT UNIVERSITY OF VALLADOLID					
BY	M ^a Dolores Bermejo	REV	Pablo Cabeza		
1	Item number	P-210	3	Manufacturer	Dossapro-MiltonRoyal
2	Service	Quenching pump	4	Type	MC 61 S(Q) 20 N
OPERATIONAL AND CONSTRUCCION DATA					
5	Liquid pumped	Water			
6	Temperature	20°C			
7	Max Flow	72 kg/h			
8	Max pressure	450 bar			
9	Min pressure	1 bar			
10	Discharge pressure	300 bar			
11	Frame	Cast iron			
12	Piston	Steel ASISI 316-L			
DRIVE					
13	Electric drive	4 kW			
14	Speed	142 r.p.m			
15	Phases	3			
16	Power factor	0.8			
17	Voltage	220 V			
18	Cycles	50			
CONTROL EQUIPMENT					
17	Backstop valve				
18	Relief valve	Pressure rating set to 6750 280 bar			
NOTES					
DATE	EDITED	VERIFIQUED	APPROBED		
22/03/12	Pablo Cabeza				

	<p>PREHEATER PROCESS DATA SHEET</p> <p>PILOT PLANT UNIVERSITY OF VALLADOLID</p>				
BY	M ^a Dolores Bermejo	REV	Pablo Cabeza		
1	Item number	E-250	3	Manufacturer	UVA
2	Service	Preheat feed	4	Type	Electric
OPERATIONAL AND CONSTRUCCION DATA					
5	Support	Brass.-cass	12	Isolation support	Aluminum frame
6	Electric resistances	4x2000W	13	Fluid	Water / waste
7	Pipe lenght	6 m	14	Cp	4,2 kJ/kg
8	Nominal diameter	¼ inch	15	Pressure	250 bar
9	thickness	0,035 mm	16	Min Temperature	25°C
10	Pipe material	Inconel 600	17	Max Temperature	550°C
11	Isolation	Wool	18	U	3310 (W/m ²)
CONTROL EQUIPMENT AND OTHER CHARACTERISTICS					
19	Temperature control	Thermocouples type K			
DIMENSIONAL CHARATTHEISTICS					
					
NOTES					
DATE	EDITED	VERIFIQUED	APPROBED		
22/03/12	Pablo Cabeza				

	<p>PREHEATER PROCESS DATA SHEET</p> <p>PILOT PLANT UNIVERSITY OF VALLADOLID</p>	
---	---	---

BY	M ^a Dolores Bermejo	REV	Pablo Cabeza
----	--------------------------------	-----	--------------

1	Item number	E-260	3	Manufacturer	UVA
2	Service	Preheat feed	4	Type	Electric

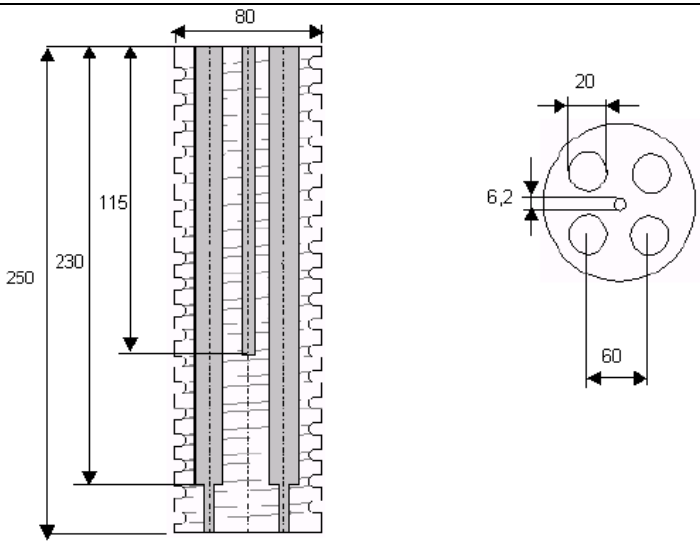
OPERATIONAL AND CONSTRUCCION DATA

5	Support	Brass.-cass	12	Isolation support	Aluminum frame
6	Electric resistances	4x2500W	13	Fluid	Water / waste
7	Pipe lenght	4.5 m	14	Cp	4,2 kJ/kg
8	Nominal diameter	¼ inch	15	Pressure	250 bar
9	thickness	0,035 mm	16	Min Temperature	25°C
10	Pipe material	Inconel 600	17	Max Temperature	550°C
11	Isolation	Wool	18	U	3740 (W/m ²)

CONTROL EQUIPMENT AND OTHER CHARACTERISTICS

19	Temperature control	Thermocouples type K
----	---------------------	----------------------

DIMENSIONAL CHARATTHEISTICS

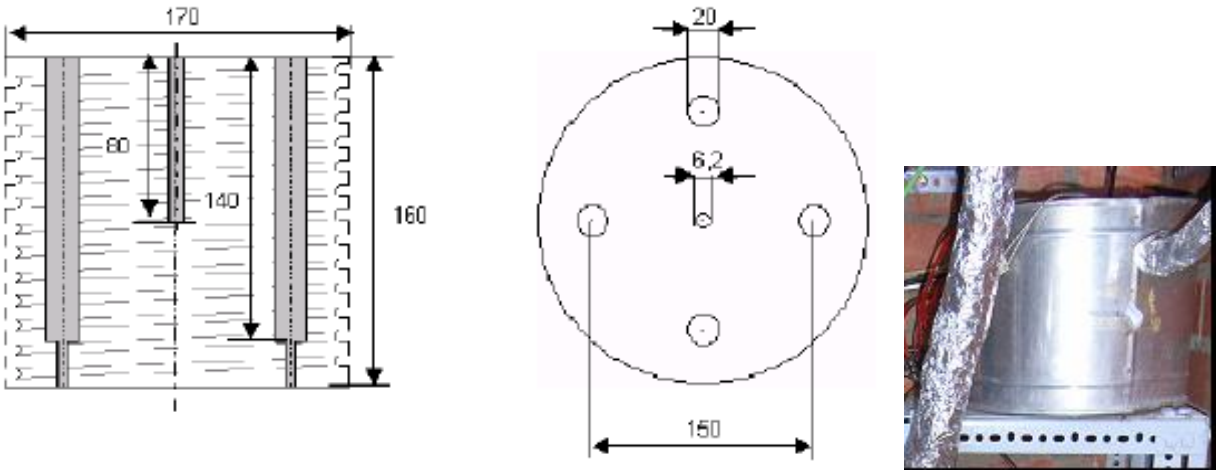


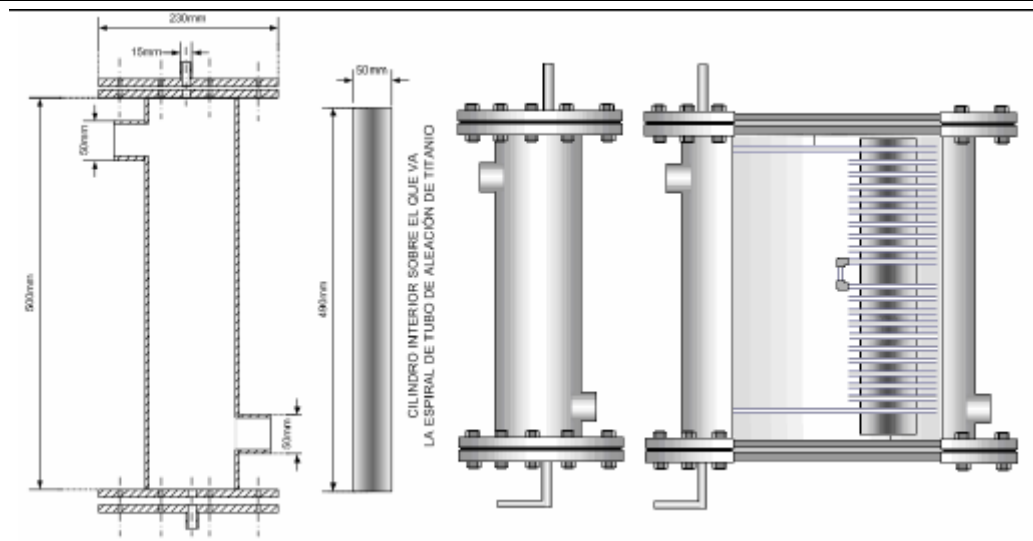


NOTES

--	--	--	--

DATE	EDITED	VERIFIQUED	APPROBED
22/03/12	Pablo Cabeza		

		PREHEATER PROCESS DATA SHEET					
PILOT PLANT UNIVERSITY OF VALLADOLID							
BY		M ^a Dolores Bermejo		REV	Pablo Cabeza		
1	Item number	E-230	3	Manufacturer	UVA		
2	Service	Preheat air	4	Type	Electric		
OPERATIONAL AND CONSTRUCCION DATA							
5	Support	Brass.-cass	12	Isolation support	Aluminum frame		
6	Electric resistances	4x15000W	13	Fluid	Air		
7	Pipe lenght	6 m	14	Cp	1.2 kJ/kg		
8	Nominal diameter	¼ inch	15	Pressure	250 bar		
9	thickness	0,035 mm	16	Min Temperature	25°C		
10	Pipe material	Inconel 600	17	Max Temperature	550°C		
11	Isolation	Wool	18	U	1716 (W/m ²)		
CONTROL EQUIPMENT AND OTHER CHARACTERISTICS							
19	Temperature control	Thermocouples type K					
DIMENSIONAL CHARATTHEISTICS							
							
NOTES							
DATE		EDITED		VERIFIQUED		APPROBED	
22/03/12		Pablo Cabeza					

		COOLER PROCESS DATA SHEET				
PILOT PLANT UNIVERSITY OF VALLADOLID						
BY	M ^a Dolores Bermejo			REV	Pablo Cabeza	
1	Item number	E-120	3	Manufacturer	UVA	
2	Service	Refrigeration of products	4	Type		
OPERATIONAL AND CONSTRUCCION DATA						
External wall			Interior			
6	Fitting diameter	50 mm	13	Fitting diameter	¾ in	
7	Fitting type	Plastic tube	14	Fitting type		
8	Material	Galvanized steel	15	Material pipe	Stainless steel	
9	lock	Bolts and joint	16	Length pipe	6 m	
10	Pressure	3 bar	17	Max pressure	250 bar	
11	Max Temperature	100°C	18	Max temperature	400°C	
12	Fluid	Water	19	Fluid	Outlet reactor	
OTHER CHARACTERISTICS						
						
CONTROL EQUIPMENT						
20	Temperature control		Thermocouples type K			
NOTES						
DATE	EDITED		VERIFIQUED	APPROBED		
22/03/12	Pablo Cabeza					

LIST OF PUBLICATIONS

- M.D. Bermejo, P. Cabeza, M. Bahr, R. Fernández, V. Ríos, C. Jiménez, M.J. Cocero, Experimental study of hydrothermal flames initiation using different static mixer configurations, *Journal of Supercritical Fluids*, 50 (2009) 240-249.
- M.D. Bermejo, P. Cabeza, J.P.S. Queiroz, C. Jiménez, M.J. Cocero, Analysis of the scale up of a transpiring wall reactor with a hydrothermal flame as a heat source for the supercritical water oxidation, *The Journal of Supercritical Fluids*, 56 (2011) 21-32.
- P. Cabeza, M.D. Bermejo, C. Jimenez, M.J. Cocero, Experimental study of the supercritical water oxidation of recalcitrant compounds under hydrothermal flames using tubular reactors, *Water Research*, 45 (2011) 2485-2495.
- M.D. Bermejo, C. Jiménez, P. Cabeza, A. Matías-Gago, M.J. Cocero, Experimental study of hydrothermal flames formation using a tubular injector in a refrigerated reaction chamber. Influence of the operational and geometrical parameters, *The Journal of Supercritical Fluids*, 59 (2011) 140-148.
- P. Cabeza, J.P.S. Queiroz, S. Arca, C. Jiménez, A. Gutierrez, M.D. Bermejo, M.J. Cocero, Sludge destruction by means of a hydrothermal flame. Optimization of ammonia destruction conditions, *Water research*. Submitted for publication (2012).

